Planktic foraminiferal response to changing SE Atlantic oceanography

Loncaric, N.

2005

document version
Publisher's PDF, also known as Version of record

Planktic foraminiferal response to changing SE Atlantic oceanography

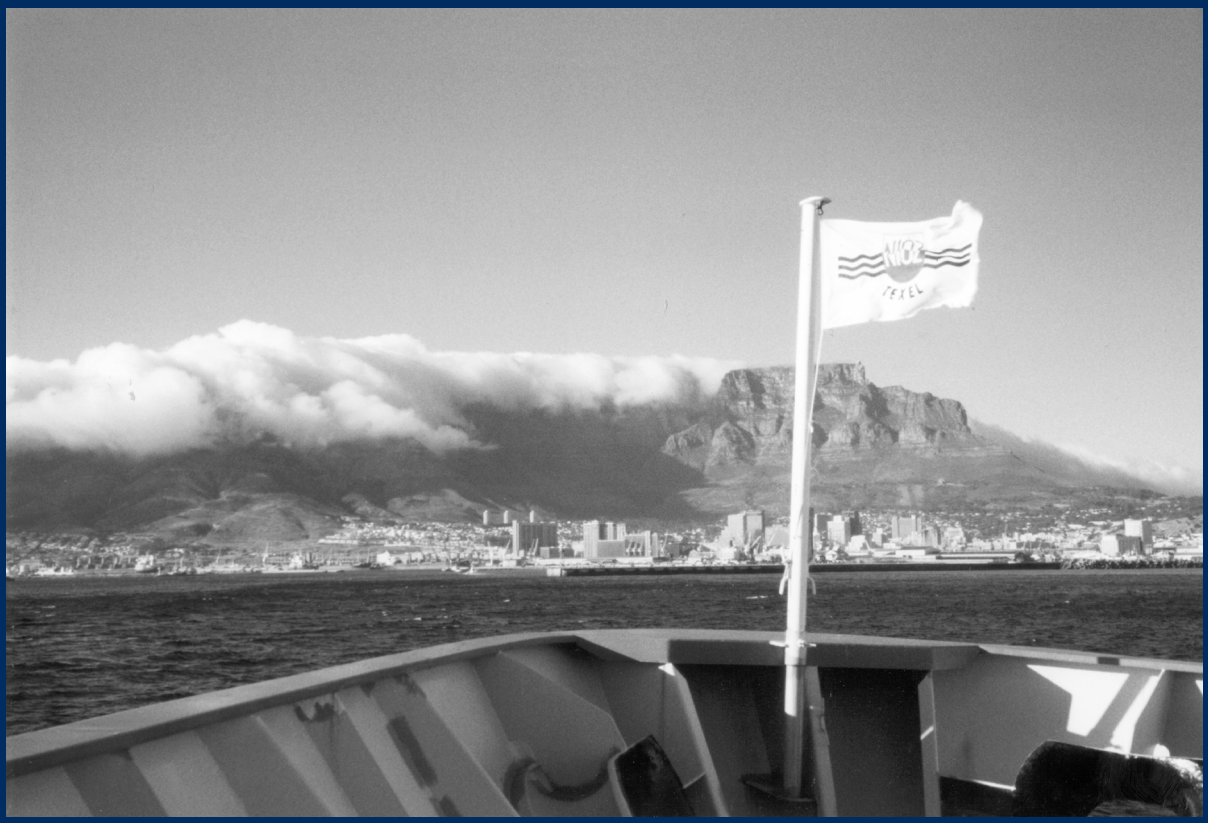

Neven Lončarić

VRIJE UNIVERSITEIT

Planktic foraminiferal response to changing SE Atlantic oceanography

ACADEMISCH PROEFSCHRIFT

ter verkrijging van de graad Doctor aan
de Vrije Universiteit Amsterdam,
op gezag van de rector magnificus
prof.dr. T. Sminia,
in het openbaar te verdedigen
ten overstaan van de promotiecommissie
van de faculteit der Aard- en Levenswetenschappen
op donderdag 15 december 2005 om 10.45 uur
in de aula van de universiteit,
De Boelelaan 1105

door

Neven Lončarić

geboren te Zagreb, Kroatië

promotor:	prof.dr. D. Kroon
copromotoren:	dr. G.-J.A. Brummer
	dr. F.J.C. Peeters

Respons van planktonische foraminiferen op oceanografische veranderingen in de Zuidoost Atlantische Oceaan

(met een samenvatting in het Nederlands)

Reakcija planktonskih foraminifera na promjenjive oceanografske uvjete jugoistočnog Atlantskog oceana

(sa sažetkom na hrvatskom jeziku)

ISBN-10: 90-9020153-X
ISBN-13: 978-909020153-5

front page cover: NIOZ research vessel Pelagia entering the harbor of Cape Town after MARE 0 cruise (photo by N. Lončarić)

Members of the evaluation committee:

prof. dr. J. Bijma
Alfred-Wegener-Institut für Polar- und Meeresforschung, Bremerhaven, Germany

dr. K. Darling
The University of Edinburgh, United Kingdom

dr. F. Jansen
Koninklijk Nederlands Instituut voor Onderzoek der Zee (NIOZ), Texel, The Netherlands

dr. S. Jung
Vrije Universiteit, Amsterdam, The Netherlands

prof. dr. C. Lange
Centro de Investigación Oceanográfica en el Pacífico Sur-Oriental (COPAS), Concepción, Chile

prof. dr. T. van Weering
Koninklijk Nederlands Instituut voor Onderzoek der Zee (NIOZ), Texel, The Netherlands

Co-authors affiliation (in order of appearance):

G.J. A. Brummer
Department of Marine Chemistry and Geology
Royal Netherlands Institute for Sea Research (NIOZ)
P.O. Box 59, 1790 AB Den Burg, Texel, The Netherlands

D. Kroon
Department of Paleoecology and Paleoclimatology
Faculty of Earth and Life Sciences, Vrije Universiteit
De Boelelaan 1085, 1081 HV Amsterdam, The Netherlands

J.M. van Iperen
Department of Marine Chemistry and Geology and
Department of Marine Ecology and Evolution
Royal Netherlands Institute for Sea Research (NIOZ)
P.O. Box 59, 1790 AB Den Burg, Texel, The Netherlands

F.J.C. Peeters
Department of Paleoecology and Paleoclimatology
Faculty of Earth and Life Sciences, Vrije Universiteit
De Boelelaan 1085, 1081 HV Amsterdam, The Netherlands

CONTENTS:

Slap

I teče, teče, teče jedan slap,
što u njem znači moja mala kap?

Gle jedna duga u njemu se stvara,
i sja i blista u hiljadu šara.

Taj san o slapu da bi mogo sjati,
i moja kaplja pomaže ga tkati.

Dobriša Cesarić (1902-1980)

1. Introduction and summary

Neven Lončarić

1. PLANKTIC FORAMINIFERA

Planktic foraminifera are single celled organisms within the Phylum Granuloreticulosa, discovered almost two centuries ago and first described by D'Orbigny (1826). During their life cycle these free floating animals form a coiled carbonate shell composed of several chambers (Fig. 1.1). They live mostly in the photic zone of the open ocean, but can control their vertical position in the water column by adjusting their buoyancy, and dwell several hundreds meter deep. Their taxonomy is traditionally based on the shell morphology (i.e. shell and chamber shape and shell surface; Fig. 1.1) and includes approximately forty-four modern species (Hemleben et al., 1989). Two major groups are distinguished, based on the presence or absence of spines, i.e. the spinose and non-spinose species, respectively (Murray, 1897). In general, spinose species are carnivorous, feeding mainly on copepods, whereas non-spinose species feed on algae as first observed by Rhumbler (1911), although several species are omnivorous, feeding on both phytoplankton and animal prey. A number of mainly spinose species may contain symbiont algae (predominantly dinoflagellates). The environmental characteristics of the upper water column such as temperature or nutrient availability determine the species composition of the faunal assemblages in the world oceans (e.g. Bé and Tolderlund, 1971). Among other factors, it is this ecosystem affiliation that makes planktic foraminifera one of the major tools in the paleoceanographic studies. In the reproductive cycle of many, if not all species, the parent's life ends upon gametogenesis, i.e. sexual reproduction where the parent organism discharges large number of gametes which later merge to form a zygote that develops into a new organism (Hemleben et al., 1989). After gametogenesis, the empty carbonate shell of the parent organism sinks to the ocean floor. Thus, this reproductive strategy directly relates pelagic carbonate production in the upper ocean to the shell deposition fluxes on the sea floor, transferring the signature of the ambient water in which the specimen lived to the fossil record on the ocean bottom (Fig. 1.2). Settling foraminiferal tests constitute a substantial part of the biogenic

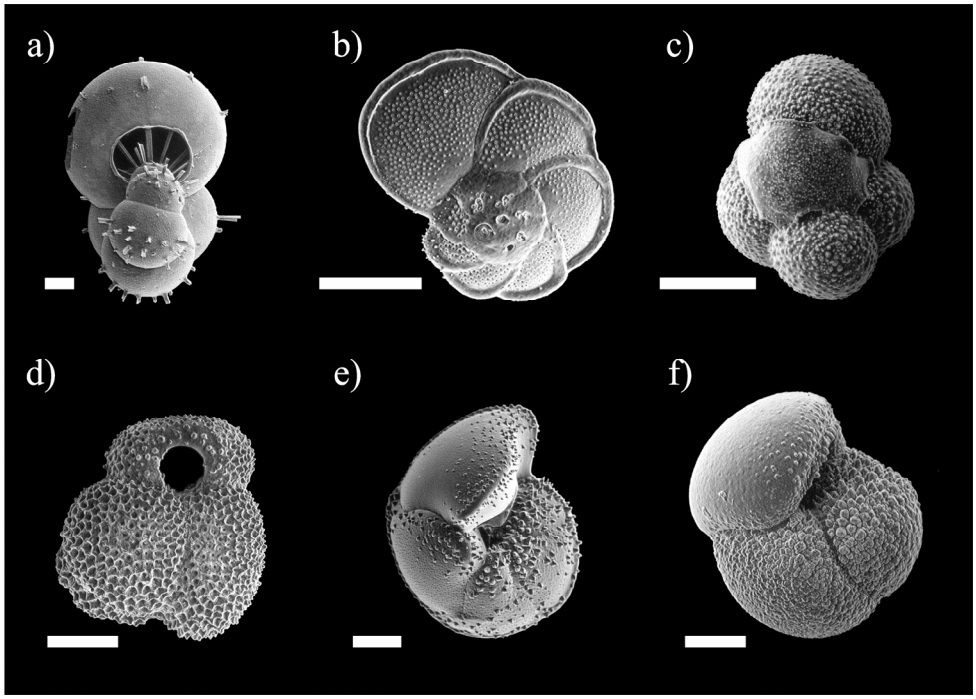

Figure 1.1: Scanning electron microscope micrographs of common central Walvis Ridge planktic foraminifera. Scale (white bars) equals 100 µm. **a)** *Hastigerina pelagica*, **b)** *Globorotalia menardii*, **c)** *Globigerinita glutinata*, **d)** *Globigerinoides ruber*, **e)** left-coiled *Globorotalia truncatulinoides*, **f)** *Globorotalia inflata.*

particulate flux and are a major component of the pelagic ocean sediment cover above the carbonate compensation depth (i.e. the depth below which the rate of carbonate dissolution exceeds the rate of shell deposition). Ryan and Pitman (1998) writing about highlights of the Ocean Drilling Program in the early days stated: "*The sedimentary layer of the ocean floor is a virtual library of information. Its acquisitions are made of mud, ooze, sand and rock with a script choreographed by climate during the erosion of mountains by precipitation, the transport of dust from deserts by wind, the wandering of the sea in meanders and gyres, the freeze and thaw of ice caps, and the life span of multitude of creatures who once colonized the ground, both wet and dry, and left behind their skeletal remains in the form of fossils. The texts in this ocean floor library are deciphered by scientists exploring the knowledge of physics, chemistry and biology."* Our knowledge on the ecology of foraminiferal species is perhaps one of the most limiting factors in decoding the information stored in this "ocean floor library". This study aims to contribute in deciphering the "script" of this peculiar "library" by documenting the biological and chemical characteristics of modern planktic foraminifera in order to improve the interpretation of ancient ocean environments.

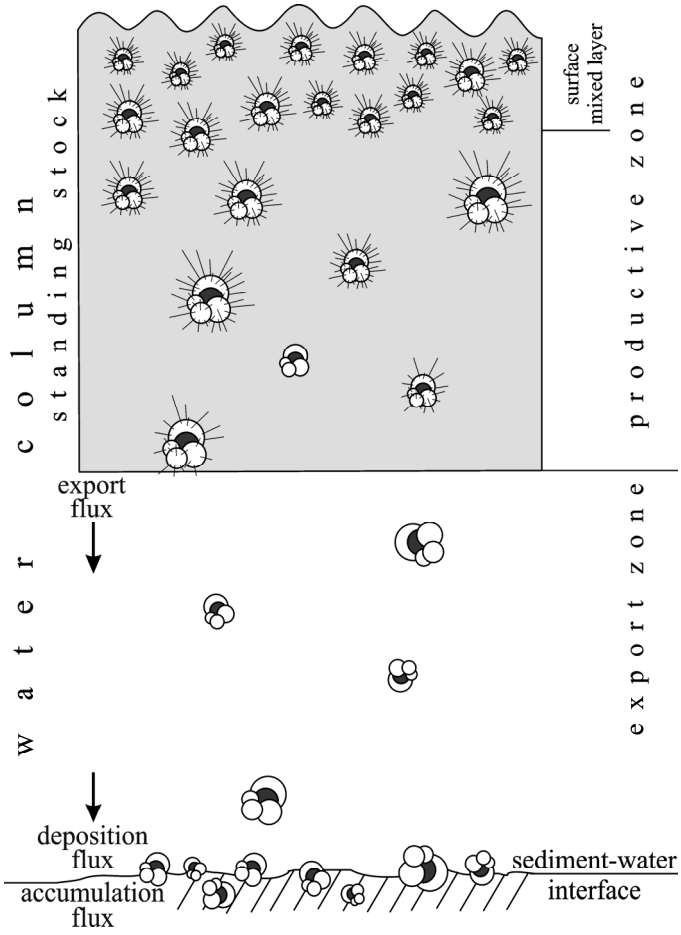

Figure 1.2: Schematic profile through the water column illustrating the foraminiferal cycle from production to sediment accumulation. The productive zone is the part of the water column where foraminifera live, calcify and build the standing stock. Dead specimens settling from the productive zone compose the export flux that may be altered by different processes during the transfer towards the sea floor. Deposition flux consists of shells that arrive at the bottom. The shells at and below the sediment-water interface compose the accumulation flux.

2. PROXIES IN PALEOCEANOGRAPHY

Characteristics of the ancient ocean environments, such as paleotemperature, paleosalinity or paleoproductivity are not directly measurable. However, they can be derived from other, measurable

parameters that are related to the targeted, non-measurable variables. Such indicators are called proxies. In paleoceanography they serve to determine the specific paleoenvironmental parameters by interpretations of the measurement results in terms of the conditions they indicate. Planktic foraminifera belong to one of the major paleoceanographic proxies. Their species assemblages and the composition of their calcite shell are used to estimate the temperature, salinity, productivity, global ice volume/sea level, ocean circulation and stratification of the past. Such properties can be estimated based on the analogy between the fossil shells found in ocean sediments with the modern species that live in the present day upper ocean. Given the wide application of planktic foraminifera and their great importance for ocean-climate reconstruction, a thorough understanding of the behaviour of modern species provides the base for firm estimates. Field observations on living populations are therefore necessary, allowing direct comparison of species assemblages and shell chemistry with the physical and chemical properties of the ambient water column.

This thesis addresses a number of questions related to the sensitivity of foraminiferal species to e.g. temperature, productivity or stratification, their vertical and lateral distribution, population dynamics and seasonal variations in shell production and export. Yet, the accurate interpretation of ancient environmental conditions from the foraminiferal records is not dependent only on a full understanding of the species ecology. The foraminiferal source signal exported from the productive zone (i.e. the part of the upper water column where foraminifera live and calcify their shells; Fig. 1.2), is also affected by the extent of preservation during the transfer to the sea floor and upon burial within the bottom sediment. Processes such as differential dissolution or diagenesis may alter the original signal and thus influence the reconstruction of specific ocean-climate parameters. In order to quantify sedimentary preservation and the impact of seasonal and interannual variability in shell production to the fossil assemblages preserved in sediment, I also examined the sediment accumulation fluxes of foraminiferal shells and contrasted them with the annual deposition (Fig. 1.2).

3. THE WALVIS RIDGE AREA

This study was carried out at the central part of the Walvis Ridge in the Southeast Atlantic Ocean (Fig. 1.3). The hydrography of the SE Atlantic is largely controlled by the Subtropical South Atlantic Gyre. The central Walvis Ridge is under the influence of the northward flowing eastern flank of this gyre, known as the oceanic branch of the Benguela Current (Peterson and Stramma, 1991; Garzoli and Gordon, 1996), with predominantly oligotrophic surface water conditions. Eastward from the study area, the surface circulation is dominated by the coastal branch of the Benguela current associated with a wind driven upwelling zone along the South African and Namibian shelf (18° - 34° S). In this zone, surface water is transported offshore by the south-eastern trade winds and replaced by colder and nutrient rich subsurface water. Benguela upwelling cells are active all year round, with filaments occasionally extending as far as 600 km offshore (Lutjeharms and Stokton, 1987). Although one of the largest upwelling regions of the world (Shannon and Nelson, 1996), the Benguela upwelling system has no direct influence on the oceanographic conditions above the central Walvis Ridge which remain oligotrophic in this respect throughout the year (Fig. 4.3).

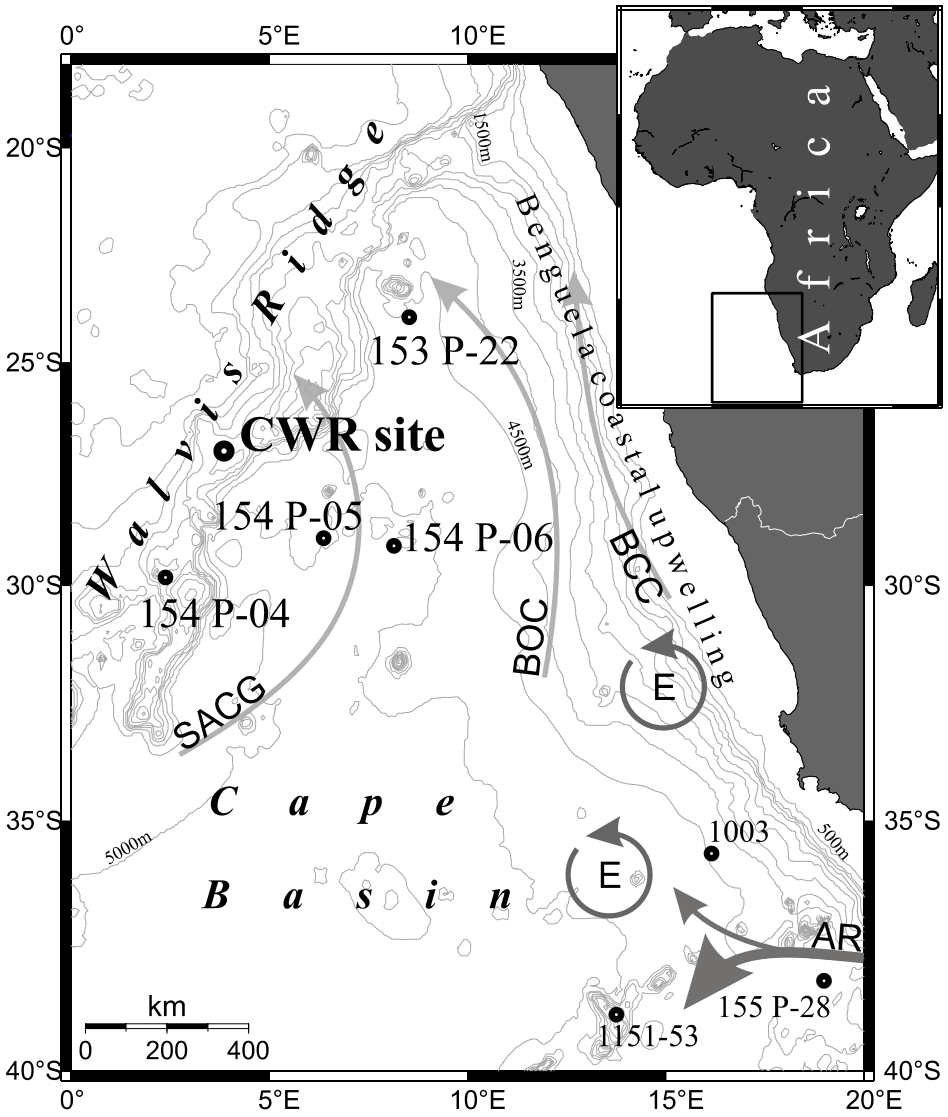

Figure 1.3: Location of the study sites (from Table 1), regional bathymetry and hydrography. SACG = South Atlantic Central Gyre, BOC = Benguela Oceanic Current, BCC = Benguela Coastal Current, AR = Agulhas Retroflection, E = Agulhas eddies.

Another prominent feature that characterizes the hydrography of the SE Atlantic is the inflow of warm and salty Agulhas Current water from the Indian Ocean into the Atlantic around the Cape of Good Hope (Schouten et al., 2000, 2002). The greatest part of the Agulhas Current retrogrades back into the Indian Ocean whereas a smaller part leaks into the Cape Basin. This occurs in the form of large scale eddies which occasionally enter the Atlantic and penetrate into the Benguela system.

Agulhas eddies are anti clockwise rotating bodies of relatively dense water, 500 to 1000 m deep and 100 to 250 km wide (Lutjeharms, 1996; van Aken et al., 2003). Once entrained in the Benguela system, they migrate northwards gradually loosing their heat and salinity to the surrounding water. This addition of warm and salty water is an important element of the global thermohaline circulation and one of the major controlling factors of the South Atlantic heat and salt budget (Gordon, 1985; Gordon et al., 1992).

Table 1.1: MARE sampling stations used in this research.

station	coordinates	type of sampling	date	chapter
CWR 154 P 03; 1008; 174 P 03	27°0' S; 3°51' E	3x double plankton tow cast 2x 24 weeks sediment trap mooring box core water sampling CTD-rosette	 19/2/00 30/7/00 2/2/01 	2 3 4 5 6
153 P 22	24°0' S; 8°30' E	water sampling CTD-rosette	12/2/00	5
154 P 04	29°50' S; 2°26' E	double plankton tow cast CTD-rosette water sampling	20/2/00	3 5
154 P 05	28°48' S; 6°18' E	double plankton tow cast CTD-rosette	21/2/00	6
154 P 06	29°10' S; 8°10' E	24 weeks sediment trap mooring double plankton tow cast CTD-rosette	22/2/00	3 6
155 P 28	38°1' S; 18°25' E	double plankton tow cast CTD-rosette	7/3/00	5
1001/ 1003	35°56' S; 16°6' E	double plankton tow cast CTD-rosette	22/7/00	5
1151/ 1153	38°40' S; 13°58' E	double plankton tow cast CTD-rosette	7/8/00	5

4. OUTLINE OF THE RESEARCH

4.1. Material and methods

The major goal of this study was to determine the ecological characteristics of modern planktic foraminiferal associations and their response to changes of the surrounding environment. Foraminifera respond to several hydrographic properties that in the natural environment interact, creating a complex system of controlling parameters. The central Walvis Ridge area in the southeast Atlantic Ocean (Fig. 1.3) is characterised by predominantly stable conditions, such as low nutrient levels within the shallow surface mixed layer during most of the year and a low seasonal temperature

gradient, which provide a suitable setting for quantification of individual ecological characteristics and species responses. It is situated approximately 1300 km westward from the African coast, out of the reach of the coastal influences and the Benguela upwelling. The central Walvis Ridge (CWR) sampling station provided therefore the framework for ecological studies presented here. At this site, the material was collected by different sampling techniques during three MARE cruises in February 2000, July/August 2000 and February 2001 (Tab. 1). The water column properties such as temperature, salinity and fluorescence were measured in-situ by a CTD (Conductivity-Temperature-Depth) rosette sampler (Fig. 1.4a), which also sampled seawater for chemical analyses (e.g. nutrient content and isotope composition) performed shipboard or later in the laboratory.

Figure 1.4: CTD-rosette **(a)** and Hydrobios Multinet system **(b)**.

Plankton from the upper 800 to 1000 m of the water column was sampled by depth-stratified tows using the NIOZ-modified Hydrobios Multinet system equipped with two flow meters and 5 nets with a 100 µm mesh in a steal frame connected to a PC-controlled deck unit (Fig. 1.4b). It allowed quantitative sampling of foraminifera and other plankton at exact depth intervals. The nets were successively opened and closed during the upcast while obliquely towed behind the slow-sailing ship, sampling between 20 and 1000 m^3 of seawater (Fig. 1.5). The sampling intervals were usually wider for the deep cast where plankton concentration is low, and narrow in the photic zone where plankton is abundant (Fig. 1.2; Tab. 2.1). This prevented the net clogging, yet allowed collecting sufficient material for the taxonomic and chemical analyses.

The particulate matter settling to the ocean floor was sampled by time-series sediment traps. These are cone-shaped devices moored close to the bottom with a 1 m^2 opening on the upper side and a carousel with 24 sampling cups at the lower, narrow side, programmed to rotate in equidistant time steps (mostly 7 or 8 days) and sample particles settling through the opening (Figs. 1.6-1.7).

Surface sediment was sampled by a box corer, a 55 cm high and 50 cm wide coring cylinder with weight on top that rapidly descends to the sea bottom and due to a gravitational force penetrates into upper few tenths of centimetres of the sea bed and closes with a lid upon retrieval. Apart from the CWR site, several additional sites in the region were also sampled to document the regional faunal and chemical composition of the water column and the impact of SE Atlantic hydrographic changes to the deep sea carbonate sedimentation patterns (Fig. 1.1; Tab. 1.1).

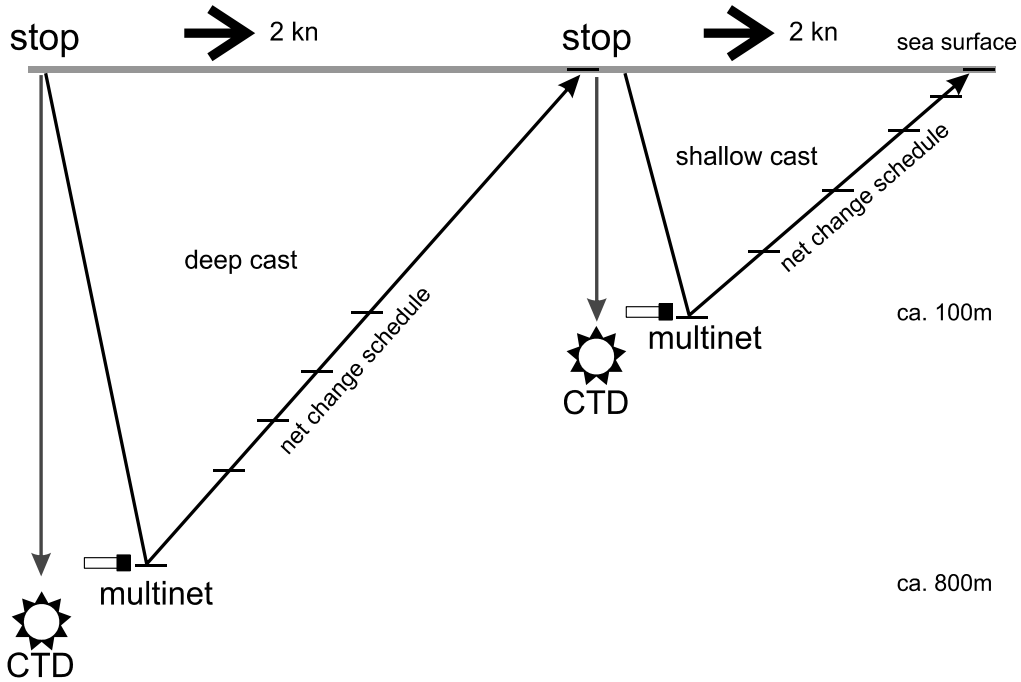

Figure 1.5: Sampling strategy of plankton towing (Multinet) and water profiling (CTD-rosette) during the MARE cruises. Kn = towing velocity in knots.

4.2. Population dynamics of planktic foraminifera

Chapter 2 addresses the population dynamics of planktic foraminifera. To that purpose I developed a methodology for determination of the depth of the productive zone (i.e. the part of the water column in which species live), the size of the foraminiferal standing stocks (i.e. number of specimens per square meter of the productive zone) and the turnover time (i.e. the time required for complete replacement of the species population by the next generation) (Fig. 2.3). The turnover time was approached by two independent methods, one using the foraminiferal deposition flux (shells settling to the ocean floor as the number of shells per m^2 per day) as recorded by sediment traps near the sea floor, and the other using the export concentration of dead specimens settling out from the productive zone in the upper water column (number of shells per m^3 of seawater), recorded by plankton tows. A simple model was developed to illustrate the significance of such turnover time, which showed that it may be interpreted as the average life span of the foraminiferal species only for the population in, or near the steady state (Figs. 2.8-2.9). In addition, the model showed that growing populations yield increased turnover times while by contrast, collapsing populations render short turnover times. This methodology was applied to the CWR plankton tow and sediment trap results from February 2000, July 2000 and February 2001, where it appeared that the spinose shallow-dwelling species *Globigerinoides trilobus* and *Globigerinoides ruber* (Fig. 1.1d) showed the most consistent values, closest to the steady state. Their turnover time in austral summer was interpreted

as an average life span of approximately two weeks. Non-spinose deep-dwellers showed an average turnover of no longer than six weeks. The CWR findings put forward that the complete refreshment of the planktic foraminiferal populations within the productive zone is a matter of weeks, rather than a seasonal or even annual cycle as previously suggested for some deep-dwelling species.

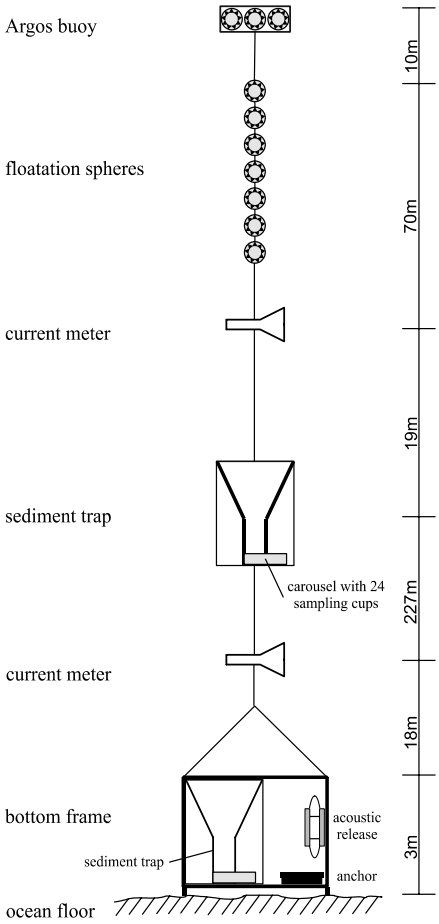

Figure 1.6: Configuration of the MARE sediment trap moorings.

4.3. Lunar cycles and seasonal variation in deposition fluxes

Chapter 3 further elaborates on foraminiferal population dynamics in terms of its reproductive cycling on a (semi)lunar frequency. Such cycling was first demonstrated in laboratory cultures of *Hastigerina pelagica* (Fig. 1.1a) and has been suggested for several planktic foraminiferal species from plankton tows and sediment traps. Therefore lunar cycling may be an important source of temporal variation for the lateral and vertical distribution of living species and a potential driving mechanism of short-term carbonate fluxes that may account to 5.7 Gt $year^{-1}$ in pelagic ocean. Yet, lunar oscillations in the foraminiferal reproduction has not been recognized in field observations as straightforwardly as in cultured *H. pelagica* and this species remained the only one for which an endogenous lunar cycle could be demonstrated in the laboratory. I field-demonstrate for the first time that lunar periodicity in *H. pelagica* determines its shell deposition fluxes at the 2700 m deep ocean floor. The CWR deposition flux maxima of this species showed a strong 30-day cyclicity arriving on average 12.5 days after the full moon. After accounting for the settling time, this coincides with the reproduction 5 days after the full moon, as it was originally observed in culture isolates. This allowed addressing the reproductive periodicity in the deposition fluxes of other planktic species at the Walvis Ridge. However, no other species exhibited lunar or any other oscillations in deposition flux within the 16 to 90 days domain of this study. Rather than lunar-driven, fluxes of all other species appeared primarily determined by seasonal responses, implying that reproduction is continuous in the lunar domain. Given that *H. pelagica* is a rare species with low fluxes and low burial efficiency, such continuous reproduction by other species greatly facilitates interpretations of the foraminiferal distribution patterns across ecological and physical gradients in the upper ocean. Furthermore, this study shows that lunar

reproductive cycling does not affect pelagic carbonate productivity and deep ocean sedimentation fluxes. Recognition of the lunar frequency in the deposition flux of *H. pelagica* also demonstrates the high accuracy of the trap sampling at this site, in particular when considering the fragility of the species and the depth of the mooring.

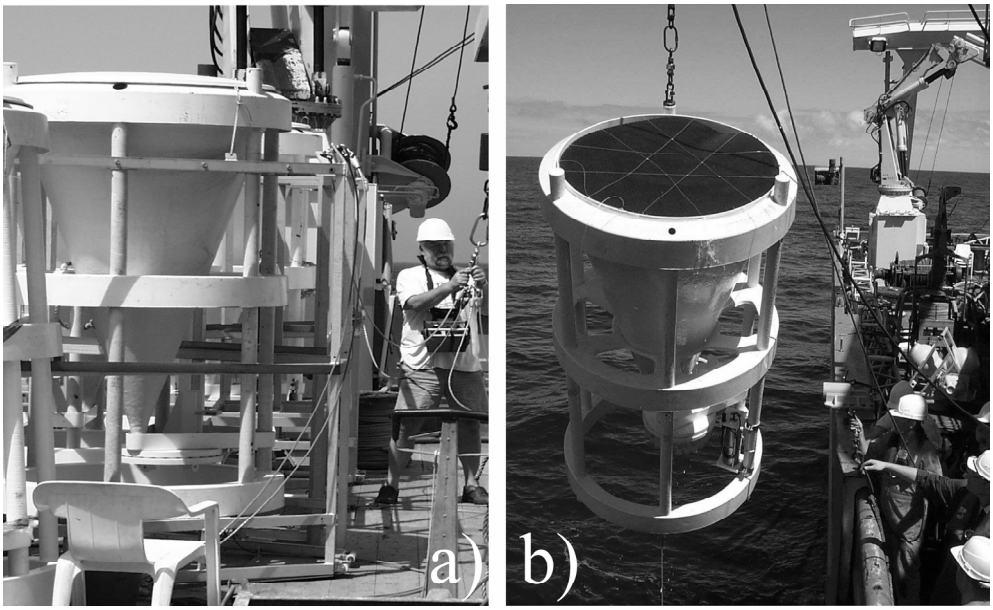

Figure 1.7: Sediment traps on board the R/V Pelagia prior deployment at the Walvis Ridge in February 2000 (**a**) and upon recovery in February 2001 (**b**).

4.4. Seasonal export and sediment preservation in a trophic gradient

Particle flux records from different areas of the world oceans point to the dynamic behaviour of plankton populations in general. **Chapter 4** addresses the seasonal changes in the predominantly oligotrophic South Atlantic Central Gyre by combining the CWR time-series deposition fluxes of phytoplankton (diatoms and silicoflagellates), zooplankton (foraminifera and pteropods) and other biogenic particles collected by the sediment traps, and contrasting them to the surface sediment from a box core of the same site. Prominent austral spring maxima characterised the CWR deposition fluxes of all major compounds. The productivity sequence was initiated by winter deepening of the surface mixed layer in response to increased wind stress during late autumn that allowed entrainment of new nutrients from the subsurface, enhancing productivity in the surface mixed layer (Fig. 4.4b). At the turn of winter, shoaling of the surface mixed layer resulted in a halt of nutrient entrainment causing collapse of the productivity. In response, nearly 25% of the annual mass flux arrived to the sea floor within a month in early spring. Both diatom and foraminiferal standing stocks were associated with the same process of nutrient entrainment in the surface mixed layer even though

separated by a one-week lag of maxima in their deposition fluxes at the sea floor due to the faster response of phytoplankton to nutrient limitation and additionally modified by their slower settling with respect to foraminifera. Principal component analysis of the time-series deposition fluxes revealed strong seasonality of foraminiferal species, whereas diatoms clustered according to the bloom and non-bloom period. Small *Nitzschia bicapitata* and *Globorotalia inflata* (Fig. 1.1f) dominated the annual deposition of diatoms and foraminifera, respectively with 60% and 25%. The deep-dwelling foraminifer *Globorotalia truncatulinoides* (Fig. 1.1e) was an important exception, since it did not follow the general seasonal pattern. Its left- and right-coiled specimens showed maximum deposition in early winter as well as late spring or in late spring only, respectively. Such a different seasonal response of chiral *G. truncatulinoides* argues for a separate taxonomic status rather than simple coiling variability within a single species in agreement with recent DNA studies, and suggests that genetic species also have different seasonality.

At the sediment water interface, intense degradation of organic matter and biogenic silica resulted in poor preservation and pronounced changes in the species composition of siliceous phytoplankton. Of all particle compounds, only foraminiferal shells showed full preservation in the sediment surface. Consequently, *G. inflata* and most other foraminiferal species appeared predominantly deposited in response to the seasonal productivity changes and preserved this upper ocean signal through their sediment assemblages at the sea floor.

The CWR data have been used as the end member to complete a productivity gradient across the Benguela system, from the oligotrophic Central Gyre to the highly productive coastal upwelling off Namibia. Along this gradient, flux maxima appeared associated with winter minima in sea surface temperature and related maxima in surface mixed layer depth, but showed an oceanward offset, first appearing along the coast in early August and two months later at the CWR site. Transition from oligotrophic to mesotrophic conditions was characterised by the increasing dominance of *G. inflata* coupled with a decreasing foraminiferal diversity and abundance of warm species, whereas in diatom assemblages small and weakly-silicified *N. bicapitata* was substituted by larger and heavier-silicified species. Closer to the coastal upwelling, decreasing dominance of *G. inflata* combined with increasing abundance of cold water *Globigerina bulloides*, dextral *Neogloboquadrina pachyderma* and ultimately sinistral *N. pachyderma* together with *Turborotalita quinqueloba* accompanied the transition from mesotrophic to eutrophic conditions. Although the total fluxes of particle compounds increased shoreward, the differences appeared rather small testifying to only moderate productivity and deposition at the Namibian margin with respect to the Central Gyre.

4.5. Oxygen isotope ecology of recent planktic foraminifera

The oxygen isotope composition ($\delta^{18}O$) of foraminiferal shells is related to the temperature and the $\delta^{18}O$ of the surrounding water. Thus, the sediment $\delta^{18}O$ signal from fossil shells will be defined by foraminiferal ecology, e.g. calcification depth and seasonality, temporal flux changes and vital effect (i.e. how the specimen incorporates $\delta^{18}O$ signal from the ambient water into its own shell). This source signal from the productive zone may be altered during the shell transfer to the sea floor and upon burial by e.g. deep encrustation of cold water calcite, partial dissolution or diagenesis. In **chapter 5**, the ecological insights gained from foraminiferal species are combined with the oxygen isotopic composition of their shells (i.e. $^{18}O/^{16}O$ ratio) to enhance our understanding of the species

depth habitat, calcification and the seasonal distribution in the upper water column and improve the sea surface temperature (SST) estimates from shell $\delta^{18}O$. To further unravel the processes relating shell production to sediment preservation, the $\delta^{18}O$ records from the CWR plankton tows are compared with the shell $\delta^{18}O$ from the annual deposition flux (sediment traps) and the fossil $\delta^{18}O$ from the core-top sediment.

The base of foraminiferal productive zone (Z_{BPZ}) is calculated using the method developed in chapter 2 and compared with the Z_{BPZ} derived from the $\delta^{18}O$ profiles. The two independent approaches agreed to a large extent, testifying to the accuracy of the primary hypothesis and suggesting that both the shell concentration and its $\delta^{18}O$ can be used confidently to determine the depth range of the species' productive zone. The results from the CWR and three additional sites in the southern Cape Basin (Fig. 1.3) promote *Globigerinita glutinata* (Fig. 1.1c) as the best SST proxy. This species calcified in equilibrium with the expected $\delta^{18}O$, showed constant isotope values with depth and it was the only CWR species that did not show any alteration in the fossil $\delta^{18}O$. Concordant with its flux maximum in early spring triggered by deep winter mixing (chapter 4), the sediment $\delta^{18}O$ signal of *G. glutinata* accurately reflected the winter SST at the CWR site. The $\delta^{18}O$ sediment record of *G. ruber* (Fig. 1.1d), a species generally considered to be shallow-dweller and thus used as a SST proxy, also provided a good estimate of the winter SST at the CWR. However, our plankton tow results suggest that the calcification zone of *G. ruber* always extends till the deep chlorophyll maximum which may be situated far below the surface mixed layer. At the CWR this occurs from autumn till spring (chapter 4), when the export $\delta^{18}O$ is partly formed in water colder than SST and therefore significantly underestimates the actual SST by more than 2°C. *G. truncatulinoides* (Fig. 1.1e) appeared to calcify in oxygen isotope equilibrium in the zone of maximum shell concentration, which is usually deeper for larger specimens. Since the calcite from the 250 µm tests of *G. truncatulinoides* contributes less than 10% of the 400 µm-fraction shell mass, the fraction of the calcite formed in shallower, warmer water is insignificant in the larger tests (Fig. 5.9). The CWR tow results show that the $\delta^{18}O$ of left-coiled *G. truncatulinoides* with a maximum test diameter of ~400 µm reflect the water temperature at about 350 m depth, and those with a diameter of ~250 µm indicate the temperature at about 200 m depth. Consequently, the $\delta^{18}O$ difference between the test size fractions in the sediment can be used to estimate the subsurface temperature gradient.

4.6. Planktic foraminifera in a mature Agulhas eddy

Chapter 6 documents the faunal composition of a mature Agulhas eddy that penetrated into the northern Cape Basin. Foraminiferal assemblages and physical characteristics of the eddy are contrasted whit those of the surrounding water and to the deposition flux, aiming to assess its imprint on sedimentation patterns in the northern Cape Basin and the Walvis Ridge. The examined eddy was at the moment of sampling still clearly recognisable on the sea surface altimetry images by its elevated surface due to its anticlockwise rotational motion. It was distinguished from the ambient ocean by a slightly higher salinity, deeper surface mixed layer and higher foraminiferal standing stocks. The faunal composition of the ring was similar to the assemblages earlier identified in the freshly formed eddies from the southern Cape Basin. However, the contrast between the faunal assemblages of the mature eddy and the surrounding ocean was weak, despite clear identification of the eddy by radar altimetry.

Remarkable was the absence of the tropical species *Globorotalia menardii* (Fig. 1.1b) within the eddy, although it was very abundant in the surrounding SE Atlantic waters. In several paleostudies from this area it has been assumed that this species has an Indian Ocean origin indicative for an "open Cape valve", i.e. full interglacial exchange between the Indian and Atlantic Ocean. However, *G. menardii* does not appear to belong to the typical mature ring fauna, corroborating findings from the freshly formed eddies from the southern Cape Basin. More likely it re-seeded the Cape Basin from the subtropical Atlantic during interglacials when ocean fronts shifted southward, rather than via Agulhas eddies from the Indian Ocean.

REFERENCES:

Bé, A.W.H. & Tolderlund, D.S., 1971. Distribution and ecology of living planktonic foraminifera in surface waters of the Atlantic and Indian Oceans. In: W.R. Riedel (Ed.), *The Micropaleontology of the Oceans.* Cambridge University Press, Cambridge, pp. 105-149.

d'Orbigny, A.D., 1826. Tableau méthodique de la classe des Céphalopodes. *Ann. Sci. Nat., 1* (7): 245-314.

Garzoli, S.L. & Gordon, A.L., 1996. Origins and variability of the Benguela Current. *Journal of Geophysical Research, 101* (C1): 897-906.

Gordon, A.L., 1985. Indian-Atlantic transfer of thermocline water at the Agulhas retroflection. *Science, 227* (4690): 1030-1033.

Gordon, A.L., 1996. Communication between oceans. *Nature, 382*(6590): 399-400.

Gordon, A.L., Weiss, R.F., Smethie, W.M. & Warner, M.J., 1992. Thermocline and intermediate communication between the South Atlantic and Indian Oceans. *Journal Geophysical Research, 97*: 7223-7240.

Hemleben, C. Spindler, M. & Anderson, O.R., 1989. *Modern Planktonic Foraminifera*. Springer-Verlag, New York, 363 pp.

Lutjeharms, J.R.E., 1996. The exchange of water between the South Indian and South Atlantic Oceans. In: G. Wefer, W.H. Berger, G. Siedler & D.J. Webb (Eds.), *The South Atlantic: Present and past circulation*. Springer-Verlag, Berlin Heidelberg, pp. 125-162.

Lutjeharms, J.R.E. & Stockton, P.L., 1987. Kinematics of Southern Africa's upwelling front. In: Brink, K.H. (Ed.), The Benguela and comparable ecosystems. Sea Fisheries Research Institute, Cape Town, pp. 35-49.

Murray, J., 1897. On the distribution of the pelagic foraminifera at the surface and on the floor of the ocean. *Nat. Sci., 11*: 17-27

Peterson, R.G. & Stramma, L., 1991. Upper-level circulation in the South Atlantic Ocean. *Progress in Oceanography, 26* (1): 1-73.

Rhumbler, L., 1911. *Die Foraminiferen (Thalamorphoren) der Plankton-Expedition*. Erste Teil: Die allgemeinen Organisations-Verhaltnisse der Foraminiferen. Ergebnisse der Plankton-expedition der Humboldt-Stiftung (1909), 3: 331 pp.

Ryan, W. & Pitman, W., 1998. *Noah's flood*. Simon and Schuster UK Ltd, London, 337 pp.

Schouten, M.W., de Ruijter, W.P.M., van Leeuwen, P.J. & Lutjeharms, J.R.E., 2000. Translation, decay and splitting of Agulhas rings in the southeastern Atlantic Ocean. *Journal of Geophysical Research, 105* (C9): 21913-21925.

Schouten, M.W., de Ruijter, W.P.M. & van Leeuwen, P.J., 2002. Upstream control of Agulhas Ring shedding. *Journal of Geophysical Research - Oceans, 107* (C8), doi:1029/2001JC000804.

Shannon, L.V. and Nelson, G., 1996. The Benguela: large scale features and processes and system variability. In: G. Wefer, W.H. Berger, G. Siedler & D.J. Webb (Eds.), *The South Atlantic: Present and past circulation*. Springer-Verlag, Berlin Heidelberg, pp. 163-210.

van Aken, H.M., van Veldhoven, A.K., Veth, C., de Ruijter, W.P.M., van Leeuwen, P.J., Drijfhout, S.S., Whittle, C.P. & Rouault, M., 2003. Observations of a young Agulhas ring, Astrid, during MARE in March 2000. *Deep-Sea Research II, 50* (1): 167-195.

More

I gledam more gdje se meni penje
i slušam more dobrojutro veli
i ono sluša mene i ja mu šapćem
o dobrojutro more kažem tiho
pa opet tiše ponovim mu pozdrav
a more sluša sluša pa se smije
pa šuti pa se smije pa se penje
i gledam more gledam more zlato
i gledam more gdje se meni penje
i dobrojutro more more kaže
i zagrli me more oko vrata
i more i ja i ja s morem zlatom
sjedimo skupa na žalu vrh brijega
i smijemo se smijemo se moru

Josip Pupačić (1928-1971)

2. Population dynamics of planktic foraminifera at the central Walvis Ridge (SE Atlantic): standing stock, export flux and turnover time

Neven Lončarić & Geert-Jan A. Brummer

ABSTRACT

We derived a set of equations, which allows to determine the depth of the productive zone and turnover time of planktic foraminifera as sampled in the field. It was applied to the combined results from plankton tows and sediment traps at a single site on the central Walvis Ridge (SE Atlantic). Turnover time, i.e. the time required for the complete replacement of the foraminiferal population by a new generation, was determined for the major planktic foraminiferal species in contrasting seasons (February and July). It is approached in two independent manners, one using the foraminiferal export flux (J_{exp}) as recorded by sediment traps close to the ocean floor and the other using the export concentration (C_{exp}) of dead specimens settling out from the upper ocean, recorded by plankton towing. Both approaches yield similar turnover patterns despite the time scale discrepancy between the two sets of samples (C_{exp} vs. J_{exp}) and the short-scale temporal changes in the population dynamics. Export concentrations are positively correlated with the standing stocks (*SS*) for the February samples (near steady state condition), and turnover times are approximately constant for most of the species. These results are interpreted as the average life span of the stable foraminiferal population. July samples however, show for some species offset in SS/C_{exp} ratio, which is interpreted as characteristic of rapid population change. A positive and negative offset from the steady state situation indicates a growing and decaying population, respectively. Our findings suggest that the complete refreshment of the planktic foraminiferal populations within the productive zone is a matter of days to weeks. The most consistent is the summer record of spinose, shallow-dwelling species *Globigerinoides trilobus trilobus* and *Globigerinoides ruber* with the average life spans of 14±2 and 14±6 days, respectively. The longest turnover times are recorded for the July populations of the non-spinose species *Globorotalia menardii* (32±11 days), dextral *Globorotalia truncatulinoides* (25±7 days), *Globigerinita glutinata* (21±5 days) and sinistral *Globorotalia truncatulinoides* (17±5 days). No evidence is found for the average foraminiferal life span longer than 6 weeks.

1. INTRODUCTION

Planktic foraminifera provide an important group of palaeoceanographic proxies. Fossil assemblages of these cosmopolitan protozoans and the isotopic composition of their shells are widely used to assess the timing and magnitude of climate changes in the past by informing on sea surface temperature, productivity and global ice volume. The robustness of palaeoceanographic interpretations from the fossil record is limited by our knowledge of the physiology and ecology of modern species. Numerous field and culture studies in the last few decades have shown that planktic foraminifera have complex life cycles involving controlling factors such as water temperature (Bé and Tolderlund, 1971; Bijma et al., 1990b; Oberhänsli et al., 1992), nutrient availability (Thiede, 1975; Deuser and Ross, 1980; Thunell and Reynolds, 1984; Sautter and Thunell, 1991; Ortiz and Mix, 1992; Sautter and Sancetta, 1992; Thunell and Sautter, 1992; Schiebel et al., 1995; Schiebel et al., 2001), light regime (Duplessy et al., 1981; Ortiz et al., 1995) and reproductive cycling (Hemleben and Spindler, 1983; Bijma et al., 1990a; Schiebel et al., 1997). So far, gametogenesis was observed for a number of cultured spinose species although it never resulted in a second generation of the foraminiferal population. Therefore culturing is performed only on mature specimens collected in the field (Hemleben et al., 1989; Bijma et al., 1990b). Such experiments provide a limited insight into the entire life cycle since they only follow the later stages of growth till reproductive maturity. On the other hand, due to the complexity of the required sampling techniques, field studies that contrast water column concentrations with export fluxes and address foraminiferal turnover at the population level remain scarce since the pioneering work of Berger and Soutar (1967) and Berger (1969).

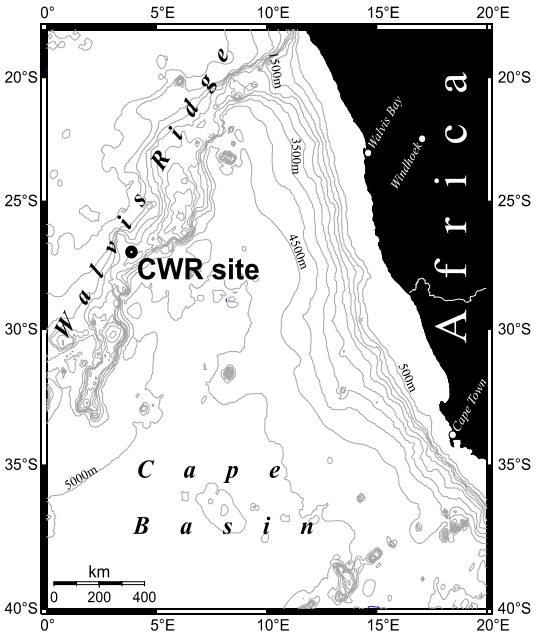

Figure 2.1: Study site location and local bathymetric features (map created by OMC at www.aquarius.geomar.de).

In this study we quantify the relationship between the standing stock of living species, and the export concentration and export flux of shells sinking to the ocean floor, among others to gain insight in their average life span. For this purpose we collected an integrated set of nested samples at a single site at the Walvis Ridge. This allows to assess the dynamics of renewal of the foraminiferal populations within the productive zone by combining their concentration profiles in the upper water column with their shell export fluxes, as obtained from three plankton tow profiles and sediment traps moored directly below.

Table 2.1: Sampling details of the plankton tows collected at the central Walvis Ridge (CWR).

CRUISE /station		date [dd-mm-yy]	LAT begin/end [deg/min]	LONG begin/end [deg/min]	tow interval [m]	volume [m^3]
MARE 0 (summer)	154 P 03a	19/Feb/00	27° 01.01' S 27° 06.01' S	3°52.13' E 3°55.65' E	804-503 503-306 306-155 155-105	669 806 421 129
	154 P 03d	19/Feb/00	27° 00.29' S 27° 00.91' S	3° 51.17' E 3° 51.88' E	107-77 77-55 55-29 29-13 13-0	73 55 74 32 18
MARE II (winter)	1086	30/Jul/00	27° 00.61' S 26° 57.71' S	3° 51.18' E 3° 58.26' E	998-499 499-300 300-202 202-152	972 576 255 143
	1089	30/Jul/00	26° 57.81' S 26° 58.84' S	3° 58.02' E 3° 55.93' E	148-100 100-75 75-52 52-24 24-0	176 112 107 91 115
MARE III (summer)	174P03-1	02/Feb/01	27° 00.87' S 27° 04.10' S	3° 51.51' E 3° 56.40' E	803-501 501-302 302-201 201-148	575 827 197 148
	174 P 03-4	02/Feb/01	27° 00.77' S 27° 00.88' S	3° 51.71' E 3° 51.86' E	154-100 100-74 74-51 51-26 26-0	113 110 92 54 98

2. MATERIAL AND METHODS

2.1. Plankton tows

At the central Walvis Ridge (CWR) site plankton tow samples were collected during three MARE cruises, in February 2000, July 2000 and February 2001 (Fig. 2.1, Tab. 2.1). A modified Hydrobios Multinet System equipped with 5 plankton nets (mesh 100 µm) and flow meters was obliquely towed behind the ship at about 1.5 knots (for detailed explanation of the sampling technique and the historical development of plankton sampling equipment see Wiebe and Benfield, 2003). The nets were opened and closed consecutively during the upcast, each sampling a specific depth interval of the water column (Tab. 2.1). Oblique plankton towing through the water column yields an average shell concentration per tow interval. In practice, the depth intervals of the tows are tuned to the expected foraminiferal shell concentration. Low concentration requires a wide depth interval to filter a sufficient volume of water for the statistically reliable analysis, while high

concentration requires narrower depth intervals filtering less water to prevent the net from clogging. For the deep cast approximately 130 – 1000 m^3 of seawater was filtered per interval, for the shallow cast approximately 20 – 180 m^3. Onboard, after removing the large swimmers, the samples were frozen at –40°C. In the laboratory the samples were freeze-dried, weighed and ashed in a low-temperature asher (T<100°C) to remove the organic matter. After wet-sieving over 100 µm mesh the samples were dry-sieved into three size fractions (100-150, 150-250, >250 µm).

2.2. Sediment traps

A Technicap PPS5 sediment trap with sampling area of 1 m^2 equipped with a 24-cup automated sampling carousel was moored at the sea floor of the CWR site (27°00' S, 3°51' E; bottom depth 2701 m; Fig. 2.1). The trap was deployed in February 2000, serviced in July 2000 and recovered in February 2001, providing a semi-continuous 1-year record. Prior to mooring, the sample cups were filled with seawater collected from the deployment depth, which was poisoned by a pH buffered solution of $HgCl_2$ (pH~8.5; 1g $HgCl_2$ per 1l seawater).

In the laboratory the non-flux large swimmers were removed from the samples. The samples were wet-split into at least two aliquots using a Folsom splitter (Sell and Evans, 1982; Griffiths et al., 1984). One aliquot was wet-sieved over 150 µm mesh, rinsed with alcohol, ashed in a low-temperature asher and then dry-sieved over a 250 µm mesh to obtain two size fractions for the foraminiferal studies. For this study, the first cup from the first mooring (resolution 7 days) and the first and last cup from the second mooring (resolution 8 days) that best correspond to the plankton tows have been used for comparison with the upper water column.

2.3. Foraminiferal analyses

Quantitative and qualitative analyses of planktic foraminifera were performed on 27 plankton tow samples and three corresponding sediment trap intervals (the first cup following the plankton towing). For the February 2001 sample, we have used the first foregoing cup. Census counts were made separately for the two coarser fractions, i.e. 150-250 and >250 µm. Large samples were split by an Otto dry splitter. On average 351 specimens (min. 170, max. 926) were picked per each tow depth interval or sediment trap cup. For the purpose of this study the counts of two size fractions were integrated in one, larger than 150 µm. For the species *Globigerinoides trilobus* we counted separately the morphotype with (= *G. trilobus sacculifer*) and without (= *G. trilobus trilobus*) the final sack-like chamber. When used as integrated counts for both morphotypes, the species name *Globigerinoides trilobus* s.l. is applied.

3. OCEANOGRAPHIC SETTING

The oceanography above the central Walvis Ridge is under the influence of the oceanic flank of the Benguela Current which forms the eastern limb of the South Atlantic Subtropical Gyre (Peterson

and Stramma, 1991). The Benguela Current is primarily fed by the South Atlantic Current, but may also receive Agulhas Current Water as well as Subantarctic Surface Water (Peterson and Stramma, 1991). The temperature range of the predominantly oligotrophic surface water at the CWR site is between 17°C (austral winter) and 24°C (austral summer) (NOAA satellite derived SST for 27°S; 4°E; www.saa.noaa.gov). The Benguela Current upwelling system is situated approximately 10° eastwards of the study site. Even though one of the greatest upwelling regions of the world with filaments of cold, nutrient rich water extending as much as 600 km offshore, the Benguela upwelling has no direct influence on the oceanography above the central Walvis Ridge (Lutjeharms and Stokton, 1987; Shannon and Nelson, 1996).

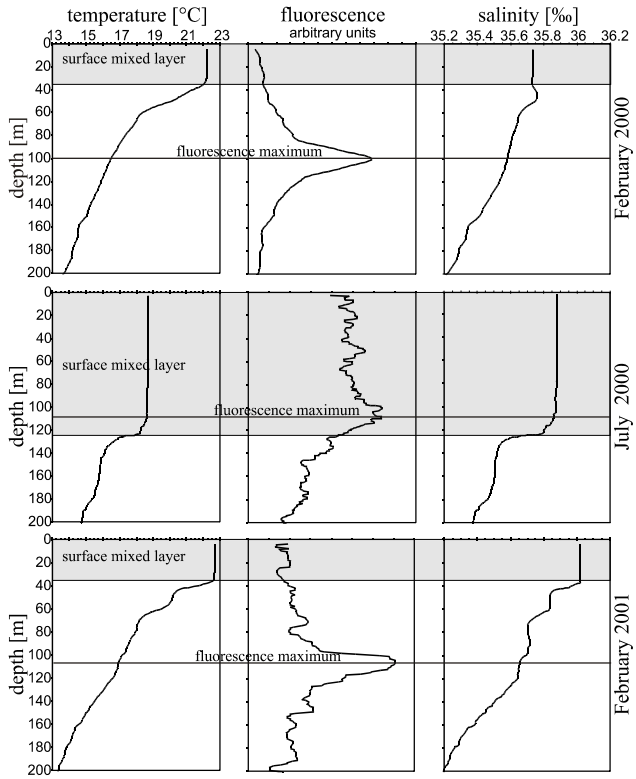

Figure 2.2: CTD profiles taken at the CWR site during the MARE cruises. All CTD profiles were retrieved immediately after or prior the corresponding plankton tow sampling.

Although with relatively similar SST ranging between 18.7 and 22.7°C, the summer and winter CTD profiles at study site, retrieved during three MARE cruises, differ to a large extent (Fig. 2.2). February 2000 is characterized by a sharp shallow thermocline at depth of 35 m, yet the prominent but narrow fluorescence maximum is traced much deeper, at 100 m. One year later, in February 2001, the surface mixed layer is of the same thickness, with slightly higher water temperature. The secondary thermocline at 60 m depth confines together with the upper thermocline a subsurface mixed layer at depth between 45 and 55 m.

In contrast to the austral summer profiles, the surface mixed layer in the austral winter exceeds the depth of 120 m and it is approximately 4°C colder (Fig. 2.2). The fluorescence is homogeneously distributed over the upper 120 m with a weak maximum at about 110 m. A subsurface mixed layer with water temperature of 16°C and low fluorescence is recorded at the depth of 140 to 180 m.

4. APPROACHING FORAMINIFERAL POPULATION DYNAMICS

Most species of planktic foraminifers live in the upper part of the water column (e.g. Oberhänsli et al., 1992). The concentrations of foraminiferal tests collected by plankton tows are usually highest near the sea surface, decreasing with depth to much lower and near constant values (Fig. 2.3). Following Peeters and Brummer (2002) we define the base of the productive zone (Z_{BPZ}) separately for each planktic foraminiferal species at the level where the concentration profile attains an approximately constant value. Below that depth these approximately constant concentrations are considered to represent only the remnant shells settling to the sea floor and are termed export concentration (C_{exp}). Foraminifers towed above the Z_{BPZ} are within the productive zone and compose the standing stock (SS). For a single tow interval the standing stock [# m^{-2}] is given by:

$$SS_i = C_i (Z_i - Z_{i-1}) \tag{1}$$

where C_i is the shell concentration [# m^{-3}] for the interval i, and Z_i and Z_{i-1} are the begin and end depth [m] of the tow interval, respectively (Fig. 2.3a). The value of i ranges from 1 to N, where N is the number of tow intervals within the productive zone. It is not very likely that the Z_{BPZ} match exactly the tow intervals. More probably it is situated within the towed interval at the transition between the export concentration zone and the productive zone, which combines low standing stock of dead specimens sinking to the sea floor and the high pelagic population standing stock measured within the productive zone (Fig. 2.3b):

$$SS_n = C_{\exp}\left(Z_n - Z_{n-1}\right) + C_{n-1}\left(Z_{BPZ} - Z_{n-1}\right) \tag{2}$$

Since the export concentration of certain species in practice often has a near, rather than exactly constant value (e.g. our MARE data and Peeters and Brummer (2002)), we follow Peeters and Brummer (2002) and for C_{exp} take the average concentration below the productive zone. Solving for Z_{BPZ}, equations (1) and (2) yield the depth of the base of the productive zone:

$$Z_{BPZ} = \frac{C_n - C_{\exp}}{C_{n-1}}\left(Z_n - Z_{n-1}\right) + Z_{n-1} \tag{3}$$

The depth integrated entire standing stock within the productive zone is then:

$$SS = \int_{Z_0}^{Z_{BPZ}} C(Z) \cdot dZ = \sum_{i=1}^{n-1} C_i (Z_i - Z_{i-1}) + C_{n-1}(Z_{BPZ} - Z_{n-1}) \tag{4}$$

where Z_{BPZ} and Z_0 are respectively base and top of the productive zone (Fig. 2.3b). We also define the average concentration of the living population C_{liv} as:

$$C_{liv} = \frac{SS}{Z_{BPZ} - Z_0} \tag{5}$$

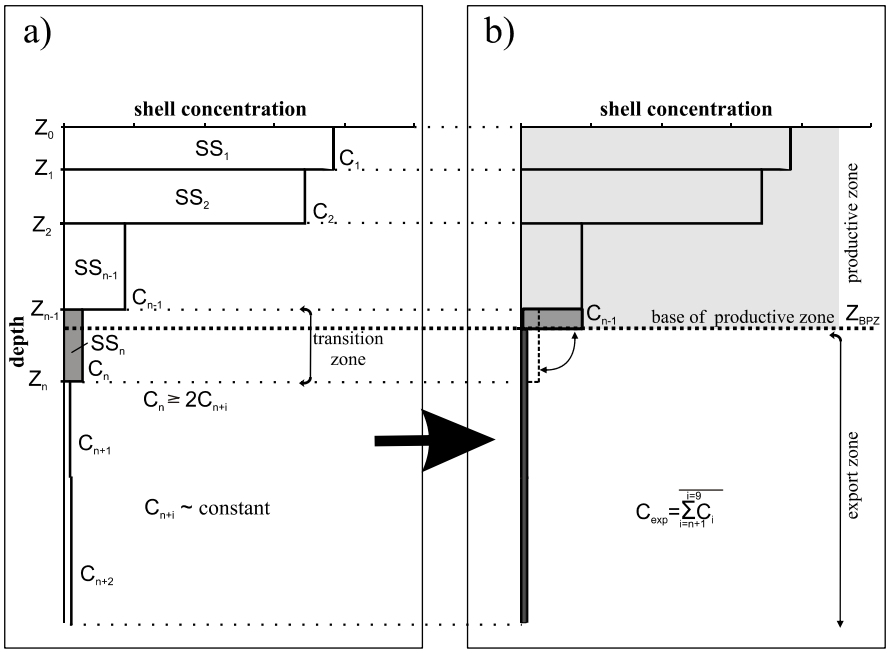

Figure 2.3: A characteristic concentration profile **(a)** with a schematic example for the calculation of the base of the productive zone (Z_{BPZ}), determination of the export concentration (C_{exp}) and the concentration correction for the dead population within the transition interval **(b)**.

In steady-state, the concentration of foraminifera living in the water column and the shell flux towards the sea floor are related by the turnover time (*TT*), i.e. time necessary for the complete renewal of the population. This turnover time can be calculated by dividing the standing stock above Z_{BPZ} by the export flux from the sediment traps (Berger and Soutar, 1967):

$$TT_J = \frac{SS}{J_{\exp}} \tag{6}$$

where TT_J is the turnover time [days], *SS* is the standing stock above the base of the productive zone [# m^{-2}] and J_{exp} is the foraminiferal export flux recorded by the underlying sediment trap [# m^{-2} day^{-1}]. Since the settling velocity of most foraminiferal species is known from e.g. experimental studies of Takahashi and Bé (1984), J_{exp} can also be calculated from the export concentration:

$$J_{\exp} = V_s \cdot C_{\exp} \tag{7}$$

where V_s is the mean settling velocity for a particular foraminiferal species [m day^{-1}]. Combining equations (6) and (7) gives an alternative expression for deciphering the turnover time under steady state conditions via the export concentrations from plankton tows:

$$TT_C = \frac{SS}{C_{\exp} \cdot V_s} \tag{8}$$

5. RESULTS

5.1. Concentration profiles

In total 27 planktic foraminiferal taxa are identified in the analyzed samples. In the February 2000 tow samples (Fig. 2.4a), eight of these taxa, i.e. *Globigerinoides trilobus* s.l.*, Globigerinoides ruber, Globorotalia menardii, Globorotalia truncatulinoides* (sin)*, Globorotalia inflata, Globigerinita glutinata, Orbulina universa* and *Globigerinella siphonifera* account for 98% of the assemblages in the size fraction larger than 150 μm. For the purpose of this study, we analyzed these eight most abundant species also for July 2000 and February 2001. Additionally, the deep-dwelling non-spinose *Globorotalia scitula* and *Globorotalia truncatulinoides* (dex) are considered when present.

Total water column shell concentrations are low in February 2000 and only the shallow-dweller species *G. trilobus* s.l., *G. ruber and G. menardii* reached concentrations higher than 1 # m^{-3} (Fig. 2.4a). These species dominate assemblages composing 84% of the total planktic foraminiferal standing stock (Tab. 2.2). Overall, concentrations are highest within the surface mixed layer (upper 25 m) and decrease rapidly with depth. At approximately 120 m the total shell concentration profile approaches a constant value of 0.6 # m^{-3}.

In contrast to the February 2000 tows, the foraminiferal concentrations, standing stocks and export concentration in July are much higher (Fig. 2.4b). Here eleven species reach a concentration higher than 1 # m^{-3}, with SS higher than 100 # m^{-2}. The non-spinose *G. glutinata, G. truncatulinoides* (sin) and (dex) and *G. inflata* dominate the standing stocks (56%). The foraminiferal production zone is broad and on average much deeper than in summer, for some species exceeding 400 m. The total foraminiferal concentration profile matches the weak bimodal pattern of the fluorescence curve with two maxima in the lower part of the surface mixed layer (Fig. 2.2 and Fig. 2.4b).

In February 2001 overall foraminiferal concentrations have a clear bimodal distribution pattern with maxima within the surface and subsurface mixed layers (Fig. 2.4c). Standing stocks are comparable to February 2000, but with lower concentrations and a deeper productive zone. *G. trilobus* s.l. is again the most abundant species, followed by *G. inflata, G. scitula* and *G. ruber*. Together they constitute 55% of the total standing stock.

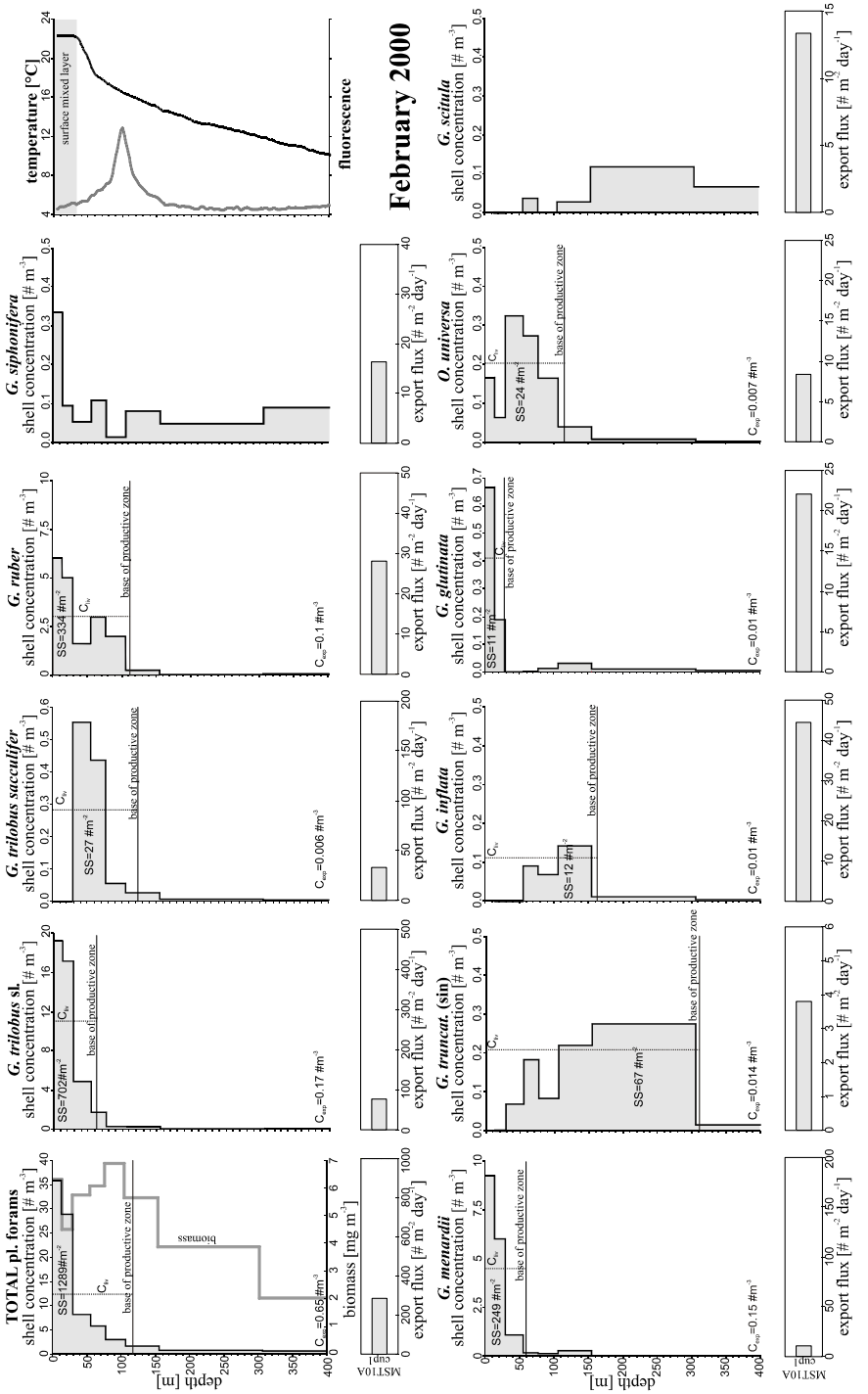
February 2000
TOTAL pl. forams
shell concentration [# m-3]
SS=1289#m-2
Cw
base of productive zone
biomass
Cex=0.65 #m-3
depth [m]
biomass [mg m-3]
export flux [# m-2 day-1]
G. trilobus sl.
SS=702#m-2
Cex=0.17 #m-3
G. truncat. (sin)
SS=67 #m-2
Cex=0.014 #m-3
G. menardii
SS=249 #m-2
Cex=0.15 #m-3
G. trilobus sacculifer
SS=27 #m-3
Cex=0.006 #m-3
G. inflata
SS=12 #m-2
Cex=0.01 #m-3
G. ruber
SS=334 #m-2
Cex=0.1 #m-3
G. glutinata
SS=11 #m-2
Cex=0.01 #m-3
G. siphonifera
O. universa
SS=24 #m-3
Cex=0.007 #m-3
G. scitula
temperature [°C]
surface mixed layer
fluorescence
MST10A
cup

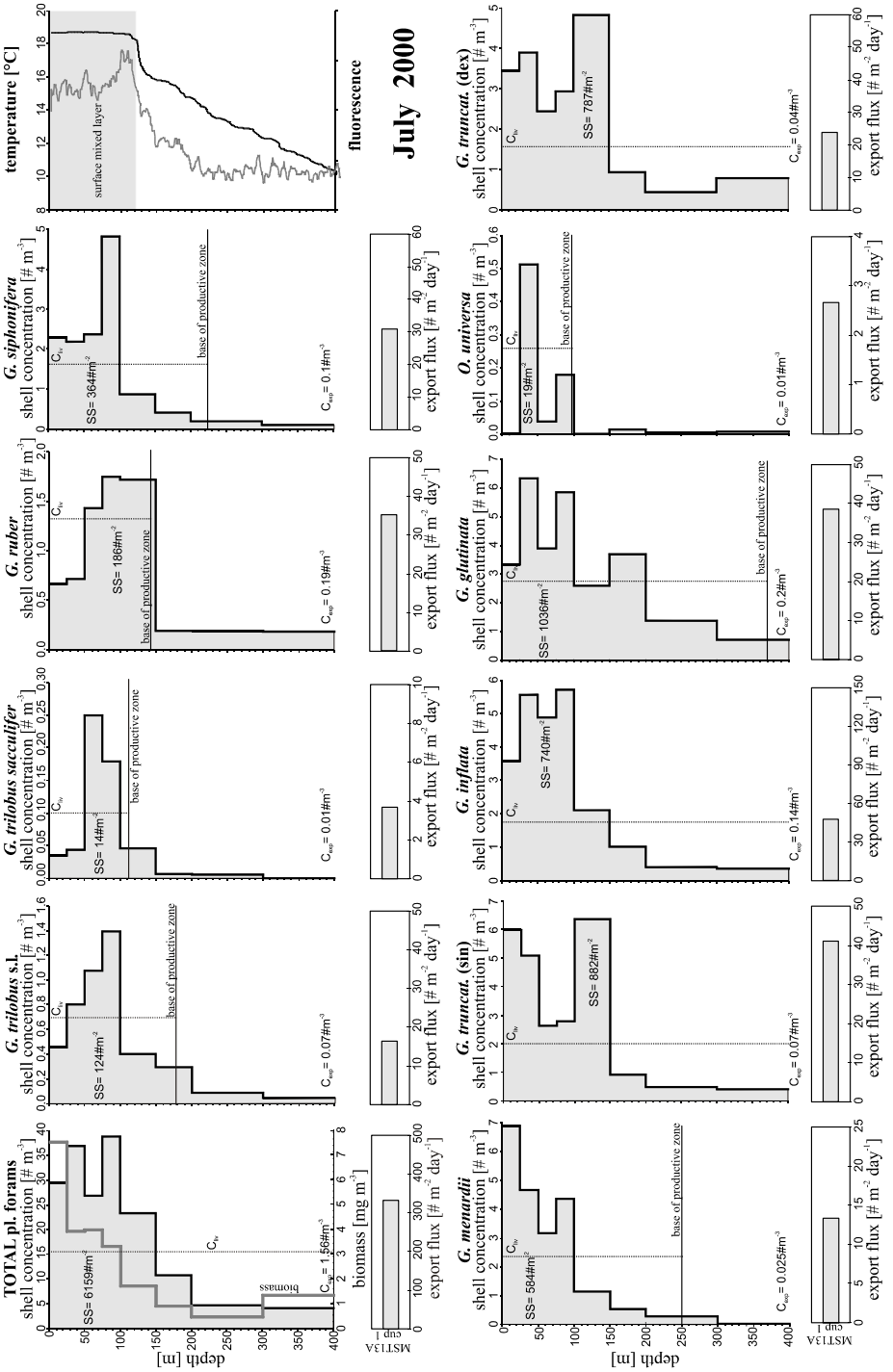
July 2000
temperature [°C]
surface mixed layer
fluorescence
TOTAL pl. forams
G. trilobus s.l.
G. trilobus sacculifer
G. ruber
G. siphonifera
G. truncat. (dex)
G. truncat. (sin)
G. inflata
G. glutinata
O. universa
G. menardii
shell concentration [# m-3]
export flux [# m-2 day-1]
depth [m]
biomass [mg m-3]
MST13A cup 1
SS= 6159#m-2
SS= 124#m-2
SS= 14#m-2
SS= 186#m-2
SS= 364#m-2
SS= 19#m-2
SS= 787#m-2
SS= 1036#m-2
SS= 740#m-2
SS= 882#m-2
SS= 584#m-2
Cw
base of productive zone
biomass
Cexp= 1.56#m-3
Cexp= 0.07#m-3
Cexp= 0.01#m-3
Cexp= 0.19#m-3
Cexp= 0.1#m-3
Cexp= 0.01#m-3
Cexp= 0.04#m-3
Cexp= 0.2#m-3
Cexp= 0.14#m-3
Cexp= 0.07#m-3
Cexp= 0.025#m-3

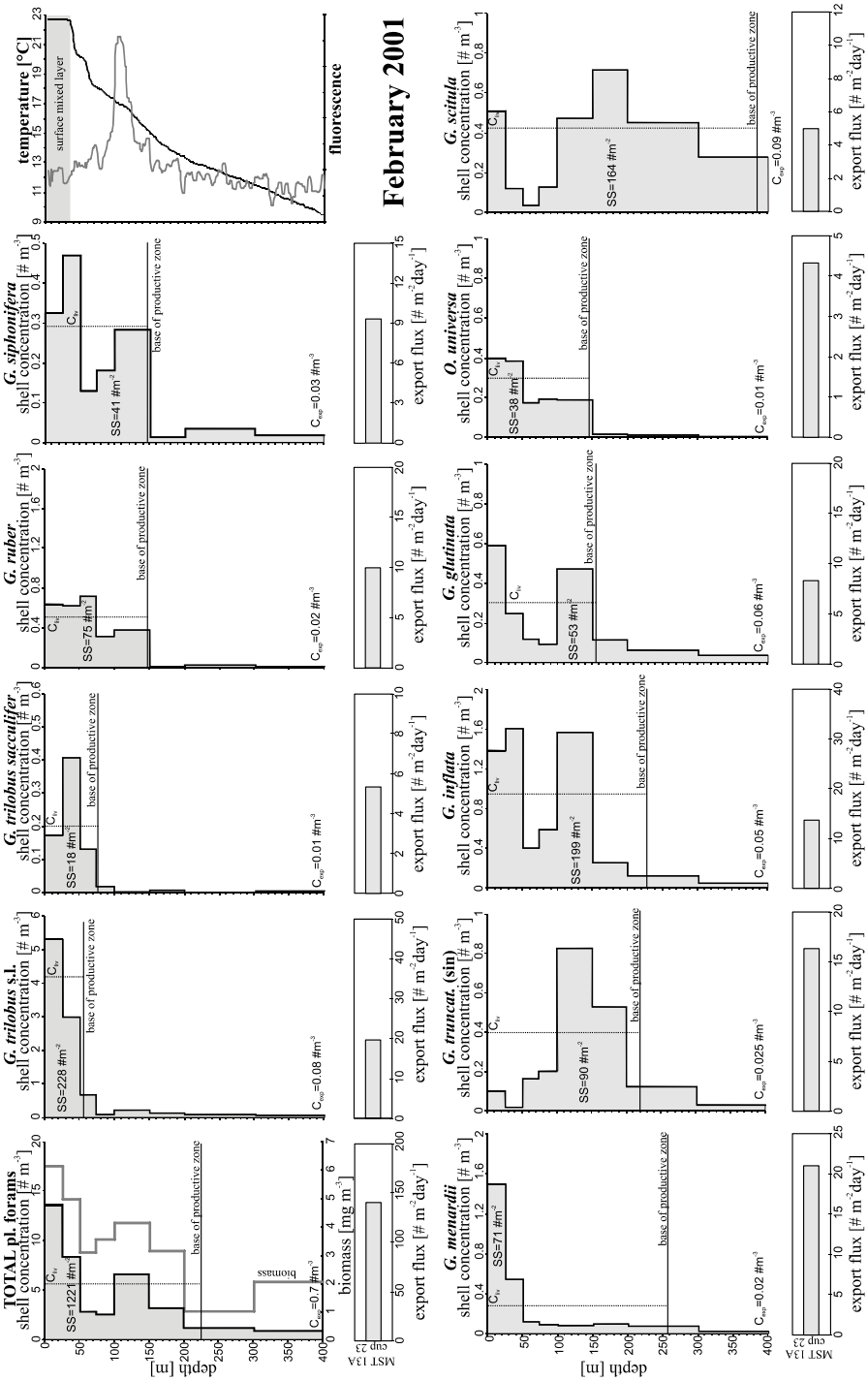
February 2001
TOTAL pl. forams
shell concentration [# m-3]
SS=1221 #m-2
base of productive zone
biomass
Cexp=0.7 #m-3
depth [m]
biomass [mg m-3]
MST 13A
cup 23
export flux [# m-2day-1]
G. trilobus s.l.
SS=228 #m-2
Cexp=0.08 #m-3
G. trilobus sacculifer
SS=18 #m-2
Cexp=0.01 #m-3
G. ruber
SS=75 #m-2
Cexp=0.02 #m-3
G. siphonifera
SS=41 #m-3
Cexp=0.03 #m-3
temperature [°C]
surface mixed layer
fluorescence
G. menardii
SS=71 #m-3
Cexp=0.02 #m-3
G. truncat. (sin)
SS=90 #m-2
Cexp=0.025 #m-3
G. inflata
SS=199 #m-2
Cexp=0.05 #m-3
G. glutinata
SS=53 #m-2
Cexp=0.06 #m-3
O. universa
SS=38 #m-3
Cexp=0.01 #m-3
G. scitula
SS=164 #m-2
Cexp=0.09 #m-3

Figure 2.4 (previous 3 pages): Foraminiferal concentration profiles [#m^{-3}] and export fluxes [#m^{-2}day^{-1}], together with the corresponding CTD temperature and fluorescence profiles. Calculated standing stocks, depth of the productive zone, export concentration and average concentration within the productive zone are also given. Concentrations and fluxes are given for the size fraction larger than 150µm. Export fluxes are calculated from the nearest corresponding sediment trap cups. February 2001 cup precedes plankton towing, as opposed to other two stations. February 2000 cup sampled with a 7-days resolution while other two cups had an 8-days resolution. **a)** February 2000, **b)** July 2000 and **c)** February 2001.

5.2. Export concentrations vs. standing stocks

Figure 2.5 illustrates the relationship between standing stocks and export concentrations for the most abundant species collected at the Walvis Ridge. For the summer stations, characterized by relatively high surface water temperatures, shallow thermoclines and fluorescence maxima below the surface mixed layer, the size of the standing stock seems to be the principal factor controlling the export concentration and a positive correlation between *SS* and C_{exp} is observed. For the winter station, distinguished by a deep thermocline, a lower SST and a fluorescence maximum within the surface mixed layer, two groups of species emerge. One group (*G. truncatulinoides* (sin) and (dex), *G. menardii, G. inflata* and *G. glutinata*) is characterized by high and the other (*G. trilobus trilobus* and *G. ruber*) by low SS/C_{exp} ratios.

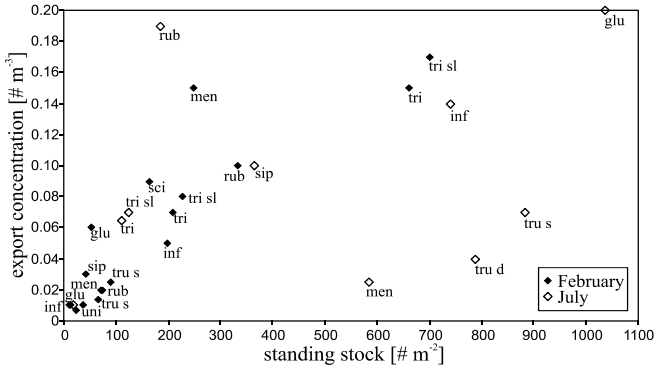

Figure 2.5: Relationship between standing stocks and the corresponding export concentrations for major species from the Walvis Ridge (data in Tab. 2.2).

5.3. Turnover time

Turnover times can be calculated in two independent ways following equation (6) and (8). The average *TT* for the total foraminiferal population ranges from 5 to 19 days (Tab. 2.2). It is short in austral summer and 2-3 times longer in winter.

The warm-water species *G. trilobus* s.l. (Bé and Tolderlund, 1971) shows the most consistent record with only a moderate seasonal variation and just a minor difference between the two calculation approaches (Fig. 2.6). Turnover time ranges between 11 and 16 days in summer and it is shorter in winter, between 6 and 9 days. The separately counted *G. trilobus sacculifer*, the reproductive stage of species *G. trilobus* s.l., distinguished by its sack-like final chamber (Hemleben et al., 1997), has always much shorter *TT* than the juvenile-to-adult form *G. trilobus trilobus* without sack-like final chamber. The average summer turnover time of *G. trilobus sacculifer* is 2±1 days (Tab. 2.2). Another warm-water species, *G. ruber* shows a very similar *TT* trend and range, albeit

with somewhat larger discrepancy between the two approaches for the second summer period. An

Table 2.2: Overview of results for: export concentration (C_{exp}) following principle from figure 2.2, standing stocks (*SS*) following equation (4), base of the productive zone (Z_{BPZ}) following equation (3), average concentration of the living population (C_{liv}) following equation (5), export flux (J_{exp}) as recorded by sediment trap and the turnover time (*TT*). *TT* is calculated by two approaches: via flux following equation 6 (TT_J) and via export concentration following equation 8 (TT_C). In the equation 8, the mean settling velocities for cytoplasm-bearing foraminifers (V_S) gained by experiments of Takahashi and Bé (1984) are used. Maximum and minimum TT_C is based on the mean V_S ± st. dev. For the species where no experimental V_S were available, the V_S of an analogue species (*G. menardii*) are used. The settling velocities at the Walvis Ridge may differ to mean V_S from Takahashi and Bé's experiments due to the possible differences in the mean size/weight ratio. The TT_C for the total foraminiferal assemblages (**) is based on estimated V_S and therefore just illustrative.

species	C_{exp} [# m^{-3}]	Z_{BPZ} [m]	SS [# m^{-2}]	C_{liv} [# m^{-3}]	V_s [m day^{-1}]	J_{exp} [# m^{-2} day^{-1}]	TT_J [day]	TT_C (mean) [day]	TT_C (min) [day]	TT_C (max) [day]	comment
February 2000											
G. trilobus trilobus	0.15	61	662	10.9	274±143	43	15.4	16.1	10.6	33.7	
G. trilobus sacculifer	0.006	123	27	0.3		33	0.8				
G. trilobus s.l.	0.17	62	702	11.3	274±143	76	9.2	15.1	9.9	31.5	
G. ruber	0.1	112	334	3.0	198±94	28	11.9	16.9	11.4	32.1	
G. menardii	0.15	59	249	4.2	1104±22	11	22.6	1.5	1.2	1.9	
G. truncatulinoides (s)	0.014	311	67	0.2	1104±22	4	16.8	4.3	3.6	5.5	V_s for *G. menardii*
G. inflata	0.01	163	12	0.1	504±91	45	0.3	2.5	2.0	2.9	
O. universa	0.007	115	24	0.2	277±144	8	2.8	2.7	8.1	25.8	
G. glutinata	0.01	28	11	0.4	328±26	22	0.5	3.5	3.1	3.6	
TOTAL pl. for.	0.6	115	1289	12.6	400**	286	4.5	5			** estimated V_s
July 2000											
G. trilobus trilobus	0.065	185	111	0.6	274±143	13	8.5	6.2	4.1	13.0	
G. trilobus sacculifer	0.01	111	14	0.1		4	3.8				
G. trilobus s.l.	0.07	179	124	0.7	274±143	17	7.3	6.5	4.2	13.5	
G. ruber	0.19	142	186	1.3	198±94	35	5.3	4.9	3.4	9.4	
G. siphonifera	0.1	223	364	1.6	271±191	31	11.7	13.4	7.9	45.5	
G. menardii	0.025	250	584	2.3	1104±22	13	43.8	21.1	17.5	26.7	
G. truncatulinoides (s)	0.07	441	882	2.0	1104±22	41	21.5	11.4	9.5	14.4	V_s for *G. menardii*
G. inflata	0.14	407	740	1.8	504±91	48	15.5	10.5	8.9	12.8	
O. universa	0.01	97	19	0.3	277±144	3	6.4	6.9	4.6	14.4	
G. glutinata	0.2	373	1036	2.8	328±26	39	26.8	15.8	14.6	17.2	
G. truncatulinoides (d)	0.04	489	787	1.6	1104±22	24	32.8	17.8	14.8	22.5	V_s for G. *menardii*
TOTAL pl. for.	1.56	407	6159	15.1	400**	332	18.6	9.9			** estimated V_s
February 2001											
G. trilobus trilobus	0.07	55	209	3.8	274±143	14	14.6	10.9	7.2	22.8	
G. trilobus sacculifer	0.01	76	18	0.2		5	3.4				
G. trilobus s.l.	0.08	56	228	4.1	274±143	19	12	10.4	6.8	21.8	
G. ruber	0.02	147	75	0.5	198±94	10	7.5	18.8	12.8	36.1	
G. siphonifera	0.03	146	41	0.3	271±191	9	4.4	5	3.0	17.1	
G. menardii	0.02	257	71	0.3	1104±22	21	3.4	3.2	2.7	4.1	
G. truncatulinoides (s)	0.025	219	90	0.4	1104±22	16	5.5	3.3	2.7	4.1	V_s for *G. menardii*
G. inflata	0.05	229	199	0.9	504±91	14	14.5	7.9	6.7	9.6	
O. universa	0.01	147	38	0.3	277±144	4	8.7	13.7	9.0	28.6	
G. glutinata	0.06	155	53	0.3	328±26	8	6.3	2.7	2.5	2.9	
G. scitula	0.09	386	164	0.4		5	32.8				
TOTAL pl. for.	0.7	227	1221	5.4	400**	140	8.7	4.4			** estimated V_s

exactly opposite trend with short summer and long winter *TT* is shown by *G. truncatulinoides, G. menardii, O. universa, G. glutinata* and possibly *G. inflata*. The species *G. menardii, G. truncatulinoides* (sin) and (dex) and *G. glutinata* have on average the longest turnover time of up to 44 days, but the disagreement between the two calculation approaches is also the largest.

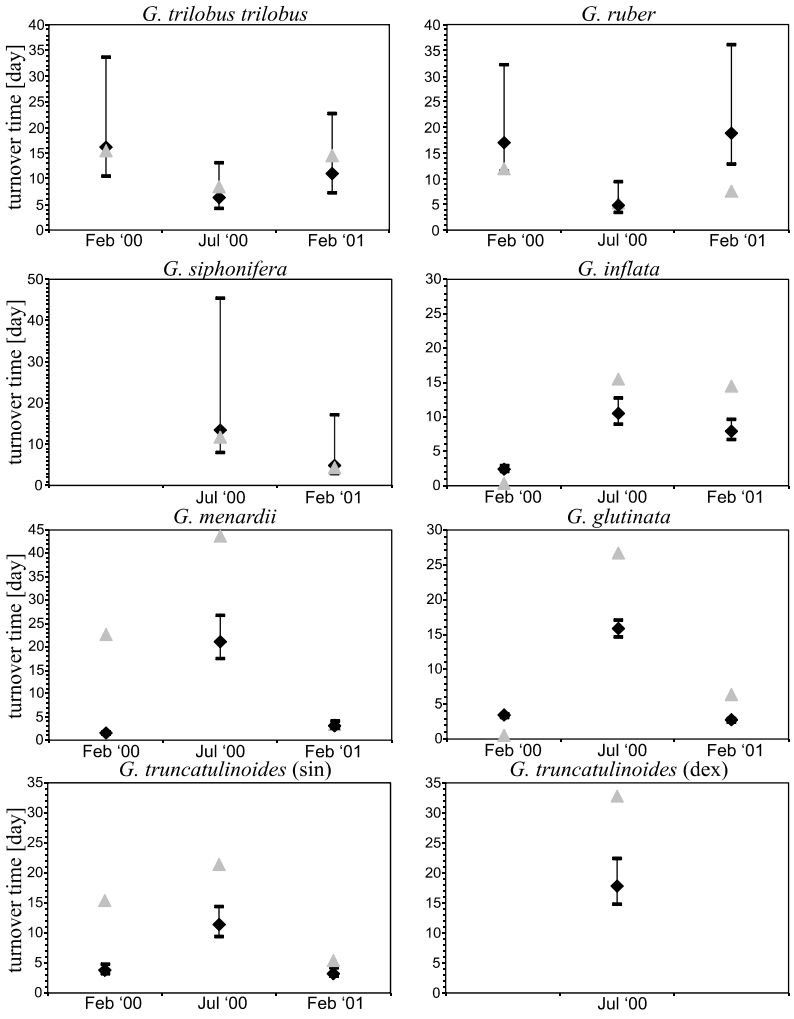

Figure 2.6: Turnover time calculations. Results based on the flux recorded by sediment trap (eq. 6) are given as grey triangles (= TT_J), while black diamonds stay for the calculations based on the C_{exp} (eq. 8) recorded by plankton tows (= TT_C). The error bars refer to TT_C and they are based on the average settling velocity for certain species ± standard deviation, as reported by Takahashi and Bé (1984). The experimental settling velocity of *G. truncatulinoides* was not available, instead V_S of *G. menardii* has been used.

6. DISCUSSION

6.1. Quantifying standing stocks

Peeters and Brummer (2002) proposed fitting of foraminiferal average concentrations by Gaussian distribution to the mid-depth tow interval points, based on their analysis of a set of samples from the Arabian Sea collected with the identical Multinet equipment and a sampling resolution comparable to our study. According to their approach, the base of the productive zone is defined at two standard deviations from the depth of the maximum concentration predicted by curve fitting. The standing stock is calculated as the area under the Gaussian or double Gaussian curve, bordered by the base of the productive zone and the sea surface. This fitting method provides consistent estimates for the base of the productive zone, coinciding approximately with the depth where concentrations approach a constant value. For simple concentration profiles, with a maximum concentration at the surface and a gradual decrease with depth, also estimates of the maximum concentration and standing stock by this approach are the same as for integrating intervals over depth. However, for the more complex profiles, the estimates of standing stocks become less precise as at least 3 and, in case of a double Gaussian distribution, 6 unknown variables need to be determined by fitting through mostly 3 to 4 data points (see figures 10 and 11 in Peeters and Brummer, 2002). We calculated that this Gaussian fitting method may overestimate the standing stocks by up to 30%, compared to the simple summing up of the tow results as defined by equation (4).

Certainly, a small portion of foraminifers within the productive zone, above the transition tow interval (above depth Z_{N-1}, Fig. 2.3) is composed of dead specimens sinking to the sea floor (Schiebel et al., 1995; Peeters and Brummer, 2002). Still, considering the huge difference between C_{exp} and C_{liv} (C_{exp} is one to three orders of magnitude smaller than C_{liv}), such contribution is only significant for the transition interval between the productive zone and the export concentration zone (Fig. 2.3). The full sinking speed is reached within the first 5 cm of settling (Takahashi and Bé, 1984) and therefore it takes only a short time for the dead specimens to settle out of the productive zone. This implies that all foraminifers above depth Z_{N-1} are regarded to be alive at the moment of sampling and that specimens recorded below depth Z_N are regarded as dead (Schiebel and Hemleben, 2000).

6.2. Time scale constraint

Our plankton towing in the upper ocean water column took approximately one hour for the shallow cast (to 100 m) and two to three hours for the deep cast (to 800 m). Takahashi and Bé (1984) experimentally demonstrated for the cytoplasm-filled tests of 10 species that the sinking speed ranges between 200 m day^{-1} (*G. ruber*) and 1100 m day^{-1} (*G. menardii*), for a mean shell diameter between 220 µm (*G. glutinata*) and 660 µm (*G. menardii*). Consequently, shell settling is sufficiently rapid not to cause a significant temporal shift between the sampled depth intervals and the actual size of the standing stock (Schiebel, 2002). However, for the longer-term record obtained by the sediment traps at the depth of 2700 m the sampling resolution of 7 to 8 days and the delay caused by settling do play an important role. Considering the average foraminiferal settling velocity, the depth and duration of the towing and the depth of the sediment trap mooring, we calculated the sinking time for

the average specimen relative to the sea surface (Fig. 2.7). The majority of the specimens will reach 100 m depth within a few hours and 800 m depth within a few days. Thus, the majority of adult empty tests will reach the export concentration zone ($>Z_{BPZ}$) within a few hours at most and represents the state of the foraminiferal population on sub-diurnal time scales. For the deep-dwelling species the sinking time will be even shorter. In contrast, for the sediment trap, due to the greater depth (2700 m for our Walvis Ridge Site) and one-week sampling resolution, the time span covered by a sampling cup will be approximately 3 weeks. Hence, the sediment trap samples that best correspond to the Multinet samples will be those sampled directly after the plankton towing, but they will represent the state of the population in the productive zone only when it had been in steady state for at least three weeks. Comparison of turnover times calculated via fluxes (eq. 6) with those calculated via export concentration (eq. 8) should on one hand reduce the time scale discrepancy for the unsteady population and, on the other hand, provide more control over the reliability of the export concentration at the expense of variable settling velocity.

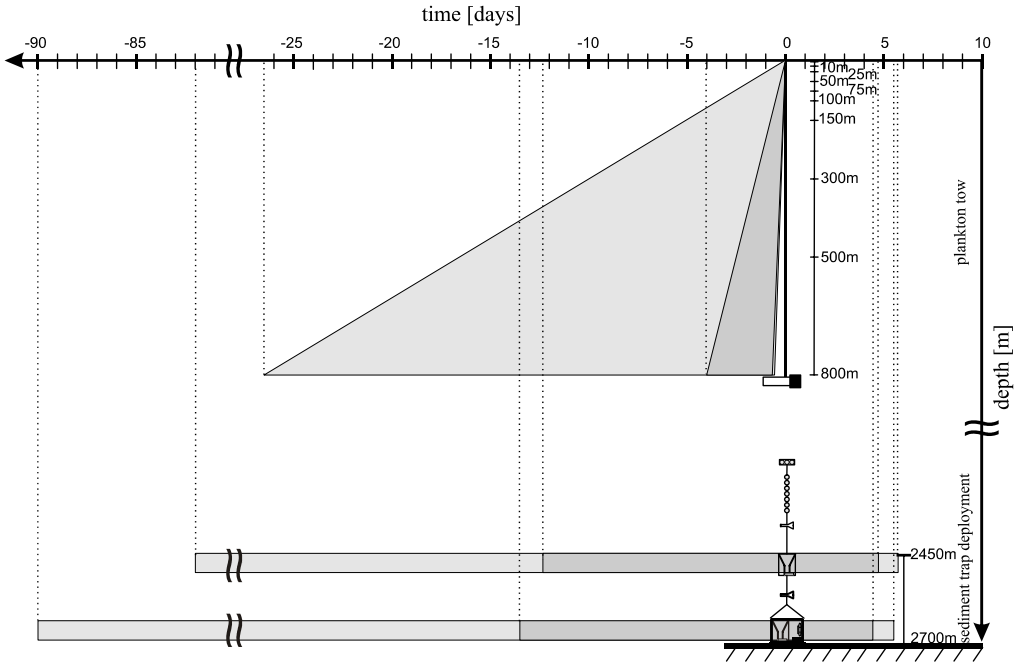

Figure 2.7: Theoretical settling time for the foraminiferal specimens relative to the sea surface. Settling time is calculated from the experimental settling velocities of Takahashi and Bé (1984). In light grey: calculations based on the fastest and slowest reported V_S for the cytoplasm-filled, net-collected specimens (i.e. P-specimens) (min. 30 m day^{-1}; max 1500 m day^{-1}); in dark grey: calculations based on the mean V_S of 10 P-species used in Takahashi and Bé experiments (min. 200 m day^{-1}; max 1100 m day^{-1}). For the sediment trap, the calculations are based on the one-week sampling interval that starts at t = 0.

6.3. Significance of the turnover times

Turnover times calculated from the sediment trap fluxes often match those calculated from the export concentrations (Fig. 2.6). Discrepancy between flux *TT* and export concentration *TT* is observed for some stages of *G. truncatulinoides and G. menardii* and less prominent for *G. ruber* and *G. glutinata*. Differences may be attributed to the temporal flux change during the sediment trap sampling time span and/or inaccuracy in determination of the export concentration. In any case, important is that even when discrepancies between two methods are significant, the trends of the resulting turnover times for both approaches are consistent.

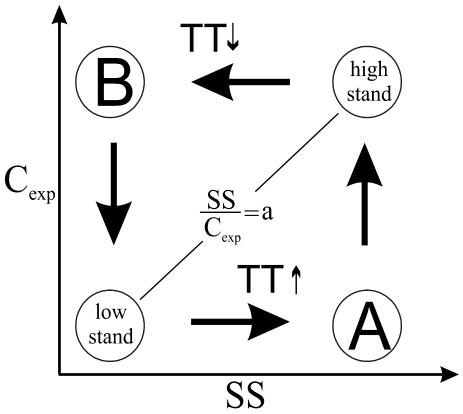

Figure 2.8: *SS/C*$_{exp}$ ratio hypothesis. In the steady state *SS* and *C*$_{exp}$ are in equilibrium and their ratio is constant. Growing population initially results in increased standing stock prior the export concentration increase and consequently a positive offset of the *SS/C*$_{exp}$ ratio (offset towards A). On the other hand decaying (dying) population initially results in increased *C*$_{exp}$ relative to the *SS* and consequently a negative *SS/C*$_{exp}$ offset towards B.

For a foraminiferal population in the steady state, the production of new specimens equals mortality. The turnover time is then the time necessary for the complete replacement of the population by new specimens, as expressed by equation (6) or (8). In nature, any shift from the "low *SS*/low *C*$_{exp}$" steady state to the "high *SS*/high *C*$_{exp}$" steady state will not follow proportionally a linear relationship (Fig. 2.8). Young, growing population will initially not produce a large export flux of adults. Consequently, the calculated turnover time will be longer than for the steady state situation. In contrast, a decaying (dying) population will have relatively low standing stocks compared to the increased number of dead specimens sinking to the sea floor. As a result, the calculated turnover time will be shorter than for the equilibrium. To further asses this hypothesis we considered the foraminiferal population illustrated by a simple logistic model for density-dependent population growth (Hastings, 1997). Density dependence here stands for the processes whose effects change as the number of individuals within the population changes. The population growth is described by the equation 4.12 of Hastings (1997):

$$SS(t) = \frac{SS_0 \cdot e^{rt}}{1 + \frac{SS_0 (e^{rt} - 1)}{K}} \tag{9}$$

assuming that, when the population standing stock is very small, the per capita growth rate is given by *r*, and denoting by *K* the value of the population density at which the per capita growth rate is zero (carrying capacity). In our model the export concentration is linearly dependent on the standing stock with a delay of 5 time units:

$$C_{\exp}(t) = SS_{t-5} \cdot 0.01 \tag{10}$$

The solution of our population dynamics model for *SS* and C_{exp} graphed in figure 2.9 clarifies the hypothetical standing stock/export concentration plot proposed in figure 2.8. The equilibrium turnover time is in the model reached for the targeted SS/C_{exp} low and high stands, while growing and decreasing populations result in significant positive and negative offsets, respectively.

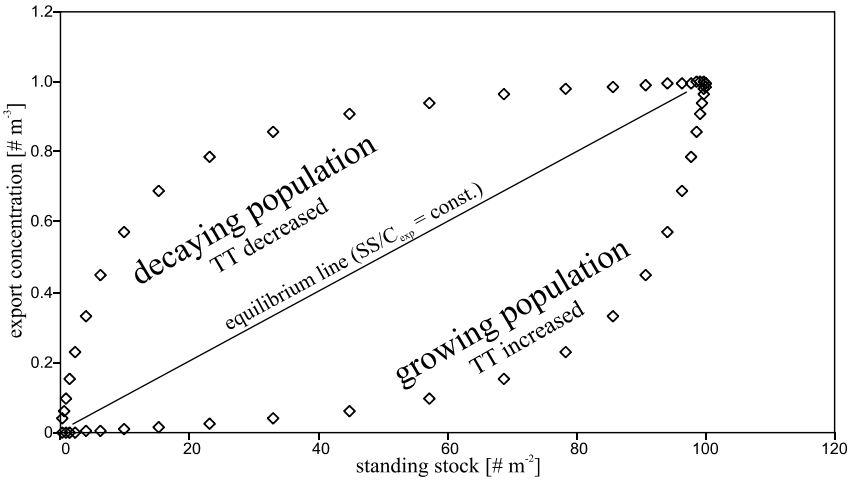

Figure 2.9: Relationship between standing stocks and export concentration for the modeled population growth and decrease according to Hastings (1997), based on equations (9) and (10), with r=±0.5 and K=100. SS/C_{exp} ratio offset from the equilibrium value is indicative for the population dynamics phase, where higher and lower SS/C_{exp} ratio points to the increasing and decreasing population size, respectively.

This implies that the calculated turnover time should be considered as a measure of the population growth state. It may be interpreted as the average foraminiferal life span only for the steady state, when the population is stable, with standing stock, export concentration and flux in the equilibrium. The offset from the equilibrium SS/C_{exp} ratios and the consequent increase or decrease in turnover time are indicative for changes in the foraminiferal population dynamics, i.e. growing or decaying population size.

6.4. Export flux as a steady state indicator

The turnover times for the set of equations, as given above, assume steady state conditions that may not apply for some periods at our Walvis Ridge station. Sediment trap records from different areas (Deuser et al., 1981; Thunell and Reynolds, 1984; Sautter and Thunell, 1991; Ortiz and Mix, 1992 Honjo and Manganini, 1993; Schiebel, 2002) point to the dynamic behaviour and significant temporal changes of the foraminiferal populations. In many cases trap records reveal covariant export fluxes at seasonal or some other frequency. Flux maxima are often short and prominent, followed by longer minima. Although on the one-week time scale foraminiferal population dynamics, as revealed by the export flux, is hardly ever in the perfect steady state, they are closest to that during the flux low-stand.

During the whole sampling period at our study site, the highest flux was recorded in the period from October to November 2000 (Fig. 2.10). That is, at the same time, the period of the strongest flux oscillation. The upper water column was sampled by tows in February 2000, July 2000 and February 2001, at the time of low to moderate total flux oscillations. Next to the low flux oscillations recorded by the sediment trap (Fig. 2.10), a linear relationship between *SS* and C_{exp} (Fig. 2.5) also points to a relatively stable environment and a near steady state conditions for the summer periods. This implies that at least one part of the foraminiferal populations was relative stable at the moment of sampling, and the turnover times calculated from these fluxes should approximate the average species age.

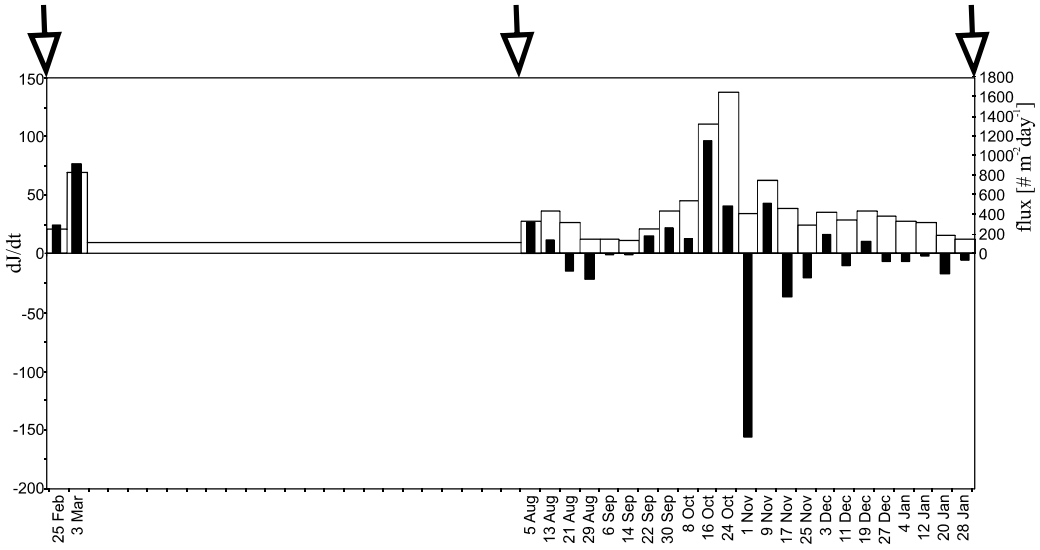

Figure 2.10: Foraminiferal flux record for the size fraction >150 µm (white bars) and the relative temporal flux change dJ/dt (black bars) at the Walvis Ridge study site for the period February 2000 – February 2001. The relative flux change is calculated as $(J_{n+1}-J_n)/t$, where t is the sediment trap sampling resolution and J_n and J_{n+1} are fluxes recorded by the sequential cups. The arrows mark the tow sampling profiles. Since the flux record prior the first mooring deployment was not available and since the first mooring failed to recover the complete record with the 7-days resolution, we used the integrated half-a-year sample from the upper trap moored 250m above sea floor at the same site as a referent J_n in the calculations of the relative flux change for the first cups in two sequences (i.e. cups 25 Feb. and 5 Aug. 2000).

6.5. Turnover times and life span

Our austral summer Walvis Ridge profiles are nearest to a steady state, as indicated by the low oscillation in the total foraminiferal flux and the positively correlated summer SS/C_{exp} ratios of major foraminiferal species. The most consistent results are those of shallow-dwelling spinose species *G. trilobus trilobus* and *G. ruber* and they are interpreted as the average life span of 14±2 and 14±6 days, respectively. *G. trilobus sacculifer*, the reproductive stage of *G. trilobus* s.l., morphologically distinguishable by forming of the sack-like final chamber, has an average life span of 1 to 3 days.

The life span we obtained for *G. trilobus* s.l. does not agree with the ontogeny driven by the lunar cycle that Bijma and Hemleben (1994) reported for this species. The same authors however, also reported that the most immature specimens of this species die prior reaching the reproductive stage. Since we determined the average turnover time of the entire population, the discrepancy between attained results is logical. Our findings do not exclude the possibility that a small portion of the population attains an age of one-month. Hemleben et al. (1987) noted that in the laboratory cultures formation of a sack-like chamber for this species precedes gamete release by 24-48 hours. The summer turnover time of 0.8 to 3.4 days (Tab. 2.2) that we calculated for the reproductive stage, *G. trilobus sacculifer* with sack-like final chamber, confirms those experimental findings.

The average life time span of *G. ruber* obtained in this study is longer than 7.8 days mean survival time reported by Bijma et al. (1990b) in their laboratory experiments. Considering partial ontogeny covered by laboratory experiments and possible exposure to stress conditions during culturing, the longer life span for specimens living in the natural environment is expected.

The longest turnover times of approximately one month are observed for winter populations of the non-spinose and/or deep-dwelling species (*G. menardii*, 32±11 days; *G. truncatulinoides* (dex), 25±7 days; *G. glutinata*, 21±5 days; *G. truncatulinoides* (sin), 17±5 days). Still, due to the less consistent record and possibly the effect of an unsteady population, the calculated winter turnover times for these species are just illustrative and should not directly be considered as the average life spans.

For some species the winter offsets in the SS/C_{exp} ratios may be explained by a (rapid) change in suitability of living conditions as postulated in figure 2.8 and modelled in figure 2.9. The winter conditions, characterized by a deep surface mixed layer with high chlorophyll content and lower SST, are presumably favourable for the majority of non-spinose and deep-dwelling species (higher *SS*). Here in contrast, some spinose shallow-dwellers suffer due to such environmental change or possibly of increased competition (lower *SS*). Unfavourable environmental conditions will result in an increase in export concentration and a standing stock decrease with, as a consequence, a negative offset of SS/C_{exp} ratio (as for *G. trilobus trilobus* and *G. ruber* in winter). On the other hand, the standing stocks respond fast on favourable environmental changes, while the resulting export concentration increase is somewhat delayed. The consequential offset in SS/C_{exp} ratio is then positive. This could be the case for some non-spinose species with high July standing stocks.

Another population dynamics scenario is likely for species that cease to grow in environments near extremes of their distributional range, like suggested by Auras-Schudnagies et al. (1989). Such stagnation periods will be characterized by the semi steady state conditions, with relatively stable SS and low C_{exp} resulting in very long turnover times. We did not find any turnover times that would point to such behaviour.

7. SUMMARY AND CONCLUSIONS

The calculated turnover time should be considered as a measure of the state of foraminiferal population. It may be interpreted as the average foraminiferal life span only for the steady state, when the population is stable regarding the sampling resolution, with standing stock, export concentration and flux in the equilibrium. The offset from the equilibrium SS/C_{exp} ratios and the consequent increase or decrease in turnover time are indicative for changes in the foraminiferal population size, i.e. growing or decaying population.

The spinose, shallow-dwelling species *G. trilobus trilobus* and *G. ruber* show in this study the most reliable records. The calculated summer turnover times of 14±2 days for *G. trilobus trilobus* and 14±6 days for *G. ruber* are consistent, based on relatively high standing stocks and small temporal oscillations of the export fluxes. Therefore these results may be interpreted as the average life spans.

The longest turnover times are recorded for the July populations of non-spinose and/or deep-dwelling species *G. menardii* (32±11 days), dextral *G. truncatulinoides* (25±7 days), *G. glutinata* (21±5 days) and sinistral *G. truncatulinoides* (17±5 days). The discrepant sampling time scales or effect of population growth dynamics however, possibly affect the July results. No evidence is found for any foraminiferal life span longer than 6 weeks and therefore there is no indication for a seasonal or annual reproductive cycle or for periods of long stagnation in the foraminiferal growth.

8. ACKNOWLEDGMENTS

The MARE program (Mixing of Agulhas Rings Experiment) was coordinated and funded by the Clivarnet project of the Netherlands Organization for Scientific Research (NWO - ALW). The captains and crews of R/V Pelagia and Agulhas are thanked for their assistance during the MARE cruises. We thank Frank Peeters and Barbara Donner for helpful suggestions on an earlier version of this manuscript. This work was financially supported by the Netherlands - Bremen Oceanography (NEBROC) program grant to the first author.

REFERENCES

Auras-Schudnagies, A., Kroon, D., Ganssen, G., Hemleben, C. & van Hinte, J.E., 1989. Distributional pattern of planktonic foraminifers and pteropods in surface waters and top core sediments of the Red Sea, and adjacent areas controlled by the monsoonal and other ecological factors. *Deep-Sea Research I, 36* (10): 1515-1533.

Bé, A.W.H. & Tolderlund, D.S., 1971. Distribution and ecology of living planktonic foraminifera in surface waters of the Atlantic and Indian Oceans. In: B.M. Funnel & W.R. Riedel (Eds.), *The Micropaleontology of the Oceans.* Cambridge University Press, Cambridge: pp. 105-149.

Berger, W.H., 1969. Ecologic patterns of living planktonic foraminifera. *Deep-Sea Research I, 16* (169): 1-24.

Berger, W.H. & Soutar, A., 1967. Planktonic foraminifera: Field experiment on production rate. *Science, 156*: 1495-1497.

Bijma, J. & Hemleben, C., 1994. Population dynamics of the planktic foraminifer *Globigerinoides sacculifer* (Brady) from the central Red Sea. *Deep-Sea Research I, 41* (3): 485-510.

Bijma, J., Erez, J. & Hemleben, C., 1990a. Lunar and semi-lunar reproductive cycles in some spinose planktonic foraminifers. *Journal of Foraminiferal Research, 20*: 117-127.

Bijma, J., Faber Jr., W.W. & Hemleben, C., 1990b. Temperature and salinity limits for growth and survival of some planktonic foraminifers in laboratory cultures. *Journal of Foraminiferal Research, 20* (2): 95-116.

Deuser, W.G., Ross, E.H., Hemleben, C. & Spindler, M., 1981. Seasonal changes in species composition, numbers, mass, size and isotopic composition of planktonic foraminifera settling into the deep Sargasso Sea. *Palaeogeography, Palaeoclimatology, Palaeoecology, 33*: 103-127.

Deuser, W.G. & Ross, E.H., 1980. Seasonal change in the flux of organic carbon to the deep Sargasso Sea. *Nature, 283*: 364-365.

Duplessy, J.-C., Blanc, P.-L. & Bé, A.W.H., 1981. Oxygen-18 enrichment of planktonic foraminifera due to gametogenic calcification below the euphotic zone. *Science, 213* (4513): 1247-1250.

Griffiths, F.B., Brown, G.H., Reid, D.D. & Parker, R.R., 1984. Estimation of sample zooplankton abundance from Folsom splitter sub-samples. *Journal of Plankton Research, 6* (5): 721-731.

Hastings, A., 1997. *Population biology: concepts and models.* Springer-Verlag, New York: 220 pp.

Hemleben, C., Spindler, M. & Anderson, O.R., 1989. *Modern Planktonic Foraminifera.* Springer-Verlag, New York: 363 pp.

Hemleben, C., Spindler, M., Breitinger, I. & Ott, R., 1987. Morphological and physiological responses of *Globigerinoides sacculifer* (Brady) under varying laboratory conditions. *Marine Micropaleontology, 12*: 305-324.

Hemleben, C. & Spindler, M., 1983. Recent advances in research on living planktonic foraminifera. In: J.E. Meulenkamp (Ed.), *Reconstruction of marine paleoenvironments.* Utrecht Micropaleontological Bulletins, Utrecht: pp. 141-170.

Honjo, S. & Manganini, S.J., 1993. Annual biogenic particle fluxes to the interior of the North Atlantic Ocean; studied at 34°N 21°W and 48°N 21°W. *Deep-Sea Research II, 40* (1-2): 587-607.

Lutjeharms, J.R.E. & Stokton, P.L., 1987. Kinematics of Southern Africa's upwelling front. In: A.I.L. Payne, J.A. Gulland & K.H. Brink (Eds.), *The Benguela and comparable ecosystems.* South African Journal of Marine Science. Sea Fisheries Research Institute, Cape Town: pp. 35-49.

Oberhänsli, H., Bénier, C., Meinecke, G., Schmidt, H., Schneider, R. & Wefer, G., 1992. Planktonic foraminifers as tracers of ocean currents in the eastern South Atlantic. *Paleoceanography, 7* (5): 607-632.

Ortiz, J.D., Mix, A.C. & Collier, R.W., 1995. Environmental control of living symbiotic and asymbiotic foraminifera of the California Current. *Paleoceanography, 10* (6): 987-1009.

Ortiz, J.D. & Mix, A.C., 1992. The spatial distribution and seasonal succession of planktonic foraminifera in the California Current off Oregon, September 1987 - September 1988. In: C.P. Summerhayes, W.L. Prell & K.C. Emeis (Eds.), Upwelling systems: evolution since the Early Miocene. Geological Society Special Publications, London: pp. 197-213.

Peeters, F.J.C. & Brummer, G.-J.A., 2002. The seasonal and vertical distribution of living planktic foraminifera in the NW Arabian Sea. In: P.D. Clift, D. Kroon, C. Gaedicke & J. Craig (Eds.), The tectonic and climatic evolution of the Arabian Sea region. Geological Society Special Publications, London: pp. 463-497.

Peterson, R.G. & Stramma, L., 1991. Upper-level circulation in the South Atlantic Ocean. *Progress in Oceanography, 26* (1): 1-73.

Sautter, L.R. & Sancetta, C., 1992. Seasonal associations of phytoplankton and planktic foraminifera in an upwelling region and their contribution to the seafloor. *Marine Micropaleontology, 18*: 263-278.

Sautter, L.R. & Thunell, R.C., 1991. Planktonic foraminiferal response to upwelling and seasonal hydrographic conditions: sediment trap results from San Pedro Basin, Southern California Bight. *Journal of Foraminiferal Research, 21* (4): 347-363.

Schiebel, R., 2002. Planktic foraminiferal sedimentation and the marine calcite budget. *Global biogeochemical cycles, 16* (4): 1065, doi:10.1029/2001GB001459.

Schiebel, R., Waniek, J., Bork, M. & Hemleben, C., 2001. Planktic foraminiferal production stimulated by chlorophyll redistribution and entrainment of nutrients. *Deep-Sea Research I, 48* (3): 721-740.

Schiebel, R. & Hemleben, C., 2000. Interannual variability of planktic foraminiferal populations and test flux in the eastern North Atlantic Ocean (JGOFS). *Deep-Sea Research II, 47* (9-11): 1809-1852.

Schiebel, R., Bijma, J. & Hemleben, C., 1997. Population dynamics of the planktic foraminifer *Globigerina bulloides* from the eastern North Atlantic. *Deep-Sea Research I, 44* (9-10): 1701-1713.

Schiebel, R., Hiller, B. & Hemleben, C., 1995. Impacts of storms on recent planktic foraminiferal test production and $CaCO_3$ flux in the North Atlantic at 47°N, 20°W (JGOFS). *Marine Micropaleontology, 26*: 115-129.

Sell, D.W. & Evans, M.S., 1982. A statistical analysis of subsampling and an evaluation of Folsom plankton splitter. *Hydrobiologia, 94* (3): 223-230.

Shannon, L.V. & Nelson, G., 1996. The Benguela: large scale features and processes and system variability. In: G. Wefer, W.H. Berger, G. Siedler & D.J. Webb (Eds.), *The South Atlantic: Present and past circulation.* Springer-Verlag, Berlin, Heidelberg: pp. 163-210.

Takahashi, K. & Bé, A.W., 1984. Planktonic foraminifera: factors controlling sinking speed. *Deep-Sea Research I, 31* (12A): 1477-1500.

Thiede, J., 1975. Distribution of foraminifera in surface waters of a coastal upwelling area. *Nature, 253*: 712-714.

Thunell, R. & Sautter, L.R., 1992. Planktonic foraminiferal fauna and stable isotopic indices of upwelling: a sediment trap study in the San Pedro Basin, Southern California Bight. In: C.P. Summerhayes, W.L. Prell & K.C. Emeis (Eds.), *Upwelling systems: evolution since the Early Miocene.* The Geological Society Special Publications, London: pp. 77-91.

Thunell, R.C. & Reynolds, L.A., 1984. Sedimentation of planktonic foraminifera: Seasonal changes in species flux in the Panama Basin. *Micropaleontology, 30* (3): 243-262.

Wiebe, P.H. & Benfield, M.C., 2003. From the Hensen net toward four-dimensional biological oceanography. *Progress in Oceanography, 56*: 7-136.

Bonaca u predvečerje

More ko žena miče pločice svojih dragulja,
u sjeni jedra čipkastu pjenu plete.
Blistaju zelenomodre, žute i sive facete,
Drveno rebro lađe voda usnom ljulja

Na dnu u tmini sivog morskog mulja
potopljene stvari miču se i svijete.
Nad zrcalom modrim bijele ptice lete.
voda je teška ko kružnica ulja.

Iz dimnjaka lađe pramen čađe kulja,
cvrči na ognju riba; vonj smole i joda.
Titraju jegulje svjetla, gluha i nijema voda.

Na pučini jedro, lik rumena broda
i ticalo bijelo svjetionika.
Pod palubom oganj. Smijeh. Harmonika.

Miroslav Krleža (1893-1981)

3. Lunar cycles and seasonal variations in deposition fluxes of planktic foraminiferal shell carbonate to the deep South Atlantic (central Walvis Ridge)

Neven Lončarić, Geert-Jan A. Brummer & Dick Kroon

ABSTRACT

Several authors have argued that lunar reproductive cycling controls the shell fluxes of planktic foraminifera, one of the major carbonate-producing groups in the global pelagic ocean. A time-series sediment trap at 2700 m depth on the central Walvis Ridge below the South Atlantic central gyre demonstrate for the first time that shell deposition fluxes of *Hastigerina pelagica* are synchronous with lunar periodicity. Spectral analysis of the 6-month time-series with 8-day resolution showed a strong 30-day cyclicity in the flux maxima of *H. pelagica* arriving at the ocean floor on average 12.5 days after each full moon. Given a shell settling velocity of about 400 m day^{-1}, which implies about seven days for settling, this coincides with the pronounced endogenous reproduction rhythm of 5 ± 2 days after full moon as originally observed in laboratory cultured isolates from off Bermuda in the North Atlantic. By contrast, no endogenous or exogenous lunar periodicity was observed in the deposition flux or size distribution of any of the 27 other shell species from austral winter (August 2000) to austral summer (February 2001). Instead, the deposition fluxes of shell species, the bulk carbonate and the total mass were dominated by a seasonal maximum during austral spring, without any periodicity in the 16 to 90 day domain of this study. Since *H. pelagica* exhibits low fluxes with a low burial efficiency, and continuous (re)production is shown by the deposition fluxes of other species, lunar reproductive cycling appears not to affect pelagic carbonate productivity and deep ocean sedimentation fluxes.

1. INTRODUCTION

In their pioneering work, Spindler et al. (1979) documented for the first time a lunar cycle in the reproduction strategy of planktic foraminifera, one of the major carbonate producing groups. In

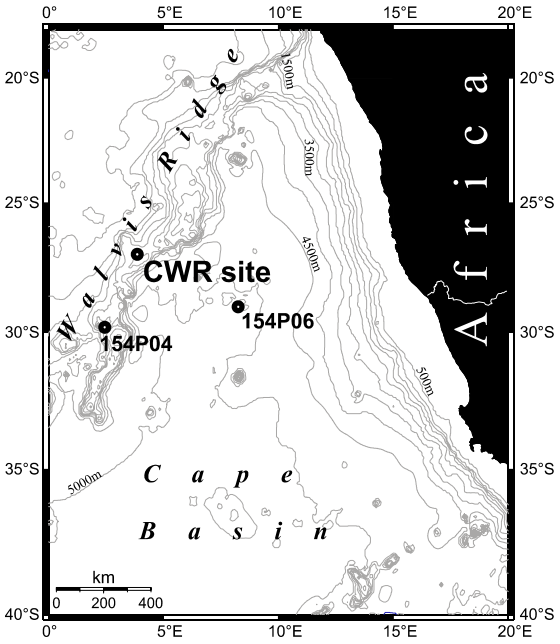

Figure 3.1: Study site location and regional bathymetry. The sediment trap was deployed at the CWR site. Plankton tows were made at all three given sites (map created using OMC at www.aquarius.geomar.de).

laboratory cultures of *H. pelagica* collected off Bermuda they showed that endogenous lunar forcing plays a dominant role in the reproductive behaviour of this species. Maximum gametogenesis of *H. pelagica* appeared to be tuned to the 29.5-day synodic cycle and occurred 5 ± 2 days after full moon for 85.4% of the culture population. Subsequent work did not disclose such endogenous forcing in a number of other species kept in laboratory culture, but this did not rule out that exogenous forcing might exist. Considerable effort was directed towards assessing lunar reproductive cycling in other species of planktic foraminifera (Hemleben et al., 1989) and its importance for foraminiferal population dynamics and carbonate flux patterns (Bijma et al., 1994). Among other authors, Bijma et al. (1990), Erez et al. (1991), Schiebel et al. (1997), Volkmann (2000) and Kawahata et al. (2002) inferred (semi-) lunar reproductive cycling for several planktic foraminiferal species from time-series plankton tows and sediment traps.

Yet, whether exogenous or endogenous, lunar oscillations have not been recognised in the field as readily as they were observed for the endogenous lunar cycle of *H. pelagica* in cultures. This seems due mainly to the non-lunar variability in population abundance and size-frequency distribution that may fully obscure the lunar signal, but also to methodological constraints inherent to the time-series sampling, e.g., the temporal resolution and spatial scatter of the available data. Ambiguities remain with respect to the proportion of the population involved, the actual timing of (semi-) lunar reproduction and the potentially associated depth migration (cf. Bijma et al., 1990; Erez et al., 1991; Kawahata et al., 2002). Moreover, these superimpose an important source of temporal variation on the spatial distribution patterns of living species and their calcification depths, which is difficult to constrain when long sampling transects across ecological and physical gradients interfere with the lunar phases (Ottens, 1991; Volkmann, 2000). Therefore, the importance of synchronised reproduction for the foraminiferal standing stocks, export and depositional fluxes needs to be clarified. Although lunar cycling is a potential driving mechanism of carbonate fluxes, variability might be more dependent on the seasonal export productivity from upper ocean waters. In this study, we aim to resolve which factor is the most important, using a high-resolution sediment trap time-series on the 2700 m deep central Walvis Ridge. Shell fluxes, species size distribution and proportion of reproductive features are examined in order to establish the effect of lunar cycling on carbonate fluxes in the South Atlantic subtropical gyre.

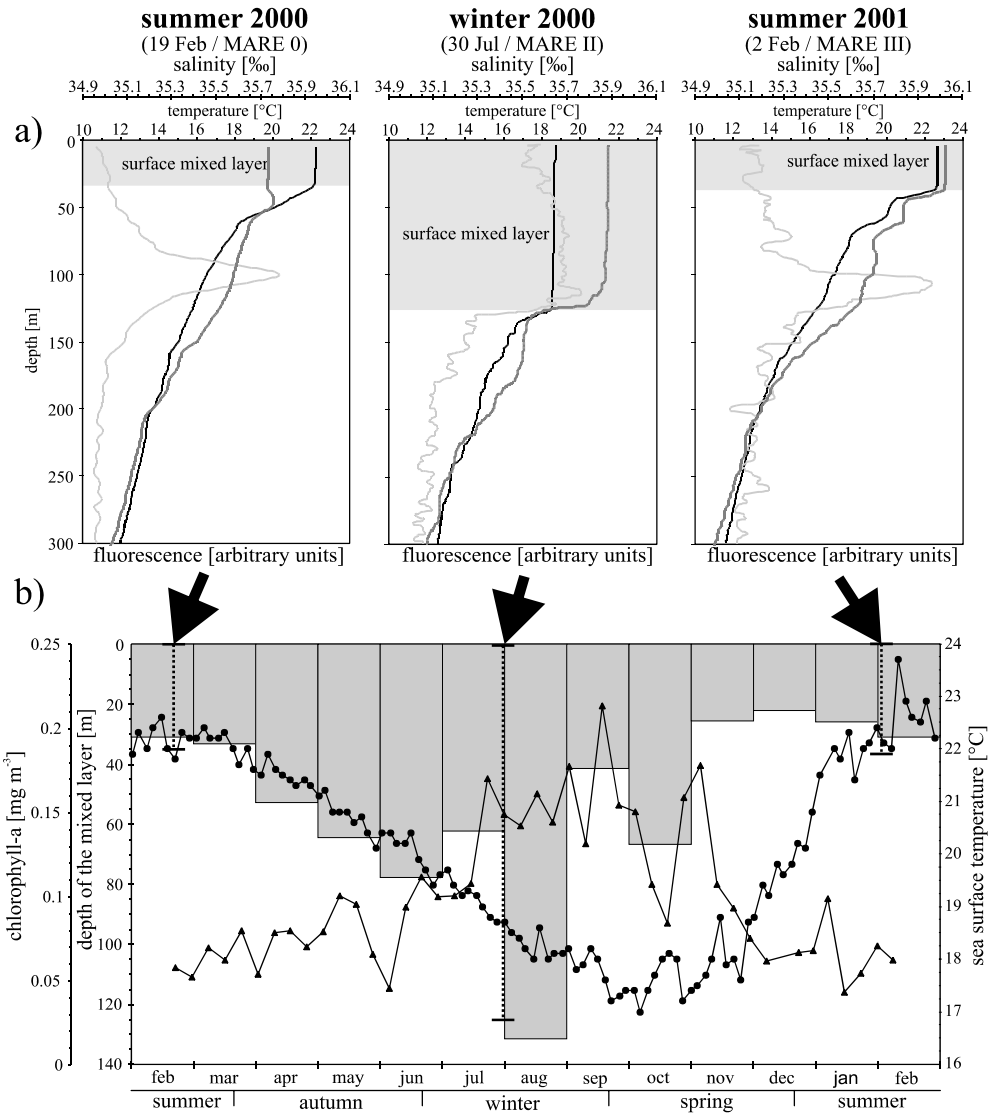

Figure 3.2: (a) Water column profiles of temperature (black; °C) and fluorescence (grey; arbitrary units) in the upper 300m taken at the CWR site. Shaded area represents the surface mixed layer. **(b)** Sea surface temperature - dots (NOAA) and chlorophyll-a concentration - triangles (SeaWiFS) at the CWR site from February 2000 to February 2001. Vertical grey bars represent monthly mean depth of the surface mixed layer extracted from http://ingrid.ldeo.columbia.edu/SOURCES/Levitus (Levitus and Boyer, 1994). Vertical dashed lines mark moments of CTD and plankton tow sampling. The length of the dashed lines corresponds to the in-situ measured surface mixed layer depths from (a). The CWR sediment trap time series covers the period from August 2000 until February 2001.

2. MATERIAL AND METHODS

During the Mixing of Agulhas Rings Experiment (MARE), a Technicap PPS5 sediment trap with sampling area of 1 m^2 and equipped with an automated sampling carousel was deployed two meters above the ocean floor of the central Walvis Ridge (SE Atlantic) at a water depth of 2700 m (Fig. 3.1). The trap sampled the settling particle flux prior to deposition on the sea floor with a 8-day sampling resolution from August 2000 till February 2001 at 27°00' S, 3°51' E. During the MARE cruises in 2000 and 2001, a number of CTD-rosette profiles were taken to characterize in-situ water column properties (Fig. 3.2). In addition, a complementary set of plankton tow samples from the upper 800 m of the water column was collected by a modified, obliquely towed Hydrobios Multinet system equipped with 5 plankton nets (mesh 100 μm) and on-line flow meters (Peeters et al., 2002). Planktic foraminiferal census counts were made separately for two size fractions, 150-250 and >250 μm. We separately counted *Globigerinoides trilobus* with and without a sac-like final chamber.

For the spectral analyses, the integrated 8-day fluxes derived from the individual sediment-trap cups were attributed to the middle of each sampling interval and, after linear integration, analysed using the AnalySeries computer program (Paillard et al., 1996). The spectral analyses were done by the Blackman-Tukey and Fast Fourier Transform algorithms. The Tukey window was used for data filtering in both cases. Our sediment-trap record covers six entire lunar cycles, each defined by three to four 8-day sample intervals. Thus, the wavelength of the critical Nyquist frequency equals 16 days, i.e. the highest frequency that can be estimated from a discrete, equally spaced record whose wavelength is exactly two distances between successive observations (Davis, 1986). Since this is far below the 29.5-day synodic cycle, this time-series record is well suited for spectral analysis of lunar oscillations in shell carbonate deposition fluxes.

3. OCEANOGRAPHIC SETTING

The central Walvis Ridge is situated below the eastern limb of the South Atlantic Subtropical Gyre, which forms the oceanic flank of the Benguela Current (Peterson and Stramma, 1991). MARE in situ observations (Fig. 3.2a) and remote sensing (Fig. 3.2b) show predominantly oligotrophic surface water conditions, with increased chlorophyll content at the end of winter (mid July - September) and in mid spring (end of October). Sea-surface temperature increased from 17°C in austral winter, when the surface mixed layer was deep, to 23°C in the shallow mixed layer during austral summer. The trap site is situated well outside the range of filaments of upwelled water that occasionally penetrate oceanwards from the Benguela upwelling system (Lutjeharms and Stockton, 1987; Shannon and Nelson, 1996). For the entire period of sampling, radar altimetry imaging (TOPEX/Poseidon) did not show any perturbations by passing Agulhas rings, i.e. meso-scale eddies of warm-core Indian Ocean waters, which occasionally cross the Walvis Ridge from the proximate Cape Basin (Lutjeharms, 1996; Schouten et al., 2000, 2002). Overall, hydrographic observations are

consistent with a typical subtropical ocean gyre system with strictly seasonal variability, without intermittent and infra-seasonal disruption.

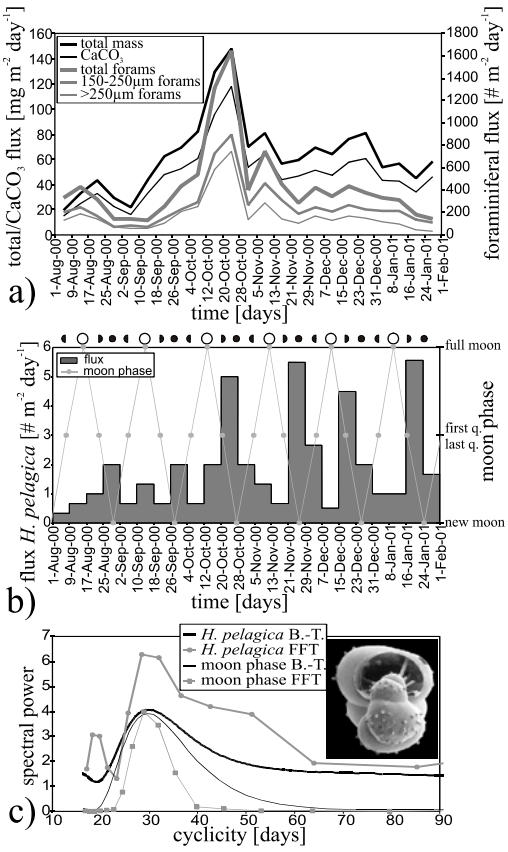

Figure 3.3: Deposition flux of foraminifera, calcium carbonate and total mass **(a)**, and *H. pelagica* (dark grey bars) vs. phases of the moon (light grey line) **(b)** from August 2000 to February 2001 recorded at 2700m by the Walvis Ridge sediment trap. Chart **(c)** presents spectral analysis of the *H. pelagica* flux (Blackman-Tukey in black; Fast Fourier Transform in grey) vs. spectral analysis of the moon phases.

4. RESULTS

Strong lunar cyclicity with a dominant 30-day cycle component was observed in *H. pelagica* despite low fluxes of only 0.3 to 5.6 shells m^{-2} day^{-1} (Fig. 3.3). A repetitive flux maximum arrived on average 12.5 days after full moon at the 2700 m-deep central Walvis Ridge, most prominently during austral spring/summer. On average, lunar maxima in shell deposition flux are 6.5 times higher than in the adjoining lunar minima, varying by a factor of 3 to 9 in lunar amplitude across the time-series. Seasonal variability is relatively small, as average spring/summer fluxes are approximately two times higher than during winter. By contrast, no other species in the time-series showed any cyclicity on the wavelengths between 16 to 90 days that are consistent with the critical Nyquist frequency (Fig. 3.4). Furthermore, the ratios of the separately counted coarse (>250 µm) versus fine (150-250 µm) size fractions reveal no oscillations with a lunar periodicity either. Instead, all other species show a short and prominent spring maximum in shell deposition fluxes, as did the bulk carbonate and total mass fluxes (Fig. 3.4).

Except for *H. pelagica*, the only other flux record that seems to vary on a lunar frequency is the proportion of sac- and non sac-bearing morphotypes of *G. trilobus*, albeit only for the last four months and with a weak 42-day periodicity (Fig. 3.5). A composite of plankton tows collected at subsequent stages of the moon cycle at the CWR site and surroundings showed that sac-bearing *G. trilobus* is present in all depth profiles (Fig. 3.6). They occurred in low concentrations in the surface-most depth interval and in enhanced concentrations within or near the thermocline and the deep chlorophyll maximum, at water depths between 25 and 100 m. The morphotypes without a sac-like chamber were always predominant and, with the exception of one profile, showed maximum concentrations shallower than sac-bearing specimens.

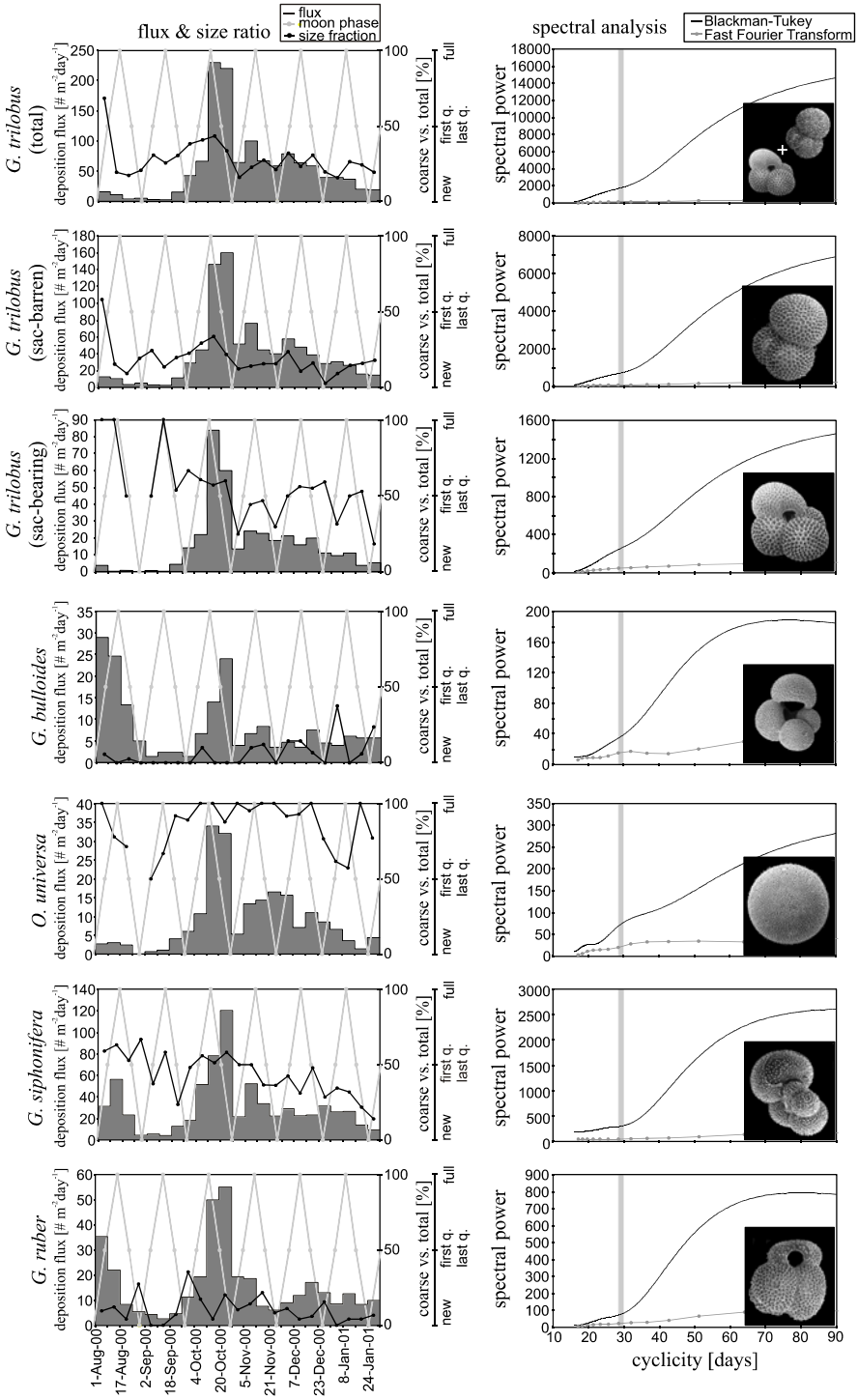
flux & size ratio
flux
moon phase
size fraction
spectral analysis
Blackman-Tukey
Fast Fourier Transform
G. trilobus (total)
G. trilobus (sac-barren)
G. trilobus (sac-bearing)
G. bulloides
O. universa
G. siphonifera
G. ruber
deposition flux [# m-2day-1]
coarse vs. total [%]
new
first q.
last q.
full
spectral power
cyclicity [days]
1-Aug-00
17-Aug-00
2-Sep-00
18-Sep-00
4-Oct-00
20-Oct-00
5-Nov-00
21-Nov-00
7-Dec-00
23-Dec-00
8-Jan-01
24-Jan-01

Figure 3.4 (previous page): Deposition flux and the size ratio (fraction >250µm vs. >150µm) of other major species for which gametogenesis with (semi-) lunar frequency has been previously suggested. Associated spectral analyses are given in the right charts. Synodic cyclicity of *H. pelagica* (vertical grey bar) is given for comparison. Results of species *G. trilobus* are given separately for morphotypes with and without sac-like final chamber as well as for the total population.

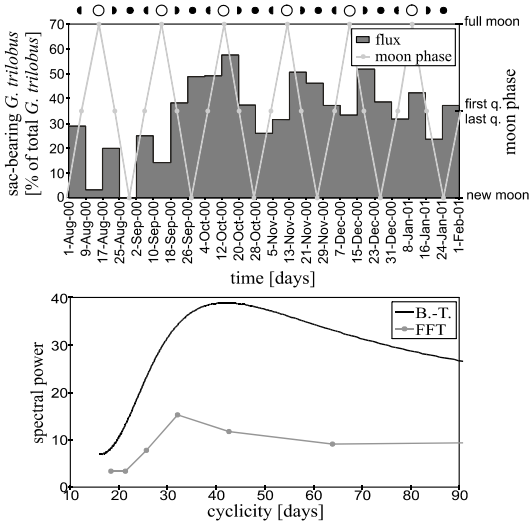

Figure 3.5: Ratio of *G. trilobus* morphotypes (sac-bearing/total * 100) given relative to the phases of the moon. The spectral analysis is performed just for the last four months of the record, covering the period from 26th September 2000 to 1st February 2001, and shows weak 41.8-day cyclicity (Blackman-Tukey algorithm).

5. DISCUSSION

In the life cycle of planktic foraminifera, a major group of pelagic carbonate producers (e.g. Schiebel and Hemleben, 2000), the parental life ends upon reproduction and its calcite shell sinks to the ocean floor (Hemleben et al., 1989). Thus reproductive strategies directly relate pelagic carbonate production in the upper ocean to shell deposition fluxes on the deep ocean floor. Although yet poorly constrained, coccolithophorid prymnesiophyte algae increasingly appear a less dominant contributor to global carbonate fluxes than previously considered (e.g. Westbroek et al., 1993). Modern estimates of the global foraminiferal carbonate flux range up to 1.3 to 3.2 Gt year^{-1}, which would make planktic foraminifera the largest contributor to the global carbonate flux (5.7 Gt year^{-1}) in open marine systems (Schiebel, 2002). Though the carbonate budget in these calculations may be overestimated (Feely et al., 2004), this is consistent with the strong infra-annual co-variability we observed in the deposition fluxes of foraminiferal shells (>150 µm, >250 µm), bulk carbonate and total mass (Fig. 3.3), as well as with the low preservation potential of coccolith carbonate on the central Walvis Ridge (Böckel and Baumann, 2004).

In a model study Bijma et al. (1994) showed that the shell carbonate export flux of planktic foraminifera would be greatly affected by synchronised lunar reproduction, thus providing a driving mechanism behind temporal variability in both plankton distribution and deep-sea shell carbonate fluxes. As a reproductive strategy, time- and depth-synchronised gamete release would increase the probability of gamete fusion in the oceanic water column (e.g. Bijma et al., 1990, 1994; Erez et al., 1991). Here, the lunar cycle provides an obvious external tuning for reproductive behaviour or may otherwise be of adaptive significance as is commonly encountered in coastal, benthic communities (e.g. Omori, 1995). Spindler et al. (1979) first recognised an endogenous reproductive cycle for an oceanic organism. In individual laboratory cultures of *H. pelagica*, they observed a maximum in

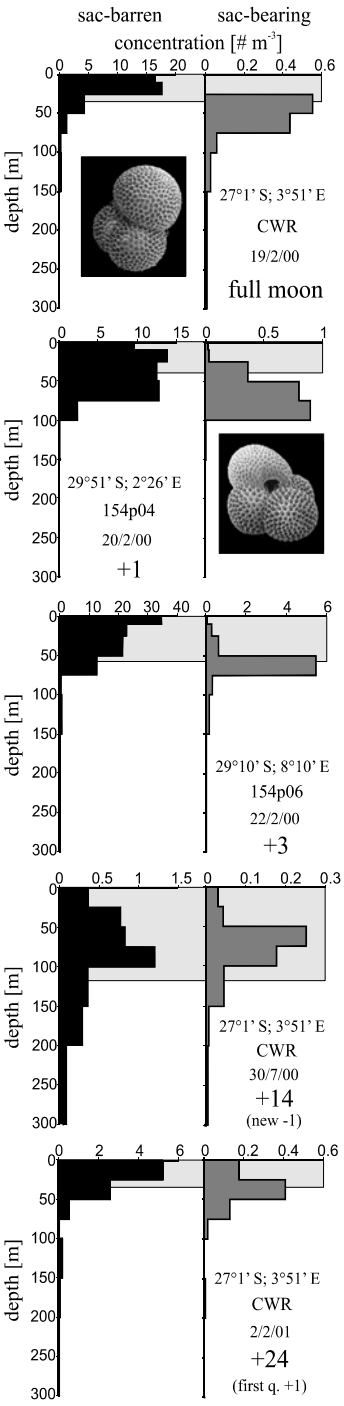

Figure 3.6 (right): Plankton tow profiles of *G. trilobus* morphotypes from the mooring site and surroundings taken during different phases of the moon. The morphotype without sac-like chamber is given in black and with sac-like chamber in grey. Shaded area represents the surface mixed layer.

gametogenesis 5 ± 2 days after full moon, which involved 85.4% of the cultured population. Discarded shells arriving from the productive upper ocean on the deep ocean floor are delayed by the settling time. If we consider reproduction 5 ± 2 days after full moon (Spindler et al., 1979) and the arrival of shells at the 2700m deep CWR site 12.5 days after full moon, then the required settling time from its depth habitat yields a sinking velocity of 390 ± 100 m day^{-1}. Although experimentally observed settling velocities for *H. pelagica* have not been reported, velocities of 300 to 500 m day^{-1} are typically found for spinose species of similar shell shape and size, e.g. *G. ruber, G. trilobus, G. siphonifera* and *G. bulloides* (Takahashi and Bé, 1984: Schiebel and Hemleben, 2000). Furthermore, the 85% of cultured individuals participating in synodic gametogenesis (Spindler et al., 1979) is consistent with the observed lunar amplitude in shell deposition fluxes of about a factor of 7 in the CWR time-series, although modified by seasonal variability. Thus, lunar oscillations in deep-sea deposition fluxes of *H. pelagica* in the South Atlantic central gyre are in full agreement with the findings of Spindler et al. (1979) of endogenous synodic gametogenesis in cultured isolates from off Bermuda in the North Atlantic central gyre. For *H. pelagica*, lunar reproductive cycling should be considered the primary driving mechanism for the rapid carbonate flux oscillations on the deep ocean floor.

Since the Walvis Ridge time-series shows such clear lunar forcing of *H. pelagica* deposition fluxes, it allows assessment of lunar flux oscillations in co-occurring species like *G. trilobus*, *G. bulloides* or *O. universa*. For these species exogenous lunar forcing of the reproductive cycle has been suggested to explain temporal variation in abundance, size distribution and shell flux (e.g. Bijma et al., 1990; Schiebel et al., 1997; Kawahata et al., 2002). Yet, only *H. pelagica* among the 28 species of planktic foraminifera at the CWR site showed such pronounced synodic cyclicity, or on any other wavelength in the 16-90 day domain. On the one hand this adds to the growing evidence that *H. pelagica*'s endogenous lunar reproductive strategy is unique among planktic foraminifera, if not among oceanic plankton in general. On the other hand it

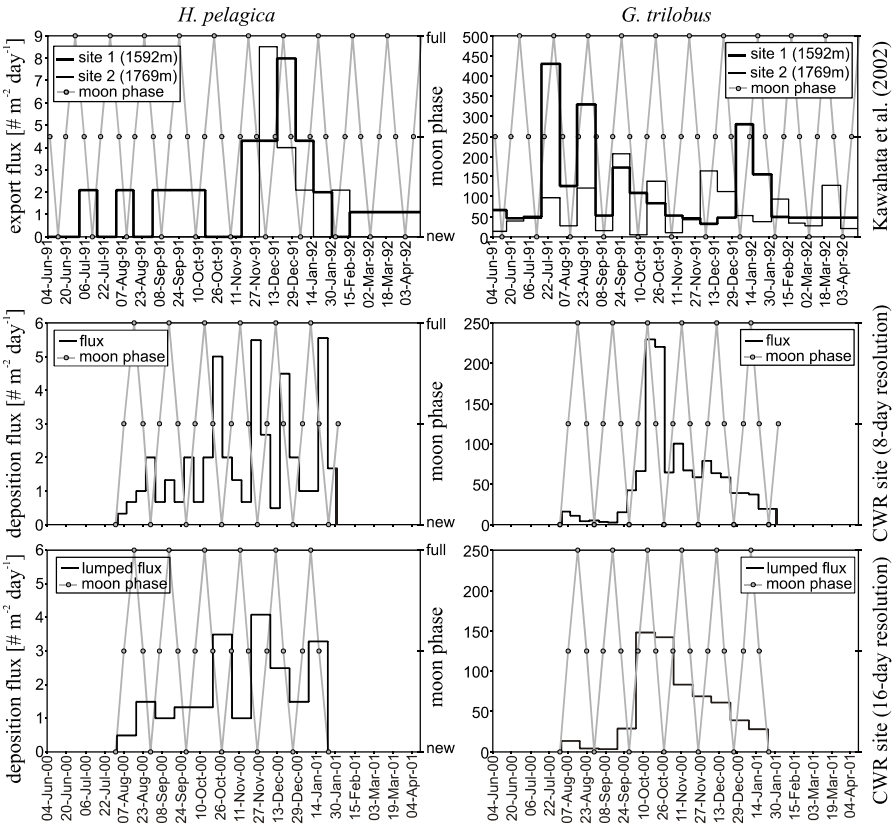

Figure 3.7: *H. pelagica* and *G. trilobus* flux records from the western Pacific after Kawahata et al. (2002) **(a)** versus CWR records **(b)**. The bottom charts **(c)** present the same CWR records from **(b)**, but with 16-day sampling resolution created by lumping of the neighbouring cups, and they illustrate constraint of low resolution sampling for the lunar cyclicity analysis.

implies that all other species (1) lacked such endogenous forcing, but also that (2) exogenous lunar forcing was insignificant relative to non-lunar temporal variability in deposition fluxes at the central Walvis Ridge (Fig. 3.3). Such exogenous lunar forcing was invoked from time-series plankton tows for *G. trilobus* in the Red Sea (Almogi-Labin, 1984; Hemleben et al., 1989; Bijma et al., 1990; Erez et al., 1991; Bijma and Hemleben, 1994) and for *G. bulloides* in the North Atlantic (Schiebel et al., 1997), which are both common in the CWR time-series. Volkmann (2000) reported lunar cycling for several other species absent in our samples, in plankton tows from the Arctic Ocean. To our knowledge Kawahata et al. (2002) were the first to report on lunar periodicity of planktic foraminifera in transit flux using sediment trap derived time-series in the western equatorial Pacific. They invoked lunar cycling for *G. trilobus* (Fig. 3.7) and *O. universa,* but also for *G. ruber* and *G. siphonifera,* which Bijma et al. (1990) suggested, may show a weak semi-lunar (bi-weekly) synchronised reproduction. However, flux maxima were apparent in only 3 or 4 out of the eleven moon cycles in the time-series of Kawahata et al. (2002), whereas no endogenous lunar periodicity was seen in their *H. pelagica* (Fig. 3.7). This may be due to the poor counting statistics at low shell

fluxes, but more probably to the prolonged sampling intervals of 15 to 16 days, well outside the constraints of the critical Nyquist frequency for resolving lunar cyclicity (Fig. 3.7). Unfortunately, neither our nor the Kawahata et al. (2002) time-series has the required temporal resolution with respect to Nyquist frequency to establish the significance of semi-lunar oscillations in shell flux which Bijma et al. (1990) inferred for reproductive cycling in *G. ruber* and *G. siphonifera.* Yet, despite the improved counting statistics and proper resolution in the lunar domain, neither *G. trilobus* nor *G. bulloides* showed any perceivable lunar periodicity in CWR deposition fluxes (Fig. 3.3), as was expected from the modelling results of Bijma et al. (1994) and suggested by the trap results of Kawahata et al. (2002). For the deposition fluxes at the CWR site, it is clear that, compared to *H. pelagica*, lunar reproductive cycles are only of subordinate importance, whether endogenous or exogenous. If existing at all, lunar forcing is much weaker than seasonal forcing on the shell export fluxes of planktic foraminifera and carbonate in general (Fig. 3.3). At the CWR site, not only shell deposition fluxes but also the ratio of the coarse (>250µm) versus fine (150-250µm) size fraction lacked any significant variation with a lunar periodicity. As Bijma et al. (1990, 1994) argued, synchronized reproduction should cause such changes, since populations of simultaneously growing individuals are formed that lead to a saw-tooth pattern in the shell size-frequency distribution over time. Importantly, this property is conserved when population size, and thus the shell export, vary for other unknown reasons, a feature Bijma et al. (1990) originally employed to disclose exogenous (semi-) lunar cycling in Red Sea surface plankton. Moreover, it allows assessment of lunar gametogenesis from the deposition flux when obscured by the effects of high mortality, e.g. when only a small portion of the foraminiferal population reaches the reproductive stage (Bijma and Hemleben, 1994). Moreover, size shifts should not significantly be obscured by differential shell settling velocity between size fractions of the same species in the size range considered here (cf. Erez et al., 1991; Bijma et al., 1994). Applied to our data, no underlying lunar pattern in size distribution emerged from the seasonally strongly variable fluxes of species.

Bijma et al. (1994) argued that the flux of *G. trilobus* is a function of the synodic cycle and is independent of the reproduction level, where a decrease in reproduction rate only shifts the flux maximum from full moon to new moon. Apart from *H. pelagica*, the only CWR record with some lunar periodicity concerns the proportion of sac-bearing individuals of *G. trilobus* with respect to the total population of both morphotypes (Fig. 3.5). Formation of the sac-like final chamber is a reproductive feature of this species which precedes gametogenesis by a few days although it is not mandatory for reproduction (Hemleben et al., 1987; Brummer et al., 1987; Bijma et al., 1990). Prior to the spring flux maximum the morphotype ratios are irregular but for the last four months they show approximate lunar cyclicity, with relative maxima in sac-bearing specimens arriving on the central Walvis Ridge 5 ± 2 days after full moon. This would coincide with maximum reproduction exactly at full moon as inferred by Almogi-Labin, (1984), Bijma et al. (1990) and Erez et al. (1991), considering the settling velocity of *G. trilobus* (Takahashi and Bé, 1984; Bijma et al., 1994; Schiebel and Hemleben, 2000), the depth of our mooring and the sampling resolution. Perhaps gametogenesis in *G. trilobus* is lunar for a small part of the population at the CWR in summer, but by the same token, it may not since our evidence is of too questionable statistical significance considering the partial, selective record with an average cyclicity of approximately 42 days, far above synodic periodicity. Even though *G. trilobus* may slightly intensify gametogenesis during full moon in summer, it is not expressed in the shell deposition flux and size-frequency distribution. Moreover, plankton tows from the CWR mooring site and surroundings (Fig. 3.5) show that sac-bearing *G.*

trilobus do not disappear from surface waters following full moon as a result of reproductive migration to greater depth or gametogenic shell export (cf. Erez et al., 1991; Bijma and Hemleben, 1994). Sac-bearing specimens did live consistently deeper, between 25 and 100 m at both the CWR site (Fig. 3.5) and in the Red Sea (Bijma and Hemleben, 1994), i.e. much shallower than the reproduction depth of 400 m Erez et al. (1991) suggested. Yet, *G. trilobus* persisted throughout the lunar cycle, in different seasons, without apparent lunar vertical migration in terms of subtle changes in shell concentration or size distribution previous authors associated with lunar time (Fig. 3.5). In this respect, sediment trap time-series, when properly resolved, are much less hindered by the effects of day-to-day changes in the spatial distribution in the lunar domain as they integrate the shell export over the entire productive zone. For the CWR site, both sediment trap and plankton tow evidence argue for continuous reproduction rather than synodic cyclicity in *G. trilobus* given the flux pattern and size distribution of morphotypes.

Whether endogenous or exogenous, at the CWR site no lunar cyclicity has been observed for any species but *H. pelagica*. This is remarkable since this species has low standing stocks and export fluxes, and a weakly calcified shell suffering from structural breakdown during gametogenesis (Hemleben et al. 1989). It underscores our observation that lunar cycling can not be important in any other species, judging from their deposition fluxes at the CWR, including *G. trilobus, G. bulloides* and *O. universa*, which have previously been inferred to show lunar reproductive cycling elsewhere. Rather than lunar-driven, species' fluxes appear determined primarily by seasonal responses, implying that reproduction is continuous in the lunar domain, except for *H. pelagica*, unique among planktic foraminifera in number of other aspects such as wall structure, presence of bubble capsule and exclusively carnivorous diet that is less susceptible to seasonal changes in phytoplankton standing stocks (Hemleben et al., 1989). Such continuous reproduction greatly facilitates interpretations of the foraminiferal distribution patterns across ecological and physical gradients in the upper ocean. Given the very low burial efficiency of *H. pelagica* (Hilbrecht, 1996) and lack of lunar oscillations in the shell flux or size distribution of other species, we conclude that the lunar cycle plays at most a subordinate role in the foraminiferal carbonate sedimentation patterns in the deep sea. It appears that deep-sea sedimentation patterns below central ocean gyre are determined predominantly by continuous reproduction in the lunar domain in response to temporal (seasonal) changes in overall shell productivity in the upper ocean.

6. ACKNOWLEDGMENTS

We wish to thank the captains and crews of R/V Pelagia and R/V Agulhas as well as the NIOZ technicians for their assistance during the MARE cruises. Jolanda van Iperen is acknowledged for the SEM photography. Thanks are due to Thomas Richter for comments. Michael Bacon and three anonymous reviewers are thanked for reviewing the manuscript. This work was supported by grants from the Dutch Ministry of Education, Arts and Sciences within the Netherlands - Bremen Oceanography (NEBROC) programme and from the Netherlands Organisation for Scientific Research (NWO - ALW) within the Mixing of Agulhas Rings Experiment (MARE). We acknowledge the additional support from the Pelagia Around Africa programme (NIOZ/NWO).

REFERENCES

Almogi-Labin, A., 1984. Population dynamics of planktic Foraminifera and Pteropoda – Gulf of Aqaba, Red Sea. *Proceedings of the Koninklijke Nederlandse Akademie van Wetenschappen, Series B, 87* (4): 481-511.

Bijma, J., Erez, J. & Hemleben, C., 1990. Lunar and semi-lunar reproductive cycles in some spinose planktonic foraminifers. *Journal of Foraminiferal Research, 20*: 117-127.

Bijma, J. & Hemleben, C., 1994. Population dynamics of the planktic foraminifer *Globigerinoides sacculifer* (Brady) from the central Red Sea. *Deep-Sea Research I, 41* (3): 485-510.

Bijma, J., Hemleben, C. & Wellnitz, K., 1994. Lunar-influenced carbonate flux of the planktic foraminifer *Globigerinoides sacculifer* (Brady) from the central Red Sea. *Deep-Sea Research I, 41* (3): 511-530.

Brummer, G-J.A., Hemleben, C. & Spindler M., 1987. Ontogeny of extant spinose planktonic foraminifera (Globigerinidae): a concept exemplified by *Globigerinoides sacculifer* (Brady) and *G. ruber* (d'Orbigny). *Marine Micropaleontology, 12* (4): 357-381.

Böckel, B. & Baumann, K.-H., 2004. Distribution of coccoliths in surface sediments of the south-eastern South Atlantic Ocean: ecology, preservation and carbonate contribution. *Marine Micropaleontology, 51* (3-4): 301-320.

Davis, J.C., 1986. *Statistics and data analysis in geology.* John Wiley & Sons, Inc., New York: 646 pp.

Erez, J., Almogi-Labin, A. & Avraham, S., 1991. On the life history of planktonic foraminifera: lunar reproduction cycle in *Globigerinoides sacculifer* (Brady). *Paleoceanography, 6* (3): 295-306.

Feely, R.A., Sabine, C.L., Lee, K., Berelson, W., Kleypas, J., Fabry, V. & Millero, F.J., 2004. Impact of anthropogenic CO_2 on the $CaCO_3$ system in the Oceans. *Science, 305* (5682): 362-366.

Hemleben, C., Spindler, M. & Anderson, O.R., 1989. *Modern planktonic foraminifera.* Springer-Verlag, New York: 363 pp.

Hemleben, C., Spindler, M., Breitinger, I. & Ott, R., 1987. Morphological and physiological responses of *Globigerinoides sacculifer* (Brady) under varying laboratory conditions. *Marine Micropaleontology, 12* (4): 305-324.

Hilbrecht, H., 1996. Extant planktic foraminifera and the physical environment in the Atlantic and Indian Oceans. *Mitteilungen aus dem Geologischen Institut der Eidgenösschen Technischen Hochschule und der Universität Zürich, Neue Folge 300*: 1-93.

Kawahata, H., Nishimura, A. & Gagan, M.K., 2002. Seasonal change in foraminiferal production in the western equatorial Pacific warm pool: evidence from sediment trap experiments. *Deep-Sea Research II, 49* (13-14): 2783-2800.

Levitus, S. & Boyer, T., 1994. *World Ocean Atlas 1994, 4.* U.S. Department of Commerce, Washington D.C.: 117 pp.

Lutjeharms, J.R.E. & Stockton, P.L., 1987. Kinematics of Southern Africa's upwelling front. In: K.H. Brink (Ed.), The *Benguela and comparable ecosystems.* Sea Fisheries Research Institute, Cape Town: pp. 35-49.

Lutjeharms, J.R.E., 1996. The exchange of water between the South Indian and South Atlantic Oceans. In: G. Wefer, W.H. Berger, G. Siedler & D.J. Webb (Eds.), *The South Atlantic: Present and past circulation.* Springer-Verlag, Berlin Heidelberg: pp. 125-162.

Omori, K., 1995. The adaptive significance of lunar or semi-lunar reproductive cycle in marine animals. *Ecological Modelling, 82*: 41-49.

Ottens, J.J., 1991. Planktic foraminifera as North Atlantic water mass indicators. *Oceanologica Acta, 14* (2): 123-140.

Paillard, D., Labeyrie, L. & Yiou, P., 1996. Macintosh program performs time-series analysis. *EOS Transactions, 77*: 379.

Peeters, F.J.C., Brummer, G.-J.A. & Ganssen, G., 2002. The effect of upwelling on the distribution and stable isotopes composition of *Globigerina bulloides* and *Globigerinoides ruber* (planktic foraminifera) in modern surface waters of the NW Arabian Sea. *Global and Planetary Change, 34* (3-4): 269-291.

Peterson, R.G. & Stramma, L., 1991. Upper-level circulation in the South Atlantic Ocean. *Progress in Oceanography, 26* (1): 1-73.

Schiebel, R., 2002. Planktic foraminiferal sedimentation and the marine calcite budget. *Global Biogeochemical Cycles, 16* (4): 1065, doi:1029/2001GB001459.

Schiebel, R., Bijma, J. & Hemleben, C., 1997. Population dynamics of the planktic foraminifer *Globigerina bulloides* from the eastern North Atlantic. *Deep-Sea Research I, 44* (9-10): 1701-1713.

Schiebel, R. & Hemleben, C., 2000. Interannual variability of planktic foraminiferal populations and test flux in the eastern North Atlantic Ocean (JGOFS). *Deep-Sea Research II, 47* (9-11): 1809-1852.

Schouten, M.W., de Ruijter, W.P.M., van Leeuwen, P.J. & Lutjeharms, J.R.E., 2000. Translation, decay and splitting of Agulhas rings in the southeastern Atlantic Ocean. *Journal of Geophysical Research - Oceans, 105* (C9): 21913-21925.

Schouten, M.W., de Ruijter, W.P.M. & van Leeuwen, P.J., 2002. Upstream control of Agulhas Ring shedding. *Journal of Geophysical Research - Oceans, 107* (C8): 3109 doi: 1029/2001JC000804.

Shannon, L.V. & Nelson, G., 1996. The Benguela: large scale features and processes and system variability. In: G. Wefer, W.H. Berger, G. Siedler & D.J. Webb (Eds.), *The South Atlantic: Present and past circulation.* Springer-Verlag, Berlin Heidelberg: pp. 163-210.

Spindler, M., Hemleben, C., Bayer, U., Bé, A.W.H. & Anderson, O.R., 1979. Lunar periodicity of reproduction in the planktonic foraminifer *Hastigerina pelagica*. *Marine Ecology Progress Series, 1*: 61-64.

Takahashi, K. & Bé, A.W., 1984. Planktonic foraminifera: factors controlling sinking speed. *Deep-Sea Research I, 31* (12A): 1477-1500.

Volkmann, R., 2000. Planktic foraminifers in the outer Laptev Sea and the Fram Strait - modern distribution and ecology. *Journal of Foraminiferal Research, 30* (3): 157-176.

Westbroek, P., Brown, C.W. van Bleijswijk, J., Brownlee, C., Brummer, G.J.A., Conte, M., Egge, J., Fernández, E., Jordan, R., Knappertsbusch, M., Stefels, J., Veldhuis, M., van der Wal, P. & Young, J., 1993. A model system approach to biological climate forcing. The example of *Emiliania huxleyi. Global and Planetary Change, 8*: 27-46.

Veličanstvo mora

Cvrčci u borovima
Cvrče pjesan bez kraja, a more uzburkano
Šumori i udara o hridi, i huči, i buči,
Pod suncem rujanskim. Dovikuju se, neprestano,
Plivači; njihovi glasi
Ulaze kroz odškrinuta vrata crkve
Na Dančama, nošeni vjetrom, i umiru
Ispred triptihona Nikole Božidarevića
(MCCCCCXVII MENSIS FEBRVARII
NICOLAVS RHAGVSINVS PINGEBAT).
U davnini i on je slušao
Šumorenje mora o kojemu sada
Učiteljica mlada, u crno odjevena,
Tumači svome razredu malih
Djevojčica i dječaka; govori im,
skupivši ih oko sebe, pokazujući rukom
More: "Svratite, djeco, pažnju
I pogledajte, kako se more razbija
O hridi, i kako se pjeni, i kako… Hej, vi,
Dođite bliže i slušajte mene…"
Sedam dječaka u košuljama zelenim,
Prestaše da osluškuju šumorenje mora
Da bi čuli glas učiteljice koja zna sve
O moru: I kako se talasa, i kako se pjeni,
A nije u nedoumici, kao ja koji sjedim
Na bliskoj klupi, u zavjetarju, i ne znam,
Premda su mi usta otvorena, kazati
Ni riječ pred veličanstvom mora,
Pred modrim šumom vječnosti.

Dragutin Tadijanović (1905)

4. Seasonal export and sediment preservation of diatom, foraminiferal and biogenic mass fluxes in a trophic gradient across the SE Atlantic

Neven Lončarić, Jolanda van Iperen, Dick Kroon & Geert-Jan A. Brummer

ABSTRACT

Seasonal deposition fluxes of phytoplankton, zooplankton and other major particle compounds, intercepted by deep-moored traps, are contrasted with their sediment accumulation flux at the 2700 m deep central Walvis Ridge, oligotrophic SE Atlantic. These data provide the first seasonally resolved record of biogenic particle fluxes in the South Atlantic Central Gyre and serve as the oligotrophic end member of a gradient across the Benguela system to the highly productive coastal upwelling off Namibia. Maximum fluxes at the central Walvis Ridge were deposited in early austral spring, following winter deepening of the surface mixed layer and associated nutrient entrainment. Nearly 25% of the annual mass flux arrived in October, when sea surface temperature rose, deep vertical mixing halted and surface production collapsed. The annual flux of diatoms was dominated by small *Nitzschia bicapitata* (60%) whereas *Globorotalia inflata* dominated the foraminiferal fluxes (25%). Diatom diversity dropped significantly during the bloom periods, when up to 80% was composed of small *N. bicapitata*, but foraminiferal diversity remained about constant. The diatom flux maximum together with C_{org} preceded that of foraminifera and pteropods by one week, in concert with the mass flux of biogenic silica and carbonate, respectively. Fluxes of the left- and right-coiled shells of the deep-dwelling foraminifer *Globorotalia truncatulinoides* peaked in different seasons, a distinctive ecological behaviour which merits their taxonomic recognition as separate "cryptic" species. These findings testify to recent evidence for the existence of several genetic species within *G. truncatulinoides* and now suggest that such species may also have a different seasonal response.

The Benguela trophic gradient showed a shoreward increase in particle fluxes but differences were surprisingly small, testifying to only moderately enhanced export productivity and deposition at the Namibian margin relative to the oligotrophic central gyre. From the open ocean towards coastal upwelling, small and weakly-silicified diatoms were substituted by other, larger and heavier-silicified species possibly in response to decreased silica limitation. Foraminiferal deposition fluxes were increasingly dominated by *G. inflata*, accompanied by a change-over from many warm- to few cold-water secondary species. The late winter maximum at the Namibian margin and the early spring maximum at the central

Walvis Ridge were generated by the same process of collapsing surface productivity in response to the shut down of nutrient entrainment at the winter to summer transition, although delayed by up to 2 months in the Central Gyre. At the sediment-water interface, intense degradation of organic matter and biogenic silica resulted in poor preservation accompanied by pronounced changes in the species composition of siliceous phytoplankton. Of all particle groups at the central Walvis Ridge, only the export of foraminiferal shells appeared to be fully transferred into the sediment, and through their species assemblage provide a sedimentary record of past seasonal productivity conditions of the upper ocean.

1. INTRODUCTION

Planktic foraminifera and diatoms are perhaps the most important global producers of carbonate and silicate particles in the pelagic ocean, respectively (e.g. Lisitzin, 1985; Schiebel and Hemleben, 2000). Their bio-geography is governed by changing ocean circulation, ambient temperature, light and nutrients among others, in the upper water column where they live (e.g. Burckle, 1978; Hemleben et al., 1989; Wefer et al., 1999). These properties together characterise productivity regimes to which specific foraminiferal or diatom species are associated. This tight relationship between species distribution patterns and environmental characteristics allow a first order approximation of past pelagic ecosystems to be reconstructed from sediment cores. Our poor understanding of the eco-physiology of modern species, however, limits the robustness of palaeoceanographic interpretations. One complicating factor is that diatoms and foraminifera often show strongly seasonal export fluxes in response to the changing oceanography (e.g. Thunell and Honjo, 1987; Deuser and Ross, 1989; Sautter and Sancetta, 1992; Schiebel and Hemleben, 2000; Romero et al., 2002; King and Howard, 2003). In addition, the plankton deposition flux is modified by diagenesis during burial, which may introduce selective preservation effects (e.g. Treppke et al., 1996a; Koning et al., 2001; Conan et al., 2002; Bárcena et al., 2004).

In this study we quantitatively analyse the seasonal deposition fluxes of diatoms and planktic foraminifera along with other major flux compounds collected by time-series sediment traps on the central Walvis Ridge (CWR) and contrast the annual deposition fluxes with the accumulation fluxes in the surface sediment directly beneath the traps. We aim to document changes in magnitude, composition and timing of the particle fluxes and examine the importance of the spring bloom within the Benguela ecosystem. Furthermore, we quantify sediment preservation and address the impact of interannual variability at the same site. Previous studies of the spatial and temporal response of calcareous and siliceous microplankton were mainly focused on the highly productive systems associated with seasonal or year-round Benguela upwelling along the African continental margin (e.g. Berger and Wefer, 1990; Giraudeau, 1993; Fischer and Wefer, 1996; Treppke et al., 1996b; Müller et al., 1997; Romero et al., 2002). The new data from the CWR site situated in the oligotrophic South Atlantic Central Gyre allow for assessing the trophic gradient crossing the Benguela Current from the open SE Atlantic to coastal upwelling off Namibia.

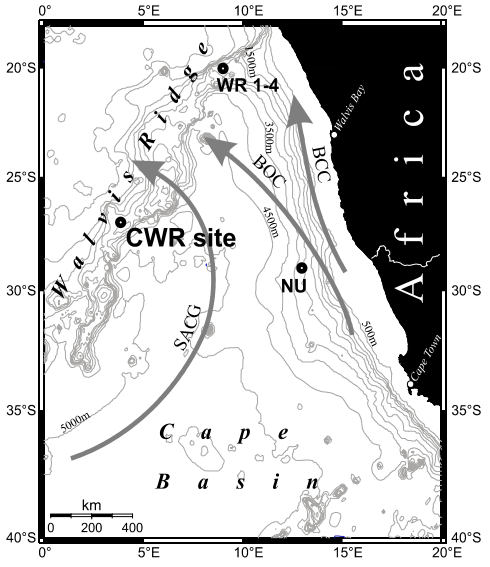

Figure 4.1: CWR site location and regional bathymetry. The NU (Romero et al., 2002) and WR 1-4 (e.g. Fischer and Wefer 1996; Treppke et al., 1996a) sediment trap sites from the Namibian margin constitute the inner part of the Benguela system gradient.

2. MATERIAL AND METHODS

2.1. Hydrographic observations

At the central Walvis Ridge site (CWR; Fig. 4.1) the entire water column was profiled during three MARE cruises using a Neill-Brown CTD-rosette sampler operated at JGOFS standards or better (Veth, 2000). We used in-situ temperature, salinity, fluorescence and nutrient concentrations to characterise the water column properties in summer 2000 (MARE 0), winter 2000 (MARE II) and summer 2001 (MARE III). For the periods in between, sea surface temperature (SST) was taken from the NOAA remote sensing records for this site, with a 50 km resolution, derived from 8 km resolution global SST observations (POES AVHRR/HIRS; www.osdpd.noaa.gov) and compared with our CWR in-situ measurements. SeaWiFS remote sensing provided the surface water concentration of chlorophyll-a at 27°S, 4°E. Surface mixed layer (SML) depth was modified after the monthly averaged values given by Levitus and Boyer (1994), that were tuned to the 3 in-situ profiles (Lončarić et al, 2005) and the temporal development of satellite-derived SST for 2000-2001. For the entire period of sampling, radar altimetry imaging of the SE Atlantic (TOPEX/Poseidon) did not show any perturbations by passing Agulhas rings, i.e. meso-scale eddies of warm-core and highly saline Indian Ocean waters, which intermittently cross the central Walvis Ridge from the proximate Cape Basin (Garzoli and Gordon, 1996; Schouten et al., 2000).

2.2. Particle flux

Two Technicap PPS5 sediment traps with a collecting area of 1 m^2 and a 24-cup automated sampling carousel have been deployed in a semi-enclosed basin on top of the central Walvis Ridge (27°00' S, 3°51' E; Fig. 4.1). One trap was moored in a bottom frame, 2 m above the sea floor at a depth of 2700 m, and the other at 2450 m depth, 250 m above. Prior to mooring, the sample cups were filled with a mercury-chloride poisoned and borax-buffered solution of seawater collected from the deployment depth (1 g l^{-1} of $HgCl_2$; pH~8.5). Moorings were deployed in February 2000, serviced in July 2000 and recovered in February 2001, programmed to sample consecutive 7 and 8-days intervals, respectively, although only an integrated half-year sample was recovered for the initial mooring period (i.e. February-July, 2000). Daily fluxes of total mass and major bulk compounds J_m [g m^{-2} day^{-1}] were calculated from individual trap collecting cups as:

$$J_m = \frac{W}{sp * t * s} \quad (1)$$

where W is the sample mass of particular component, sp is the fraction of the trap sample taken, t is the collecting time in days and s is the collecting area of the trap in m^2. Annual deposition fluxes were derived from the cumulative half-year period and all 8-days intervals from February 22, 2000 to February 1, 2001 and extrapolated for one year exactly.

After recovery, the collecting cups were subsampled shipboard for dissolved phase analysis (silica, phosphate, ammonia) and stored dark at 4°C. In the laboratory, any larger "swimmers" were removed and the residue subdivided into at least 2 aliquots using a Folsom wet-splitter (Sell and Evans, 1982; Griffiths et al., 1984) with a precision of >95%. One aliquot was used for plankton analysis as outlined below (diatoms, foraminifera, silicoflagellates, pteropods). A second aliquot was filtered on acid-cleaned pre-weighed polycarbonate filters (0.45 µm pore-size; 47 mm diameter), rinsed with pure water to remove the salts, exicator-dried at room temperature and back-weighed to the nearest 0.01 mg at constant humidity to obtain the total mass (Bonnin et al., 2002). After removal from the filter, the cake was homogenised in an agate mortar and subsampled by dry weight for analysis of bulk parameters. Carbon and nitrogen were separately analysed on weight-aliquots of the bulk material before and after removal of the carbonate-carbon (Bonnin et al., 2002), using a Carlo/Erba-Flash EA-1112. This yielded total carbon, organic carbon and nitrogen, which were converted into weight percent organic matter (= 2 x C_{org}; following Romero et al., 2002) and calcium carbonate ($CaCO_3$ = 8.33 x [C_{tot}–C_{org}]). Opaline silica was determined by continuous alkaline leaching that accounts for contributions by co-leaching of Al-silicates (Koning et al., 2002). This left a residual mass fraction conventionally referred to as the "lithogenic" contribution (Romero et al., 2002). In addition, the nitrogen isotope composition was measured by continuous flow mass spectrometry on bulk aliquots weighed to equal N mass (30 µg), using a Fisons CN analyser interfaced with a Finnigan Delta S mass spectrometer with an error of less than 0.2‰ in $\delta^{15}N$ (for details see Middelburg and Nieuwenhuize, 2000).

2.3. Foraminiferal analysis

All aliquots designated for the foraminiferal analysis were wet-sieved over a 150 µm mesh, rinsed with ethanol, ashed in a low-temperature asher and then dry-sieved over a 250 µm mesh to obtain 2 size fractions. The fraction smaller than 150 µm from the same aliquots was kept for diatom analysis. Planktic foraminifera were enumerated in the size fractions 150-250 µm and >250 µm. Large samples were split by an Otto dry splitter. On average 349 specimens (93 to 749) were counted per size fraction. We also counted the number of pteropod shells present in the foraminiferal samples, yet these were not identified to the species level. Taxonomy mainly followed Hemleben et al. (1989). For the species *Globigerinoides trilobus* we distinguished between the morphotype with and without the terminal elongated, sack-like chamber. The name *G. trilobus trilobus* is used for specimens without a sack-like chamber (= *Globigerina triloba* Reuss, 1850), whereas those with a sack-like chamber were referred to as *G. trilobus sacculifer* (= *Globigerina sacculifera* Brady, 1877). When referring to the entire species, the name *G. trilobus* s.l. is applied. Left- and right-coiled specimens of the *Globorotalia truncatulinoides* were treated separately. The daily foraminiferal flux J_f [# m^{-2} day^{-1}] is given by:

$$J_f = \frac{N_f}{sp * t * s} \quad (2)$$

where N_f is the number of counted specimens, *sp* is the fraction of the trap sample taken, *t* is the collecting time in days and *s* is the trap collecting area (m^2).

2.4. Diatom analysis

For diatom analyses, we employed the fraction <150 μm of the same aliquots as used for enumeration of the foraminifera. Considering that not all diatoms are smaller than 150 μm, the 6-month integrated sample from the upper trap of the first deployment was used to compare the diatom content of the <150 μm fraction with the original bulk samples. Since the compared samples had at least a 94% match, we used the <150 μm fractions to provide sufficient material for further analyses. The only exception was identification of half to complete valves of the giant *Ethmodiscus* that were counted in the foraminiferal fraction >150 μm, as these were fragmented during preparation of the Naphrax slides. In the preparation procedure, centrifugation (10 min at 1200 r/min) instead of decantation was used for improved separation of the residue (i.e. less flocks and no suspended diatoms) and to minimise silica dissolution (i.e. shorter processing time), thus enhancing the recovery of the small and fragile specimens. In a number of centrifugation/decantation experiments we did not find any evidence for the increased fragmentation or lower abundance of fragile species, as some authors reported for sediment samples (e.g. Abrantes et al., 2005). For sample preparation of both trap and sediment samples the standard cleaning method of Schrader (1974) was applied, with some modifications such as only a moderate use of chemicals (1N HCl and 10% H_2O_2 in quantities tuned to the subsample size) at a lower incubation temperature of 60°C to minimise dissolution (A.J. van Bennekom, pers. comm.). Quantitative slides were prepared in evaporation trays (∅ 96 mm) following Batterbee (1973) with three circular LM cover slips (∅ 19 mm) and one SEM slip (∅ 10 mm). Two dried LM slips were embedded in Naphrax (r.i. = 1.72) at 140ºC and subsequently examined at 1000x magnification.

For each slide at least 300 individuals (150 on each slip) were counted and identified to species level. In case of difficulties in distinguishing between two or more species, they were combined in a single counting group (Tab. 4.1). Diatom specimens representing more than one half of the valve were counted as one. For long pennate diatoms (*Alveolus marinus*, *Fragilariopsis doliolus*, *Lioloma* spp., *Pseudonitzschia* spp., *Thalassionema* spp. and *Thalassiothrix* spp.) each pole was counted as one half. Other fragments were not counted except the easily recognisable bristles of *Chaetoceros messanensis*. Capitate species of the genus *Nitzschia* were allotted to four size groups: (1) the *N. bicapitata* group 1 (<22 μm), (2) the *N. bicapitata* group 2 (22-33 μm), (3) the *N. braarudii* group (>33 μm) and (4) the *Pseudonitzschia inflatula* var. *capitata* group (>50 μm and narrow). In addition, several specimens of the genus *Ethmodiscus* were determined to species level by scanning electron microscopy (i.e. *E. gazellae*). Specimen counts were converted into species fluxes J_d [# m^{-2} day^{-1}] using:

$$J_d = \frac{N_d * A/a * V/v}{sp * t * s} \quad (3)$$

species code	FORAMINIFERAL species	rel.abundance Aug'00-Feb'01 [%]	deposition flux [# m^{-2} yr^{-1}]	[%]	accumulation flux [# m^{-2} yr^{-1}]	[%]	burial factor
DIG	*Beella digitata*	1.2	1418	1.3	364	0.2	0.26
BUL	*Globigerina bulloides*	1.6	2054	2.0	3277	2.3	1.59
FAL	*Globigerina falconensis*	2.2	2213	2.1	4005	2.7	1.81
SIP	*Globigerinella siphonifera*	6.1	7707	7.3	9102	6.3	1.18
CAL	*Globigerinella calida*	3.8	3886	3.7	2184	1.5	0.56
GLU	*Globigerinita glutinata*	7.6	7848	7.4	8374	5.8	1.07
RUB	*Globigerinoides ruber*	3.1	5839	5.6	12742	8.8	2.18
TRI	*Globigerinoides trilobus trilobus* (-sac)	7.7	14044	13.3	6553	4.5	0.47
SAC	*Globigerinoides trilobus sacculifer* (+sac)	3.2	4584	4.4	2184	1.5	0.48
HIR	*Globorotalia hirsuta*	3.4	3368	3.2	7281	5.0	2.16
INF	*Globorotalia inflata*	26.5	26853	25.5	41140	28.2	1.53
MEN	*Globorotalia menardii*	5.9	9177	8.7	10922	7.5	1.19
SCI	*Globorotalia scitula*	2.0	2080	2.0	3641	2.5	1.75
TRD	*Globorotalia truncatulinoides* (d)	1.1	1539	1.5	6189	4.3	4.02
TRS	*Globorotalia truncatulinoides* (l)	4.7	5153	4.9	7281	5.0	1.41
DUT	*Neogloboquadrina dutertrei*	1.0	968	0.9	1820	1.3	1.88
PAC	*Neogloboquadrina pachyderma* (d)	3.0	2981	2.8	9466	6.5	3.18
UNI	*Orbulina universa*	1.8	2222	2.1	4733	3.3	2.13
	total:	**85.8**		**98.7**		**97.0**	
	Hastigerina pelagica		426	0.4	0	0	0

Table 4.1: Foraminiferal and diatom species and species groups with relative abundance higher than 1% included in the principal component analyses during the high-resolution sediment trap sampling period (August 2000 – February 2001). For diatoms, the most important species in the species groups are given in bold. Burial factors (BF) are given by equation 7.

species code	DIATOM species and species groups	rel. abundance Aug '00-Feb'01 [%]	deposition flux [# $10^6 m^{-2} yr^{-1}$]	deposition flux [%]	accumulation flux [# $10^6 m^{-2} yr^{-1}$]	accumulation flux [%]	burial factor
ALVMAR	*Alveolus marinus*	1.2	16	0.8	0.19	4.2	0.012
AZPNEO	*Azpeitia neocrenulata*	1.2	29	1.4	0.28	6.3	0.010
CHAVEG	*Chaetoceros* vegetative cells	1.5	22	1.1	0.00	0	0.000
FRADOL	*Fragilariopsis doliolus*	1.7	32	1.6	0.50	11.1	0.016
NITBI1	*Nitzschia bicapitata* group 1 (<22 µm) ***bicapitata,*** *bifurcata, ikeana, leehyi, villaredii*	60.2	1208	59.4	0.91	20.3	0.001
NITBI2	*Nitzschia bicapitata* group 2 (22-33 µm)	1.9	61	3.0	0.13	2.8	0.002
NITBRA	*Nitzschia braarudii* group (>33 µm, broad) ***braarudii,*** *capitellata, dietrichii, lodicula, longicollum, oceanica, reimersenii*	2.4	62	3.0	0.11	2.5	0.002
NITSIC	*Nitzschia sicula*	1.6	28	1.4	0.04	0.9	0.002
PNICAP	*Pseudonitzschia inflatula* var. *capitata* group (>50 µm, narrow) ***inflatula* var. *capitata,*** *N. dietrichii, N. lodicula*	2.1	42	2.0	0.20	4.4	0.005
PNIDSG	*Pseudonitzschia* pointed ends group *australis, cuspidata, delicatissima, inflatula, fraudulenta, lineola, multiseries, pseudodelicatissima, pungens, pungiformis, subfraudulenta, subpacifica, turgidula*	2.8	46	2.2	0.01	0.2	0.000
RHIBER	*Rhizosolenia bergonii*	1.7	26	1.3	0.21	4.7	0.008
TNEINC	*Thalassionema nitzschioides* var. *incurvatum*	6.1	116	5.7	0.33	7.3	0.003
TNEINF	*Thalassionema nitzschioides* var. *inflatum*	2.4	54	2.6	0.19	4.2	0.004
TSIOLI	*Thalassiosira lineata* group *lineata, lineoides*	1.5	32	1.6	0.11	2.5	0.003
TSIOVG	*Thalassiosira oestrupii* *oestrupii* var. *oestrupii, oestrupii* var. *venrickae*	2.7	60	3.0	0.39	8.8	0.007
TTHSPA	*Thalassiothrix spathulata* group ***spathulata,*** *gibberula, lanceolata*	1.0	19	1.0	0.10	2.2	0.005
	total:	**91.9**		**91.1**		**82.4**	

Table 4.1: continued

where N_d is the number of specimens counted along an area of traverses *a* as a fraction of the total area of the evaporation tray *A*, *v* is the subvolume of the total suspension volume *V* used in the tray, *sp* is the fraction of the trap sample taken, *t* is the collecting time and *s* is the trap collecting area. Along with marine diatoms, also allochthonous epibiontic, littoral benthic and continental diatom species were counted, as well as pelagic silicoflagellates, benthic sponge spicules and terrestrial phytoliths albeit the latter three groups were not identified to species level.

2.5. Diversity and covariability

The diatom and foraminiferal species diversities were calculated using the Shannon-Weaver Information Measure (h'):

$$h' = -\sum_{i=1}^{n} p_i * \log_2 p_i \tag{4}$$

where p_i is the proportion of specimens belonging to the *i*-th species to the total number of specimens in the sample, *n* (Shannon, 1949). This measure of diversity is thus mainly determined by the proportion of common species. In addition, the Buzas – Gibson index of equitability (E) is given as:

$$E = \frac{e^{h'}}{s} \tag{5}$$

in which *s* is the number of species in the sample (Buzas and Gibson, 1969). This index renders the deviation of an assemblage from a sample of equally contributing species. Equitability decreases when sample size increases because of the addition of rare species, unlike the Shannon-Weaver information measure (Gibson and Buzas, 1973) that is useful for comparing diversities in samples of different size (Giraudeau, 1993).

In order to examine the temporal covariability between species fluxes, a principal component analysis (PCA) (SYSTAT 10©; Wilkinson, 1988) was carried out on the data sets from the high–resolution sampling period. Only species contributing more than 1% to the deposition fluxes were included, yielding a total of 18 foraminiferal and 16 diatom species for analyses (Tab. 4.1). To increase the normality of the data set, the flux values were logarithmically transformed and standardised to mean zero and one standard deviation for each species, resulting in similar importance for all included species. Analysis was performed on fluxes of both foraminifera and diatoms, separately and combined.

2.6. Sediment record

In order to determine the burial efficiencies of deposition fluxes, a 43 cm long box core (174 P 03 - 6) was taken at the approximate location of the trap site (26°59' S; 3°56' E) during the recovery cruise in February 2001 (MARE III). The sediment was subsampled by two 50 cm long plastic liners, one of which was later subsampled for ^{14}C and ^{210}Pb analyses by syringes (5 cm^3; Ø = 1 cm) at 1 cm depth intervals. The remaining upper 0.5 cm of the core was sampled onboard directly after recovery and kept frozen at -40°C. All samples were freeze-dried and weighed to determine their dry

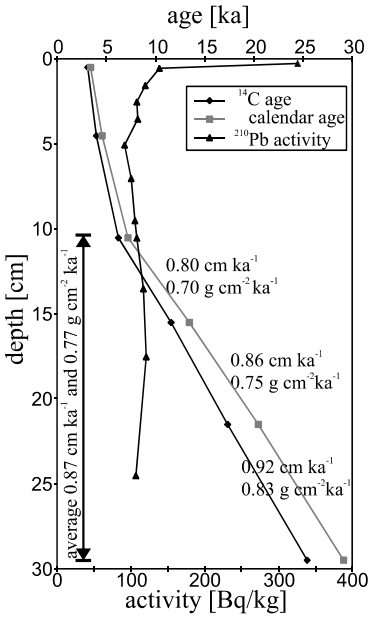

Figure 4.2: Cored sediment at the CWR mooring site (box core 174P03-6; 26°59'S, 3°56'E). Analyses of ^{14}C on *G. inflata* and ^{210}Pb activity showed modern topmost sediment, low mixing rate and an almost constant sedimentation of 0.87 cm ka^{-1} and 0.77 g cm^{-2} ka^{-1} for the interval between 10 and 30 cm. For details see text.

bulk density (DBD). After wet-sieving over 100 μm mesh the samples were dry-sieved into 3 fractions (>250 μm, 150-250 μm and 100-150 μm).

Twelve samples from the upper 25 cm of the core were analysed for ^{210}Pb. The ^{210}Pb activity profile showed that the topmost sediment at the CWR site is modern in age and mixing rates are very low within the approximately 5 cm upper mixed layer (Fig. 4.2). The linear sedimentation rate (LSR) was given by six samples from the upper 30 cm of the box core that were dated by radiocarbon AMS on the shells of the planktic foraminifera *Globorotalia inflata* (Fig. 4.2; Tab. 4.2). ^{14}C dates were corrected for a reservoir age of –400 yr and converted to calendar years by the CALIB program (Stuiver and Reimer, 1993; Stuiver et al., 1998). For the oldest control point, which is out of the CALIB range, the calibration of Voelker et al. (2000) was used.

Dating revealed an almost constant sedimentation rate of 0.87 cm ka^{-1} for the interval between 10.5 cm and 29.5 cm below a mixed top layer ($LSR_{10.5\text{-}29.5cm}$; Fig. 4.2). To minimise the effect of compaction with respect to the saturated topmost sediment, its weight (W_{0cm}) was recalculated to volume (V_{0cm}) using the average DBD of 0.89 g cm^{-3} from the dated interval with the constant sedimentation rate. The sediment accumulation flux J_{acc} [# m^{-2} yr^{-1}] or [g m^{-2} yr^{-1}] was then given by:

$$J_{acc} = N * \frac{LSR}{V} = N * \frac{LSR_{(10.5-29.5cm)} * DBD_{(10.5-29.5cm)}}{W_{(0cm)}} \qquad (6)$$

where N was the number of counted specimens or weight of the biogenic component in the surface sediment. The burial efficiency factor BF is given by:

$$BF = \frac{J_{acc}}{J_{dep}} \qquad (7)$$

and defines what part of the annual deposition flux 2000-2001 (J_{dep}) was incorporated in the bottom sediment.

Table 4.2: 210Pb activity and 14C ages from the CWR box core 174P03-6 presented in Figure 4.2.

average depth (cm)	^{210}Pb(tot) (mBq/g)	^{14}C age - 400 (yr)	calendar age (yr)	source
0,2	325,5			
0,5	138,7	3105	3375	calib
1,5	119,5			
2,5	108,6			
3,5	109,6			
4,5		4040	4581	calib
5,0	91,3			
7,0	100,2			
9,5	105,2			
10,5	108,3	6270	7208	calib
13,5	117,6			
15,5		11610	13461	calib
17,5	121,0			
21,5		17290	20460	calib
24,5	107,2			
29,5		25460	29160	Voelker et al.

3. RESULTS

In this section we outline the oceanographic conditions at the CWR site as recorded by in-situ measurements and remote sensing in order to relate biogenic particle production in the upper water column with the deposition fluxes on the deep ocean floor. We document seasonal change of skeletal export from phyto- and zooplankton groups (diatoms, silicoflagellates, foraminifera and pteropods) with respect to major mass fluxes ($CaCO_3$, organic matter, opaline silica). Furthermore, we quantitatively analyse the response of diatom and foraminiferal species and their communality in relation to temporal changes in ambient conditions. Finally, we compare the annual deposition as recorded by the sediment traps with the accumulation fluxes in the bottom sediment at the same site to assess the impact of sedimentary preservation on seasonal deposition fluxes.

3.1. Regional oceanography

The hydrography of the Southeast Atlantic Ocean is largely controlled by the Subtropical Atlantic Gyre with the central Walvis Ridge on its eastern flank, known as the oceanic branch of the Benguela Current (Fig. 4.1) (Peterson and Stramma, 1991; Garzoli and Gordon 1996). Flowing northwards, the Benguela Current incorporates the thermocline and Atlantic Intermediate Water stratum and is primarily fed by the gyral South Atlantic Current, but can also receive Agulhas Current Water as well as Subantarctic Surface Water (Peterson and Stramma, 1991). Off southwestern Africa, the eastern boundary current known as the coastal branch of the Benguela

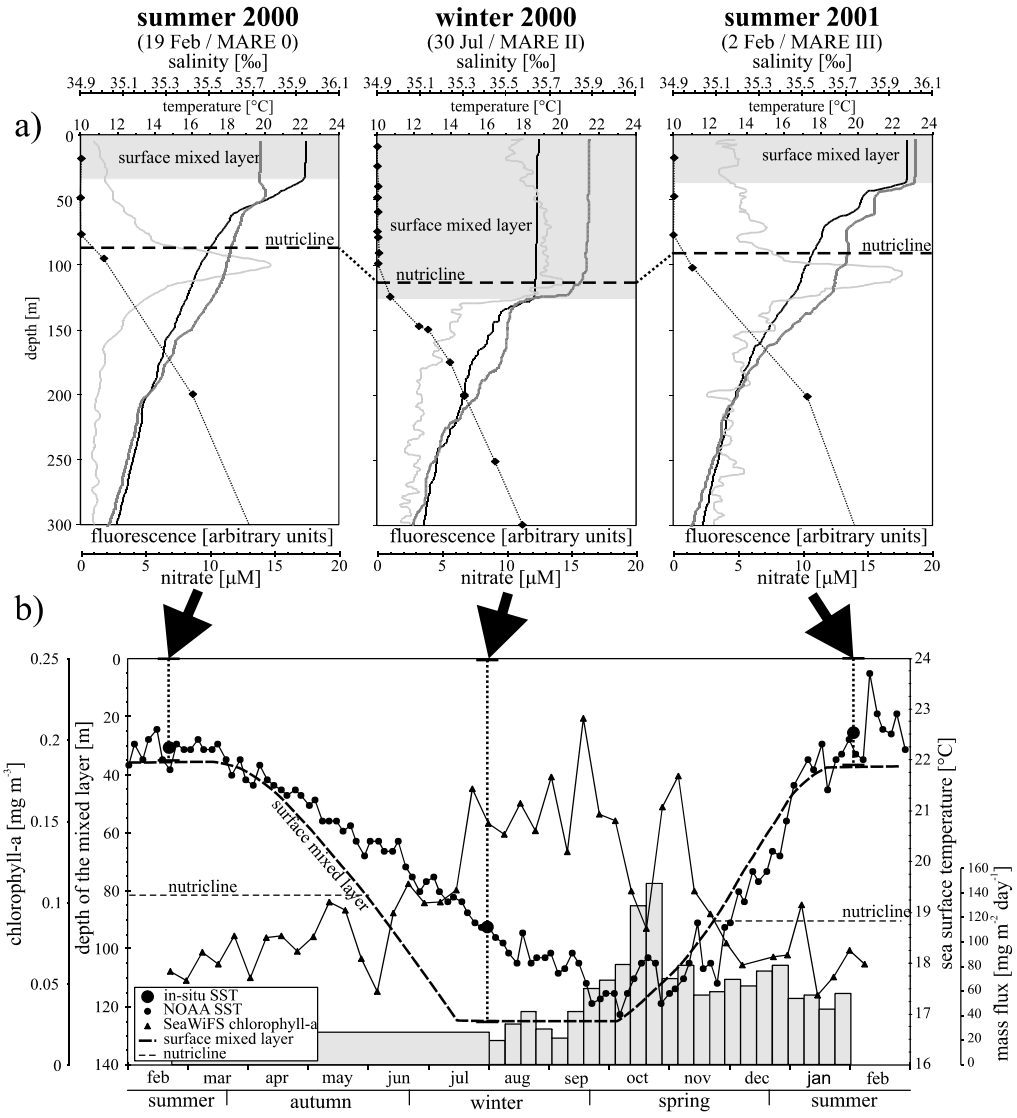

Figure 4.4a) Water column profiles of temperature (black; °C), fluorescence (light grey, arbitrary units), salinity (dark grey; ‰) and nitrate concentration (diamonds; µM) in the upper 300 m taken at the CWR. Shaded areas represent the surface mixed layer. **b)** Satellite-derived sea surface temperature (dots; NOAA-POAS AVHRR/HIRS), chlorophyll-a concentration (triangles; SeaWiFS) and depth of the surface mixed layer (dashed line; modified after Levitus and Boyer (1994) and tuned to the in-situ profiles) at the CWR site from February 2000 to February 2001. Vertical dashed lines mark times of CTD profiling. The length of the vertical dashed lines corresponds to the in-situ measured SML depths (from a) and the bold dots represent the in-situ measured SST. Vertical grey bars represent the mass deposition flux.

Current, is associated with the highly productive and globally important Benguela coastal upwelling system. Filaments of cold, nutrient rich water may extend for as much as 600 km offshore Namibia across the NU and WR sites (Fig. 4.3 in appendix "colour figures"), but do not affect the predominantly oligotrophic conditions at the CWR situated about 10° further oceanward (Lutjeharms and Stokton, 1987; Shannon and Nelson, 1996).

In summer 2000 the upper water column at the CWR site was characterised by a sharp shallow thermocline at a depth of 35 m at the bottom of the 22.2°C warm surface mixed layer (Fig. 4.4a). A prominent but narrow fluorescence maximum was situated much deeper, just below the nutricline at about 90 m. A similar water column structure was found one year later in the summer of 2001, except for a slightly warmer SML (22.6°C) and a better-developed subsurface mixed layer between 45 m and 55 m (to about 20°C). By contrast, in austral winter the SML exceeded a depth of 120 m, well into the nutricline and was approximately 4°C colder (Fig. 4.4a). The enhanced fluorescence reflection was measured over the entire deep SML, with a weak maximum at about 110 m. During the mooring period satellite-derived SST decreased gradually from summer values of 23°C (February – March) to an early spring minimum of 17°C (early October; Fig. 4.4b), in response to enhanced wind stress and reduced insolation (Shannon, 1985). As a result, the SML and seasonal thermocline deepened, breaching the nutricline and entraining new nutrients from depths down to 120 m. This lead to enhanced concentrations of chlorophyll-a in winter (mid July) which rapidly declined in early spring (late September/early October) when deepening of the SML and nutrient entrainment ceased (Fig. 4.4b). As SST rose during spring, a weak surface stratification developed which was briefly disrupted by deep vertical mixing in late spring judging from a drop in SST to winter values and a concomitant maximum in surface chlorophyll-a (late October/early November; Fig. 4.4b). Persistent re-stratification during spring/summer warming was accompanied by shoaling of the deep thermocline, separation of the SML from the nutricline at about 90 m by December, and the development of a new warm SML at 30 m by late January. In response, surface chlorophyll concentrations declined and a deep chlorophyll maximum developed below the nutricline in a stepped gradient toward the stable summer stratification (January-March).

3.2. Major element and particle composition of deposition fluxes

Total mass fluxes are characterised by a prominent maximum in early austral spring (October), following the collapse of winter maxima in surface chlorophyll at the CWR (Fig. 4.4b). The early spring maximum dominated the annual deposition flux (Fig. 4.5; Tab. 4.3) and accounted for nearly 25% of the 17 g m^{-2} $year^{-1}$ in 2000-2001. Deposition fluxes ranged from 20 mg m^{-2} day^{-1} (late winter) to 150 mg m^{-2} day^{-1} in the early spring maximum, and were mainly composed of carbonates (75%), with smaller contributions of organic matter (8%), biogenic silica (7%) and a residual ("lithogenic") mass fraction (10%). All mass compounds show a minor maximum in mid winter, a gradual rise towards the dominant maximum in early spring, enhanced fluxes in late spring and low to moderate fluxes in summer (Fig. 4.5; Tab. 4.3). This seasonal pattern is well developed in organic carbon (C_{org}) with fluxes rising from 1 mg m^{-2} day^{-1} in late winter to 6.5 mg m^{-2} day^{-1} in early spring. Deposition fluxes of C_{org} were only slightly enhanced in late spring, similar to $CaCO_3$ but opposite the significantly higher residual mass (RM), whereas biogenic silica (BSi) peaked at the turn of spring (Fig. 4.5). In terms of dry weight percent, organic carbon showed an increasing trend from

3.6% in winter to 5.1% at its early spring maximum in the deposition flux, followed by a decreasing trend to nearly 2% in summer. Within the early spring maximum C_{org}, BSi and RM peaked one week earlier than the total mass flux and its main constituent $CaCO_3$ (Fig. 4.5).

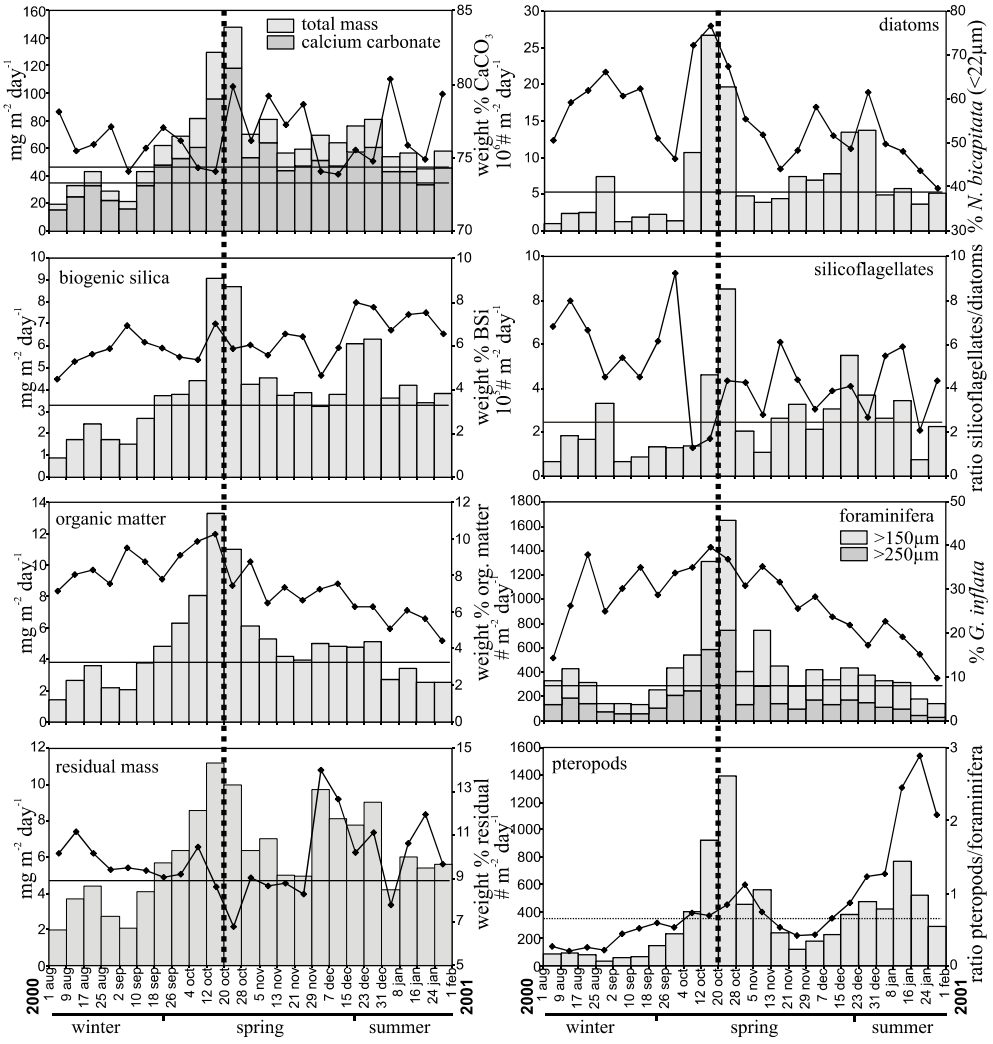

Figure 4.5: Deposition flux (bars) and relative abundance (diamonds) of major particle constituents at the CWR during the high-resolution sampling period and their annual flux (horizontal lines). For pteropods only the average from Aug. 2000 to Feb. 2001 is given (stippled horizontal line).

Table 4.3: Deposition and accumulation fluxes of the major particulate phases and their composition at the CWR from the sediment traps and box corer surface sediment, respectively. The last four columns (Ctot – BSi) are given as the weight percentage. "<dl" stands for "below the detection limit" and "na" for "data not available".

sampling period	mass [mg m^{-2}day^{-1}]	$CaCO_3$ [mg m^{-2}day^{-1}]	BSi [mg m^{-2}day^{-1}]	org. matt. [mg m^{-2}day^{-1}]	residual [mg m^{-2}day^{-1}]	$\delta^{15}N$ [‰]	diatoms [#10^{6}m^{-2}day^{-1}]	*N. bicapitata* [<22µm %]	silicoflagellates [#10^{5}m^{-2}day^{-1}]	foraminifera [#m^{-2}day^{-1}] >250	foraminifera [#m^{-2}day^{-1}] >150	*G. inflata* [>150µm %]	pteropods [#m^{-2}day^{-1}] >250	pteropods [#m^{-2}day^{-1}] >150	C_{tot} [%]	C_{org} [%]	N [%]	BSi [%]
1/8/00-9/8/00	19.5	15.3	0.9	1.4	2.0	6.1	0.97	50.5	0.66	132.3	331.7	14.4	23.7	89.0	12.95	3.57	0.53	4.51
9/8/00-17/8/00	32.8	24.8	1.7	2.6	3.7	4.6	2.33	59.2	1.87	186.3	431.7	26.3	34.3	92.3	13.08	4.03	0.53	5.29
17/8/00-25/8/00	43.4	32.9	2.4	3.6	4.4	4.8	2.55	62.0	1.69	146.0	315.7	38.0	50.0	83.7	13.26	4.15	0.57	5.62
25/8/00-2/9/00	29.2	22.5	1.7	2.2	2.7	4.6	7.40	66.1	3.33	72.0	144.0	25.0	12.5	31.5	13.03	3.78	0.50	5.89
2/9/00-10/9/00	21.8	16.2	1.5	2.1	2.1	5.0	1.22	60.8	0.66	57.0	141.7	30.1	43.0	62.7	13.63	4.73	0.67	6.91
10/9/00-18/9/00	43.3	32.8	2.7	3.8	4.1	5.4	1.92	62.3	0.87	58.7	133.0	35.1	44.3	70.0	13.45	4.36	0.62	6.16
18/9/00-26/9/00	62.3	48.0	3.7	4.8	5.7	6.1	2.21	51.0	1.36	103.3	253.0	28.9	49.0	150.0	13.14	3.88	0.59	5.92
26/9/00-4/10/00	69.2	52.7	3.8	6.3	6.4	5.6	1.39	46.3	1.29	208.7	434.7	33.7	49.3	232.7	13.69	4.54	0.69	5.48
4/10/00-12/10/00	81.9	60.9	4.4	8.1	8.6	5.2	10.72	72.2	1.39	250.7	540.7	35.0	71.3	397.3	13.84	4.92	0.70	5.37
12/10/00-20/10/00	129.4	95.8	9.1	13.3	11.2	5.4	26.68	76.7	4.62	584.0	1314.0	39.6	208.0	924.0	14.02	5.13	0.74	7.00
20/10/00-28/10/00	147.6	118.0	8.7	11.0	10.0	5.7	19.69	67.5	8.54	749.0	1647.0	36.8	479.0	1391.0	13.31	3.72	0.61	5.89
28/10/00-5/11/00	70.1	53.4	4.2	6.1	6.3	6.1	4.82	55.5	2.06	134.7	403.3	30.9	177.3	451.3	13.50	4.36	0.67	6.06
5/11/00-13/11/00	81.1	64.2	4.5	5.3	7.0	5.4	3.87	51.8	1.08	284.0	747.3	35.1	232.7	555.3	12.76	3.25	0.50	5.60
13/11/00-21/11/00	56.8	43.9	3.7	4.2	5.0	6.4	4.35	44.2	2.66	142.3	454.3	31.8	99.0	245.0	12.95	3.67	0.68	6.56
21/11/00-29/11/00	59.7	47.0	3.8	4.0	4.9	5.7	7.43	48.2	3.27	101.5	287.0	25.6	52.5	120.5	12.75	3.31	0.52	6.44
29/11/00-7/12/00	69.3	51.4	3.2	5.0	9.7	5.1	6.97	58.1	2.14	172.0	422.0	28.4	57.7	183.7	12.50	3.61	0.49	4.65
7/12/00-15/12/00	64.1	47.4	3.8	4.8	8.1	5.7	7.85	51.6	3.05	133.0	342.5	23.8	84.5	226.5	12.63	3.76	0.61	5.91
15/12/00-23/12/00	76.3	57.6	6.1	4.8	7.8	5.2	13.51	48.8	5.52	170.5	434.5	21.9	132.0	377.0	12.20	3.13	0.45	7.98
23/12/00-31/12/00	80.9	60.5	6.3	5.1	9.0	5.8	13.73	61.6	3.69	150.0	379.5	17.3	187.0	468.0	12.12	3.15	0.43	7.78
31/12/00-8/1/01	53.8	43.2	3.6	2.7	4.2	5.0	4.86	49.7	2.66	116.0	329.5	22.8	130.0	419.5	12.19	2.54	0.38	6.72
8/1/01-16/1/01	56.6	42.9	4.2	3.4	6.0	5.5	5.86	48.1	3.45	100.5	314.0	19.3	107.5	769.0	12.14	3.04	0.42	7.43
16/1/01-24/1/01	45.3	33.9	3.4	2.5	5.4	5.4	3.62	43.7	0.76	45.7	179.0	15.3	66.0	517.1	11.80	2.81	0.42	7.51
24/1/01-1/2/01	58.1	46.1	3.8	2.6	5.6	5.2	5.21	39.6	2.28	31.0	140.3	9.7	45.3	292.0	11.72	2.20	0.38	6.57
23/2/00-1/8/00	27.6	19.5	2.4	2.6	3.1	5.6	4.00	58.0	2.35	50.2	113.0	3.1	n.a.	n.a.	13.14	4.65	0.53	8.58
annual deposition	46.7	35.0	3.3	3.7	4.7	5.4	5.57	59.4	2.46	119.6	288.4	25.5	n.a.	n.a.	13.01	4.01	0.55	6.99
annual accumulat.	21.1	19.3	0.04	0.04	1.8	9.4	0.01	20.3	0.01	146.6	399.0	28.3	0	0	11.04	0.08	<d.l.	0.19
burrial factor	0.45	0.55	0.01	0.01	0.37	n.a.	0.002	0.0008	0.0056	1.23	1.38	1.53	0	0	0.38	0.01	<d.l.	<d.l

Deposition fluxes of siliceous phytoplankton and calcareous zooplankton alike showed a strong similarity to the seasonal pattern of mass fluxes (Fig. 4.5). All are characterised by highest deposition in early spring, those of diatoms arriving one week earlier than the foraminiferal shells, in line with the mass fluxes of biogenic silica and $CaCO_3$ of which they are composed (Fig. 4.5, Tab. 4.3). This coupling is also observed for the diatom and silicoflagellate secondary maxima in late spring. A clear seasonal shift was observed within the calcareous zooplankton community with a changing dominance from foraminifera in austral winter to pteropods in austral summer (Fig. 4.5). A less pronounced shift occurred within the phytoplankton community, with a proportionally higher contribution of silicoflagellates in winter and diatoms in summer (Fig. 4.5). Diatom and foraminiferal fluxes were dominated by the small *Nitzschia bicapitata* of group 1 (60%) and *Globorotalia inflata* (25%), respectively (Tab. 4.3). Deposition fluxes of either dominant species also correlated highly with those of biogenic silica and $CaCO_3$, respectively, and thus with total mass. In addition, the relative abundance of *G. inflata* showed the same seasonal trend observed in the weight % C_{org} (Fig. 4.5), i.e. low winter and summer values culminating in the early spring maximum.

3.3. Diatoms and foraminiferal deposition fluxes

Figure 4.6 presents the temporal deposition fluxes of the sixteen most dominant diatom species for the high-resolution mooring period from August 2000 to February 2001, together with the giant species *Ethmodiscus gazellae.* Most of these species showed a pronounced early spring maximum during October (27 #10^6 m^{-2} day^{-1}), followed by a moderate late spring/early summer maximum in December (14 #10^6 m^{-2} day^{-1}). In addition, some of the species contributed to a weak winter maximum in August (4 #10^6 m^{-2} day^{-1}). Nearly 83% of the entire diatom assemblage belonged to the order of Pennales, of which 80% was composed of only two very small and fragile species, i.e. *N. bicapitata* (<22 µm) and *Thalassionema nitzschioides* var. *incurvatum* that dominated the spring bloom. Small *N. bicapitata* dominated the diatom assemblage with 40% to 77% (60% on average) and valve fluxes of 0.5 to 20.5 # 10^6 m^{-2} day^{-1} (Figs. 4.5 and 4.6) often found aggregated in brownish flocs of organic matter. The other Pennales (e.g. the *Pseudonitzchia* pointed ends group with a needle-like outline, and the *N. bicapitata* group 2 (22-33 µm)) were generally larger and appeared in the late spring/early summer maximum together with centricate *Chaetoceros* vegetative cells. Other centricates were secondary contributors to the spring and winter maxima. The only exception was the giant pillbox-shaped *E. gazellae* that generated highest fluxes in summer (December), outside the periods of the main diatom blooms. This was a minor CWR species in terms of the flux of valves. Yet, we calculated that approximately 22.000 specimens of *N. bicapitata* (group 1) would equal one specimen of *E. gazellae*, if the diatom surface area is considered to be proportional to its silica weight, making it an equally important contributor to the total silica mass flux as the other secondary diatom species. Our samples were barren in continental species, whereas epibiontic and benthic species contributed only 0.2 and 0.1% to the total assemblages, respectively. This suggests a negligible lateral input derived by wind and/or advective transport of resuspended sediments.

Globorotalia inflata dominated foraminiferal assemblages both during the spring bloom and in the annual deposition flux, amounting to 38% and 25% of the total shell flux, respectively (Figs. 4.5 and 4.7). Its daily flux ranged from 10 to 600 # m^{-2} day^{-1} with an annual average of 74 # m^{-2} day^{-1} (Fig. 4.7). Most secondary species followed this general trend of maximum flux during October (e.g.

Figure 4.6: Deposition fluxes of major diatom species included in the PCA for the period Aug. 2000 – Feb. 2001, grouped according to their principal component scores (numbers given in upper corners). Fluxes of *E. gazellae* were not included in the PCA (counts in cups 4 and 6 are missing).

Figure 4.7 (next page): Deposition fluxes of major foraminiferal species included in the PCA for the period Aug. 2000 – Feb. 2001, grouped according to their principal component scores (numbers given in upper corners) in the size fraction >250 µm (dark grey bars) and 150-250 µm (light grey bars). Fluxes of *H. pelagica* were not included in the PCA.

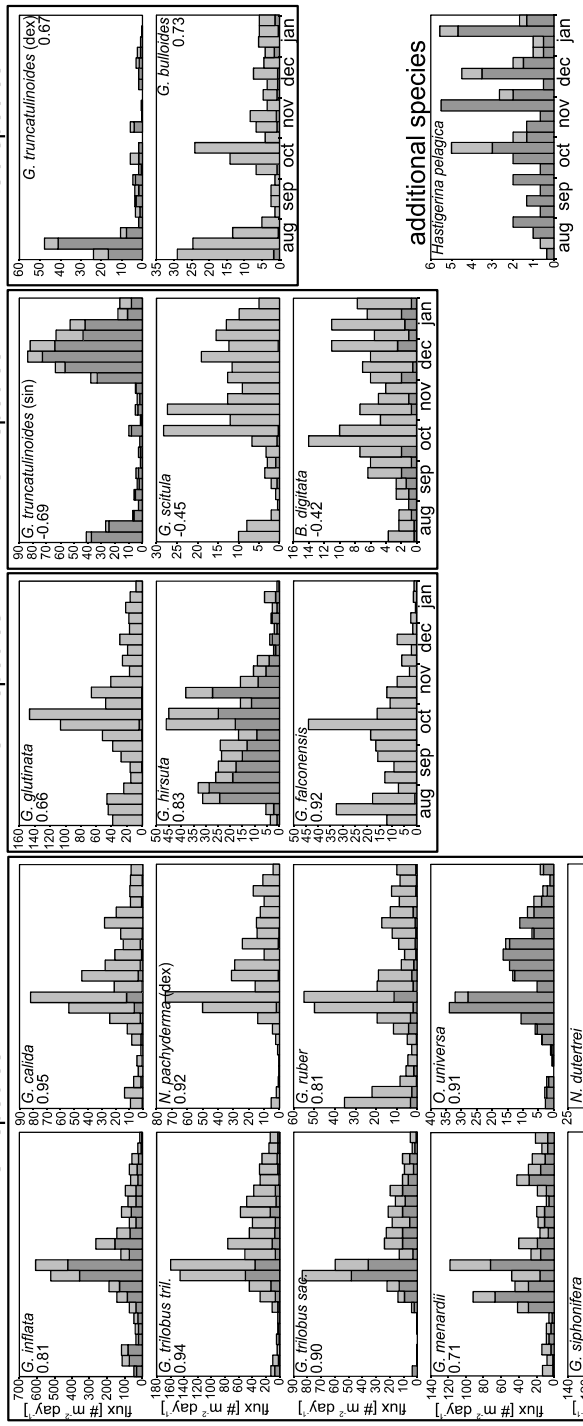
PC1 species
PC2+ species
PC2- species
PC3 species
additional species
G. inflata 0.81
G. calida 0.95
G. truncatulinoides (dex) 0.67
G. truncatulinoides (sin) -0.69
G. glutinata 0.66
G. bulloides 0.73
G. scitula -0.45
N. pachyderma (dex) 0.92
G. hirsuta 0.83
G. trilobus tri.
G. trilobus sac. 0.90
G. ruber 0.81
G. falconensis 0.92
B. digitata -0.42
O. universa 0.91
G. menardii 0.71
N. dutertrei 0.85
G. siphonifera 0.92
Hastigerina pelagica
flux [# m-2 day-1]
aug sep oct nov dec jan

G. trilobus s.l., *Globigerinita glutinata*, *Globorotalia menardii, Globigerinella siphonifera*, *Globigerinella calida*, *Globigerinoides ruber* and *Orbulina universa*). The most contrasting taxa to the general pattern were deep dwelling *Globorotalia truncatulinoides* sinistral and dextral, *Globorotalia hirsuta*, and *Hastigerina pelagica*, which all peaked outside the total flux maximum. Uniquely, *H. pelagica* showed a pronounced lunar cyclicity in deposition flux (Lončarić et al., 2005), despite its low abundance (Fig. 4.7), the required shell settling time and seasonal oceanography. This also testifies to the accuracy of time-series fluxes sampling and complete preservation of foraminiferal shells as collected by the 2700 m deep CWR sediment traps.

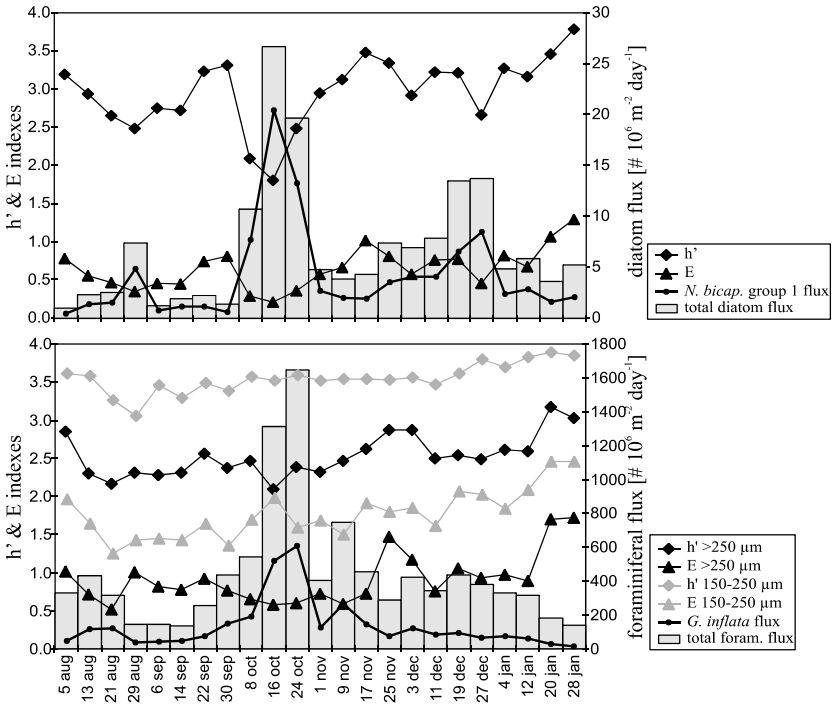

Figure 4.8: Diversity (Shannon – Weaver Information Measure h'; diamonds) and equitability (Buzas – Gibson index E; triangles) with the total fluxes (grey bars) and major species fluxes (small dots) of diatoms (upper panel) and foraminifera (lower panel) for the period August 2000 – February 2001.

3.4. Community structure of plankton deposition fluxes

3.4.1. Diversity and covariability

The diatom Shannon-Weaver diversity index dropped sharply from 3.8 to 1.8 during the diatom spring maximum overwhelmed by high fluxes of small *N. bicapitata* (Fig. 4.8). Diversity minima also accompanied the other flux maxima in August and December. The diatom equitability index closely followed this trend, although smaller in magnitude. For foraminifera by contrast, the Shannon-Weaver diversity remained remarkably constant with only a weak increasing trend from

winter 2000 to summer 2001, although the deposition flux increased by a factor of five during the spring maximum. Only a minor decrease was found in the coarse size fraction during the periods of high flux, due to the enhanced dominance of large *G. inflata* (Fig. 4.8). The diversity of the fine fraction (150-250 µm) was higher, but with a smaller amplitude of change (3.1 to 3.9) than in the coarse fraction (>250 µm) (2.1 to 3.2), testifying to the increased contribution of small, but important CWR species like *G. glutinata*, *N. pachyderma* and *G. falconensis* that rarely attain a size larger than 250 µm (Fig. 4.7). The foraminiferal equitability index followed diversity, except for the coarse fraction during the spring maximum, when it increased together with the shell flux.

Table 4.4: Factor scores and loadings from the principle component analysis on the species flux of foraminifera and diatoms, combined and separately, from the high-resolution sampling period (Aug. 2000 – Feb. 2001). For species codes see table 4.3.

FACTOR SCORES

mid time	foraminifera +diatoms			foraminifera			diatoms		cup no.
	PC 1	PC 2	PC 3	PC 1	PC 2	PC 3	PC 1	PC 2	
5/Aug/2000	-0.81	0.53	2.47	-0.07	0.29	2.51	-1.28	-0.30	1
13/Aug/2000	-0.78	0.83	2.11	-0.23	1.18	2.71	-1.01	-0.14	2
21/Aug/2000	-1.04	0.81	0.19	-0.83	1.53	0.81	-0.96	0.07	3
29/Aug/2000	-0.99	-0.20	-2.01	-1.72	0.95	-0.26	-0.13	0.33	4
6/Sep/2000	-1.59	0.05	-0.87	-1.66	0.63	-0.59	-1.27	-0.01	5
14/Sep/2000	-1.56	-0.12	-1.03	-1.78	0.58	-0.54	-1.10	-0.11	6
22/Sep/2000	-0.81	0.54	-0.52	-0.57	0.54	-0.96	-0.90	0.31	7
30/Sep/2000	-0.64	1.03	-0.33	-0.04	0.91	-1.49	-1.05	0.12	8
8/Oct/2000	0.49	0.81	-0.31	0.72	0.65	-0.56	0.24	0.49	9
16/Oct/2000	1.99	1.17	-0.85	1.80	1.34	-0.41	1.93	0.99	10
24/Oct/2000	2.33	1.49	-0.47	2.27	0.73	0.08	2.00	2.59	11
1/Nov/2000	0.07	0.73	-0.53	0.34	0.24	-0.98	-0.22	0.86	12
9/Nov/2000	0.38	1.32	0.76	1.12	0.57	-0.25	-0.32	0.77	13
17/Nov/2000	0.26	0.47	0.18	0.64	-0.11	-0.55	-0.15	0.36	14
25/Nov/2000	0.30	-0.45	-1.03	-0.03	-0.55	-0.98	0.48	0.32	15
3/Dec/2000	0.30	-0.43	0.33	0.43	-0.81	-0.43	0.10	-0.52	16
11/Dec/2000	0.22	-1.37	0.70	0.00	-1.22	0.31	0.37	-1.59	17
19/Dec/2000	1.19	-1.97	0.41	0.41	-0.72	0.62	1.80	-2.78	18
27/Dec/2000	0.98	-1.59	0.30	0.35	-1.45	0.44	1.37	-1.17	19
4/Jan/2001	-0.04	-0.64	0.76	0.04	-1.13	0.35	-0.15	-0.39	20
12/Jan/2001	0.23	-0.82	0.47	0.11	-1.47	0.30	0.18	-0.04	21
20/Jan/2001	-0.41	-0.84	0.00	-0.57	-1.07	-0.01	-0.28	-0.32	22
28/Jan/2001	-0.10	-1.34	-0.73	-0.71	-1.63	-0.13	0.33	0.17	23
var. explained	**49.8**	**17.5**	**8.3**	**53.1**	**20.9**	**12.5**	**65.1**	**15.9**	

3.4.2. Multivariate analysis

For the combined species fluxes of foraminifera and diatoms, principal component analysis (PCA) yielded three components that explained 76% of the total variance (Tab. 4.4), out of six with eigen values higher than 1 in the period from August 2000 to February 2001. Biplots of scores of the first and second component showed clear seasonal clustering in winter, spring and summer groups (Fig. 4.9a). The first component (49.8%) rendered high positive loadings for both diatoms (*T. nitzschioides* var. *incurvatum*, small *N. bicapitata*, *Thalassiosira lineata* and *Thalassiothrix spathulata*) and foraminifera (*G. trilobus* s.l., *G. calida*, dextral *N. pachyderma* and *O. universa*). The scores of PC 1 were positively correlated with the total mass flux as all species of this component as well as BSi and $CaCO_3$ shared a similarly prominent flux maximum in October (Figs.

4.5-4.7; Tab. 4.5). Three-dimensional plots of the component loadings (Fig. 4.9a) showed separate clusters for diatoms and foraminifera. Although most species from both groups shared high loadings on PC 1, they are separated by different loadings on other two components. PC 2 explained 17.5% of the total variance, with high positive loadings for foraminifera (*Globigerina falconensis*, *G. glutinata*, *G. hirsuta* and *G. inflata*), but negative loadings for diatoms (large *N. bicapitata*, *Pseudonitzschia* pointed ends group, *Chaetoceros* vegetative cells and *P. inflatula* var. *capitata*) (Fig. 4.9a; Tab. 4.4). Of all PC 2 foraminifera, only sinistral *G. truncatulinoides* showed a negative loading together with diatoms. The scores of PC 2 are inversely related to the SST and consequently, positively related to the SML depth (Tab. 4.5). Although *G. inflata* is the major foraminiferal contributor to the spring bloom, its loadings are equally high on the first and second component. High loadings on PC 3 (8.3% of the total variance) were found exclusively for deep-dwelling or rare foraminiferal species that flourished outside the spring bloom (positive for sinistral and dextral *G. truncatulinoides*, *Globigerina bulloides* and *Globorotalia scitula*; negative for *G. hirsuta*; Fig. 4.9a; Tab. 4.4).

Table 4.4: continued

FACTOR LOADINGS

species	foraminifera +diatoms			foraminifera			diatoms		
code	PC 1	PC 2	PC 3	PC 1	PC 2	PC 3	PC 1	PC 2	PC 3
DIG	0.76	-0.10	0.09	0.73	-0.42	-0.19			
GLU	0.51	0.79	0.13	0.72	0.66	0.08			
SIP	0.75	0.41	0.47	0.92	0.12	0.29			
BUL	0.37	0.33	0.52	0.47	0.26	0.73			
CAL	0.89	0.28	0.16	0.95	0.02	-0.03			
FAL	-0.01	0.80	0.01	0.21	0.92	0.05			
HIR	-0.02	0.78	-0.48	0.11	0.83	-0.44			
INF	0.64	0.65	0.07	0.81	0.50	-0.11			
MEN	0.63	0.37	-0.11	0.71	0.08	-0.36			
SCI	0.69	-0.11	0.52	0.75	-0.45	0.24			
TRD	-0.26	0.42	0.54	-0.06	0.58	0.67			
TRS	0.17	-0.69	0.61	0.05	-0.69	0.62			
TRI	0.90	0.15	0.10	0.94	-0.18	-0.19			
RUB	0.70	0.37	0.41	0.81	0.18	0.39			
SAC	0.88	0.10	0.02	0.90	-0.21	-0.31			
DUT	0.79	0.12	0.34	0.85	-0.25	0.15			
PAC	0.89	0.08	0.15	0.92	-0.28	-0.14			
UNI	0.87	0.19	0.10	0.91	-0.08	-0.18			
ALVMAR	0.77	0.02	-0.17				0.74	0.31	-0.52
AZPNEO	0.83	-0.12	-0.10				0.85	0.01	0.18
CHAVEG	0.56	-0.61	0.08				0.69	-0.57	-0.32
FRADOL	0.75	-0.04	-0.18				0.72	0.21	0.44
NITBI1	0.85	-0.06	-0.28				0.92	0.14	0.07
NITBI2	0.47	-0.75	-0.01				0.68	-0.66	-0.12
NITBRA	0.75	-0.46	-0.07				0.88	-0.29	0.22
NITSIC	0.76	0.16	-0.45				0.79	0.51	0.06
PNICAP	0.71	-0.47	-0.08				0.85	-0.37	0.18
PNIDSG	0.56	-0.75	0.08				0.71	-0.63	-0.05
RHIBER	0.67	0.29	-0.42				0.62	0.66	-0.15
TNEINC	0.88	-0.21	-0.17				0.92	-0.09	0.15
TNEINF	0.81	-0.19	-0.25				0.89	0.13	-0.03
TSIOLI	0.84	0.23	-0.28				0.79	0.53	0.00
TSIOVG	0.81	-0.28	-0.08				0.83	0.05	-0.32
TTHSPA	0.84	-0.18	-0.14				0.91	0.02	0.04

a) foraminifera & diatoms

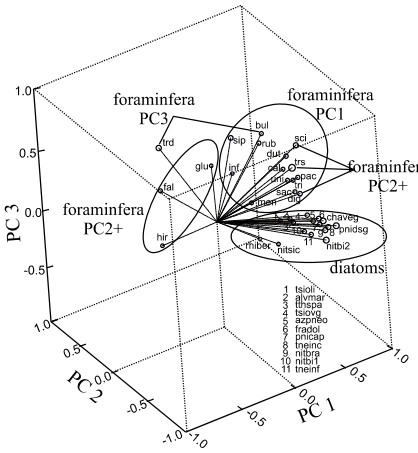

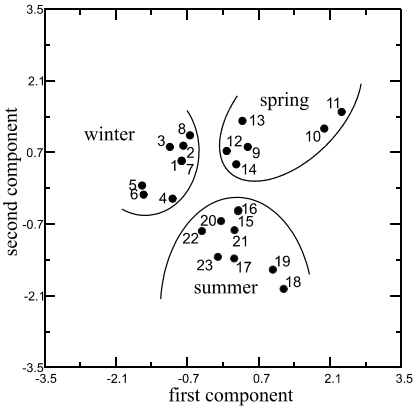

b) foraminifera

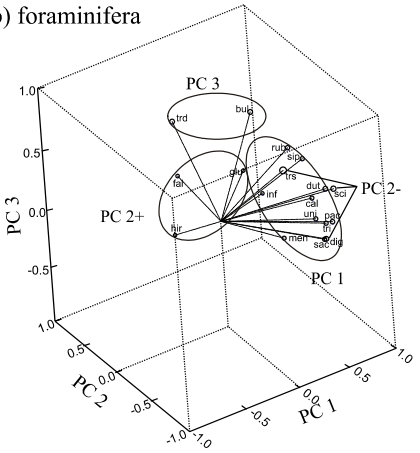

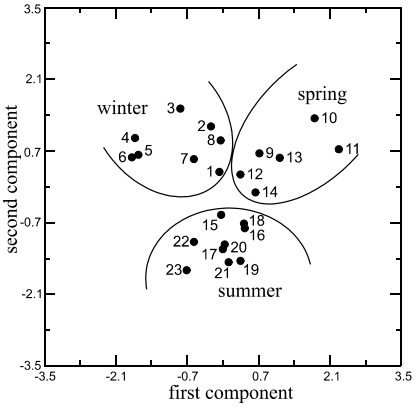

c) diatoms

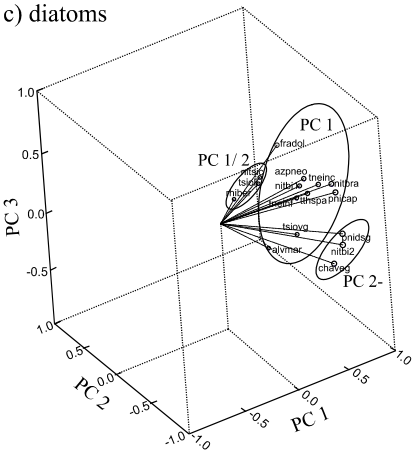

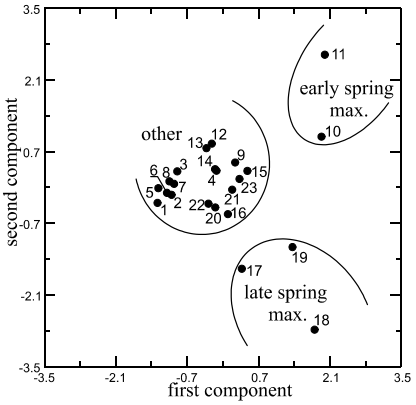

loadings scores

Figure 4.9 (previous page): Plots of factor loading (left panels) and scores (right panels) of the PCA based on the combined **(a)** and separated foraminiferal **(b)** and diatom **(c)** deposition fluxes from August 2000 – February 2001. Abbreviations and numbers refer to the species (Tab. 1) and sediment trap cups (Tab. 4), respectively. In the loading plots, long vectors in the same direction indicate a high positive correlation between species.

Principal component analysis performed on foraminiferal fluxes alone resulted in 3 components that together explained 87% of the total variance (Tab. 4.4). Most species had high loadings on PC 1 (Figs. 4.7 and 4.9b; Tab. 4.4) and typically showed maximum deposition in early spring. Species with high loadings on PC 2 had an additional flux peak in August, or reached the maximum completely outside the spring bloom, whereas PC 3 species had flux maxima in August. Similar to the combined fluxes, foraminifera showed clear seasonal clustering of the scores in the first and second component (Fig. 4.9b) and covariance with the calcium carbonate flux and SST, respectively (Tab. 4.5). The covariation of PC 2 with SST, chlorophyll-a concentration and depth of the SML was higher for the separated than for the combined fluxes (Tab. 4.5).

Separate analysis of diatom fluxes yielded only two components with eigen values higher than 1 which explained 81% of the total variance (Tab. 4.4). Species with high loadings on PC 1 had a prominent maximum in early spring and a weaker one in late spring (Fig. 4.6). Species with high loadings on both PC 1 (65%) and PC 2 (16%) did not have a clearly defined December peak and those with negative loadings on PC 2 bloomed only during late spring. Consequently, scores of PC 1 and PC 2 clustered according to the periods of bloom (Fig. 4.9c). Inasmuch as PC 1 scores were strongly related to the mass and BSi fluxes, PC 2 scores lacked significant covariation with any of the measured properties (Tab. 4.5).

Table 4.5: Linear correlation coefficients between the plankton fluxes and PCA scores, and the major flux compounds, SST, surface chlorophyll concentration and SML depth.

	linear correlation coefficient	mass	$CaCO_3$	BSi	C_{org}	SST	Chl-a	SML
flux	foraminifera	0.879	0.886	0.777	0.866	-0.257	0.006	0.255
	pteropods	0.840	0.850	0.818	0.717	0.181	-0.253	-0.187
	diatoms	0.832	0.812	0.858	0.816	-0.001	-0.284	-0.038
	silicoflagellates	0.720	0.733	0.735	0.563	0.107	-0.166	-0.149
PC scores	PC1 forams	0.847	0.847	0.766	0.766	-0.088	-0.326	-0.049
	PC2 forams	0.061	0.060	-0.044	0.325	-0.812	0.722	0.939
	PC3 forams	-0.300	-0.295	-0.284	-0.331	0.260	0.010	-0.042
	PC1 diatoms	0.794	0.785	0.846	0.647	0.225	-0.473	-0.345
	PC2 diatoms	0.402	0.431	0.254	0.460	-0.403	0.372	0.450
	PC1 combined	0.894	0.890	0.883	0.759	0.107	-0.458	-0.251
	PC2 combined	0.256	0.269	0.086	0.446	-0.723	0.560	0.787
	PC3 combined	-0.205	-0.203	-0.232	-0.261	0.210	-0.160	-0.142

3.5. Annual deposition and sediment accumulation

On an annual basis, 75% of the mass deposition flux during 2000 – 2001 was composed of calcium carbonate, with approximately equal secondary contributions by organic matter, biogenic silica and residual mass (Fig. 4.10 in appendix "colour figures"; Tab. 4.3). The foraminiferal deposition flux was dominated by *G. inflata* that contributed more than 25% of the assemblages, followed by *G. trilobus* s.l. (18%), *G. menardii* (9%), *G. glutinata* (7%), *G. siphonifera* (7%) and *G. ruber* (6%) (Tab. 4.1). Diatom annual deposition fluxes were overwhelmed by small *N. bicapitata*. This species group was an order of magnitude more abundant than *T. nitzschioides* var. *incurvatum*

and twenty times more abundant than *N. braarudii*, large *N. bicapitata* and *Thalassiosira oestrupii* (Tab. 4.1; Fig. 4.10 in appendix "colour figures").

Total mass accumulation flux of the surface sediment amounted to 45% of the deposition flux, with a calcium carbonate content of more than 90% and very low biogenic silica and organic carbon (Fig. 4.10 in appendix "colour figures"). *G. inflata* appeared the most dominant foraminiferal species in the accumulating sediment at approximately 3 to 5 times higher fluxes than *G. ruber, G. menardii, N. pachyderma* (dex), *G. siphonifera, G. trilobus* s.l. and *G. glutinata*, in that order (Fig. 4.10 in appendix "colour figures"; Tab. 4.1). The diatom sediment fluxes were dominated by small *N. bicapitata* with approximately two times higher fluxes than those of *F. doliolus* and *T. oestrupii* and three times higher than that of *T. nitzschioides* var. *incurvatum* (Fig. 4.10 in appendix "colour figures"; Tab. 4.1). Overall, the annual foraminiferal deposition flux during 2000 – 2001 was slightly lower than the accumulation flux in the sediment and similar in species composition (Fig. 4.10 in appendix "colour figures"). By contrast, the diatom fluxes showed large differences between the deposited and accumulating assemblages.

4. DISCUSSION

Transfer of skeletal remains and other particles exported from the productive upper water column to the deep ocean floor generally takes days to weeks. At the 8-day scale of sediment trap sampling at the CWR, this resulted in delayed deposition of particles at 2700 m depth with respect to the ambient conditions at the time the export flux was generated in the upper ocean. For the large, but thin tests of the foraminifer *Hastigerina pelagica*, we found settling velocities between 300 to 500 m day^{-1} at the CWR site using external tuning to its lunar reproduction cycle (Lončarić et al., 2005). In laboratory experiments, Takahashi & Bé (1984) observed that sinking speeds ranged between 320 and 1270 m day^{-1} for a number of foraminiferal species with shells larger than 150 μm. Although the heaviest shells of large species of foraminifera may arrive to the CWR ocean floor 2 days after export from the productive zone, they are considerably rare with respect to weakly calcified shells of small species, which would arrive at least 9 days later at CWR depth. Consequently, the delay between surface export and bottom deposition of foraminiferal shells should be in the order of a week, close to the 8-day interval of sampling.

For individual diatom frustules settling velocities as low as 0.3 to 0.5 m day^{-1} have been reported for some small species, including *Nitzschia* spp. (Margalef, 1961; Smayda and Boleyn, 1965; Lisitzin, 1972). Such low settling velocities imply that most individual diatom valves will have been dissolved before reaching the ocean floor in the silica-undersaturated water column. Therefore those diatoms that have reached the bottom are thought to have arrived in aggregates and pellets (Lisitzin, 1972), at much higher settling velocities (e.g. Smetacek, 1985; Alldredge and Gotschalk, 1988-1989). Such settling in aggregates results in 1 to 2 orders of magnitude higher velocities with respect to settling as individual valves, nearing the velocities of individually settling shells of small foraminifera. However, settling velocities of diatom-ballasted aggregates seem generally half that of a modal foraminiferal shell in the size fractions considered here (Smetacek, 1985), even accounting

for aggregate acceleration with depth (Berelson, 2002). Moreover, settling in aggregates also provides physical protection against dissolution prior to arrival, as evidenced by the high deposition flux of small diatoms and the reactivity of their biogenic silica at the CWR. We conclude that the settling velocities are not widely different between diatoms and foraminifera, probably by a week, which increases the difference between the export maxima in addition to the one week difference observed between their maxima in the deposition flux at the CWR (Fig. 4.5). Most large foraminiferal shells should settle to the CWR within a few days, those of small species within a week, perhaps 2 for thin-shelled ones, whereas aggregated particulate matter and the diatoms they carry should arrive about 2 weeks after export from the photic ocean.

4.1. Deposition fluxes of major particle compounds

The most pronounced maximum in the deposition flux at the deep CWR in early spring followed the collapse of surface chlorophyll concentrations after the SML had reached its greatest depth at the turn of winter. Departing from the summer stratification, the deposition cycle started with deep mixing in response to winter cooling and increased wind stress during late autumn. This resulted in breaching the nutricline and entraining new nutrients in the deepening SML followed by a steep rise in surface chlorophyll-a (Fig. 4.4). The delayed export from such new production was short-lived, judging from the $\delta^{15}N$ minimum in the enhanced deposition flux, suggesting that further nutrient entrainment was efficiently taken up by the winter community associated with a 120 m deep SML, albeit at rising losses to the deposition flux (Figs. 4.5 and 4.11). At the turn of winter, chlorophyll-a concentrations collapsed after shoaling of the SML and the associated nutrient entrainment came to a halt, followed by maximum deposition fluxes that arrived in early spring given the settling delay to the 2700 m deep sea floor of the CWR. Within a month, 23% of the annual mass, 25% of the diatom valves and 33% of the foraminiferal flux arrived in a sequence of coupled deposition maxima which marked the transition from winter to summer conditions at the CWR. It started with maxima in organic matter, BSi and diatom fluxes, and was followed by carbonate, foraminifera and pteropods about a week later (Figs. 4.5 and 4.11), related to the differential turn-over of (siliceous) phytoplankton and (carbonate) zooplankton groups in response to a changing upper ocean (see below). This was accompanied by the shifting "rain ratios" of carbonate carbon to C_{org} as well as BSi/C_{org}, which both showed a winter trend to low values and a summer trend to high values separated by the deposition maximum in early spring (Fig. 4.11). Spring deposition fluxes rapidly declined when stratification of the upper water column intensified and SST rose, apart from a brief disruption of the weak shallow stratification and enhanced productivity induced by the shoaling nutricline in November. This resulted in a short-lived maximum in surface water chlorophyll-a and a secondary maximum in phytoplankton silica that arrived in late spring in response to the development of a new, shallow and warm SML. Organic carbon and zooplankton carbonate fluxes appeared less affected, resulting in a short but significant drop in the BSi/C_{org} while the C_{carb}/C_{org} rain ratio only showed a minor minimum in the trend to high values in the low fluxes deposited during summer re-stratification.

On an annual basis the total mass deposition of 17 g m^{-2} yr^{-1} at the CWR site in 2000-2001 is within the range of typical ocean values but considerably lower than along the adjacent, more productive African continental margin (30 – 45 g m^{-2} yr^{-1}; Fischer and Wefer, 1996). Calcium carbonate accounts for 75% of the total mass flux of 12.8 g m^{-2} yr^{-1} which is on the high end of

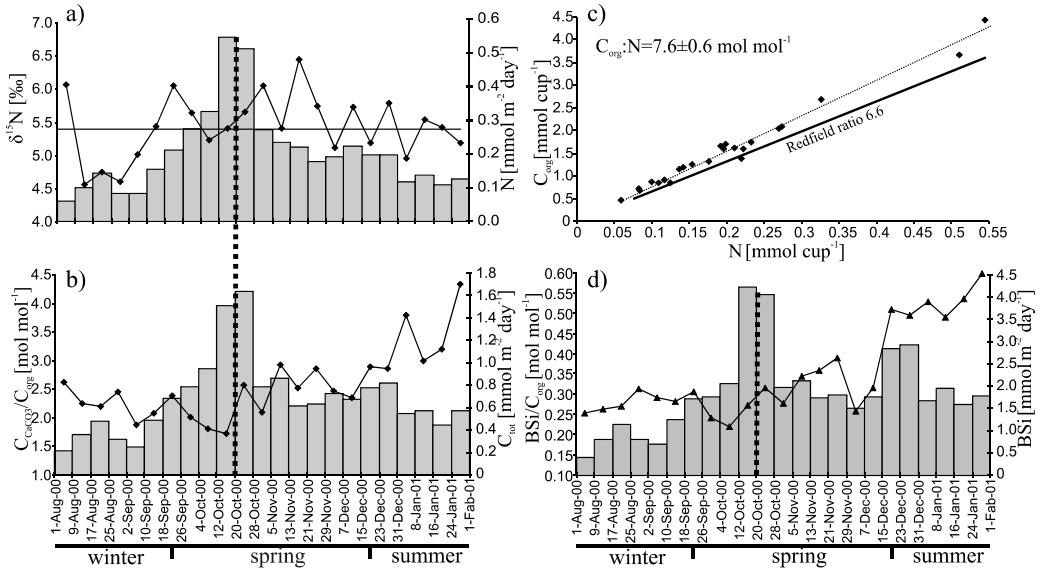

Figure 4.11: Deposition flux (bars) of nitrogen (**a**), total carbon (**b**) and biogenic silica (**d**) versus $\delta^{15}N$ record, carbonate carbon to organic carbon ratio and biogenic silica to organic carbon ratio (lines), respectively. The horizontal line in panel (**a**) refers to the flux normalized annual $\delta^{15}N$. Vertical dashed lines represent centre of the spring deposition maxima. Panel (**c**) shows the ration of organic carbon versus nitrogen in the deposition fluxes from August 2000 to February 2001 with the average of 7.6±0.6 mol mol^{-1} (dashed line). The Redfield ratio is given for comparison (bold line). For details see text.

typical deep-sea fluxes but well within the range reported from subtropical open oceans elsewhere (Milliman, 1993). At the CWR, C_{org} and total nitrogen were tightly bound in organic matter at a ratio of 7.6 ± 0.6 on a molar basis, and remained surprisingly constant from winter to summer despite an order of magnitude variability in deposition fluxes (Fig. 4.11). CWR values are only little higher than the organic C:N stoichiometric molar ratio of 7.3 (Anderson and Sarmiento, 1994) although significantly so relative to the classical Redfield ratio of 6.6 (Fig. 4.11) emanating from dissolved nutrient fields. Such higher C:N ratios in suspended and settling particulate matter are thought to result from the faster remineralisation of N with respect to C_{org} and are considered depth-dependent increasing by approximately 0.2 per km in the global ocean (Schneider et al., 2003). After accounting for this depth dependency at the 2700 m deep CWR, C:N ratios become statistically indistinguishable from upper ocean living plankton, despite the considerable spatial and temporal variability which Schneider et al. (2003) also reported for settling particles fluxes from the few available SE Atlantic sites.

4.2. Species fluxes and group-specific responses

4.2.1. Diatoms

All CWR diatom species are characteristically found in open ocean environments, except for some species of *Chaetoceros* which are also known from neritic habitats (Hustedt 1930-1959).

Pennate diatoms that composed 83% of the CWR diatom population are characterised by a longitudinal symmetry with an aligned surface pattern (Horner, 2002). Such dominance of pennate species in pelagic environments is striking because many genera within the pennate order have a raphe system with slits through each valve that allows benthic species to adhere to and move on a substrate (Wetherbee et al., 1998). However, many of the pelagic pennate species at the CWR lack this raphe system (Araphideae e.g. *Thalassionema* spp.) or have a (pseudo) keel-raphe system (*Nitzschia* spp., *Pseudonitzschia* spp.) as an adaptation to a pelagic mode of life (Buck and Chavez 1994; Iriarte and Fryxell, 1995; Romero et al., 2000). One of the pennates with a keel-raphe is *N. bicapitata*, the most dominant species at the CWR. Although this species may occur solitary, it is often found aggregated to organic matter and is therefore regarded to be pseudo-benthic (Fryxell, 2000). Its pseudo-benthic way of life attached to detritus promotes its survival since the substrate organic matter is an important source of nutrients supplied by bacterial regeneration and provides protection against filter-feeder grazing (Fryxell, 2000). In addition, this promotes the transfer of valves from the productive zone by enhancing their settling velocity in aggregated matter, as is also suggested by thigh correlation between fluxes of diatoms and C_{org} (Tab. 4.5), and provides protection against dissolution in the silica undersaturated ocean.

Within the pennate group we observed seasonal changes in valve size and shape. Spring samples were dominated by tiny and fragile solitary or aggregated pennate species while the long needle-like pennates together with large centricate *E. gazellae* predominated in summer, suggesting that changes in valve size and morphology are part of the species survival strategy in response to the seasonally changing conditions. This is clearly demonstrated by the dominance of the *N. bicapitata* group 1 in the spring maximum which may have resulted from rapid asexual cell division under favourable conditions, without auxospore production and resizing, yielding a large population of small specimens. Koning et al. (2001) associated high fluxes of *N. bicapitata* with the retreating monsoonal upwelling which similar to the CWR site also resulted in a productivity collapse and a maximum in deposition following the shutdown of nutrient entrainment and the onset of stratification. Among other important CWR diatoms are *T. nitzschioides*: *incurvatum* and *inflatum*, two varieties known from warm and saline waters of the Subtropical Gyre in the North Pacific (Tanimura, 1999). Apparently these represent oceanic oligotrophic modifications of the primarily euthrophic *T. nitzschioides* sensu stricto, which is characteristic for highly productive and less saline waters (Tanimura, 1999). The long needle-like species of the genus *Pseudonitzschia* are also known from generally warm and oligotrophic Sargasso Sea (Kaczmarska et al., 1986). The high abundance of *Pseudonitzschia* spp. in the CWR early spring flux maximum is therefore consistent with the elevated nutrient input, but still low availability in the SML during winter (Fig. 4.4).

One of the most characteristic oligotrophic species found in the deposition flux at the CWR is *E. gazellae*, although only sporadic valve fragments were preserved in the surface sediment. The species can reach a diameter of 2 mm (Hustedt, 1930-1959) and is the largest known diatom genus. *Ethmodiscus* is capable of vertical migration within the water column by controlling its buoyancy which thus allows access to an alternative, deep nutrient source. Such vertical migration is an algal survival strategy in nutrient-poor conditions and it has been reported for many larger non-motile phytoplankton species (Villareal and Carpenter, 1994). This strategy may explain the relatively uniform deposition fluxes of *E. gazellae* throughout the sampling period at the CWR, with a maximum flux outside the main diatom summer bloom, when stratification was strong and nutrient supply to the SML was subdued. Synchronous flux maxima of *E. gazellae* and the deep-dwelling

planktic foraminifera *G. truncatulinoides* (sin), suggest a similar survival strategy of these two species (Figs. 4.6-4.7), both profiting from alternative resources in the deeper water column rather than competing for them in the starved SML.

4.2.2. Planktic foraminifera

Foraminiferal deposition and accumulation fluxes at the CWR are dominated by *G. inflata* that formed 25% and 28% of total assemblages, respectively. Most secondary species followed the general flux pattern of *G. inflata* and other particle compounds, with a pronounced spring maximum in October (i.e. *G. trilobus* s.l., *G. menardii*, *G. siphonifera*, *G. calida* and *G. ruber*; PC1; Fig. 4.7). Shallow-dwelling *Globorotalia menardii* was distinguished by a prominent flux maximum of almost 100 # $m^{-2}day^{-1}$ in late September that preceded the main spring maximum by about 3 weeks. Although the first maximum coincided with that of chlorophyll-a in the surface water, its deposition maximum at the CWR is more likely triggered by nutrient entrainment into the SML in early August given the delayed arrival. Deposition fluxes of most deep-dwellers differed to some extent from the first order flux pattern. Only in *H. pelagica* a clear lunar frequency was recognised, despite the low deposition fluxes of weakly calcified shells and the strongly seasonal oceanography at the site (Lončarić et al, 2005). Deep-dwelling *Globorotalia hirsuta* (max. 45 # $m^{-2}day^{-1}$) appeared as a winter species following the breaching of the nutricline and the enhanced chlorophyll concentration in the deep SML until the collapse of the productive system in early spring. In addition to the main October maximum, low abundant *Globorotalia scitula* and *Beella digitata* showed a secondary flux peak during December and January that paralleled the secondary diatom bloom and was likely related to the brief interruption of the water column restratification in November.

Remarkably, both left- and right-coiled *G. truncatulinoides* peaked exclusively outside the early spring bloom. *G. truncatulinoides* is considered as one of the deepest-dwelling species among planktic foraminifera, with maximum concentrations far below the surface mixed layer and the photic zone (e.g. Hemleben et al., 1989; Lohmann and Schweitzer 1990; Lohmann, 1992). It has been known for decades that *G. truncatulinoides* in sediment cores shows distinct provinces in terms of the coiling direction of its trochospiral test (Ericson et al., 1954; Thiede, 1971). In plankton tows from South Atlantic surface waters, Bé and Tolderlund (1971) reported dominantly sinistral *G. truncatulinoides* southwards of 30-35°S, as was later confirmed by surface sediment assemblages (summarised by Kemle-von Mücke and Hemleben, 1999). Surprisingly, sinistral shells dominate both deposition and accumulation fluxes at the CWR site (27°S), which is more consistent with the findings from the Namibian and S. African margins, where sinistral *G. truncatulinoides* dominated and dextral populations only occurred northwards of 23°S (Giraudeau, 1993). In the CWR time-series, dextral *G. truncatulinoides* flourished during a single winter maximum (August), whereas the more abundant sinistral *G. truncatulinoides* showed a weak maximum in August and a second, strong one in summer (December-January) (Figs. 4.7 and 4.12). Sinistral *G. truncatulinoides* dominated throughout the CWR time-series and therefore largely determined the total flux pattern of *G. truncatulinoides* (Fig. 4.12), similar to the tow results reported by Lohmann and Schweitzer (1990) for the NW Atlantic winter. Its CWR maximum in winter suggests that the transition between sinistral and dextral *G. truncatulinoides* does not follow the seasonal migration of the South Atlantic thermal fronts, or at least not the associated local fluctuation in SST. Rather, the temporal switch in coiling dominance is related to the differential export productivity in response to the seasonal

stratification and/or governed by advection considering the poleward subsurface circulation (Reid 1989; Mohrholz et al., 2001).

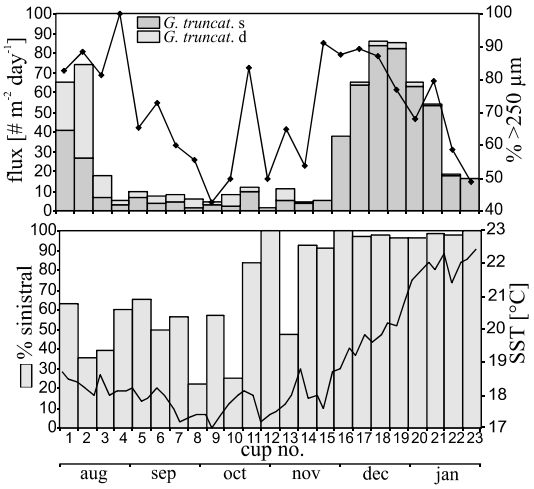

Figure 4.12: Deposition flux and relative abundance of sinistral and dextral *G. truncatulinoides* for the period Aug. 2000 – Feb. 2001. Upper panel shows the shell flux (bars) and percentage of the coarse size fraction (diamonds) and the lower panel the relative abundance of the sinistral shells in the total flux of *G. truncatulinoides* (bars) vs. SST (line).

Among others Lohmann and Schweitzer (1990) and Martinez (1994) associated enhanced abundances of the sinistral *G. truncatulinoides* with a very deep thermocline, and reported the dextral variety as the more tolerant to increased stratification and shoaling of the thermocline. At the CWR site only the weak winter peak, composed of both dextral and sinistral *G. truncatulinoides* was associated with a deep surface mixed layer. However, the most pronounced flux maximum exclusively composed of sinistral *G. truncatulinoides* occurred during the spring/summer transition characterised by a rapid increase in SST, shoaling of the surface mixed layer and restratification of the upper water column. The left/right-coiling ratio appeared better synchronised with these changing conditions than the absolute fluxes, with highest ratios in the period of high SST and shallow SML (Fig. 4.12). The spring increase in the overall shell size paralleled the dominance of the left-coiled shells (Fig. 4.12), similar to the sediment observations of Thiede (1971) and combined plankton tow/sediment results of Lohmann and Schweitzer (1990), a phenomenon attributed to the shoaling of the main thermocline.

The different seasonal response of left- and right-coiled *G. truncatulinoides* in the CWR time-series merits their taxonomic recognition as distinct "cryptic" species, rather than mere coiling varieties of a single species. This interpretation is in line with recent DNA studies on planktic foraminifera (e.g. Darling et al., 1999). More specifically, de Vargas et al. (2001) identified a complex of genetic species within *G. truncatulinoides* separated by significant distances in ribosomal genes. The CWR flux record provides additional evidence that such genetic species not only differ in their genome, but also show a different seasonal ecology. In addition, the cryptic speciation within *G. truncatulinoides* morphotypes may explain ecological discrepancies between the CWR in the South Atlantic and the Sargasso Sea in the North Atlantic (Lohmann and Schweitzer, 1990).

4.3. Diversity and communal responses

The Shannon-Weaver diversity index (h') shows a strong inverse relationship with the diatom flux (Fig. 4.8), particularly in spring when productivity is overwhelmed by *N. bicapitata*. Also the equitability (E) shows this trend, with relative minima during the periods of high deposition flux at

the CWR. A similar, although less distinct antithetic relationship between the diatom flux and (h') has been observed at the Namibian margin (Treppke et al., 1996b), even though the species composition was entirely different. Such diatom diversity as a unimodal function of standing stocks, with maximum diversity at intermediate levels of standing stocks and minima during bloom periods, is common in marine phytoplankton and terrestrial plants (Irigoien et al., 2004). By contrast, the diversity of foraminifera remains unchanged during periods of maximum flux, apart from a weak increasing trend from winter towards summer and slightly enhanced values during the period of highest SST and strongest stratification (Fig. 4.8). Different trends in diversity of phyto- and zooplankton have been interpreted as due to uncoupling of producer and consumer communities of marine plankton that react differently to the changing environmental conditions (Irigoien et al., 2004). Such uncoupling may be caused by the nature of their diet, where most phytoplankton are specialised feeders and most zooplankton, in turn, are generalists (Irigoien et al., 2005). At the CWR, such uncoupling can also be recognised between protistan and metazoan plankton, where foraminifera predominated in winter and pteropods in summer (Fig. 4.5), reflecting their different manner of feeding and trophic position within the oligotrophic food web.

Rather than be caused by uncoupling, the one-week lag between deposition maxima of diatoms and foraminifera may alternatively have resulted from the faster response of phytoplankton to nutrient limitation, following the collapse of surface water productivity at the turn of winter. Foraminifera would have survived for at least another week, possibly 2 considering their faster settling with respect to diatoms. This is consistent with the observations of Sauter and Sancetta (1992) who encountered a similar one-week offset with foraminiferal flux lagging diatoms in the upwelling region of the San Pedro Basin.

Such delay between the deposition maxima is reflected in separate clustering of diatoms and foraminifera on the three-dimensional loadings plot, which also revealed strong seasonal clustering of species fluxes with distinct winter, spring and summer community sequences (Fig. 4.9a). This seasonality was most pronounced for foraminifera (Fig. 4.9b), whereas diatoms clustered according to the bloom and non-bloom periods (Fig. 4.9c). Both diatom and foraminifera deposition maxima showed strong coherence with those of organic carbon (Tab. 4.5), testifying to their dependence on wind-driven deep mixing that controls resources at this oligotrophic open ocean site. Surprisingly, the CWR diatom fluxes showed little correspondence with the satellite-derived chlorophyll-a. This record, derived from colour reflectance by remote sensing, yields the surface water concentrations which can be taken as representative for the SML, but does not account for the diatom populations below, e.g. in the deep chlorophyll maximum zone for most of the year. Furthermore, in the oligotrophic surface waters over the CWR, other pico- and nano-plankton autotrophs rather than diatoms may account for 60-70% of the total primary production, similar to other predominantly oligotrophic areas (Herbland et al., 1985; Chavez and Barber, 1987; Rodier and Borgne, 1997). Therefore the CWR record argues that most diatom export productivity is generated at greater depth, associated with the deep chlorophyll maximum and the nutricline (Fig. 4.4). None of the particle fluxes correlated with SST except for the PC 2 foraminifera. The strong inverse correlation is remarkable since the foraminiferal PC 2 is mostly composed of deep-dwelling species that live below the seasonal thermocline and are not directly related to the SST. Inverse correlation of PC 2 foraminifera with SST is accompanied by a strong positive correlation with the SML depth (Tab. 4.5). Since the SST record at the CWR site is about the inverse of the SML depth this may suggest

that foraminiferal species from PC 2 benefit from deep winter mixing and weak surface stratification rather than be related to the SST change.

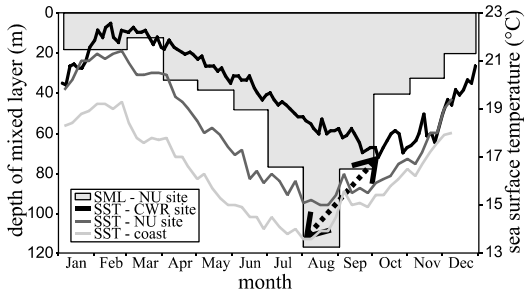

Figure 4.13: SST record along the Benguela trophic gradient from coastal Namibia to the CWR. Note the oceanward delay in the SST winter minimum and higher absolute SST.

4.4. Benguela trophic gradient

From the open oligotrophic SE Atlantic to the highly productive Namibian margin flux maxima appeared associated with parallel winter minima in SST and maxima in SML depth, but may be offset by up to 2 months. Along the Benguela trophic gradient, SST minima/SML maxima first occur in early August along the coast in the area of permanent upwelling, then at the outer margin in late August (NU site; Romero 2002) and finally in the open ocean at the CWR during October (Fig. 4.13). This oceanward delay is related to the annual fluctuation in the sea-air heat exchange modulated by fluctuation in upwelling intensity along the gradient. Consequently, the NU winter blooms are triggered by the same mechanism as at the CWR, related to the nutricline breaching despite the 2 months delay that separates the deposition flux maxima. Annual fluxes of most major components increase shoreward, from the open ocean CWR site towards the NU and WR sites at the Namibian margin (Romero et al., 2002; Fischer and Wefer, 1996; Treppke et al., 1996b), (Tab. 4.6). In the open ocean, the total mass flux is half that at the margin. Also the ratio of carbonate carbon to organic carbon decreases shoreward, similar to the trends observed in the eastern boundary current of the Pacific Ocean (Ortiz and Mix, 1992).

Remarkably, the annual diatom deposition is much higher at the CWR ($20x10^8$ valves m^{-2} $year^{-1}$) than Romero et al. (2002) found at the NU site ($1.5x10^8$ valves m^{-2} $year^{-1}$) and identical with the WR site (Treppke et al., 1996b), although both are under direct influence of Benguela upwelling where diatom productivity and export should be enhanced (Fig. 4.3 in appendix "colour figures"; Tab. 4.6). Whereas small *N. bicapitata* constitutes 60% of the diatom deposition flux at the CWR, the entire group contributes only 6% at the WR site, with order of magnitude lower maxima in spring and fall (Treppke et al., 1996b). Instead of small *N. bicapitata*, larger taxa dominate assemblages associated with the Benguela upwelling, i.e. *Flagilariopsis, Azpeitia* and *Actinocyclus* at the NU site and *Thalassionema, Pseudonitzschia* and *Rhizosolenia* at the WR (Treppke et al., 1996b; Romero et al., 2002). Diatom fluxes found at the CWR were higher than in the equatorial regions (southern Guinea Basin: Lange et al., 1994; off western equatorial Africa: Romero et al., 2000; off north Mauritania: Lange et al., 1998), where small *N. bicapitata* is also abundant (Lange et al., 1994, 1998; Treppke et al., 1996a, 1996b; Romero et al., 1999), and they were similar to the non-upwelling winter periods off Somalia (Koning et al., 2001). Yet, they were lower than characteristically found within coastal upwelling, e.g. off Somalia (Koning et al., 2001), California (Sautter and Sancetta, 1992; Thunell et al., 1994; Thunell, 1998) and in the northern Guinea Basin (Lange et al., 1994; Treppke et al., 1996a). The dominance of small and weakly-silicified species such as *N. bicapitata* may additionally be controlled by silica limitation on the Benguela trophic gradient in respect to the larger and well-silicified species near the Namibian margin. Thus small shell size and weak silification of the

dominant species may account for such discrepancy of high valves at low silica fluxes at the oligotrophic CWR site (Tab. 4.6).

	CWR (27°00'S, 3°51'E)	NU (29°12'S, 13°07'E)	WR (20°03'S, 9°09'E)	
annual fluxes	trap depth 2699 m	trap depth 2516 m	trap depth 599 m	trap depth 1663 m
total mass [g m^{-2} yr^{-1}]	17.0	30.7	43.9	31.1
calcium carbonate [g m^{-2} yr^{-1}]	12.8 (74.9%)	21.3 (69.4%)	27.5 (62.5%)	17.7 (56.9%)
biogenic opal [g m^{-2} yr^{-1}]	1.2 (7.0%)	2.9 (9.4%)	3.9 (8.8%)	3.7 (11.9%)
organic carbon [g m^{-2} yr^{-1}]	0.7 (4.0%)	1.6 (5.2%)	4.6 (10.5%)	3.2 (10.3%)
residual [g m^{-2} yr^{-1}]	1.6 (9.4%)	4.4 (14.3%)	3.4 (7.8%)	3.6 (11.6%)
foraminifera [# m^{-2} yr^{-1}]	$1.1x10^5$	$1.3x10^5$	$3.4x10^5$	
diatoms [# m^{-2} yr^{-1}]	$20x10^8$	$1.5x10^8$	$20x10^8$	
season of highest flux	spring	summer and winter	fall and spring	
foraminiferal composition	*G. inflata* dominates spring bloom and annual flux; secondary contributors: *G. trilobus, G. glutinata, G. siphonifera, G. ruber*	*G. inflata* year round, secondary contributors *N. pachyderma* (dex), *G. bulloides, O. universa*	*G. inflata* and *N. dutertrei* dominate flux, secondary contributors *N. pachyderma* (dex) *G. bulloides, O. universa*	
diatom composition	*N. bicapitata* overwhelms (60%), secondary contributor: oceanic *T. nitzschioides* var. *incurvatum* (6%); occurrence of oligotrophic genus *Ethmodiscus*	pelagic *F. doliolus*, high contribution of coastal species in summer	neritic *T. nitzschioides* accompanied by oceanic/tropical and subtropical species *Pseudonitzschia* spp., *R. bergonii*, *N. bicapitata* (6%)	

Table 4.6 (previous page): Comparison of the major particle flux compounds along the Benguela trophic gradient represented by the CWR, NU (Romero et al, 2002) and WR (Treppke et al., 1996, Fischer and Wefer, 1996 and Romero et al., 1999) sediment trap sites. For locations see Figure 4.1.

Annual deposition fluxes of foraminifera were remarkably similar along the Benguela trophic gradient (Tab. 4.6) considering the pronounced influence of coastal upwelling near the Namibian margin. (Fig. 4.3 in appendix "colour figures"). At the CWR, *G. inflata* dominated the foraminiferal fluxes and constituted 25% and 28% of the annual deposition and accumulation assemblage, respectively, ranging from 10% in periods of low productivity to over 30% during the early spring maximum. By contrast, its deposition flux increased by a factor of 3 at the higher productivity levels prevailing at the NU and WR sites adjacent to the Benguela upwelling, where it formed up to 90% of the assemblages (Romero et al., 2002). This is accompanied by a significant change in the composition and flux of secondary species along the gradient, from the warm species in the open ocean (e.g. *G. trilobus* s.l., *G. ruber, G. menardii, G. siphonifera, G. calida, G. falconensis*) to cold water species at the margin (e.g. *G. bulloides, G. pachyderma* (dex); Romero et al., 2002) whose maximum abundance in the surface sediment coincides with the seaward limit of the upwelled water (Giraudeau, 1993). Further coastward in the sediments below permanent coastal upwelling, the foraminiferal assemblages are dominated by *N. pachyderma* sin. and *T. quinqueloba* (Giraudeau, 1993) that were virtually absent at the CWR. The absolute temperature difference of about 3.5°C may have contributed to the species change along the Benguela gradient (Fig. 4.13). At about the same absolute flux of foraminifera (Tab. 4.6), the species diversity in the open ocean is much higher than at the margin, as 28 and 12 species have been encountered at the CWR and NU sites, respectively. The modest increase in deposition fluxes of major particle compounds, from the oligotrophic Subtropical Gyre towards the eutrophic coastal upwelling, argues for only moderate productivity and deposition at the Namibian continental margin. In summary we conclude that increasing dominance of *G. inflata* coupled with a decreasing diversity and abundance of secondary warm species mark the transition from oligotrophic to mesotrophic conditions along the Benguela trophic gradient. A decreasing dominance of *G. inflata* combined with the absence of warm species and increasing abundance of *G. bulloides*, dextral *N. pachyderma* and ultimately sinistral *N. pachyderma* together with *T. quinqueloba* accompany transition from mesotrophic conditions to the eutrophic coastal ocean.

4.5. Sediment accumulation and preservation

Whereas the residence time of particles settling to 2700 m depth is in the order of a few days to weeks, it will usually take decades before the seasonal deposition fluxes are actually buried in the deep ocean sediment. As a consequence, the long residence time at the sediment-water interface generates ample exposure to transient microbial degradation and chemical decomposition. In order to determine the burial transfer and sedimentary preservation of seasonal and annual deposition fluxes, they are contrasted to the sediment accumulation flux (Fig 4.10 in appendix "colour figures"; Tabs. 4.1 and 4.3). Such a direct comparison appears warranted at the CWR, since the ^{210}Pb core profile showed a high activity in the topmost 0.5 cm (Fig. 4.2) indicating modern sediment accumulation and low sediment mixing at the time scale of ^{210}Pb decay with a half-life of 22 years. Furthermore, the sediment trap records of organic matter, δ^{15}N, biogenic silica, residual mass and plankton

assemblages offered no evidence of any significant lateral input from resuspended sediment or rebound fluxes, allowing direct comparison of the annual deposition and centennial accumulation fluxes.

Of all particle groups, only foraminiferal shells appear to be transferred fully to the sediment judging from a burial factor close to unity (1.4), implying full preservation consistent with the supersaturation of the bottom water with respect to their calcite shell. Moreover organic matter fluxes were too low to induce any significant metabolic driven dissolution in the sediment or to support strong bioturbation and concomitant fragmentation. Foraminiferal shells in the >150 µm fraction appear to be better transferred than biogenic carbonate in general as the dominant phase in the mass deposition flux with a burial factor of 0.55. Undoubtedly aragonite dissolution contributed importantly to this loss, as only fragments remained of the large deposition flux of pteropod shells after prolonged exposure to the undersaturated bottom water at the CWR (Tab. 4.3). For the shallower Namibian margin, Fischer and Wefer (1996) reported a better apparent preservation of the total carbonate at a burial factor of 0.8, consistent with bottom water saturation with respect to all carbonate phases in the deposition flux, rather than calcite alone. Residual deposition fluxes, including labile biogenic phosphates appear less well transferred at the CWR (BF 0.45), compared to the Namibian margin (Fischer and Wefer, 1996; Romero et al., 2000). Despite lower total mass fluxes at the CWR, its burial (BF = 0.45) is within the range reported for the Eastern Atlantic (0.38-0.63) and identical to the WR site at the Namibian margin (Fischer and Wefer, 1996).

Organic matter and biogenic silica showed intense degradation and losses to the bottom water, yielding burial factors that are lower by two orders of magnitude with respect to the deposition flux at the CWR (BF < 0.01). Consequently, the preservation of these phases is poor, testifying to their reactivity on the time scales of the sediment accumulation at the central Walvis Ridge and elsewhere in the eastern Atlantic, including the Namibian margin (Fischer and Wefer, 1996). Such considerable losses are typically caused by the selective removal of organic matter by microbial decomposition and of biogenic silica by dissolution in the undersaturated bottom waters. Extensive microbial degradation of organic matter is also evidenced by the highly enriched $\delta^{15}N$ in the topmost sediment with respect to the deposition flux (+ 3.9‰) that typically result from nitrogen-limited if not carbon-limited oxidation (Altabet, 1996; Brummer et al., 2002). As a result the contribution of C_{org} dropped from 4.0% to 0.08% in the topmost sediment of the CWR, resulting in a pronounced increase in the ratio of C_{carb} to C_{org} relative to the annual rain-ratio in the deposition flux from 2.2 to 131.

Biogenic silica is severely affected by dissolution in the undersaturated ocean water, resulting in a burial factor of only 0.002 at the CWR, even lower than the efficiencies summarised by Koning et al. (1997) for a wide range of sites in the world oceans. The onset of dissolution could already be traced in the increased concentration of dissolved silica during deployment of the sediment traps and sample storage (Fig. 4.14). Severe dissolution is accompanied by pronounced changes in the species assemblages of silicious phytoplankton at the sediment-water interface prior to burial (Fig. 4.10 in appendix "colour figures"). Whereas *N. bicapitata* constitutes 60% of the diatom deposition flux, it only comprises 20% in the topmost sediment, with a burial factor as low as 0.001. The sediment surface is relatively enriched in the larger more heavily silicified species of centricate diatoms which are known to preserve much better than the small specimens of weakly silicified pennates (Lange et al., 1994; Treppke et al., 1996b; Lange et al., 1998; Romero et al., 2000; Koning et al, 2001; Seeberg-Elverfeld et al., 2004). Yet, even for the best preserved centricate species *F. doliolus* and *A.*

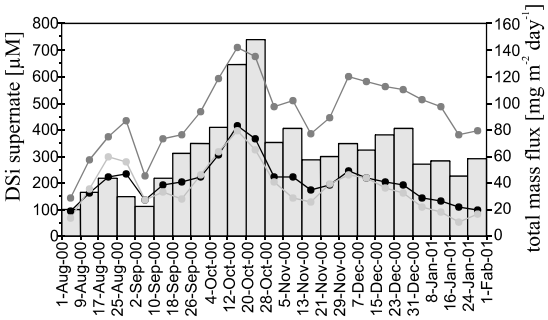

Figure 4.14: Dissolved silica concentration in the collecting bottles of the sediment trap moored 250 m (light grey) and 2 m (black) above the sea floor measured immediately after recovery, as well as several moths later in the laboratory for the bottom trap (dark grey), illustrating the high reactivity of the intercepted biogenic silica flux (bars).

marinus, accumulation did not exceed 2% of the annual deposition flux. At such high levels of dissolution, species valve size and specific mass determine the residual composition of sedimentary assemblages rather than the seasonal export flux, thus complicating paleoceanographic interpretation of diatom fluxes and assemblages from sediment records. As it appears, most biogenic silica produced in the photic ocean is rapidly exchanged with the deep bottom water, refuelling productive surface waters on the long time scale of ocean overturning circulation.

With a burial factor of 1.4, foraminiferal calcite shells showed the highest level of efficiency in the transformation of seasonal deposition to centennial sediment accumulation, both in terms of shell fluxes and in species composition (Fig. 4.10 in appendix "colour figures"). At such a high level of overall preservation, variability due to interannual change in the timing and magnitude of deposition fluxes may be invoked with respect to the single year we sampled, apart from possible errors associated with determining the sediment accumulation flux. Both depositional and accumulation fluxes are dominated by *G. inflata* at a burial factor of 1.5, followed by about equal proportions of secondary species. The non-spinose *G. truncatulinoides* and dextral *N. pachydema* were enriched by a factor of 4.0 and 3.2 in the sediment, respectively. Some spinose species, including *G. ruber*, *O. universa* and *G. falconensis* appear less enriched, whereas *G. trilobus* s.l. and *G. calida* were equally depleted by a factor of 0.5 with respect to their deposition flux. The absence of the rare spinose species *H. pelagica* (BF = 0) and virtual absence of *Beella digitata* (BF = 0.3) in the sediment should be attributed to fragmentation during burial rather than dissolution of their fragile large shell. Rather, inter-annual changes in seasonal productivity will have contributed to the inter-specific differences on the centennial time scale of sediment accumulation with respect to the deposition flux, perhaps as non-analogue conditions with respect to anthropogenic change.

5. CONCLUSIONS

A prominent early spring maximum of all biogenic particles characterised the time-series flux records from the CWR sediment traps, when about one quarter of total mass annual flux arrived at the sea floor following the ceased nutrient supply in the SML. In terms of its particulate export, foraminiferal shell fluxes closely followed the seasonally changing productivity regime as appears from a comparison with diatom fluxes and other siliceous phytoplankton, but also with total mass, organic carbon and biogenic silica fluxes. However, only for foraminiferal shells we could ascertain

full preservation in the topmost sediment, as moderate to severe diagenesis at the sediment-water interface affected the seasonal deposition fluxes of all other components. Consequently, sediment *G. inflata*, *G. glutinata* and most other species appear predominantly deposited in response to and as part of the seasonal productivity changes in the pelagic system as a whole. Thus they followed the seasonally enhanced productivity by nutrient entrainment during deep winter mixing, generating maximum deposition fluxes in early spring. Important exceptions include both sinistral and dextral *G. truncatulinoides*, which did not show a maximum at that time, but instead had a maximum in early winter as well as late spring, or in late spring alone, respectively. Such different seasonal response of *G. truncatulinoides* argues for a separate taxonomic status, rather than only a variation in the shell coiling of the single species. In view of recent DNA studies these findings suggest that genetic species differ not only in their DNA structure, but also in the ecology behaviour.

Along the Benguela trophic gradient, from oligotrophic open ocean towards the continental margin associated with the coastal upwelling, the foraminiferal fluxes were characterised by the increasing dominance of *G. inflata* (from <40% to >80%) and change over in secondary species, from warm to intermediate/cold water assemblages. In diatom fluxes shoreward along the gradient, longer and heavier-silicified species substituted the small and weakly silicified genus *Nitzschia*. Although the annual fluxes of all major particle components increased shoreward, the differences were rather small. Central Gyre particle deposition accounted for 40-60% and 20-70% of the outer and inner margin deposition, respectively. This testifies to only moderate productivity and deposition at the Namibian margin with respect to the open Subtropical Gyre.

6. ACKNOWLEDGEMENTS

We acknowledge the captains, crews and scientific parties onboard the R/V Pelagia and Agulhas for their assistance during the MARE cruises. Gene Carl Feldman and Norman Kuring from the SeaWiFS are acknowledged for providing the satellite derived chlorophyll-a records. We thank Henko de Stigter and Thomas Richter for helpful suggestions considering the box core stratigraphy, Erica Koning and Sharyn Crayford for the analyses of biogenic opal, C_{tot} and C_{org} and Wim Boer for the ^{210}Pb activity measurements. This work was financially supported by the Netherlands - Bremen Oceanography (NEBROC) and Mixing of Agulhas Rings Experiment (MARE) programs of the Netherlands Organisation for Scientific Research (NWO - ALW) as well as the bilateral NWO-DFG proxy development program.

REFERENCES

Abrantes, F. Gil, I., Lopes, C. & Castro, M., 2005. Quantitative diatom analyses – a faster cleaning procedure. *Deep-Sea Research I, 52* (1): 189-198.

Alldredge, A.L. & Gotschalk, C.C., 1988. In situ settling behaviour of marine snow. *Limnology and Oceanography, 33* (3): 339-351.

Alldredge, A.L. & Gotschalk, C.C., 1989. Direct observations of the mass flocculation of diatom blooms: characteristics, settling velocities and formation of diatom aggregates. *Deep-Sea Research, 36*: 159-171.

Altabet, M., 1996. Nitrogen and Carbon isotopic tracers of the source and transformation of particles in the deep sea. In: V. Ittekkot, P. Schaefer, S. Honjo, & P.J. Depetris (Eds.), *Particle Flux in the Ocean, SCOPE Report*, *57*, Wiley, Chichester: pp. 155-184.

Anderson, L.A. & Sarmiento, J.L., 1994. Redfield ratios of remineralization determined by nutrient data-analysis. *Global Biogeochemical Cycles, 8* (1): 65-80.

Bárcena, M.A., Flores, J.A., Sierro, F.J., Pérez-Folgado, M., Fabres, J., Calafat, A. & Canals, M., 2004. Planktonic response to main oceanographic changes in the Alboran Sea (Western Mediterranean) as documented in sediment traps and surface sediments. *Marine Micropaleontology*, *53* (3-4): 423-445.

Berelson, W.M., 2002. Particle settling rates increase with depth in the ocean. *Deep-Sea Research II, 49*, 237-251.

Batterbee, R.W., 1973. A new method for the estimation of absolute microfossil numbers, with reference especially to diatoms. *Limnology and Oceanography, 18*: 647-653.

Bé, A.W.H. & Tolderlund, D.S., 1971. Distribution and ecology of living planktonic foraminifera in surface waters of the Atlantic and Indian Oceans. In: W.R. Riedel (Ed.), *The Micropaleontology of the Oceans*). Cambridge University Press, Cambridge: pp. 105-149.

Berger, W.H. & Wefer, G., 1990. Export production: seasonality and intermittency, and paleoceanographic implications. *Palaeogeography, Palaeoclimatology, Palaeoecology (Global and Planetary Change Section), 89* (3): 245-254.

Bonnin, J., van Raaphorst, W., Brummer, G.J.A., van Haren H. & Malschaert, H., 2002. Intense mid-slope resuspension of particulate matter in the Faeroe-Shetland Channel: short-term deployment of near-bottom sediment traps. *Deep-Sea Research I, 49* (8): 1485-1505.

Brummer, G.-J.A., Kloosterhuis, H.T. & Helder, W., 2002. Monsoon-driven export fluxes and early diagenesis of particulate nitrogen and its $\delta^{15}N$ across the Somalia margin. In: P.D Clift, D. Kroon, C. Gaedicke & J. Craig (Eds.), *The Tectonic and Climatic Evolution of the Arabian Sea Region*. Geological Society, Special Publications, 195, London: pp. 353-370.

Buck, K.R. & Chavez, F.P., 1994. Diatom aggregates from the open ocean. *Journal of Plankton Research, 16* (10): 1449-1457.

Burckle, L.H., 1978. Marine diatoms. In: B.U. Haq & A. Boersma (Eds.), *Introduction to marine micropaleontology*. Elsevier, New York: pp. 245-266.

Buzas, M.A. & Gibson, T.G., 1969. Species diversity: benthonic Foraminifera in western North Atlantic. *Science, 163* (3862): 72-75.

Chavez, F.P. & Barber, R.T., 1987. An estimate of new production in the equatorial Pacific. *Deep-Sea Research, 34* (7): 1229-1243.

Conan, S.M.H., Ivanova, E.M. & Brummer, G.-J.A., 2002. Quantifying carbonate dissolution and calibration of foraminiferal dissolution indices in the Somali Basin. *Marine Geology, 182* (3-4): 325-349.

Darling, K.F., Wade, C.M., Kroon, D. & Brown, A.J.L., 1999. The diversity and distribution of modern planktic foraminiferal small subunit ribosomal RNA genotypes and their potential as tracers of present and past ocean circulations. *Paleoceanography, 14* (1): 3-12.

Deuser, W.G. & Ross, E.H., 1989. Seasonally abundant planktonic foraminifera of the Sargasso Sea: succession, deep-water fluxes, isotopic compositions, and paleoceanographic implications. *Journal of Foraminiferal Research, 19* (4): 268-293.

de Vargas, C., Renaud, S., Hilbrecht, H. & Pawlowski, J., 2001. Pleistocene adaptive radiation in *Globorotalia truncatulinoides*: genetic, morphologic and environmental evidence. *Paleobiology, 27* (1): 104-125.

Ericson, D.B., Wollin, G. & Wollin, J., 1954. Coiling direction of *Globorotalia truncatulinoides* in deep-sea cores. *Deep-Sea Research, 2* (2): 152-158.

Fischer, G. & Wefer, G., 1996. Long-term observation of particle fluxes in the Eastern Atlantic: seasonality, changes of flux with depth and comparison with the sediment record. In: G. Wefer, W.H. Berger, G. Siedler & D.J. Webb (Eds.), *The South Atlantic - present and past circulation*. Springer-Verlag, Berlin Heidelberg: pp. 325-344.

Fryxell, G.A., 2000. *Nitzschia bicapitata* (Bacillariophyceae) and related taxa from oceanic aggregations. *Diatom Research, 15* (1): 43-73.

Garzoli, S.L. & Gordon, A.L., 1996. Origins and variability of the Benguela Current. *Journal of Geophysical Research, 101* (C1): 897-906.

Gibson, T.G. & Buzas, M.A., 1973. Species diversity: patterns in Modern and Miocene Foraminifera of the eastern margin of North America. *Bulletin Geological Society of America, 84* (1): 217-238.

Giraudeau, J., 1993. Planktonic foraminiferal assemblages in surface sediments from the southwest African continental margin. *Marine Geology, 110* (1-2): 47-62.

Griffiths, F.B., Brown, G.H., Reid, D.D. & Parker, R.R., 1984. Estimation of sample zooplankton abundance from Folsom splitter sub-samples. *Journal of Plankton Research, 6* (5): 721-731.

Hemleben, C., Spindler, M. & Anderson, O.R., 1989. *Modern planktonic foraminifera*. Springer-Verlag, New York: 363 pp.

Herbland, A., Le Bouteiller, A. & Raimbault, P., 1985. Size structure of phytoplankton biomass in the equatorial Atlantic Ocean. *Deep-Sea Research, 32* (7A): 819-836.

Horner, R.A., 2002. *A taxonomic guide to some common phytoplankton*. Biopress Limited, Dorset Press, Dorchester: 200 pp.

Hustedt, F., 1930-1959. Die Kieselalgen Deutschlands, Östereichs, und der Schweiz. In L. Rabenhorst (Ed), *Kryptogamenflora von Deutschland, Östereichs und der Schweiz*. Akademische Verlagsgesellschaft Geest und Portig K.-G., Leipzig: pp. 920 and 845.

Iriarte, J.L. & Fryxell, G.A., 1995. Micro-phytoplankton at the equatorial Pacific (140° West) during the JGOFS EqPac Time Series studies: March to April and October 1992. *Deep-Sea Research II, 42* (2-3): 559-583.

Irigoien, X., Huisman, J. & Harris, R.P., 2004. Global biodiversity patterns of marine phytoplankton and zooplankton. *Nature, 429*: 863-867, doi: 10.1038/nature02593.

Irigoien, X., Huisman, J. & Harris, R.P., 2005. Different measures of biodiversity. *Nature, 433*: E9, doi: 10.1038/nature03321.

Kaczmarska, I., Fryxell, G.A. & Watkins, T.P., 1986. Effect of two Gulf Stream warm-core rings on distributional patterns of the diatom genus *Nitzschia*. *Deep-Sea Research, 33* (11-12): 1843-1868.

Kemle-von Mücke, S. & Hemleben, C., 1999. Foraminifera. In: D. Boltovskoy (Ed*.), South Atlantic Zooplankton.* Backhuys Publishers, Leiden: pp. 43-73.

King, A.L. & Howard, W.R., 2003. Planktonic foraminiferal flux seasonality in Subantarctic sediment traps: a test for paleoclimate reconstructions. *Paleoceanography, 18* (1): 1019, doi:10.1029/2002PA000839.

Koning, E., Epping, E. & van Raaphorst, W., 2002. Determining biogenic silica in marine samples by tracking silicate and aluminium concentrations in alkaline leaching solutions. *Aquatic Geochemistry 8* (1): 37-67.

Koning, E., van Iperen, J.M., van Raaphorst, W., Helder, W., G.J.A., Brummer & van Weering, T.C.E., 2001. Selective preservation of upwelling-indicating diatoms in sediments off Somalia. *Deep-Sea Research I, 48* (11): 2473-2495.

Koning, E., Brummer, G.-J.A., van Raaphorst, W., van Bennekom, A.J., Helder, W. & van Iperen, J.M., 1997. Settling, dissolution and burial of biogenic silica in the sediments off Somalia (northwestern Indian Ocean). *Deep-Sea Research II, 44* (6-7): 1341-1360.

Lange, C.B., Romero, O.E., Wefer, G. & Gabric, A.J., 1998. Offshore influence of coastal upwelling off Mauritania, NW Africa, as recorded by diatoms in sediment traps at 2195m water depth. *Deep-Sea Research I, 45* (6): 985-1013.

Lange, C.B., Treppke, U.F. & Fischer, G., 1994. Seasonal diatom fluxes in the Guinea Basin and their relationships to trade winds, ITCZ migrations and upwelling events. *Deep-Sea Research I, 41* (5-6): 859-878.

Levitus, S. & Boyer, T., 1994. *World Ocean Atlas 1994, 4.* U.S. Department of Commerce, Washington D.C.: 117 pp.

Lisitzin, A. P., 1972. Sedimentation in the World Ocean. *Society of Economic Paleontologists Mineralogists, Special Publication, 17*: 218 pp.

Lisitzin, A. P., 1985. The silica cycle during the last ice age*. Palaeogeography, Palaeoclimatology, Palaeoecology, 50*: 241-270.

Lohmann, G.P., 1992. Increasing seasonal upwelling in the subtropical South Atlantic over the past 700,000 yrs: evidence from deep-living planktonic foraminifera*. Marine Micropaleontology, 19* (1-2): 1-12.

Lohmann, G.P. & Schweitzer, P.N., 1990. *Globorotalia truncatulinoides*' growth and chemistry as probes of the past thermocline: 1. shell size. *Paleoceanography, 5* (1): 55-75.

Lončarić, N., Brummer, G.-J.A., & Kroon, D., 2005. Lunar cycles and seasonal variations in deposition fluxes of planktic foraminiferal shell carbonate to the deep South Atlantic (central Walvis Ridge). *Deep-Sea Research I, 52* (7): 1178-1188.

Lutjeharms, J.R.E. & Stokton, P.L., 1987. Kinematics of Southern Africa's upwelling front. In K.H. Brink (Ed.), *The Benguela and comparable ecosystems*. Sea Fisheries Research Institute, Cape Town: pp. 35-49.

Margalef, R., 1961. Hidrografía y fitoplancton de un área de la costa meridional de Puerto Rico. *Investigacion Pesquera, 18*: 33-96.

Martinez, I.J., 1994. Late Pleistocene paleoceanography of the Tasman Sea: Implications for the dynamics of the warm pool in the western Pacific. *Palaeogeography, Palaeoclimatology, Palaeoecology, 112* (1-2): 19-62.

Middelburg, J.J. & Nieuwenhuize, J., 2000. Uptake of dissolved inorganic nitrogen in turbid, tidal estuaries. *Marine Ecology Progress Series, 192*: 79–88.

Milliman, J.D., 1993. Production and accumulation of calcium carbonate in the ocean: budget of a nonsteady state. *Global Biogeochemical Cycles, 7* (4): 927-957.

Müller, P.J., Cepek, M., Ruhland, G. & Schneider, R.R., 1997. Alkenone and coccolithophorid species changes in late Quaternary sediments from the Walvis Ridge: Implications for the alkenone paleotemperature method. *Palaeogeography, Palaeoclimatology, Palaeoecology, 135* (1-4): 71-96.

Ortiz, J.D. & Mix, A.C. (1992). The spatial distribution and seasonal succession of planktonic foraminifera in the California Current off Oregon, September 1987 - September 1988. In: C.P. Summerhayes, W.L. Prell & K.C. Emeis (Eds.), *Upwelling Systems: Evolution Since the Early Miocene*. Geological Society Special Publication, London: pp. 197-213.

Peterson, R.G. & Stramma, L., 1991. Upper-level circulation in the South Atlantic Ocean. *Progress in Oceanography, 26*(1): 1-73.

Reid, J.L., 1989. On the total geostrophic circulation of the South Atlantic Ocean: flow patterns, tracers and transport. *Progress in Oceanography, 23* (3): 149-244.

Rodier, M. & Le Borgne, R., 1997. Export flux of particles at the equator in the western and central Pacific Ocean. *Deep-Sea Research II, 44* (9-10): 2085-2133.

Romero, O., Boeckel, B., Donner, B., Lavik, G., Fischer, G. & Wefer, G., 2002. Seasonal productivity dynamics in the pelagic central Benguela System inferred from the flux of carbonate and silicate organisms. *Journal of Marine Systems, 37* (4): 259-278.

Romero, O.E., Fischer, G., Lange, C.B. & Wefer, G., 2000. Siliceous phytoplankton of the western equatorial Atlantic: sediment traps and surface sediments. *Deep-Sea Research II, 47* (9-11): 1939-1959.

Romero, O.E., Lange, C.B., Fischer, G., Treppke, U.F. & Wefer, G., 1999. Variability in export production documented by downward fluxes and species composition of marine planktic diatoms: observations from the tropical and equatorial Atlantic. In: G. Fischer & G. Wefer (Eds.), *Use of proxies in paleoceanography: examples from the South Atlantic*. Springer-Verlag, Berlin, Heidelberg: pp. 365-392.

Sautter, L.R. & Sancetta, C., 1992. Seasonal associations of phytoplankton and planktic foraminifera in an upwelling region and their contribution to the seafloor. *Marine Micropalenotology, 18* (4): 263-278.

Schiebel, R. & Hemleben, C., 2000. Interannual variability of planktic foraminiferal populations and test flux in the eastern North Atlantic Ocean (JGOFS). *Deep-Sea Research II, 47* (9-11): 1809-1852.

Schneider, B., Schlitzer, R., Fischer, G., & Nöthig, E.-M., 2003. Depth-dependent elemental compositions of particulate organic matter (POM) in the ocean. *Global Biogeochemical Cycles, 17* (2): 1032, doi: 10.1029/2002GB001871

Schouten, M.W., de Ruijter, W.P.M., van Leeuwen, P.J. & Lutjeharms, J.R.E., 2000. Translation, decay and splitting of Agulhas rings in the southeastern Atlantic Ocean. *Journal of Geophysical Research - Oceans, 105* (C9): 21913-21925.

Schrader, H.J., 1974. Proposal for a standardized method of cleaning diatom bearing deep-sea and land-exposed marine sediments. *Nova Hedwigia, 45*: 403-409.

Seeberg-Elverfeldt, I.A., Lange, C.B. & Pätzold, J., 2004. Preservation of siliceous microplankton in surface sediments of the northern Red Sea. *Marine Micropaleontology, 51* (3-4): 193-211.

Sell, D.W. & Evans, M.S., 1982. A statistical analysis of subsampling and an evaluation of the Folsom plankton splitter. *Hydrobiologia, 94* (3): 223-230.

Shannon, C.E., 1949. The mathematical theory of environment. In: C.E. Shannon (Ed.), *The mathematical theory of communication*. University Illinois Press, Urbana: pp. 1-93.

Shannon, L.V., 1985. The Benguela Ecosystem. Part I. Evolution of the Benguela, physical features and processes. *Oceanography and Marine Biology, 23*: 105-182.

Shannon, L.V. & Nelson, G., 1996. The Benguela: large scale features and processes and system variability. In: D.J. Webb (Ed.), *The South Atlantic: Present and past circulation.* Springer-Verlag, Berlin, Heidelberg: pp. 163-210.

Smayda, T.J. and Boleyn, B.J., 1965. Experimental observations on the flotation of marine diatoms. I. *Thalassiosira* cf. *nana*, *Thalassiosira rotula* and *Nitzschia seriata*. *Limnology and Oceanography, 10* (4): 499-509.

Smetacek, V.S., 1985. Role of sinking in diatom life-history cycles: ecological, evolutionary and geological significance. *Marine Biology, 84* (3): 239-251.

Stuiver, M. & Reimer, P.J., 1993. Extended ^{14}C database and revised CALIB 3.0 ^{14}C age calibration program. *Radiocarbon, 35* (1): 215-230.

Stuiver, M., Reimer, P.J., Bard, E., Beck, J.W., Burr, G.S., Hughen, K.A., Kromer, B., McCormack, G., Van der Plicht, J. & Spurk, M., 1998. INTCAL98 radiocarbon age calibration, 24,000-0 cal BP. *Radiocarbon, 40* (3): 1041-1083.

Takahashi, K. & Bé, A.W., 1984. Planktonic foraminifera: factors controlling sinking speed. *Deep-Sea Research I, 31* (12A): 1477-1500.

Tanimura, Y., 1999. Varieties of a single cosmopolitan diatom species associated with surface water masses in the North Pacific. *Marine Micropalenotology, 37* (2): 199-218.

Thiede, J., 1971. Variations in coiling ratios of Holocene planktonic foraminifera. *Deep-Sea Research, 18* (8): 823-831.

Thunell, R.C., 1998. Particle fluxes in a coastal upwelling zone: sediment trap results from Santa Barbara Basin, California. *Deep-Sea Research II, 45* (8-9): 1863-1884.

Thunell. R.C. & Honjo, S., 1987. Seasonal and interannual changes in planktonic foraminiferal production in the North Pacific. *Nature, 328*: 335-337.

Thunell, R.C., Pride, C.J., Tappa, E. & Muller-Karger, F.E., 1994. Biogenic silica fluxes and accumulation rates in the Gulf of California. *Geology, 22* (4): 303-306.

Treppke, U.F., Lange, C.B. & Wefer, G., 1996a. Vertical fluxes of diatoms and silicoflagellates in the eastern equatorial Atlantic and their contribution to the sedimentary record. *Marine Micropaleontology, 28* (1): 73-96.

Treppke, U.F., Lange, C.B., Donner, B., Fischer, G., Ruhland, G. & Wefer, G., 1996b. Diatom and silicoflagellate fluxes at the Walvis Ridge: An environment influenced by coastal upwelling in the Benguela system. *Journal of Marine Research, 54* (5): 991-1016.

Veth, C., 2000. RV Pelagia Cruise Report: Cruise 64PE155, Project MARE-1, Mixing of Agulhas Rings Experiment. *NIOZ cruise reports*, NIOZ, Texel: 42 pp.

Villareal, T.A. & Carpenter, E.J., 1994. Chemical composition and photosynthetic characteristics of *Ethmodiscus rex* (Bacillariophyceae): evidence for vertical migration. *Journal of Phycology, 30* (1): 1-8.

Voelker, A.H.L., Grootes, P.M., Nadeau, M.-J. & Sarnthein, M., 2000. Radiocarbon levels in the Iceland Sea from 25-53 kyr and their link to the earth's magnetic field intensity. *Radiocarbon, 42* (3): 437–452.

Wefer, G., Berger, W.H., Bijma, J. & Fischer, G., 1999. Clues to ocean history: a brief overview of proxies. In G. Fischer & G. Wefer (Eds.), *Use of proxies in paleoceanography: examples from the South Atlantic*. Springer-Verlag, Berlin, Heidelberg: pp. 1-68.

Wetherbee, R., Lind, J.L., Burke, J. & Quatrano, R.S., 1998. The first kiss: establishment and control of initial adhesion by raphid diatoms. *Journal of Phycology, 34* (1): 9-15.

Wilkinson, 1988. *SYSTAT, the system for statistics.* SYSTAT Inc., Evanston: 822 pp.

More

More mrmlja, more stenje, more urla, more plače;
podiže se, pa se ruši, ko da više talas neće
ustat da se snova baca; mržnja, očaj njih će dići
da bez kraja bjesne, huče, i da ludo o hrid ginu.
Što je moru? Sad je bilo tako mirno, bezazleno.
Ne zbog vjetra, već zbog duše svoje tako sad mahnita.
More mračno, iz dubine tvoje raste ova bura,
koja krije strasnu snagu i neznanu još sudbinu.

More vrije. Propinje se, ali neće, još ne može
izlit sebe: nemir, buru; a ipak će, svo, polako
prijeći žale, il će opet u svoj tamni poći bezdan.
Obala mu smeta, da se svoga tijela oslobodi,
stog je grize, mrvi, kida, kolikogod bila kruta.
Ona čini moru među, makar more slobodno je.
Nesputano ludo more, ti si bilo nekad svuda;
nekad davno to je bilo, jednom opet bit će tako.

Zlatko Tomčić (1930)

Appendix

Colour figures of chapter 4

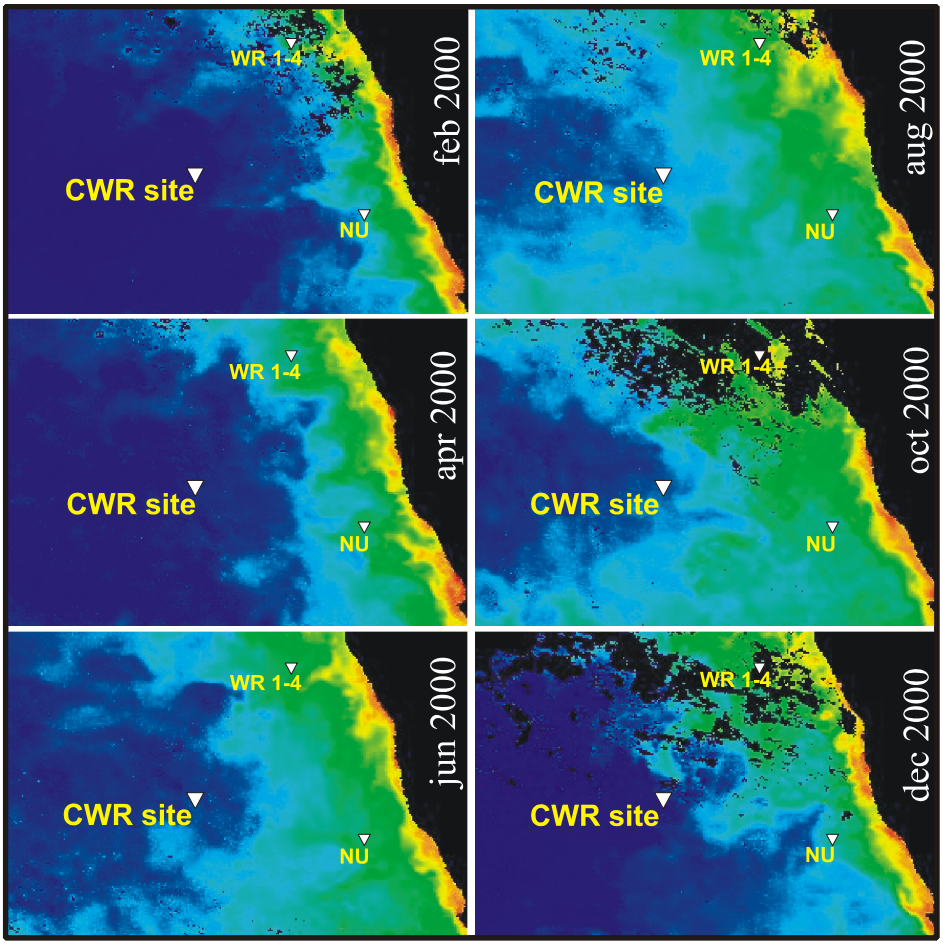

Figure 4.3: Monthly averaged surface chlorophyll-a concentration (SeaWiFS) for the CWR trap sampling period. Note enhanced concentrations at the NU and WR trap sites nearer to the Namibian margin.

Figure 4.10 (next page): Comparison of the annual deposition flux from the traps with the accumulation flux from the box core sediment. Only the foraminiferal deposition flux appeared fully transferred to sediment, whereas the diatom species assemblage is severely affected by silica dissolution.

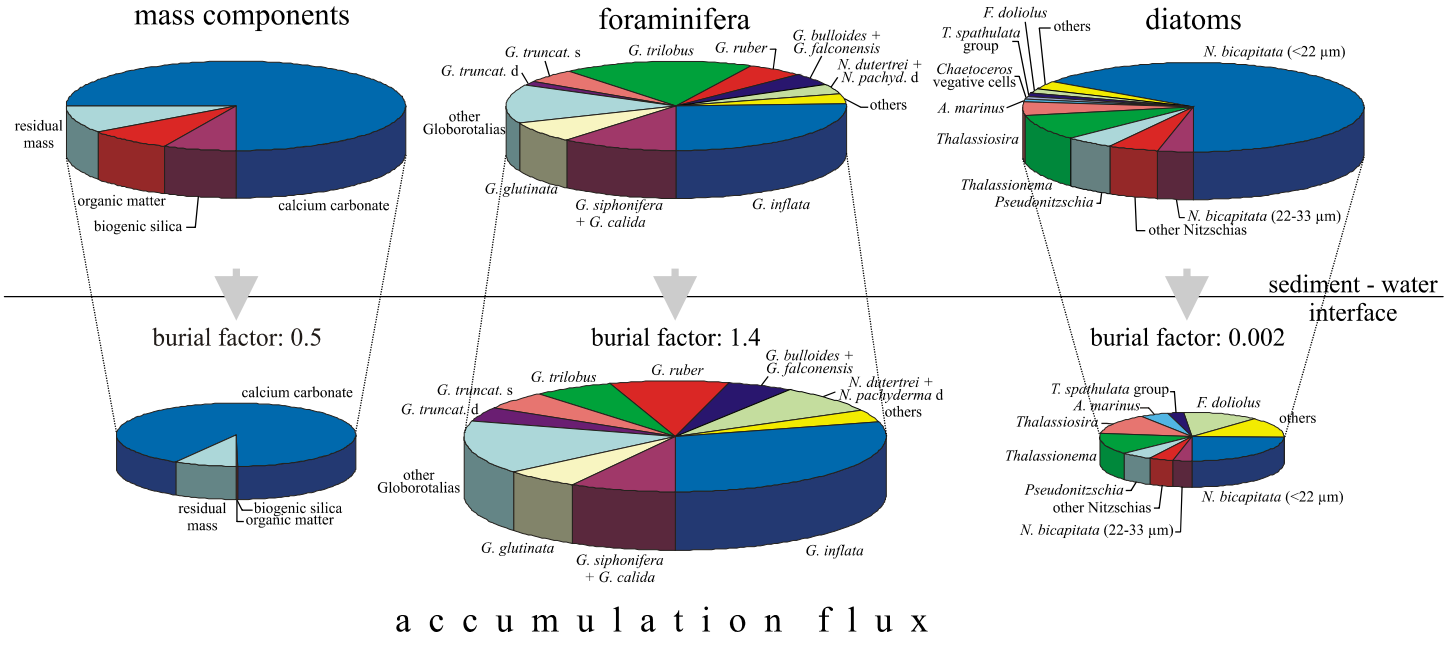
deposition flux
mass components
residual mass
organic matter
biogenic silica
calcium carbonate
foraminifera
G. truncat. s
G. truncat. d
G. trilobus
G. ruber
G. bulloides + G. falconensis
N. dutertrei + N. pachyd. d
others
other Globorotalias
G. glutinata
G. siphonifera + G. calida
G. inflata
diatoms
F. doliolus
T. spathulata group
others
Chaetoceros vegative cells
A. marinus
Thalassiosira
Thalassionema
Pseudonitzschia
N. bicapitata (<22 µm)
N. bicapitata (22-33 µm)
other Nitzschias
sediment - water interface
burial factor: 0.5
burial factor: 1.4
burial factor: 0.002
G. bulloides + G. falconensis
N. dutertrei + N. pachyderma d
T. spathulata group
accumulation flux

5. Oxygen isotope ecology of recent planktic foraminifera at the central Walvis Ridge (SE Atlantic)

Neven Lončarić, Frank J.C. Peeters, Dick Kroon and Geert-Jan A. Brummer

ABSTRACT

Seasonal and depth related changes in the oxygen isotope composition ($\delta^{18}O_c$) of six planktic foraminiferal taxa are documented from depth-stratified plankton tows collected at the central Walvis Ridge (CWR) site in the SE Atlantic Ocean. Our goal was to further develop the usage of $\delta^{18}O$ as a temperature proxy in South Atlantic sediments by improving our understanding of the habitat and calcification depth of planktic foraminifera. The $\delta^{18}O_c$ composition and characteristics in shell concentration profiles, such as the depth of maximum shell concentration and the depth at which shell concentration rapidly declines (i.e. base of the productive zone), are related to in-situ physical and chemical properties of ambient water. Records from the foraminiferal productive zone, where species live and calcify, are compared to the average annual export flux-weighted $\delta^{18}O_c$ from the sediment traps and the interannual average $\delta^{18}O_c$ in a top-sediment from a box core at the same site. CWR tow results show that both shell concentration and oxygen isotope composition can be used confidently to determine the depth range of the foraminiferal productive zone. The $\delta^{18}O_c$ of the spinose species *G. ruber* and *G. trilobus* showed a negative offset with respect to the expected isotope equilibrium for inorganically precipitated calcite (Kim and O'Neil, 1997) of ca. -0.30 and ca. -0.15‰, respectively, whereas non-spinose *G. glutinata*, *G. inflata* and *G. truncatulinoides* appeared to calcify close to equilibrium. Sea surface temperature (SST) appeared best reflected in the export flux $\delta^{18}O_c$ of *G. glutinata*. By contrast, *G. ruber* continues to calcify below the surface mixed layer (SML), down to the deep chlorophyll maximum (DCM) and its export flux $\delta^{18}O_c$ reflects the SST only in winter when SML incorporates DCM. The $\delta^{18}O_c$ of ~400 µm tests of left-coiling *G. truncatulinoides* at the CWR mirrored the sea-water temperature at approximately 340 m, whereas shells with a size of ~250 µm reflected the temperature at about 180 m. Deposition flux and core-top observations from the same site indicated that the flux weighted annual $\delta^{18}O_c$ signal of *G. glutinata* can be used as a robust proxy for the austral winter/spring sea surface temperature, where small and large specimens of left-coiled *G. truncatulinoides* provide a good estimate of summer temperature at 180 and 340 meter depth, respectively.

1. INTRODUCTION

In 1947, Urey suggested that stable oxygen isotope ratio of calcite might be used to deduce paleotemperatures. Based on Urey's proposal, Epstein et al. (1953) developed the first paleotemperature equation for biogenic carbonates. Emiliani (1955) followed this work and showed that the temperature equation can be applied on planktic foraminifera from deep-sea cores to reconstruct sea surface paleotemperature. Ever since, the stable oxygen isotope composition ($\delta^{18}O$) of the foraminiferal carbonate shell has been used widely for estimates of past global ice volume/sea level (e.g. Shackleton & Opdyke, 1973), sea surface temperature (e.g. Erez and Luz, 1983; Deuser, 1987), salinity (e.g. Duplessy et al., 1992) and ocean stratification (Williams et al., 1981; Mulitza et al., 1997; Niebler et al., 1999; Simstich et al., 2003). Seawater temperature derived from foraminiferal $\delta^{18}O$ can only be quantified and understood from sediment cores when the foraminiferal depth habitat and seasonal distribution are known. Field observations on living foraminifera are therefore necessary, allowing direct comparison of $\delta^{18}O$ in shells with the physical and chemical properties of the ambient water column. In this way foraminiferal depth habitat and isotopic disequilibrium (*i.e.* the "vital effect") can be quantified (Fairbanks et al., 1980, 1982; Ortiz et al., 1996; Peeters and Brummer, 2002), essential to constrain paleotemperature estimates and arrive at more robust reconstructions of past hydrographic conditions.

In this paper we present results on an integrated study on ecology of planktic foraminifera and their associated isotope signal from the central Walvis Ridge (CWR) site in the South Atlantic Ocean. In order to unravel the process from shell production to sediment preservation, we discuss the seasonal and vertical distribution, ecology and oxygen isotope composition of a number of foraminiferal species from plankton tows, sediment traps and a box corer. The shell concentration profiles of species *Globigerinoides trilobus, Globigerinoides ruber, Globigerinita glutinata, Globorotalia truncatulinoides* and *Globorotalia inflata* and the oxygen isotope composition of their shells are examined to estimate "calcification temperature" and depth habitat in contrasting seasons. We quantify the oxygen isotope disequilibrium ("vital effect") within the productive zone in the upper water column (i.e. the interval where foraminifer calcifies its shell) and determine the isotopic signature of the exported shells at greater depth. Since the flux of planktic foraminifera is seasonally variable (e.g. Deuser et al., 1981; Thunell and Sautter, 1992; Schiebel and Hemleben 2000), we also compare the annual flux-weighted $\delta^{18}O$ of different species from the sediment traps to the $\delta^{18}O$ of fossil specimens on the sea floor directly underneath.

2. MATERIAL

2.1. Plankton tows

During the MARE (Mixing of Agulhas Rings Experiment) cruises in February 2000, July 2000 and February 2001, depth stratified plankton tows were collected at the CWR site (Fig. 5.1; Tab. 5.1). Each station covered nine depth intervals from the upper 800-1000 m of the water column. The

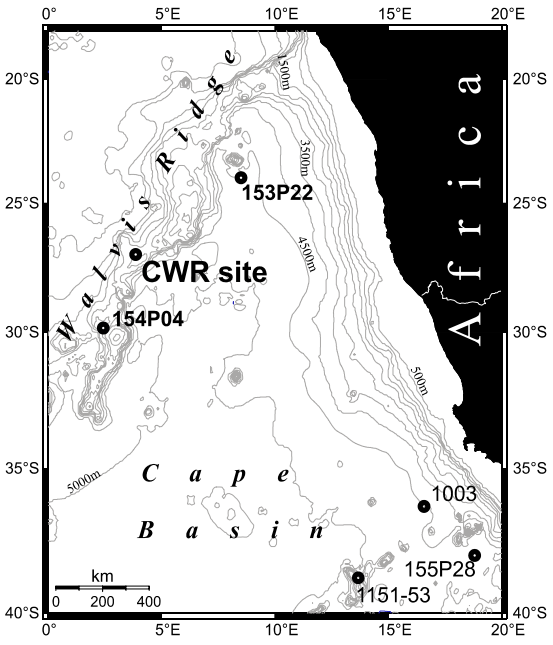

Figure 5.1: Regional bathymetry and location of the CWR site sampled by CTD, plankton tows, sediment traps and box-corer. The water samples used for the $\delta^{18}O_w$ measurements (Fig. 5.3) were taken at three Walvis Ridge sites. Additional $\delta^{18}O_c$ data for *G. glutinata* (Fig. 5.8) are from the southern Cape Basin stations (thin labels).

plankton was collected using a Hydrobios multinet system modified for oblique towing and equipped with two flow meters and five plankton nets with a 100 µm mesh (Tab. 5.1). The nets were successively opened and closed during the upcast while obliquely towed behind the ship, sampling approximately 130-1000 m^3 of seawater for the deep cast and 20-180 m^3 for the shallow cast (Tab. 5.1) (for further details on plankton sampling equipment see Wiebe and Benfield (2003)). Large metazoans were removed from the samples prior to freezing at -40°C. In the laboratory, the samples were freeze-dried and ashed in a Low Temperature Asher (LTA) to remove organic matter and concentrate the foraminiferal shells. After ashing, the residue was wet sieved over a 100 µm mesh to remove the ashed organic matter and dry-sieved into two size fractions (150-250 and >250 µm) for foraminiferal census counts. Large samples were split by an Otto dry splitter. On average 351 specimens (170 to 926) were counted per depth interval. For *Globigerinoides trilobus* only the specimens without a sac-like final chamber were considered.

2.2. Sediment traps

At the CWR site (Fig. 5.1) a Technicap PPS5 sediment trap with a 1 m^2 collecting area and 24 sampling cups was moored at 2 m above the sea floor. The trap was deployed in February 2000, serviced in July 2000 and recovered in February 2001, providing a semi-continuous 1-year record. Prior to mooring, the sample cups were filled with a $HgCl_2$-poisoned and Borax-buffered solution in seawater collected from the deployment depth. After trap recovery the samples were stored at 4°C. In the laboratory they were wet-split into at least two aliquots using a Folsom splitter (Sell and Evans, 1982; Griffiths et al., 1984). One aliquot was wet-sieved over 150 µm mesh, rinsed with ethanol, ashed in a LTA and than dry-sieved over a 250 µm mesh to obtain two size fractions for the foraminiferal studies. The first deployment provided an integrated half-a-year sample, whereas the second yielded a complete record with an eight-day sampling resolution. The samples were analysed individually and afterwards pooled into one annual value for comparison with sediment.

Table 5.1: Sampling details of the plankton tows collected at the central Walvis Ridge (CWR) site for each MARE cruise.

CRUISE /station		date (dd-mm-yy)	LAT begin/end (deg/min)	LONG begin/end (deg/min)	tow interval (m)	volume (m^3)
MARE 0 (summer)	154 P 03a	19/Feb/00	27° 01.01' S 27° 06.01' S	3°52.13' E 3°55.65' E	804-503 503-306 306-155 155-105	669 806 421 129
	154 P 03d	19/Feb/00	27° 00.29' S 27° 00.91' S	3° 51.17' E 3° 51.88' E	107-77 77-55 55-29 29-13 13-0	73 55 74 32 18
MARE II (winter)	1086	30/Jul/00	27° 00.61' S 26° 57.71' S	3° 51.18' E 3° 58.26' E	998-499 499-300 300-202 202-152	972 576 255 143
	1089	30/Jul/00	26° 57.81' S 26° 58.84' S	3° 58.02' E 3° 55.93' E	148-100 100-75 75-52 52-24 24-0	176 112 107 91 115
MARE III (summer)	174P03-1	02/Feb/01	27° 00.87' S 27° 04.10' S	3° 51.51' E 3° 56.40' E	803-501 501-302 302-201 201-148	575 827 197 148
	174 P 03-4	02/Feb/01	27° 00.77' S 27° 00.88' S	3° 51.71' E 3° 51.86' E	154-100 100-74 74-51 51-26 26-0	113 110 92 54 98

2.3. Box core

The box core 174P03-6 with a 43 cm sediment recovery was taken at the CWR site during the MARE III cruise (February 2001). The sediment was subsampled onboard directly after recovery by two 50 cm long plastic liners, one of which was later subsampled for ^{14}C and ^{210}Pb analyses by syringes (5 cm^3; Ø = 1 cm) at 1 cm depth interval. These analyses showed that the topmost sediment at the CWR site is modern in age and mixing rates are very low (Lončarić et al., submitted – chapter 4). The remaining upper 0.5 cm of the core was sampled for foraminiferal analyses and kept frozen at -40°C. In the laboratory, the samples were freeze-dried and sieved into 150-250 and >250μm fractions.

2.4. Hydrographic observations

Prior to each plankton tow cast, the upper water column was profiled by a Neill-Brown CTD rosette sampler operated at JGOFS standards or better (Veth, 2000). Twenty-two water samples collected from the upper 620 m of the water column were poisoned and stored dark in sealed bottles

at 4°C. These samples were later used for $\delta^{18}O$ analysis of seawater ($\delta^{18}O_w$). CTD-measured temperature, salinity, fluorescence and nutrient concentration were used to characterise water column properties in summer 2000, winter 2000 and summer 2001. Between the in-situ observations, sea surface temperature (SST) was obtained from the NOAA remote sensing records for this site, with a 50 km resolution, derived from 8 km resolution global sea surface temperature observations (POES AVHRR/HIRS), tuned to the in-situ data at 1m depth (www.osdpd.noaa.gov) and compared with our CWR measurements. SeaWiFS remote sensing provided the surface water chlorophyll-a concentration at 27° S; 4° E. The average depth of the surface mixed layer (SML) between the CTD measurements was taken from the World Ocean Atlas of Levitus and Boyer (1994) (http://ingrid.ldeo.columbia.edu/SOURCES/.LEVITUS).

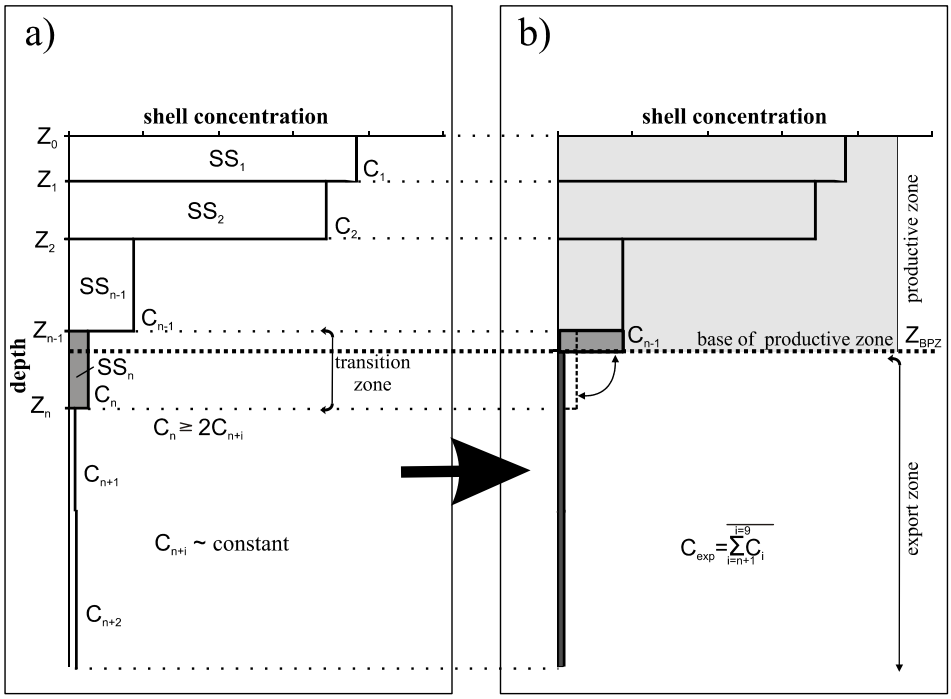

Figure 5.2: Schematic diagram of a foraminiferal concentration profile in the upper water column illustrating the definition of the base of productive zone (Z_{BPZ}). Shell concentrations (C_n) decrease gradually with depth to an approximately constant value representing only dead specimens (C_{exp}). Foraminifera collected above Z_{BPZ} are considered productive part of the standing stock (*SS*). In tow intervals across the interface between productive and export zone the shell population is composed of both living and dead (exported) specimens, which after correction for the export population yields Z_{BPZ}. For further explanation see in text.

3. METHODS

3.1. Foraminiferal productive zone and export flux

Previous studies on field collected planktic foraminifera show that the shell concentrations down the water column share a characteristic pattern (e.g. Oberhänsli et al., 1992; Ortiz et al. 1995; Peeters and Brummer, 2002; Field, 2004). In general, concentrations are relatively high in the upper part of the water column, where the foraminifera mainly live, and low at greater depth. This characteristic pattern of decreasing shell concentrations with depth can be used to identify its depth habitat, *i.e.* the productive zone (e.g. Berger and Soutar, 1967; Peeters and Brummer, 2002). We define the base of the productive zone (Z_{BPZ}) for each planktic foraminiferal species at the depth where the concentration profile attains an approximately constant value (Fig. 5.2a) (Peeters and Brummer, 2002). Foraminifera collected above the Z_{BPZ} are considered living and reflect the standing stock (*SS*). Below Z_{BPZ} concentrations are considered to represent only the remnant shells of dead specimens settling to the sea floor (Schiebel and Hemleben, 2000), and are termed export concentration (C_{exp}) (Fig. 5.2b). The standing stock (# m^{-2}) is given by:

$$\sum_{i=1}^{N} SS_i = C_i(Z_i - Z_{i-1}) \tag{1}$$

where C_i is the shell concentration (# m^{-3}) for the interval i, and Z_i and Z_{i-1} are the start and end depth (m) of each tow interval, respectively (Fig. 5.2a). Since oblique plankton towing through the upper water column per definition integrates foraminiferal concentrations over a depth interval, we derive species standing stocks by addition of all discrete interval concentrations within the productive zone. The value of i ranges from 1 to N, where N is the number of tow intervals within the productive zone. Given the towing technique used, Z_{BPZ} is probably situated somewhere within a towed interval, which combines low concentrations of dead specimens settling to the sea floor and the high pelagic population standing stock measured within the productive zone (Fig. 5.2a). We identify this transition zone as the tow interval between export and productive zone where the upcast shell concentration increases by a factor of two or higher (Fig. 5.2a). In the transition interval the standing stock (SS_n) is therefore given by:

$$SS_n = C_{\exp}(Z_n - Z_{n-1}) + C_{n-1}(Z_{BPZ} - Z_{n-1}) \tag{2}$$

where Z_n and Z_{n-1} are the begin and end depth of the transition tow interval (Fig. 5.2b). Since the export concentration of species often has a near, rather than exactly constant value, we follow Peeters and Brummer (2002) and for C_{exp} take the average concentration below the productive zone. Solving for Z_{BPZ}, equations (1) and (2) yield the nominal depth of the base of the productive zone (Fig. 5.2b):

$$Z_{BPZ} = \frac{C_n - C_{\exp}}{C_{n-1}}(Z_n - Z_{n-1}) + Z_{n-1} \tag{3}$$

Table 5.2: List of water samples analyzed for $\delta^{18}O_w$ and used for linear regression with salinity (Fig. 3). For station position see Fig. 5.1.

depth	salinity	$\delta^{18}O_w$(V-SMOW)	temperature
[m]	[‰]	[‰]	[°C]
station CWR			
18	35.73	0.45	22.20
48	35.76	0.47	18.65
77	35.64	0.41	17.38
95	35.62	0.41	16.31
200	35.26	0.09	13.61
378	34.83	0.11	10.23
501	34.57	-0.02	7.86
617	34.40	-0.26	5.99
station 154p04			
35	35.89	0.55	21.27
75	35.69	0.50	18.21
95	35.61	0.47	16.94
125	35.55	0.42	16.20
226	35.24	0.35	13.95
300	35.10	0.30	12.63
456	34.79	0.06	9.88
756	34.35	-0.20	7.40
station 153p22			
29	35.55	0.41	22.83
103	35.45	0.40	18.29
133	35.29	0.36	16.85
226	35.06	0.25	15.72
367	34.71	0.08	14.43
617	34.43	-0.15	13.24

3.2. Oxygen isotope analysis

Six taxa yielded sufficient shells within a given size fraction for stable isotope analysis (i.e. 40 to 80 µg of shell carbonate). The included species are *G. ruber, G. trilobus, G. glutinata*, left- and right-coiled *G. truncatulinoides* and *G. inflata*. In order to minimise size-related isotope variability, the tests used were microscopically selected according to maximum shell diameter (e.g. Kroon and Darling, 1995). Tests selected from the fine sieve fraction had a maximum test diameter range of 200 to 300 µm (hereafter referred to as "small") and from the coarse sieve fraction a maximum diameter range of 350 to 450 µm (hereafter referred to as "large"), respectively. Specimens selected from the box core surface sediment were cleaned ultrasonically prior to isotope measurement. The box core surface and integrated sediment trap samples were measured in duplicate or triplicate. In total 382 isotope measurements were performed on tests of six planktic foraminiferal species using a Finnigan MAT 252 mass spectrometer equipped with an automated carbonate extraction line at the Vrije Universiteit, Amsterdam (The Netherlands). The standard deviation of the external reproducibility was 0.07‰.

The oxygen isotope composition of the seawater ($\delta^{18}O_w$) was analyzed at the University of California, Davis (USA) (Tab. 5.2). Following Craig and Gordon (1965) we established a linear regression of $\delta^{18}O_w$ versus salinity in the upper water column (Fig. 5.3):

$$\delta^{18}O_W(V-SMOW) = 0.52 \times S - 17.90 \quad (4)$$

This equation (4) was used to obtain continuous depth profiles of $\delta^{18}O_w$ using the in-situ CTD salinity. Isotope values were converted from the V-SMOW to the V-PDB standard by subtracting 0.27‰ (Hut, 1987). The equation of Kim and O' Neil (1997) was used to calculate the expected equilibrium value for the oxygen isotope composition of calcite ($\delta^{18}O_{eq}$). This relationship between temperature, $\delta^{18}O_{eq}$ and $\delta^{18}O_w$ was obtained from precipitation experiments of inorganic calcite and thus excludes life processes like calcification rate (Ortiz et al., 1996), photosynthesis (Spero and Lea, 1993) or respiration (Wolf-Gladrow et al., 1999), but potentially includes the carbonate ion effect (Spero et al., 1997; Russell and Spero, 2000). Following Kim and O' Neil (1997):

$$T = 15.2 - 4.6 \times (\delta^{18}O_{eq} - \delta^{18}O_W) + 0.09 \times (\delta^{18}O_{eq} - \delta^{18}O_W)^2 \quad (5)$$

The expected equilibrium can be calculated solving equation (5) for $\delta^{18}O_{eq}$, yielding:

$$\delta^{18}O_{eq} = \delta^{18}O_W + 25.56 - 3.33\sqrt{T + 43.58} \quad (6)$$

The annual flux-weighted isotope signal $\delta^{18}O_J$ is calculated as:

$$\overline{\delta^{18}O_J} = \frac{\sum_{i=1}^{N} J_i \times \delta^{18}O_i}{J_{annual}} \quad (7)$$

where J_{annual} is the annual flux of a species recorded by sediment traps, J_i is the flux of a particular species recorded by cup i, $\delta^{18}O_i$ is the foraminiferal isotope composition from cup i and N is the total number of cups. The cups that contained an insufficient amount of foraminiferal carbonate for isotope analysis were not included in the calculations.

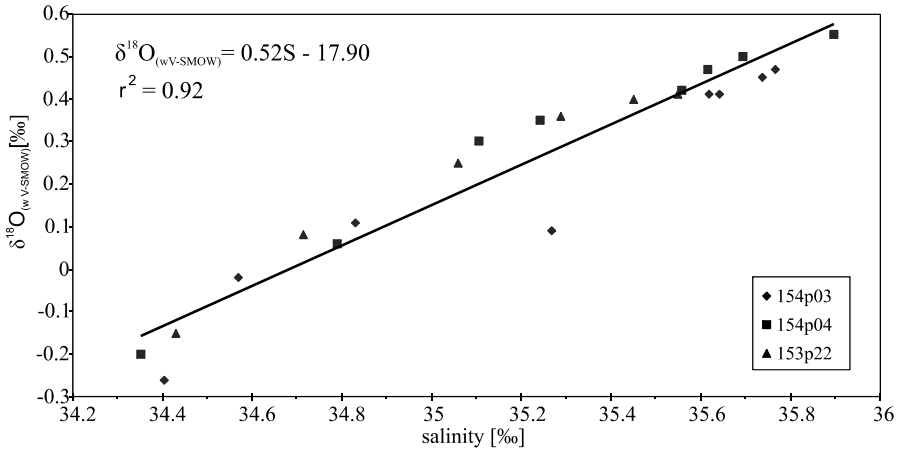

Figure 5.3: Linear regression of $\delta^{18}O_w$ vs. salinity measured at three sites above the Walvis Ridge (Fig. 5.1).

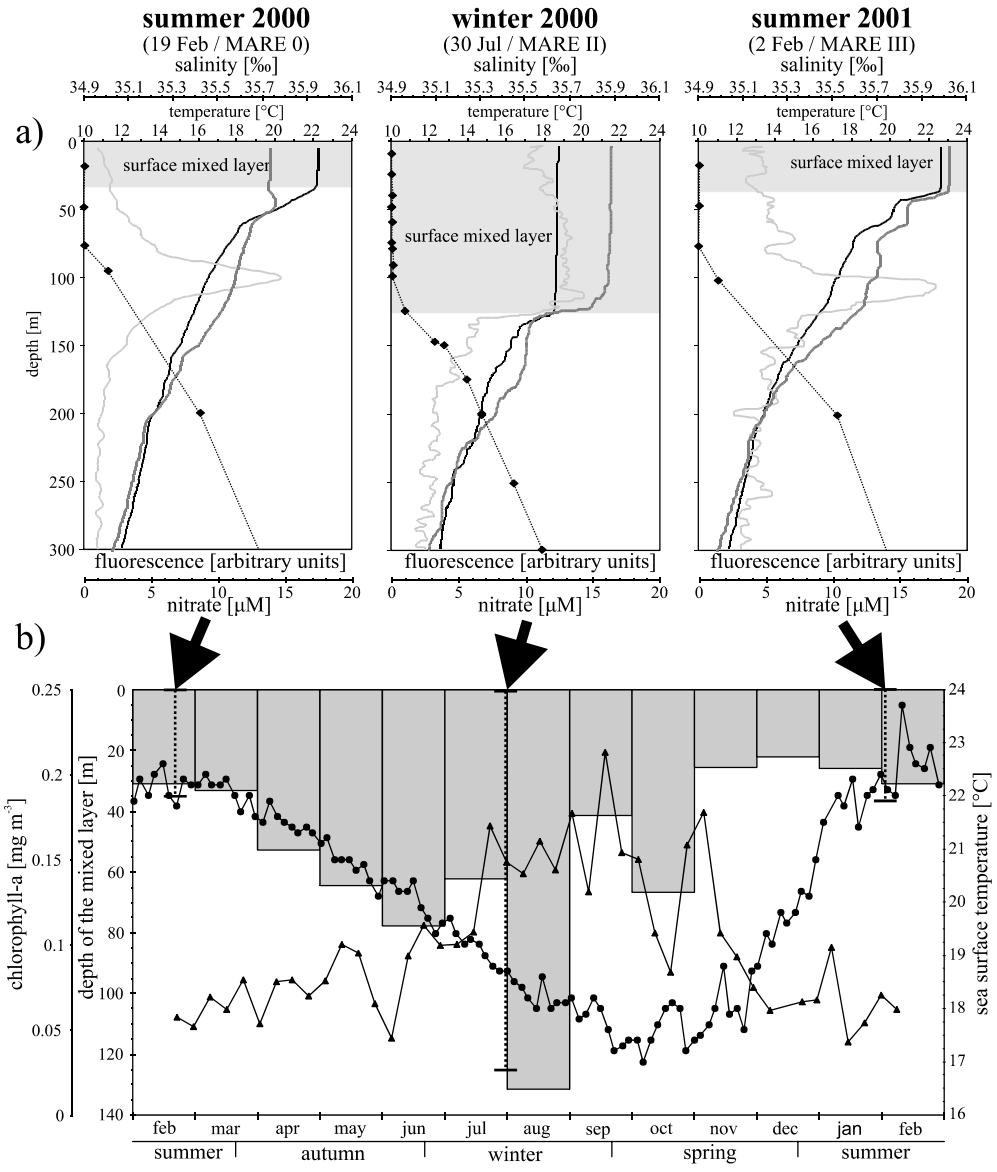

Figure 5.4: a) CTD profiles taken at the CWR site in February 2000, July 2000 and February 2001, showing temperature (black line; °C) fluorescence (light gray line; arbitrary units) salinity (dark gray line; ‰) and nitrate concentration (black diamonds; µM) in the upper 300 m of the water column.
b) Satellite-derived sea surface temperature (dots) (NOAA–POES AVHRR/HIRS), and chlorophyll-a (triangles) (SeaWiFS) for the CWR site from February 2000 to February 2001 and mean depth of the surface mixed layer (gray bars) (Levitus and Boyer, 1994). Vertical dashed lines mark the CTD and plankton tow sampling (from 5.4a). The length of the vertical dashed lines corresponds to the CTD measured depths of the surface mixed layer.

4. RESULTS

4.1. Regional oceanography

Circulation in the central Southeast Atlantic Ocean is largely controlled by the Subtropical South Atlantic Gyre. The central Walvis Ridge is under the influence of the eastern flank of this gyre, known as the oceanic branch of the Benguela Current (Peterson and Stramma, 1991; Garzoli and Gordon, 1996). The northward flowing current primarily involves the thermocline and Atlantic Intermediate Water stratum (Reid, 1989). The CWR site is situated ca. 1300 km westwards from the African continent and the coastal branch of the Benguela Current, associated with the Benguela coastal upwelling system. Although Benguela upwelling belongs to one of the greatest upwelling regions of the world with filaments of upwelled water reaching hundreds of kilometres offshore, it did not influence our sampling station (Lutjeharms and Stockton, 1987; Shannon and Nelson, 1996; Lončarić et al., submitted – chapter 4).

The summer 2000 CTD profile was characterised by a sharp shallow thermocline at a depth of 35 m below a SML of 22.2°C (Fig. 5.4a). Yet, the prominent but narrow fluorescence maximum was situated much deeper, at 100 m, just below the nutricline. One year later, in summer 2001, a slightly higher SST was measured (i.e. 22.7°C), but the surface mixed layer fluorescence maximum and nutricline were approximately at the same depth. In contrast to the austral summer profiles, the SML in the austral winter exceeded the depth of 120 m and included the nutricline. The surface water temperature was approximately 4°C lower and the fluorescence signal was homogeneously distributed over the upper 120 m with a weak maximum at about 110 m, just above the nutricline (Fig. 5.4a).

The SeaWiFS chlorophyll-a record revealed predominantly oligotrophic surface water conditions, with increased chlorophyll content at the end of the austral winter (mid July - September) and mid austral spring (late October) (Fig. 5.4b). The NOAA sea surface temperatures (Fig. 5.4b) ranged from 17°C (austral winter) to 23°C (austral summer) and matched our in-situ measurements with an offset of only 0.2°C, 0.0°C and 0.6°C on February 19th, 2000, July 30th, 2000 and February 2nd, 2001, respectively. For the entire period of sampling, radar altimetry imaging (TOPEX/Poseidon) did not show any perturbations by passing Agulhas rings, i.e. meso-scale eddies of warm-core Indian Ocean waters, which occasionally cross the Walvis Ridge from the proximate Cape Basin (Lutjeharms, 1996; Schouten et al., 2000, 2002). According to the Levitus World Ocean Atlas (Levitus and Boyer, 1994) the average SML at the CWR site was deepest in August (131 m) and shallowest from November through March (26-33 m) (Fig. 5.4b). Our CTD profiles agreed well within a few meters with average Levitus SML depths (Fig. 5.4b).

4.2. Water column distribution and oxygen isotope composition of foraminifera

In this section, shell concentration and $\delta^{18}O_c$ profiles are given to independently estimate the depth of the productive zone in which foraminifera live and calcify, in contrast to their shell export settling towards the deep ocean floor. For six taxa we address the depth distribution, standing stock and seasonal occurrence, as well as their oxygen isotope composition (Fig. 5.5; Tabs. 5.3-5.4), using

two size fractions from the depth-stratified tows collected in summer and winter. These are contrasted with the water column structure in terms of the depth of the SML, seasonal nutricline and chlorophyll-a concentration, as obtained from the CTD-rosette casts. In order to assess apparent (dis)equilibria between the foraminiferal shell and ambient water, we also consider the in-situ equilibrium values for inorganically precipitated calcite (Kim and O'Neil, 1997), using the CTD-measured salinity and temperature, and linear regression of $\delta^{18}O_w$ (eq. 4).

4.2.1. *Globigerinoides trilobus*

Although rare in winter, *G. trilobus* was abundant in both summer profiles and typically showed highest concentrations near the surface and a rapid decline with depth (Fig. 5.5a). According to the concentration profiles, the base of the productive zone was situated at a depth of approximately 60 m (Z_{BPZ}; eq. 3), i.e. 30 m deeper than the base of the SML, but 40-50 m shallower than the chlorophyll maximum around the seasonal thermocline. With a Z_{BPZ} of only 60 m, *G. trilobus* stands out as the shallowest of all species, with a standing stock of 662 # m^{-2} in summer 2000 and 208 # m^{-2} in 2001.

In all profiles *G. trilobus* showed continuously increasing $\delta^{18}O_c$ value in the upper water column, down to a depth of approximately 60 m, where it dropped close to a value found at the base of the SML. At greater depth, its $\delta^{18}O_c$ remained about constant whereas the equilibrium values for ambient water rapidly increased. This demonstrates that the calcification only occurred in the topmost 60 m, well above the DCM and indicates that the shells collected below that level should be considered as the settling export flux. Consequently the Z_{BPZ} defined by $\delta^{18}O_c$ was situated at about 60 m, identical to the depth estimate derived from the concentration profiles. Within the SML, *G. trilobus* showed a negative offset of -0.15 to -0.36‰ and -0.13 to -0.18‰ with respect to equilibrium calcification for small and large specimens, respectively (Tab. 5.4). Remarkably, the absolute 0.20‰ difference between small and large shells was retained down the export zone.

4.2.2. *Globigerinoides ruber*

In contrast to *G. trilobus*, high shell concentrations of *G. ruber* were also found deep below SML and within the seasonal thermocline down to the DCM (Fig. 5.5b). Although the highest concentrations typically occurred in the SML, the concentration-derived Z_{BPZ} extended to 112-147 m and coincided with the base of the DCM. Below Z_{BPZ}, the shell concentrations were approximately constant. Despite the deeper productive zone, the population of *G. ruber* was smaller than the one of *G. trilobus*, with the highest standing stock of 336 # m^{-2} in summer 2000.

All $\delta^{18}O_c$ profiles of *G. ruber* showed continuously increasing values through the upper water column down to the base of DCM, at a depth of approximately 125 m. Hereinafter the $\delta^{18}O_c$ dropped below values found at the DCM and remained approximately constant regardless rapidly increasing equilibrium values in the ambient water. Thus, the $\delta^{18}O_c$–derived Z_{BPZ} was situated at about 125 m, well in the range of the Z_{BPZ} as revealed from the shell concentrations. Within the summer SML, *G. ruber* showed a negative offset with respect to $\delta^{18}O_{eq}$ of -0.40‰ to -0.41‰ and -0.32‰ to -0.39‰ for the small and large shells, respectively (Tab. 5.4). In the deep winter SML, this offset was on average -0.20‰ for the small shells. Notably, the $\delta^{18}O_c$ increase through the upper water column always extended to the DCM, regardless the depth of the SML and the associated thermocline. By

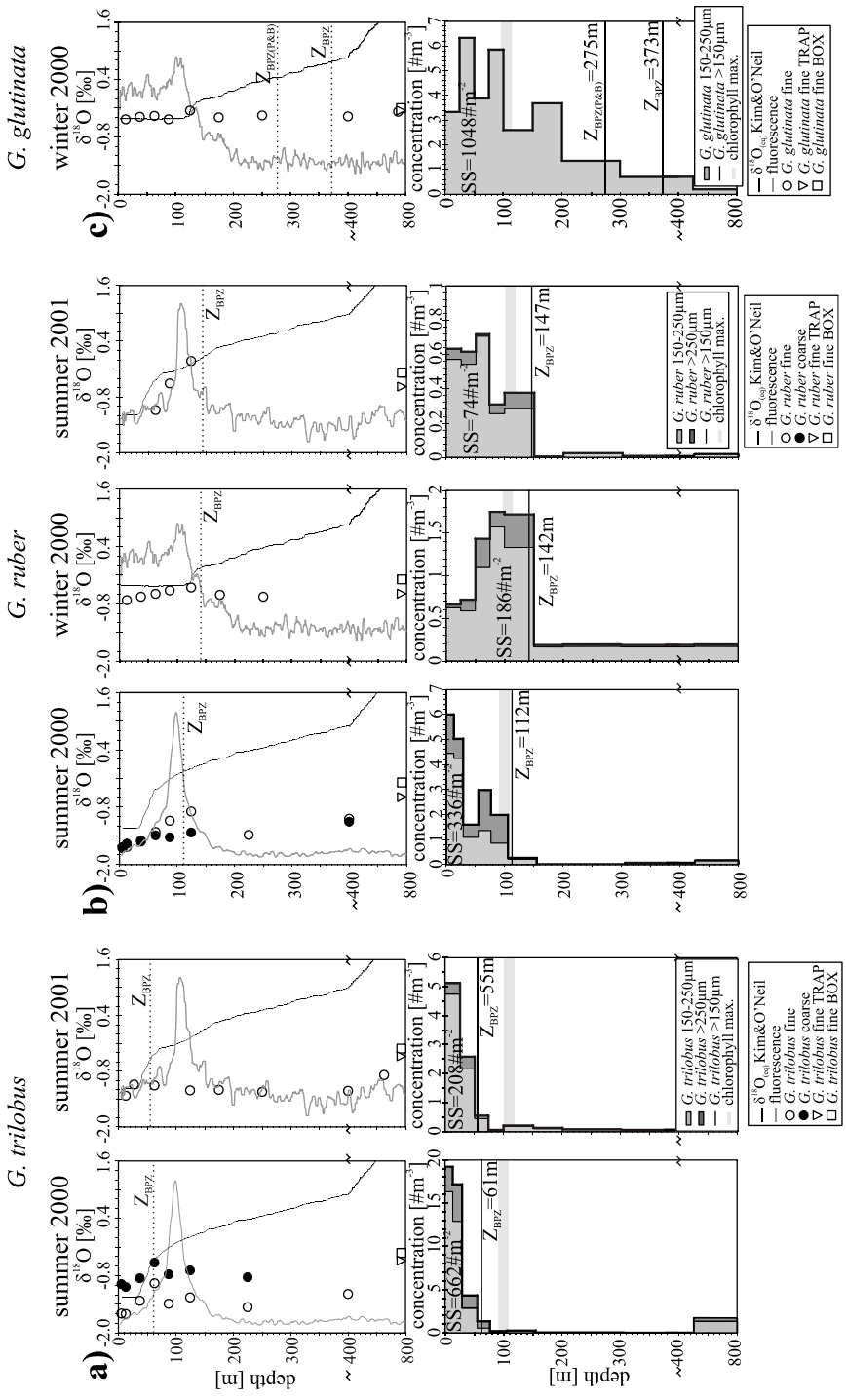
G. trilobus
G. ruber
G. glutinata
summer 2000
summer 2001
winter 2000
summer 2001
a)
b)
c)
depth [m]
δ18O [‰]
concentration [#m-3]
ZBPZ
ZBPZ=61m
ZBPZ=55m
ZBPZ=112m
ZBPZ=142m
ZBPZ=147m
ZBPZ=373m
ZBPZ(P&B)=275m
SS=662#m-2
SS=208#m-2
SS=336#m-2
SS=186#m-2
SS=74#m-2
SS=1048#m-2
δ18Osw Kim&O'Neil
fluorescence
G. trilobus fine
G. trilobus coarse
G. trilobus fine TRAP
G. trilobus fine BOX
G. trilobus 150-250µm
G. trilobus >250µm
G. trilobus >150µm
chlorophyll max.
G. ruber fine
G. ruber coarse
G. ruber fine TRAP
G. ruber fine BOX
G. ruber 150-250µm
G. ruber >250µm
G. ruber >150µm
G. glutinata fine
G. glutinata fine TRAP
G. glutinata fine BOX
G. glutinata 150-250µm
G. glutinata >150µm

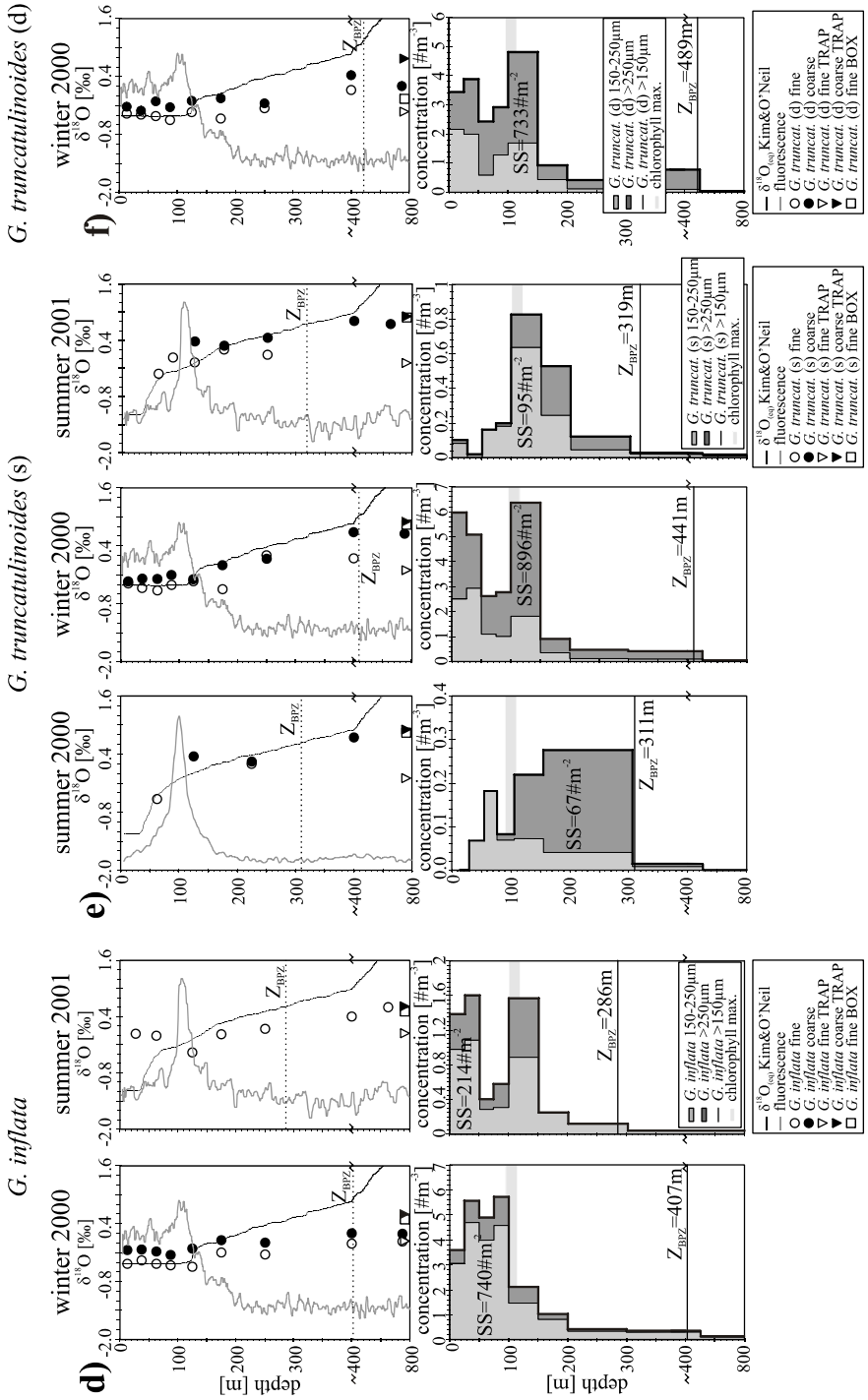
G. inflata
G. truncatulinoides (s)
G. truncatulinoides (d)
d)
e)
f)
winter 2000
summer 2001
summer 2000
winter 2000
summer 2001
δ18O [‰]
depth [m]
concentration [#m-3]
SS=740#m-2
SS=214#m-2
SS=67#m-2
SS=896#m-2
SS=95#m-2
SS=733#m-2
ZBPZ=407m
ZBPZ=286m
ZBPZ=311m
ZBPZ=441m
ZBPZ=319m
ZBPZ=489m
δ18Ocal Kim&O'Neil
fluorescence
G. inflata 150-250µm
G. inflata >250µm
G. inflata >150µm
chlorophyll max.
G. inflata coarse
G. inflata fine TRAP
G. inflata coarse TRAP
G. inflata fine BOX
G. truncat. (s) 150-250µm
G. truncat. (s) >250µm
G. truncat. (s) >150µm
G. truncat. (s) fine
G. truncat. (s) coarse
G. truncat. (s) fine TRAP
G. truncat. (s) coarse TRAP
G. truncat. (s) fine BOX
G. truncat. (d) 150-250µm
G. truncat. (d) >250µm
G. truncat. (d) >150µm
G. truncat. (d) fine
G. truncat. (d) coarse
G. truncat. (d) fine TRAP
G. truncat. (d) coarse TRAP
G. truncat. (d) fine BOX

Figure 5.5 (previous 2 pages): Oxygen isotope composition (upper panels) and foraminiferal shell concentration (lower panels) given in two size fractions, in the upper 800 m of the water column at the CWR site for: **a)** *G. trilobus*; **b)** *G. ruber*; **c)** *G. glutinata*; **d)** *G. inflata*; **e)** *G. truncatulinoides* (sin); **f)** *G. truncatulinoides* (dex). The gray line in the upper panels and horizontal gray bars in the lower panels mark the chlorophyll maximum zone. The core-top (squares) and the flux-weighted annual $\delta^{18}O_c$ (triangles) are given at the base of the isotope panel. The depth of the base of the productive zone (Z_{BPZ}) is derived from the concentration profiles by eq. 3. Note change of the vertical scale at 400 m.

contrast to all other species, only for *G. ruber* we measured higher $\delta^{18}O_c$ values in the small rather than in the corresponding large shell fraction (Tab. 5.3).

4.2.3. *Globigerinita glutinata*

This species was found almost exclusively in winter, in the size fraction smaller than 250 µm (Fig. 5.5c). Very high standing stock with more than 1000 # m^{-2} resulted from the high concentrations recorded throughout the deep SML, where two maxima coincided with fluorescence peaks, but also from the unusually low concentration decrease with depth, which contributed to the deep estimate for the Z_{BPZ} at ca. 370 m, or at 275 m using the approach of Peeters and Brummer (2002).

In contrast to the concentration profile, the $\delta^{18}O_c$ profile of *G. glutinata* was very consistent and suggested a much shallower calcification zone extending from the SML to the top of the seasonal thermocline at approximately 150 m. In the upper four tows collected within the winter SML, the $\delta^{18}O_c$ closely agreed with the expected $\delta^{18}O_{eq}$ (Fig. 5.5c; Tab. 5.4). Below 150 m depth, the shell $\delta^{18}O_c$ was approximately constant and on average 0.06‰ (below analytical precision) higher than the SML value.

4.2.4. *Globorotalia inflata*

The standing stock of *G. inflata* was higher in winter 2000, where shell concentrations closely resembled the fluorescence signal with a double maximum within SML, in contrast to summer 2001 where it had two separate maxima at the base of the SML and around the DCM. The concentration decrease below the DCM was not as rapid as for *G. ruber*, therefore suggesting the base of the productive zone be situated between 300 m in summer and 400 m in winter (Fig. 5.5d).

Winter $\delta^{18}O_c$ profiles showed approximately constant values within the SML down to the DCM, increasing below it to a depth of approximately 400 m. This demonstrates that the shell calcification ceased below 400 m, which agrees with the depth estimate of the productive zone derived from the concentration profile. Small specimens calcified in equilibrium within the SML, in the zone of maximum concentration, whereas large specimens were in equilibrium between 100 and 200 m depth. The absolute difference between small and large specimens of 0.25±0.06‰ was remarkably constant in the productive and export zones. Two summer tows collected above the DCM showed increased $\delta^{18}O_c$ values that correspond to the equilibrium values at ~150 m and may be related to vertical migration.

Table 5.3 (next page): $\delta^{18}O_c$ results from the CWR plankton tows with corresponding expected $\delta^{18}O_{eq}$, $\delta^{18}O_w$, temperature and salinity of ambient water.

	depth	*G. trilobus*		*G. ruber*		*glut.*	*G.inflata*		*G. truncat.* (s)		*G. truncat.* (d)		Kim&O'Neil	water	temp.	sal.
		fine	coarse	fine	coarse	fine	fine	coarse	fine	coarse	fine	coarse	expected $\delta^{18}O$	$\delta^{18}O$		
		[%]	[‰]	[‰]	[‰]	[‰]	[‰]	[‰]	[‰]	[‰]	[‰]	[‰]	[‰]	[‰]	[°C]	[‰]
	5	-1.59	-1.37	-1.65	-1.63								-1.24	0.24	22.23	35.72
	12.5	-1.60	-1.42	-1.64	-1.56								-1.24	0.24	22.22	35.72
	37.5	-1.33	-1.24	-1.50	-1.52								-1.15	0.24	21.77	35.72
	62.5	-0.96	-0.92	-1.32	-1.39				-0.53				-0.43	0.20	18.13	35.63
	87.5	-1.39	-1.16	-1.08	-1.43								-0.21	0.17	16.97	35.58
	125	-1.25	-1.08	-0.89	-1.32					0.36			0.01	0.13	15.76	35.49
	225	-1.46	-1.22	-1.37					0.21	0.25			0.38	-0.06	13.21	35.14
	400	-1.18		-1.05	-1.10					0.76			0.90	-0.23	10.09	34.79
	650												1.75	-0.46	5.46	34.35
	12.5			-0.73		-0.43	-0.42	-0.14	-0.37	-0.32	-0.37	-0.22	-0.42	0.33	18.70	35.88
	37.5			-0.65		-0.38	-0.36	-0.13	-0.47	-0.28	-0.39	-0.31	-0.42	0.33	18.71	35.88
	62.5			-0.59		-0.35	-0.43	-0.17	-0.52	-0.29	-0.42	-0.12	-0.43	0.33	18.71	35.88
	87.5			-0.52		-0.43	-0.46	-0.24	-0.41	-0.22	-0.50	-0.24	-0.42	0.32	18.67	35.87
	125			-0.46		-0.24	-0.49	-0.11	-0.34	-0.31	-0.34	-0.10	-0.27	0.22	17.45	35.67
	175			-0.62		-0.39	-0.19	0.06	-0.50	0.00	-0.47	-0.05	0.05	0.12	15.53	35.48
	250			-0.65		-0.35	-0.24	0.01	0.20	0.14	-0.26	-0.15	0.37	-0.04	13.34	35.18
	400					-0.37	-0.02	0.20	0.14	0.68	0.13	0.43	0.86	-0.21	10.39	34.84
	750					-0.27	0.04	0.19		0.65		0.20	1.93	-0.44	4.78	34.39
	12.5	-1.33											-1.18	0.40	22.73	36.03
	27.5	-1.09					0.03						-1.18	0.40	22.70	36.03
	62.5	-1.10		-1.08			-0.01		-0.31				-0.43	0.25	18.40	35.74
	87.5			-0.51					0.03				-0.26	0.24	17.53	35.71
	125	-1.22		-0.02			-0.36		-0.08	0.37			-0.08	0.19	16.45	35.62
	175	-1.21					0.03		0.22	0.28			0.26	0.02	14.12	35.29
	250	-1.25					0.14		0.09	0.46			0.50	-0.08	12.55	35.10
	400	-1.23					0.40			0.81			0.99	-0.25	9.65	34.76
	650	-0.89					0.60			0.75			1.79	-0.46	5.31	34.36

summer 2000 (MARE 0) **winter 2000 (MARE II)** **summer 2001 (MARE III)**

4.2.5. *Globorotalia truncatulinoides*

Shell counts and isotope measurements were performed separately for the left- and right-coiled variety. For the left-coiled specimens an increase in the test size with depth has been observed in all concentration profiles (Fig. 5.5e). The maximum abundance of large specimens was found consistently below the SML, in or below the DCM. By contrast, the small specimens showed highest concentrations above or at the DCM. The base of the productive zone, as defined by shell concentrations, was found below 300 m in summer and at approximately 440 m in winter, when the standing stock was higher by an order of magnitude.

In both size fractions the $\delta^{18}O_c$ of *G. truncatulinoides* (sin) was identical (winter 2000 and summer 2001) or very close (summer 2000) to the expected $\delta^{18}O_{eq}$ at the depths of maximum shell concentration (Fig. 5.5e, Tab. 5.4). Above these depths large specimens showed $\delta^{18}O_c$ higher than expected $\delta^{18}O_{eq}$, whereas below them the $\delta^{18}O_c$ followed the expected $\delta^{18}O_{eq}$ with a negative offset, demonstrating that the calcification zone extended to 400 m. Consequently the $\delta^{18}O_c$-derived Z_{BPZ} was within the range of the depth estimate derived from the concentration profiles. By contrast, the $\delta^{18}O_c$ of the fine fraction was approximately constant below 250 m in winter and 175 m in summer. This indicates that the calcification of the test fraction 200-300 µm ceased shallower than the fraction 350-450 µm and that the export $\delta^{18}O_c$ of small and large specimens originated from different depths in the water column.

Although absent in summer, right-coiled *G. truncatulinoides* showed high winter standing stock of 730 # m^{-2}, with concentrations resembling the left-coiled variety in magnitude and vertical distribution. According to the concentration profiles, the base of the productive zone was situated at a depth of approximately 490 m (Fig. 5.5f). This was the deepest Z_{BPZ} estimate of all species. Similar to left-coiled variety, the $\delta^{18}O_c$ of right-coiled *G. truncatulinoides* was approximately equal to the expected $\delta^{18}O_{eq}$ in the zones of maximum shell concentration. The $\delta^{18}O_c$ profile suggests that calcification ceased below 400 m, which is in agreement with the concentration-derived Z_{BPZ}.

Table 5.4: Shell oxygen isotope disequilibrium relative to the Kim and 'O Neil (1997) equation measured for two test size fractions. For species marked with (*) the disequilibrium is determined within the surface mixed layer and for those marked with (**) approximately at the depth level where shell concentrations were maximal.

species	offset from equilibrium [‰] maximum test diameter	
	200-300 µm	350-450 µm
*G. ruber**	-0.20 to -0.41	-0.32 to -0.39
*G. trilobus**	-0.36 to -0.03	-0.13 to -0.16
*G. glutinata**	+0.02	
G. truncatulinoides (s)**	-0.10 to 0.00	-0.14 to +0.01
G. truncatulinoides (d)**	0.00	-0.10 to +0.16
*G. inflata***	+0.02	+0.01 to +0.25

4.3. Sediment traps and core-top sediment

The annual flux of species was recorded in the sediment trap and yielded the annual $\delta^{18}O_c$ export signal (eq. 7), which can be compared with the $\delta^{18}O_c$ signal in the core-top sediment (Fig. 5.5; Tab. 5.5). All deep-dwellers showed significant difference between the size fractions in the trap $\delta^{18}O_c$ record. Large specimens of both left- and right-coiling *G. truncatulinoides* were 1.0‰ heavier than the corresponding fine ones, where for *G. inflata* the difference amounted to +0.55‰ (Tab. 5.5). The sea-floor $\delta^{18}O_c$ (measured only on the small

fraction) that represents centennials average (Lončarić et al., submitted - chapter 4) was consistently heavier than in the corresponding average deposition flux ($\Delta\delta^{18}O_c$ in Tab. 5.5). The difference was more pronounced for the deep-dwellers *G. truncatulinoides* and *G. inflata* than for the shallow-dwellers *G. trilobus* and *G. ruber*. The $\Delta\delta^{18}O_c$ for *G. glutinata* of only +0.03‰ was insignificant, i.e. below the analytical precision.

The winter profile of *G. glutinata* showed the best agreement between the $\delta^{18}O_c$ of the export flux recovered by the deep plankton tows, the average deposition flux from the sediment trap and the surface sediment from the box core (Fig. 5.5c). Three $\delta^{18}O_c$ values differ by only ±0.07‰, just within the analytical error. Other species that showed a good agreement between the tow export flux $\delta^{18}O_c$ and the trap annual $\delta^{18}O_c$ are the large fraction of left-coiled *G. truncatulinoides* in all tow profiles and fine fractions of *G. ruber* and *G. inflata* in winter tow profiles (Tab. 5.5).

Table 5.5: Annual flux weighted and centennial mean $\delta^{18}O_c$ of planktic foraminifera at the CWR site. $\Delta\delta^{18}O$ is the difference between box core-top and sediment trap results for the ~250µm fraction.

species	annual flux-weighted $\delta^{18}O_c$ (sediment traps)		centennial average $\delta^{18}O_c$ (sediment surface)	$\Delta\delta^{18}O$
	~250µm	~400µm	~250µm (average)	~250µm (box-trap)
G. truncatulinoides (s)	-0.10	0.91	0.84	0.94
G. truncatulinoides (d)	-0.32	0.77	-0.07	0.25
G. inflata	0.04	0.59	0.49	0.45
G. trilobus	-0.48		-0.32	0.16
G. ruber	-0.59		-0.29	0.30
G. glutinata	-0.23		-0.20	0.03

5. DISCUSSION

5.1. Foraminiferal productive zone

The productive zone is the part of the upper water column where planktic foraminiferal species live, calcify and generate the shell export which supplies the sedimentary record. We have used two independent methods to deduce the lower limit of the productive zone Z_{BPZ} for individual species, i.e. from the shell concentrations by equation 3 and from the $\delta^{18}O_c$ as the depth where shell growth ceases and $\delta^{18}O_c$ attains approximately constant value. In the analyzed profiles, the $\delta^{18}O_c$ kept increasing approximately till the Z_{BPZ} as derived from the concentration profiles, which implies that the two independent approaches for the determination of the Z_{BPZ} generally agreed well. Consequently, both shell concentration and $\delta^{18}O_c$ can be used confidently to determine the depth range of the foraminiferal productive zone for different species. In addition, the CWR $\delta^{18}O_c$ patterns suggest that foraminifera indeed grow, add chambers and/or thicken their walls over the entire productive zone as established from the concentration profiles. The depth reconstructed from the

$\delta^{18}O_c$ of exported shells below productive zone and in the sediments therefore represents the apparent calcification depth, which integrates the entire calcification cycle of the species (Fig. 5.6).

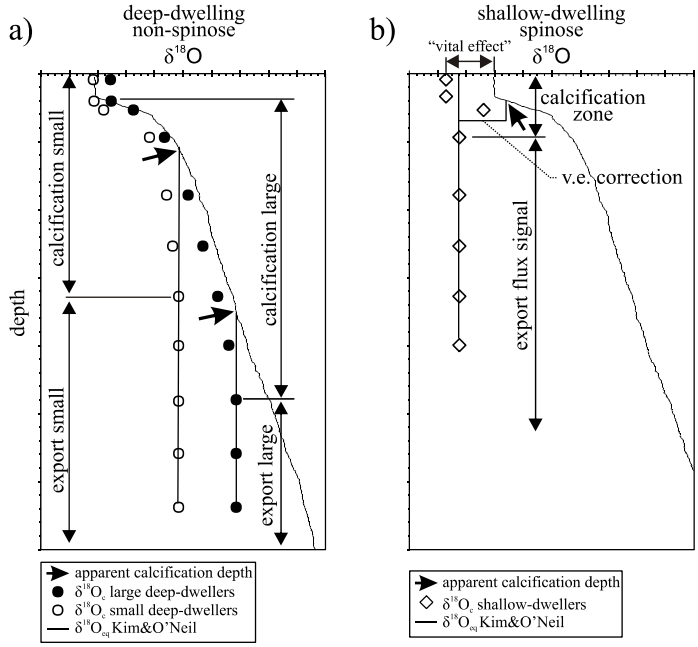

Figure 5.6: Schematic representation of the $\delta^{18}O_c$ of **(a)** deep-dwelling non-spinose (e.g. *G. truncatulinoides* and *G. inflata*) and **(b)** shallow-dwelling spinose species (e.g. *G. ruber* and *G. trilobus*) in the upper ocean. Non-spinose species calcify in oxygen isotope equilibrium in the zone of maximum concentration, while spinose ones show a negative offset. Most deep-dwellers calcify throughout the entire productive zone and therefore is their export $\delta^{18}O_c$ identical to $\delta^{18}O_c$ at the Z_{BPZ}. By contrast, only a small part of shallow dwellers calcifies until their Z_{BPZ}. Consequently, their export flux is mixture of shells formed exclusively in the SML and those that continued with calcification within seasonal thermocline. Note the difference between the apparent calcification depth deduced from the export $\delta^{18}O_c$ and the corresponding depth of the calcification zone.

The shallowest-dwelling species was *G. trilobus* with the Z_{BPZ} around 60 m and highest concentration near the surface, within the summer SML. Interestingly, we observed the productive zone of *G. ruber* to be consistently 50-90 m deeper than for *G. trilobus*. This species is generally considered as shallow-dwelling (e.g. Duplessy et al, 1981; Ravelo and Fairbanks, 1992; Niebler et al., 1999, Field, 2004) and a good indicator of the near surface conditions (Hemleben et al., 1989). Rather than confined to the SML, at the CWR the productive zone of *G. ruber* extends down to the DCM, with the Z_{BPZ} between 110 and 150 m (Fig. 5.5b). Although different from e.g. studies of Deuser and Ross (1989) (Sargasso Sea) and Kemle-von Mücke and Oberhänsli (1999) (Eastern Equatorial S. Atlantic), such maxima of *G. ruber* at the DCM have already been reported elsewhere (e.g. Fairbanks and Wiebe, 1980; Peeters et al., 2002). Thus, at the sites with a "typical tropical ocean" structure (Herbland and Voituriez, 1979; Mann and Lazier, 1991), where a shallow SML is well developed and separated from the DCM, *G. ruber* only partly reflects the SML conditions. The deepest-dwelling taxa at the CWR site were *G. truncatulinoides* and *G. inflata*, with the Z_{BPZ} ranging between 310 and 490 m (Figs. 5.5e-f) and 290 to 410 m (Fig. 5.5d), respectively. Although

concentration profiles of *G. inflata* resulted in a somewhat shallower Z_{BPZ} than for left- and right-coiled *G. truncatulinoides*, its $\delta^{18}O_c$ profiles suggest similar productive zones extending to approximately 400 m. Generally, shallow-dwellers *G. ruber* and *G. trilobus* showed a better match between two Z_{BPZ} approaches than deep-dwellers *G. inflata* and *G. truncatulinoides*, which can be attributed to the higher resolution of shallow tow intervals. The only mismatch was observed for the Z_{BPZ} of *G. glutinata* (Fig. 5.5c). The concentration profile situates the Z_{BPZ} at 370 m, or at 275 m using the approach of Peeters and Brummer (2002), whereas the $\delta^{18}O_c$ profile suggests a much shallower productive zone. Such discrepancy may arise from a number of factors such as the state of population dynamics or vertical migration. However, the $\delta^{18}O_c$ data strongly suggest that the Z_{BPZ} of *G. glutinata* is not deeper than 130-150 m.

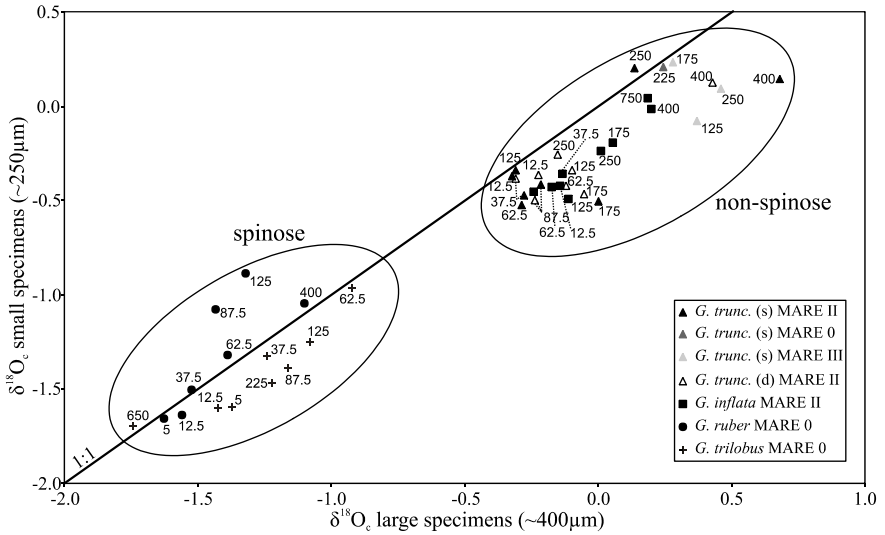

Figure 5.7: Relationship between $\delta^{18}O_c$ of small and large shells from the plankton tows at corresponding depth intervals. Large tests are isotopicaly heavier than the small ones for all species except deep *G. ruber*. Labels refer to the mid-point tow depth interval.

5.2. Species-specific and size-related $\delta^{18}O_c$ changes

Oxygen isotope analyses of living foraminifera demonstrate species-specific vital effects, where spinose species usually show larger negative offset from the expected $\delta^{18}O_{eq}$ than the non-spinose species (e.g. Fairbanks et al., 1980). In addition, planktic foraminifera commonly show a lower $\delta^{18}O_c$ in small specimens than measured for large ones of the same species (Fig. 5.7) (Erez and Honjo, 1981; Kroon, 1988). Such $\delta^{18}O_c$ shifts are also observed at the CWR, where size-related effect has been attributed to a growth at different depth and hence different calcification temperature, but may also be caused by ontogenic altering of the $\delta^{18}O_c$ composition during growth (Kroon and Darling, 1995; Bemis et al., 1998).

For all spinose species at the CWR site we observed a negative $\delta^{18}O_c$ offset with respect to the expected $\delta^{18}O_{eq}$ (Fig. 5.6). *G. ruber* showed the offset value of -0.4‰ to -0.2‰ within the mixed layer during both seasons (Fig. 5.5b; Tab. 5.4). This is within the range reported by Peeters et al. (2002) for the monsoonal-influenced Arabian Sea, as well as by Fairbanks et al. (1980) for the western N. Atlantic and by Erez and Honjo (1981) the central N. Atlantic, taking into account the heavier reference equilibrium value (see Tab. 5.6 and Appendix 5.1). For *G. trilobus* we found smaller offsets of -0.15‰ to -0.35‰ within the SML. These agree with findings from the Panama Basin, where Fairbanks et al. (1982) reported in the similarly shallow SML the "vital effect" of approximately -0.10 to -0.30‰, after reference $\delta^{18}O_{eq}$ correction.

Table 5.6: The temperature equation used in this study (Kim & O'Neil, 1997) and published prior to 1997. The oxygen isotopic composition of foraminifera is expressed as $\Delta\delta^{18}O_f$ and equals the difference between the shell and seawater (i.e. $\delta^{18}O_c - \delta^{18}O_w$) (equation format after Bemis et al. (1998, 2000)).

reference	$T = \mathbf{a} + \mathbf{b}(\Delta\delta^{18}O_f) + \mathbf{c}(\Delta\delta^{18}O_f)^2$		
	a	**b**	**c**
Kim and O'Neil, 1997	**15.2**	**-4.6**	**0.09**
Epstein et al., 1953	16.4	-4.2	0.13
Craig, 1965	16.9	-4.2	0.13
Shackleton, 1974	16.9	-4.38	0.1
Erez and Luz, 1983	17.0	-4.52	0.03

The CWR summer 2000 concentration profiles for small and large tests of shallow-dwelling *G. trilobus* and *G. ruber* show a similar vertical distribution, both having maximum within the SML (Fig. 5.5). Yet, two size fractions show different $\delta^{18}O_c$. Small tests of *G. trilobus* have within the summer SML an offset of -0.18 to -0.22‰ relative to the $\delta^{18}O_c$ from the large shells, whereas *G. ruber* shows only insignificant $\delta^{18}O_c$ difference between the shell size fractions (Fig. 5.7). Since the calcification environment is the same within the SML, the $\delta^{18}O_c$ offset between the size-fractions of *G. trilobus* has to be of an internal, ontogenic nature. Bemis et al. (1998) showed conclusively for small and large *G. bulloides* that a considerable ontogenetic $\delta^{18}O_c$ effect exists. Remarkably, difference between small and large *G. trilobus* was retained below the productive zone, indicating that calcification of both fractions at the CWR was largely restricted to the SML. For paleoceanographic applications, it has also to be considered that morphotypes of *G. trilobus* without sac-like final chamber presented in figure 5.5a, always occur shallower than those with sac-like chamber at the CWR (Lončarić et al., 2005 – chapter 3) and elsewhere (e.g. Erez et al., 1991; Bijma and Hemleben, 1994). The sac-like chamber is formed within the seasonal thermocline, where also the calcite crust may be added prior the gametogenesis (Lohmann, 1995). Consequently, the $\delta^{18}O$ analysis performed on the fossil record of entire population including two morphotypes would result in significant underestimation of the SST. Notable $\delta^{18}O_c$ increase in the *G. ruber* fine fraction down the deep winter SML, from –0.73‰ to –0.46‰ (Fig. 5.5b), suggests an additional controlling mechanism affecting $\delta^{18}O_c$ within the same fraction and in the same ambient water, which may be related to the symbiont activity under different light conditions (Spero and Lea, 1993). The exceptionally low $\delta^{18}O_c$ values of large *G. ruber* in summer 2000 (Figs. 5.5b and 5.7) could have resulted from temporal migration towards the DCM, or could be a consequence of distinct populations of small specimens calcifying both within the SML and around the DCM, which is consistent with the concentration profiles.

The oxygen isotope composition of non-spinose species is close to the expected $\delta^{18}O_{eq}$ near the depth where shell concentrations are maximal (Figs. 5.5c-f and 5.6). Given that the zone of maximum concentration indicates the preferred depth habitat of the species (Schiebel and Hemleben,

2000) and is the place where most of the foraminiferal calcite is formed (Peeters and Brummer, 2002), then the studied non-spinose species, *G. truncatulinoides*, *G. inflata* and *G. glutinata* appear to calcify in oxygen isotope equilibrium (Figs. 5.5c-f). The concentration profiles of deep-dwellers, in particular *G. truncatulinoides*, show an increase in test size with depth. Small specimens predominate at shallower depths in the water column and therefore calcify in warmer water, resulting in a lighter shell $\delta^{18}O_c$. Small specimens from the subsurface calcified larger part of their test in the relatively warm water of the SML, resulting in a negative $\delta^{18}O_c$ offset compared to large specimens from the same depth interval. Conversely, large specimens found in the SML may have migrated, or were expatriated from greater depth where they calcified most of their shell at higher $\delta^{18}O_{eq}$, resulting in a positive $\delta^{18}O_c$ offset (Fig. 5.6).

5.3. Calcification temperature vs. $\delta^{18}O_c$ export flux

Plankton towing combined with the CTD profiling attained at the CWR allows for direct comparison of the $\delta^{18}O_c$ signal from the foraminiferal export zone to the in-situ measured temperature applying equation (5) of Kim and O'Neil (1997). In this section the export $\delta^{18}O_c$ of spinose *G. ruber* and *G. trilobus* are compared to the measured SST, after correction for the in-situ observed "vital effect" from the SML. Since the non-spinose *G. glutinata*, *G. truncatulinoides* and *G. inflata* did not show a significant "vital effect", their export $\delta^{18}O_c$ is directly compared to the expected $\delta^{18}O_{eq}$ profile and recalculated to ambient temperature.

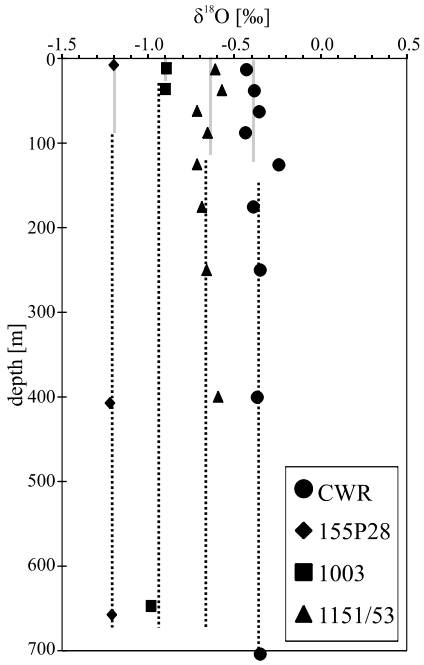

Figure 5.8: Oxygen isotope composition of *G. glutinata* from plankton tows collected at the CWR site (dots) and elsewhere in the Cape Basin (diamonds: 155P28, 38°1'S, 18°25'E; squares: 1003, 35°56'S, 16°6'E; triangles: 1153, 38°40'S, 13°58'E). Solid grey and stippled black lines represent average $\delta^{18}O_c$ within the surface mixed layer and below it, respectively.

5.3.1. Shallow-dwellers

As previously shown, *G. trilobus* is the shallowest-dwelling species at the CWR, with only few specimens that continue to calcify below the SML, down to approximately 60 m depth. Still, this part of the shell that calcified below SML results in a positive shift of the export $\delta^{18}O_c$ relative to the $\delta^{18}O_c$ value from the SML with a range of 0.17‰ to 0.28‰ in the fine, and about 0.25‰ in the coarse fraction, respectively. Consequently, the summer temperature estimates based on the export $\delta^{18}O_c$ are after in-situ "vital effect" correction lower than the measured SST, with an underestimate of 0.9 to 1.3°C for the small and approximately 1.2°C for the large shells.

The CWR tow results indicate the DCM as the level in the water column that borders the

productive zone of *G. ruber* and suggest that the calcification extends from the sea surface to the chlorophyll maximum. Both $\delta^{18}O_c$ and the concentration profiles show surprisingly high numbers of *G. ruber* calcifying always down to 125 m depth where the DCM occurs (Fig. 5.5b). In winter, when the deep SML includes the DCM, the temperature estimate from the export $\delta^{18}O_c$ of *G. ruber* matches exactly the measured SST. However, in summer when the DCM occurs 60-70 m below the SML, the temperature estimate from *G. ruber* export $\delta^{18}O_c$ underestimates the in-situ SST for 2.1 to 2.4°C for the fine and coarse fraction, respectively. Thus, in the "typical tropical ocean", where SML and DCM are well separated and consequently, the chlorophyll maximum temperature departs significantly from the surface temperatures, the SST estimates based on the export $\delta^{18}O_c$ of *G. ruber* may be inadequate.

Of all CWR species, the $\delta^{18}O_c$ record of *G. glutinata* is the most constant throughout the water column (Figs. 5.5c; Tab. 5.3). Its winter export $\delta^{18}O_c$ yields a temperature of 18.4°C, only 0.3°C lower than the in-situ measured SST. Also elsewhere in the Cape Basin (Fig. 5.8), differences between the average $\delta^{18}O_c$ of *G. glutinata* within the SML and from its export flux appear identical within the analytical error and the SST is accurately reflected in the $\delta^{18}O_c$ of exported specimens. Consequently, *G. glutinata* stands out as a robust proxy for the SST.

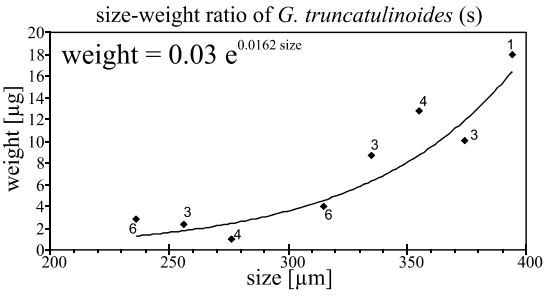

Figure 5.9: Size-weight relationship of left-coiled *G. truncatulinoides* from the sediment trap at the CWR site. Size refers to the microscopically measured largest test diameter. Due to the low weights and balance limitations several tests of the same size (labels next to symbols) are lumped together and weighed. Note that the weight of average 400 µm test is more than 11 times higher than the 250 µm test. For more shell size measurements see Lohmann and Schweitzer (1990).

5.3.2. Deep-dwellers

The deepest-dwelling taxa encountered in this study are right- and left-coiled *G. truncatulinoides* with a max. Z_{BPZ} at 490 and 440 m, respectively, as well as *G. inflata* at 410 m, as inferred from the concentration profiles (Figs. 5.5d-f). These taxa calcify in oxygen isotopic equilibrium in the zone of maximum shell concentration, which is for the small specimens usually shallower than for the large ones. Since the test weight is proportional with the amount of foraminiferal calcite, we established from morphometric analysis on left-coiled *G. truncatulinoides* that calcite from the 250 µm tests contributed less than 10% of the 400 µm-fraction mass (Fig. 5.9). Hence, even if the 250 µm test were completely precipitated within the SML, the contribution of that "warm water" calcite in the 400 µm test would be negligible. Additional argument pointing to only a minor contribution of the calcite from SML to the shells exported from the productive zone is the similarity between the $\delta^{18}O_c$ of the exported shells and those from the base of the productive zone (Figs. 5.5d-f and 5.6a). This suggests that most of the population continues calcification down to Z_{BPZ} where the export $\delta^{18}O_c$ is generated, in contrast to shallow-dwellers, where only smaller part of the population calcifies till Z_{BPZ} (Fig. 5.6). Consequently, we may conclude that *G. truncatulinoides* and *G. inflata* predominantly calcified below the SML. Although large specimens of these taxa occasionally occur within the SML (e.g. in

the summer profiles), this has no significant impact on the isotopic composition of exported shells settling to the sea floor. Such population behaviour has important consequence for the apparent calcification temperature and depth reconstructed from the exported shells. From the CWR $\delta^{18}O_c$ profiles it appears that the calcification zone for large specimens of *G. truncatulinoides* and *G. inflata* is approximately 300 m wide and covers the temperature gradient of about 7°C. Yet, in spite the wide calcification zone, the apparent calcification range calculated from export $\delta^{18}O_c$ is narrow. Left-coiled *G. truncatulinoides* manifests amongst all deep-dwellers a most consistent record in contrasting hydrographic seasons (i.e. a summer SML of 35 m vs. winter SML of 125 m). Its apparent calcification derived from the export $\delta^{18}O_c$ coarse fraction spans only 18 m for large specimens, ranging between 335 and 353 m depth, which corresponds to a temperature span of 0.7°C, ranging from 10.8°C to 11.5°C (Tab. 5.7). The apparent calcification depth at approximately 340 m derived from $\delta^{18}O_c$ of large *G. truncatulinoides* matches the modelling results (350 m) of LeGrande et al. (2004). Small specimens show warmer and shallower, but comparably narrow apparent calcification intervals (temp. range 14.1°C to 14.7°C; depth range 165 to 202 m). The apparent calcification depth of *G. inflata* varies from approximately 150-200 m in summer till ca. 250 m in winter. Thus, *G. truncatulinoides* and *G. inflata* from the CWR show a wide calcification zone, but a narrow apparent calcification temperature/depth with low seasonal variability. Furthermore, it stands out that the shell size of deep-dwellers appears as an important parameter that influences calculated apparent calcification temperatures.

Table 5.7: Export $\delta^{18}O_c$ of *G. truncatulinoides* (sin) from the summer 2000 (M-0), winter 2000 (M-II) and summer 2001 (M-III) tow profiles in the fine and coarse size fractions, with the corresponding water isotope composition and temperature, and resulting estimate for apparent calcification temperature (T) and apparent calcification depth (Z_c). The calcification temperature *T* is calculated using eq. 5. The calcification depth Z_c is the depth at which the calcification temperature *T* equals the water temperature as measured in-situ by CTD.

		~250µm	~400µm	water $_{200m}$	water $_{350m}$
$\delta^{18}O$ [‰]	M 0	0.21	0.76	-0.03	-0.18
	M II	0.17	0.67	0.07	-0.15
	M III	0.16	0.16	-0.02	-0.19
T [°C]	M 0	14.1	11.0	13.5	11.0
	M II	14.7	11.5	14.8	11.3
	M III	14.4	10.8	13.5	10.6
Z_c [m]	M 0	186	353		
	M II	202	341		
	M III	165	335		

5.4. Seasonality and annual $\delta^{18}O_c$

Seasonal and vertical calcification weight the annual $\delta^{18}O_c$ of a foraminiferal population towards the values associated with hydrographic conditions in the preferred ecological niche (Mulitza et al., 2003). The importance of seasonal events for the general sedimentation pattern and the prevailing signal that reaches the sediment can be illustrated by comparison of export $\delta^{18}O_c$ derived from plankton tows during contrasting seasons with the annual flux-weighted $\delta^{18}O_c$ derived from near-bottom sediment traps. This provides a valuable link between the modern oceanographic conditions and the information stored in the fossil record.

The best agreement between the export $\delta^{18}O_c$ and the annual $\delta^{18}O_c$ is found for *G. glutinata*, which was at the CWR abundant in winter. The calcification temperature calculated from the annual flux $\delta^{18}O_c$ is 18.3°C, identical to the austral mid winter (late July) and mid spring (October-November) SST (Fig. 5.4b), when its highest flux is recorded at the CWR site (Lončarić et al., submitted – chapter 4). Consequently, annual flux $\delta^{18}O_c$ of *G. glutinata* is an excellent proxy for the winter/spring surface temperature in this part of the ocean.

Flux-weighted annual $\delta^{18}O_c$ of *G. ruber* is identical to the winter plankton tow export $\delta^{18}O_c$ flux. At the CWR it provided a good estimate of the winter/spring SST, after in-situ "vital effect" correction. However, as we already showed, if the larger part of its annual flux is deposited in the period of "typical tropical ocean" structure such as in summer at CWR, its $\delta^{18}O_c$ may underestimate the SST by more than 2°C.

For left-coiled *G. truncatulinoides* we observed a good agreement between the export and annual average $\delta^{18}O_c$ signals particularly in summer populations. The deposition flux of *G. truncatulinoides* (sin) at the CWR is highest in December and January (Lončarić et al., submitted – chapter 4), suggesting that most of the annual flux arrives to the sea floor during the austral early summer. This explains why we found a better agreement between the export and annual $\delta^{18}O_c$ in February rather than July tows. The trap annual $\delta^{18}O_c$ yielded a temperature of 10.3°C for the depth of 350 m and 15.5°C for the 200 m depth, which is close to the average in-situ temperature of 10.8°C and 13.6°C measured by summer CTD profiles. The larger temperature overestimate at about 200 m (+1.9°C) is probably due to the steeper temperature gradient at shallower depths and the fact that the seasonal flux maximum precedes our CTD/plankton tow sampling by 1-2 months. Likely was the average CWR December/January temperature at 200 m depth higher than in-situ measured in February 2000 and 2001. The annual $\delta^{18}O_c$ of *G. inflata* gives a good estimate for the winter sea temperature at about 150 m, which agrees well with the maximum seasonal flux of this species observed at the CWR during winter/spring (Lončarić et al., submitted – chapter 4).

5.5. Sediment record

The CWR core-top $\delta^{18}O_c$ values were consistently higher than in the corresponding annual fluxes (Tab. 5.5), as commonly observed in the S. Atlantic (Mulitza et al., 2003) and elswhere (e.g. Duplessy et al., 1981; Erez and Honjo 1981; Deuser, 1987; Lohmann 1995). Differences ($\Delta\delta^{18}O_c$) were larger for the non-spinose *G. truncatulinoides* (sin) and *G. inflata* than for spinose *G. ruber and G. trilobus* (Tab. 5.5). For *G. glutinata*, $\Delta\delta^{18}O_c$ was within the analytical error and its sediment $\delta^{18}O_c$ accurately reflects the winter/spring SST (Fig. 5.5c; Tab. 5.5).

Mulitza et al. (2003) emphasized two primary mechanisms that may account for the observed deviation between the annual mean and core-top $\delta^{18}O_c$: (1) a shell flux biased towards seasons or periods when the ambient temperature was lower than the annual mean, or (2) subsurface calcification at lower temperatures. Addition of secondary calcite in waters deeper than where shells normally grow may account for one third or more of a shell's mass (Erez and Honjo, 1981; Schweitzer and Lohmann, 1991). Since we observed relatively constant export $\delta^{18}O_c$ in most of the plankton tows, secondary calcification at the CWR takes place below 800-1000 m, either as deep encrustation of shells, or abiotic precipitation of the cold water calcite in the export zone and at the sea floor. In contrast to the trap $\delta^{18}O_c$ record, which covers one year of deposition of the foraminiferal carbonate at the CWR, the core-top $\delta^{18}O_c$ represents a centennial average, since it takes hundreds of years before actual shell burial across the sediment-water interface (Lončarić et al., submitted – chapter 4). Therefore, the interannual variability in the seasonal flux may account for the higher core-top $\delta^{18}O_c$, e.g. by the relatively higher flux of deep-dwellers in winter, compared to the season 2000-2001.

The foraminiferal isotope signal in the sediment may also be altered by postdepositional processes (e.g. Mulitza et al, 2003). Mechanical processes at the sea bottom, such as fragmentation of thin-walled, non-encrusted adult shells with relatively low $\delta^{18}O_c$, or selective accumulation of heavy (mass and $\delta^{18}O_c$) specimens, but also differential dissolution related to heterogene shell chemistry (e.g. Brummer et al., 1987; Hemleben et al., 1989; Lohmann, 1992; Lohmann1995), can result in a positive $\delta^{18}O_c$ shift. Yet, it is unlikely that the partial dissolution at the CWR affected most severely only the initial chambers of the deep-dwelling, non-spinose species, which are generally characterized by the more robust shells (summarized in Hemleben et al., 1989), leaving in tact relatively delicate tests of *G. glutinata, G. trilobus* and *G. ruber*.

Although at this stage of the research it is difficult to pinpoint the true mechanism causing the observed $\Delta\delta^{18}O_c$, it is most likely related to the interannual flux changes, perhaps combined with other processes like deep encrustation of deep-dwellers, fragmentation of thin-walled calcite or selective accumulation of heavy specimens. Independently of this, *G. glutinata* stands out as a good proxy of the SST in the CWR surface sediments.

6. CONCLUSIONS

In this study, we have used two independent methods to deduce the base of the productive zone for six foraminiferal taxa at the central Walvis Ridge: (1) from the shell concentrations and (2) from the shell $\delta^{18}O_c$. In the analyzed profiles, two approaches generally agreed well yielding similar Z_{BPZ}. This implies that both shell concentration and $\delta^{18}O_c$ can be used confidently to determine the depth range of the foraminiferal productive zone for different species.

G. glutinata appeared as the best proxy of the sea surface temperature. It calcified in equilibrium with the expected $\delta^{18}O$ and showed constant $\delta^{18}O_c$ in the export flux recovered by plankton tows, the annual average deposition flux from the sediment traps and the surface sediment from the box core of the same site. In the CWR surface sediment, *G. glutinata* stands out as an excellent proxy of the winter/spring SST, as confirmed by the annual flux-weighted $\delta^{18}O_c$ and the satellite-derived temperature record.

The annual $\delta^{18}O_c$ of left-coiled *G. truncatulinoides* provides a good estimate of the summer (December-January) sub-surface temperature. The $\delta^{18}O_c$ from the specimens with a maximum test size of ~400 µm reflects the temperature at about 350 m and those with tests of ~250 µm at about 200 m. Consequently, the $\delta^{18}O_c$ difference between small and large specimens in the sediment may be used to estimate the subsurface temperature gradient.

The $\delta^{18}O_c$ record of *G. ruber* from the surface sediment provided a good estimate of the winter SST at the CWR. However, our tow results show that the calcification zone of *G. ruber* always extends down to the deep chlorophyll maximum. Therefore, in the water column structure where SML and DCM are separated by a seasonal thermocline, such as in summer at the CWR, the export $\delta^{18}O_c$ of *G. ruber* can underestimate the SST by more than 2°C.

7. ACKNOWLEDGMENTS

We thank the captains and crews of R/V Pelagia and R/V Agulhas as well as the NIOZ shipboard scientific parties for their assistance during the MARE cruises. Gene Carl Feldman and Norman Kuring from the SeaWiFS provided the satellite derived chlorophyll-a records. B. Hönisch (AWI – Bremerhaven) analyzed the $\delta^{18}O_w$ samples at the UC-Davis, by courtesy of H. Spero. This study was supported by the Netherlands - Bremen Oceanography (NEBROC) and the Mixing of Agulhas Rings Experiment (MARE) programs of the NWO/DFG and the NWO - ALW.

REFERENCES

Bemis, B.E., Spero, H.J., Bijma, J. & Lea, D.W., 1998. Reevaluation of oxygen isotopic composition of planktonic foraminifera: experimental results and revised paleotemperature equations, *Paleoceanography*, *13* (2): 150-160.

Bemis, B.E., Spero, H.J. Lea, D.W. & Bijma, J., 2000. Temperature influence on the carbon isotopic composition of *Globigerina bulloides* and *Orbulina universa* (planktonic foraminifera), *Marine Micropaleontology*, *38* (3-4): 213-228.

Berger, W.H. & Soutar, A., 1967. Planktonic foraminifera: Field experiment on production rate, *Science*, *156*: 1495-1497.

Bijma, J. & Hemleben, C., 1994. Population dynamics of the planktic foraminifer *Globigerinoides sacculifer* (Brady) from the central Red Sea, *Deep-Sea Research I*, *41* (3): 485-510.

Brummer, G.-J.A., Hemleben, C. & Spindler, M., 1987. Ontogeny of extant spinose planktonic foraminifera (Globigerinidae): a concept exemplified by *Globigerinoides sacculifer* (Brady) and *G. ruber* (d'Orbigny), *Marine Micropaleontology*, *12* (4): 17-49.

Craig, H. & Gordon, L.I., 1965. Isotopic oceanography: deuterium and oxygen 18 variations in the ocean and the marine atmosphere, In: D.R. Schink & J.T. Corless (Eds.), *Marine geochemistry*. University of Rhode Island Occasional Publications: pp. 277-374.

Deuser, W.G., 1987. Seasonal variations in isotopic composition and deep-water fluxes of the tests of perennially abundant planktonic foraminifera of the Sargasso Sea: results from sediment trap collections and their paleoceanographic significance, *Journal of Foraminiferal Research*, *17* (1): 14-27.

Deuser, W.G. & Ross, E.H., 1989. Seasonally abundant planktonic foraminifera of the Sargasso Sea: succession, deep-water fluxes, isotopic compositions, and paleoceanographic implications, *Journal of Foraminiferal Research*, *19* (4): 268-293.

Deuser, W.G., Ross, E.H., Hemleben, C. & Spindler, M., 1981. Seasonal changes in species composition, numbers, mass, size and isotopic composition of planktonic foraminifera settling into the deep Sargasso Sea, *Palaeogeography, Palaeoclimatology, Palaeoecology*, *33* (1-3): 103-127.

Duplessy, J.C., Bé, A.W.H. & Blanc, P.L., 1981. Oxygen and carbon isotopic composition and biogeographic distribution of planktonic foraminifera in the Indian Ocean, *Palaeogeography, Palaeoclimatology, Palaeoecology*, *33* (1-3): 9-46.

Duplessy, J.C., Labeyrie, L., Arnold, M., Paterne, M., Duprat, J. & van Weering, T.C.E., 1992. Changes in surface salinity of the North Atlantic Ocean during the last deglaciation, *Nature*, *358*: 485-488.

Emiliani, C., 1955. Pleistocene temperatures, *Journal of Geology*, *63*: 538-578.

Epstein, S., Buchsbaum, R., Lowenstam, H.A. & Urey, H.C., 1953. Revised carbonate-water isotopic temperature scale, *Bulletin of the Geological Society of America*, *64*: 1315-1326.

Erez, J. & Honjo, S., 1981. Comparison of isotopic composition of planktonic foraminifera in plankton tows, sediment traps and sediments, *Palaeogeography, Palaeoclimatology, Palaeoecology*, *33* (1-3): 129-156.

Erez, J. & Luz, B., 1983. Experimental paleotemperature equation for planktonic foraminifera, *Geochimica et Cosmochimica Acta*, *47* (6): 1025-1031.

Erez, J., Almogi-Labin, A. & Avraham, S., 1991. On the life history of planktonic foraminifera: lunar reproduction cycle in *Globigerinoides sacculifer* (Brady), *Paleoceanography*, *6* (3): 295-306.

Fairbanks, R.G. & Wiebe, P.H., 1980. Foraminifera and chlorophyll maximum:vertical distribution, seasonal sucession and paleoceanographic significance, *Science*, *209* (4464): 1524-1526.

Fairbanks, R.G., Wiebe, P.H. & Bé, A.W.H., 1980. Vertical distribution and isotopic composition of living planktonic foraminifera in the Western North Atlantic, *Science*, *207* (4426): 61-63.

Fairbanks, R.G., Sverdlove, M.S., Free, R., Wiebe, P.H. & Bé, A.W.H., 1982. Vertical distribution and isotopic fractination of living planktonic foraminifera from Panama Basin, *Nature*, *298* (5877): 841-844.

Field, D.B., 2004. Variability in vertical distributions of planktonic foraminifera in the California Current: Relationships to vertical ocean structure, *Paleoceanography*, *19*: PA2014 doi:10.1029/2003PA000970.

Garzoli, S.L. & Gordon, A.L., 1996. Origins and variability of the Benguela Current, *Journal of Geophysical Research*, *101* (C1): 897-906.

Griffiths, F.B., Brown, G.H., Reid, D.D. & Parker, R.R., 1984. Estimation of sample zooplankton abundance from Folsom splitter sub-samples, *Journal of Plankton Research*, *6* (5): 721-731.

Hemleben, C., Spindler, M. & Anderson, O.R., 1989. *Modern planktonic foraminifera*, Springer-Verlag, New York: 363 pp.

Herbland, A. & Voituriez, B., 1979. Hydrological structure analysis for estimating the primary production in the tropical Atlantic Ocean, *Journal of Marine Research*, *37*: 87-101.

Hut, G., 1987. Stable isotope reference samples for geochemical and hydrological investigations, Consultants Group Meeting, Int. At. Energy Agency (I.A.E.A.), Vienna, Austria: 42 pp.

Kemle-von Mücke, S. & Oberhänsli, H., 1999. The distribution of living planktic foraminifera in relation to Southeast Atlantic oceanography, In: G. Fisher & G. Wefer (Eds.) *Use of proxies in paleoceanography: examples from the South Atlantic*. Springer-Verlag, Berlin, Heidelberg: pp. 91-115.

Kim, S.T. & O'Neil, J.R., 1997. Equilibrium and nonequilibrium oxygen isotope effects in synthetic calcites, *Geochimica et Cosmochimica Acta*, *61* (16): 3461-3475.

Kroon, D., 1988. The planktic $\delta^{13}C$ record, upwelling and climate, In: *Planktonic foraminifers as tracers of ocean-climate history*, PhD thesis, Vrije Universiteit, Amsterdam: pp. 335-346.

Kroon, D. & Darling, K., 1995. Size and upwelling control of the stable-isotope composition of *Neogloboquadrina dutertrei* (D' Orbigny), *Globigerinoides ruber* (D' Orbigny) and *Globigerina bulloides* (D' Orbigny): examples from the Panama Basin and Arabian Sea, *Journal of Foraminiferal Research*, *25* (1): 39-52.

LeGrande, A.N., Lynch-Stieglitz, J. & Farmer, M.C., 2004. Oxygen isotopic composition of *Globorotalia truncatulinoides* as a proxy for intermediate depth density, *Paleoceanography, 19* (4): PA4025, doi:10.1029/2004PA001045.

Levitus, S. & Boyer, T., 1994. World Ocean Atlas 1994, 4, U.S. Department of Commerce, Washington D.C.: 117 pp.

Lohmann, G.P., 1992. Increasing seasonal upwelling in the subtropical South Atlantic over the past 700,000 yrs: evidence from deep-living planktonic foraminifera, *Marine Micropaleontology*, *19* (1-2): 1-12.

Lohmann, G.P., 1995. A model for variation in the chemistry of planktonic foraminifera due to secondary calcification and selective dissolution, *Paleoceanography*, *10* (3): 445-457.

Lohmann, G.P. & Schweitzer, P.N., 1990. *Globorotalia truncatulinoides*' growth and chemistry as probes of the past thermocline: 1. shell size, *Paleoceanography*, *5* (1): 55-75.

Lončarić, N., Brummer, G.-J.A. & Kroon, D., 2005. Lunar cycles and seasonal variations in deposition fluxes of planktic foraminiferal shell carbonate to the deep South Atlantic (central Walvis Ridge), *Deep Sea Research I*, *52* (7): 1178-1188.

Lončarić, N., van Iperen, J.M., Kroon, D. & Brummer, G.-J.A., submitted. Seasonal export and sediment preservation of diatom, foraminiferal and biogenic mass fluxes in a trophic gradient across the SE Atlantic, *Progress in Oceanography*.

Lutjeharms, J.R.E., 1996. The exchange of water between the South Indian and South Atlantic Oceans, In: G. Wefer, W.H. Berger, G. Siedler & D.J. Webb (Eds.) *The South Atlantic: Present and past circulation.* Springer-Verlag, Berlin Heidelberg: pp. 125-162.

Lutjeharms, J.R.E. & Stockton, P.L., 1987. Kinematics of Southern Africa's upwelling front, In: A.I.L. Payne, J.A. Gulland & K.H. Brink, *The Benguela and comparable ecosystems.* Sea Fisheries Research Institute, Cape Town: pp. 35-49.

Mann, K.H. & Lazier, J.R.N., 1991. *Dynamics of marine ecosystems*, Blackwell Scientific Publications, Boston: 466 pp.

Mulitza, S., Dürkoop, A., Hale, W., Wefer, G. & Niebler, H.-S., 1997. Planktonic foraminifera as recorders of past surface-water stratification, *Geology*, *25* (4): 335-338.

Mulitza, S., Donner, B., Fischer, G., Paul, A., Pätzold, J., Rühlemann, C. & Segl, M., 2003. The South Atlantic oxygen isotope record of planktic foraminifera, In: G. Wefer, S. Mulitza & V. Ratmeyer (Eds.), *The South Atlantic in the Late Quaternary: reconstruction of material budgets and current systems.* Springer-Verlag, Berlin, Heidelberg: pp. 121-142.

Niebler, H.-S., Hubberten, H.-W. & Gersonde, R., 1999. Oxygen isotope values of planktic foraminifera: a tool for the reconstruction of surface water stratification, In: G. Fischer & G. Wefer, *Use of proxies in paleoceanography: examples from the South Atlantic.*Springer-Verlag, Berlin, Heidelberg: pp. 165-189.

Oberhänsli, H., Bénier, C., Meinecke, G., Schmidt, H., Schneider, R. & Wefer, G., 1992. Planktonic foraminifers as tracers of ocean currents in the eastern South Atlantic, *Paleoceanography*, *7* (5): 607-632.

Ortiz, J.D., Mix, A.C. & Collier, R.W., 1995. Environmental control of living symbiotic and asymbiotic foraminifera of the California Current, *Paleoceanography*, *10* (6): 987-1009.

Ortiz, J.D., Mix, A.C., Rugh, W., Watkins, J.M. & Collier, R.W., 1996. Deep-dwelling planktonic foraminifera of the northeastern Pacific Ocean reveal environmental control of oxygen and carbon isotopic disequilibria, *Geochimica et Cosmochimica Acta*, *60* (22): 4509-4523.

Peeters, F.J.C. & Brummer, G.-J.A., 2002. The seasonal and vertical distribution of living planktic foraminifera in the NW Arabian Sea, In: P.D. Clift, D. Kroon, C. Gaedicke & J. Craig (Eds.), *The tectonic and climatic evolution of the Arabian Sea region* Geological Society of London - Special Publications, London: pp. 463-497.

Peeters, F.J.C., Brummer, G.J.A. & Ganssen, G., 2002. The effect of upwelling on the distribution and stable isotope composition of *Globigerina bulloides* and *Globigerinoides ruber* (planktic foraminifera) in modem surface waters of the NW Arabian Sea, *Global Planetary Change*, *34* (3-4): 269-291.

Peterson, R.G. & Stramma, L., 1991. Upper-level circulation in the South Atlantic Ocean, *Progress in Oceanography*, *26* (1): 1-73.

Ravelo, A.C. & Fairbanks, R.G., 1992. Oxygen isotopic composition of multiple species of planktonic foraminifera: Recorders of the modern photic zone temperature gradient, *Paleoceanography*, *7* (6): 815-831.

Reid, J.L., 1989. On the total geostrophic circulation of the South Atlantic Ocean: flow patterns, tracers and transport, *Progress in Oceanography*, *23* (3): 149-244.

Russell, A.D. & Spero, H.J., 2000. Field examination of the oceanic carbonate ion effect on stable isotopes in planktonic foraminifera, *Paleoceanography*, *15* (1): 43-52.

Schiebel, R. & Hemleben, C., 2000. Interannual variability of planktic foraminiferal populations and test flux in the eastern North Atlantic Ocean (JGOFS), *Deep-Sea Research II*, *47* (9-11): 1809-1852.

Schouten, M.W., de Ruijter, W.P.M., van Leeuwen, P.J. & Lutjeharms, J.R.E., 2000. Translation, decay and splitting of Agulhas rings in the southeastern Atlantic Ocean, *Journal of Geophysical Research* - Oceans, *105* (C9): 21913-21925.

Schouten, M.W., de Ruijter, W.P.M. & van Leeuwen, P.J., 2002. Upstream control of Agulhas Ring shedding, *Journal of Geophysical Research* - Oceans, *107* (C8): doi: 10.1029/2001JC000804.

Schweitzer, P. & Lohmann, G.P., 1991. Ontogeny and habitat of modern menardiiform planktonic foraminifera, *Journal of Foraminiferal Research, 21* (4): 332-346.

Sell, D.W. & Evans, M.S., 1982. A statistical analysis of subsampling and an evaluation of Folsom plankton splitter, *Hydrobiologia*, *94* (3): 223-230.

Shackleton, N.J. & Opdyke, N.D., 1973. Oxygen isotope and paleomagnetic stratigraphy of Equatorial Pacific core V28-238: Oxygen isotope temperatures and ice volumes on a 10^5 and 10^6 year scale, *Quaternary Research*, *3*: 39-55.

Shannon, L.V. & Nelson, G., 1996. The Benguela: large scale features and processes and system variability, In: G. Wefer, W.H. Berger, G. Siedler & D.J. Webb (Eds.), *The South Atlantic: Present and past circulation.* Springer-Verlag, Berlin, Heidelberg: pp. 163-210.

Simstich, J., Sarnthein, M. & Erlenkeuser, H., 2003. Paired $\delta^{18}O$ signals of *Neogloboquadrina pachyderma* (s) and *Turborotalita quinqueloba* show thermal stratification structure in Nordic Seas, *Marine Micropaleontology*, *48* (1-2): 107-125.

Spero, H.J. & Lea, D.W., 1993. Intraspecific stable isotope variability in the planktic foraminifera *Globigerinoides sacculifer*: results from laboratory experiments, *Marine Micropaleontology*, *22* (3): 221-234.

Spero, H.J., Bijma, J., Lea, D.W. & Bemis, B.E., 1997. Effect of seawater carbonate ion concentration on foraminiferal carbon and oxygen isotopes, *Nature*, *390*: 497-500.

Thunell, R. & Sautter, L.R., 1992. Planktonic foraminiferal fauna and stable isotopic indices of upwelling: a sediment trap study in the San Pedro Basin, Southern California Bight, In: C.P. Summerhayes, W.L. Prell & K.C. Emeis (Eds.), *Upwelling systems: evolution since the Early Miocene.* The Geological Society Special Publications, London: pp. 77-91.

Urey, H.C., 1947. The thermodynamic properties of isotopic substances, *Journal of the Chemical Society*, *1*: 562-581.

Veth, C., 2000. RV Pelagia Cruise Report: Cruise 64PE155, Project MARE-1, Mixing of Agulhas Rings Experiment. *NIOZ cruise reports*. Texel, NIOZ: 42 pp.

Wiebe, P.H. & Benfield, M.C., 2003. From the Hensen net toward four-dimensional biological oceanography, *Progress in Oceanography*, *56*: 7-136.

Williams, D.F., Bé, A.W. & Fairbanks, R.G., 1981. Seasonal stable isotopic variations in living planktonic foraminifera from Bermuda plankton tows, *Palaeogeography, Palaeoclimatology, Palaeoecology*, *33* (1-3): 71-102.

Wolf-Gladrow, D.A., Bijma, J. & Zeebe, R.E., 1999. Model simulation of the carbonate chemistry in the microenvironment of symbiont bearing foraminifera, *Marine Chemistry*, *64* (3): 181-198.

Appendix 5.1 (next page): Carbonate oxygen isotopic equilibrium ($\delta^{18}O_{eq}$) calculated following five different temperature equations versus water oxygen isotopic composition ($\delta^{18}O_w$) at the CWR site during three MARE cruises.

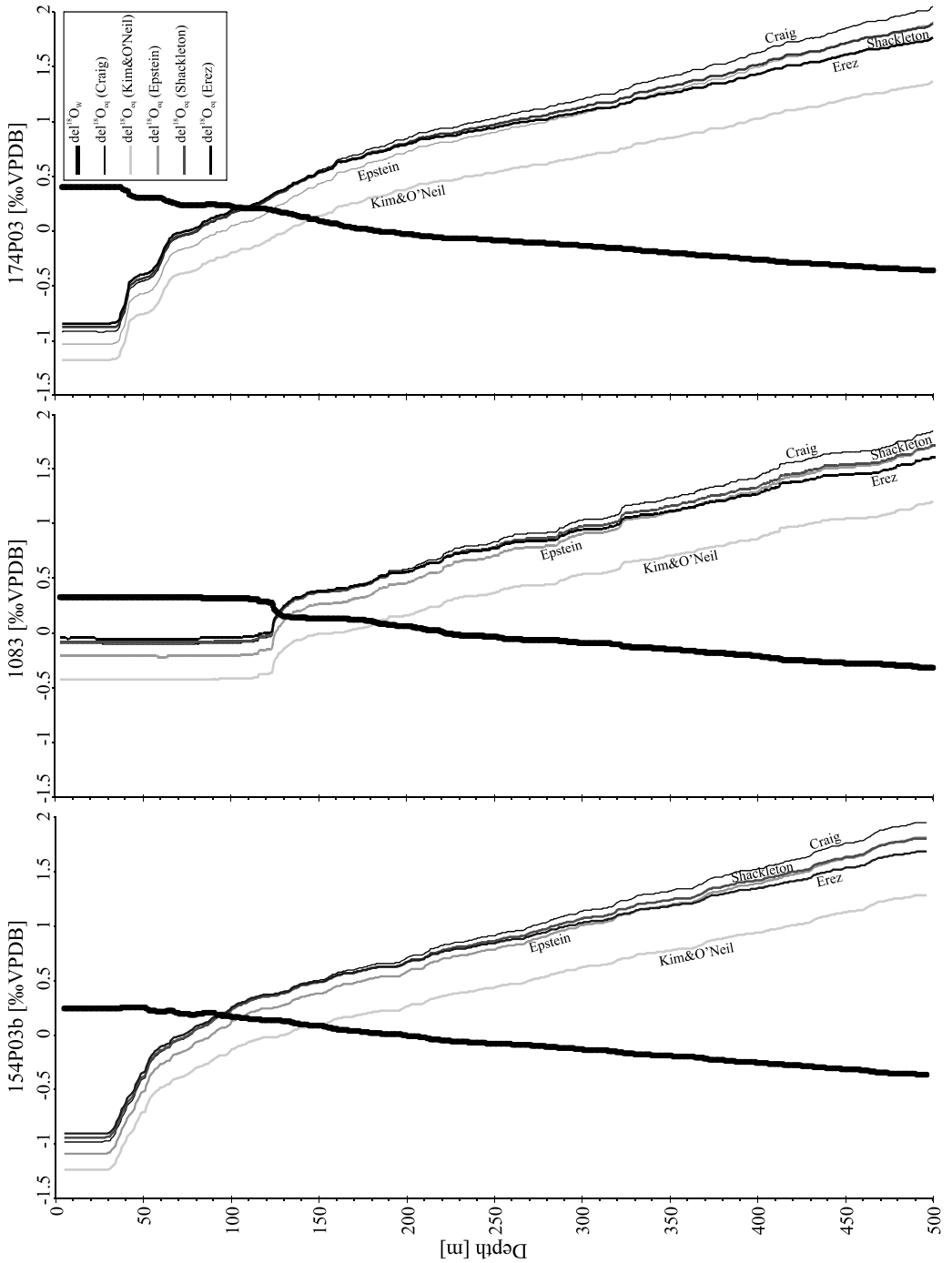
174P03 [‰VPDB]
1083 [‰VPDB]
154P03b [‰VPDB]
Depth [m]
del18Ow
del18Oeq (Craig)
del18Oeq (Kim&O'Neil)
del18Oeq (Epstein)
del18Oeq (Shackleton)
del18Oeq (Erez)
Craig
Shackleton
Erez
Epstein
Kim&O'Neil

6. Planktic foraminiferal content in a mature Agulhas eddy from the SE Atlantic: any influence on foraminiferal export fluxes?

Neven Lončarić

ABSTRACT

The Agulhas eddies, large-scale rings of dense, saline and warm water, occasionally intrude into the Benguela Current system from the Indian Ocean and progress northwards across the Cape Basin and the Walvis Ridge. In this paper is described the composition of the modern planktic foraminiferal assemblages collected from a mature Agulhas eddy when it entered into the northern Benguela Current system. In particular, I examined the effect of the eddy's gradual decay on the foraminiferal communities in the upper water column using plankton tow and CTD-rosette profiles obtained within and outside the ring. In addition, I investigated the impact of exported foraminiferal fluxes beneath the eddy on the assemblages in sediment traps moored near the sea floor and in the core-top sediment from a box corer.

The examined mature eddy "W" was clearly evident on altimetry images by its elevated surface. It was distinguished from the surrounding ocean by a slightly higher salinity, deeper surface mixed layer and higher planktic foraminiferal standing stocks. Similar to planktic foraminiferal fauna in freshly formed eddies from the Agulhas retroflection, species such as *Globigerinoides trilobus* s.l., *Globigerinoides ruber*, *Orbulina universa*, *Globigerinella siphonifera* and *Globorotalia scitula* dominated in the ring "W" assemblages. However, *Globorotalia menardii*, a species previously believed to be characteristic for the Agulhas leakage into the S. Atlantic, was virtually absent in eddy "W" fauna. Also *Globoquadrina hexagona*, a species endemic in Indian Ocean waters was not found in the water column, in the export flux or underlying sediment. The February to July foraminiferal flux patterns recorded by the sediment traps mirror the February standing stocks from the water column. Here in contrast, the core-top results show dominance of intermediate/cold water species that originate from the seasonal spring bloom. This signal prevails in sediment to the extent that any potential Agulhas eddy signature in the sediment got overprinted.

1. INTRODUCTION

The oceanography of the southern part of the SE Atlantic is characterized by two prominent features: (1) the Benguela Current flowing northwards along the African continent and (2) the inflow of the Indian Ocean water into the Atlantic around the Cape of Good Hope. The Benguela upwelling system (18° - 34°S) is nowadays one of the four major eastern boundary current regions of the World Oceans, distinguished by cold and nutrient rich water (Peterson and Stramma, 1991; Shannon and Nelson, 1996). In the Southern Cape Basin, the area where the Benguela Current originates, the warm, salty Agulhas Current intrudes from the Indian Ocean (Peterson and Stramma, 1991). A greater part of the Agulhas Current water retrogrades back into the Indian Ocean, whereas a smaller part leaks into the SE Atlantic (Lutjeharms and van Ballegooyen, 1988). This occurs in the form of large scale eddies that on average 5 to 7 times per year enter the Atlantic in the zone of Agulhas retroflection (Goñi et al., 1997; Schouten et al., 2000). The Agulhas eddies are anti-clockwise rotating bodies that average 250 km in diameter and extend to more than 1000 m depth (Lutjeharms, 1996; van Aken et al., 2003). Due to their rotational motion they are distinguished by an elevated surface relative to the surrounding ocean, traceable on satellite sea surface altimetry (SSH) images (Byrne et al., 1995). Once formed, the Agulhas eddies migrate within the Benguela Current northwards, gradually mixing with the surrounding water losing heat and salinity. The decay of such a ring can take up to a few years, by the time they cross the central Walvis Ridge (Schouten et al., 2000). This addition of warm and saline water to the South Atlantic is an important element of the global thermohaline circulation (Gordon, 1985-1996; de Ruijter et al., 1999) and one of the major controlling factors of the South Atlantic heat and salt budget (Lutjeharms, 1996; Weijer et al., 1999). The effectiveness of the retroflection in generating warm eddies depends on the position of the subtropical front (de Ruijter, 1982). It may be assumed that this front moves northwards during glacial periods (Berger and Wefer, 1996a), cutting off the supply of heat to the South Atlantic with direct consequences for the North Atlantic Deep Water formation (Weijer et al 2001). Due to such decisive role of this system in the global ocean circulation and assumed high variability on the glacial-interglacial scale, the influence of the Agulhas eddies on the sedimentation patterns in the South Cape Basin was subject of several paleostudies (Berger and Wefer, 1996b; Flores et al., 1999; Chen et al., 2002; Rau et al., 2002). Recently Peeters et al. (2004) studied the modern system and provided firm evidence for the characteristic foraminiferal signature of a freshly-formed eddy that allowed documentation of the interocean exchange dynamics for the last 500 kyrs from the sediments of the southern Cape Basin.

Although sea surface temperature anomalies of Agulhas rings tend to disappear quickly (Olson et al., 1992), satellite altimetry monitoring (e.g. TOPEX/Poseidon) documented that approximately two third of the eddies formed at the Agulhas retroflection, cross over the northern Cape Basin and the central Walvis Ridge (e.g. Garzoli and Gordon 1996; Goñi et al., 1997, Schouten et al., 2000). Such older eddies within northern Cape Basin surface waters have never been an subject of in-situ ecological studies. Therefore their faunal characteristics and the importance for sedimentation patterns are largely unknown. The purpose of this study is to determine for the first time the faunal and physical signature of a long-lived eddy and better understand the coupling between such oceanographic source signal in the water column and the exported flux directly below.

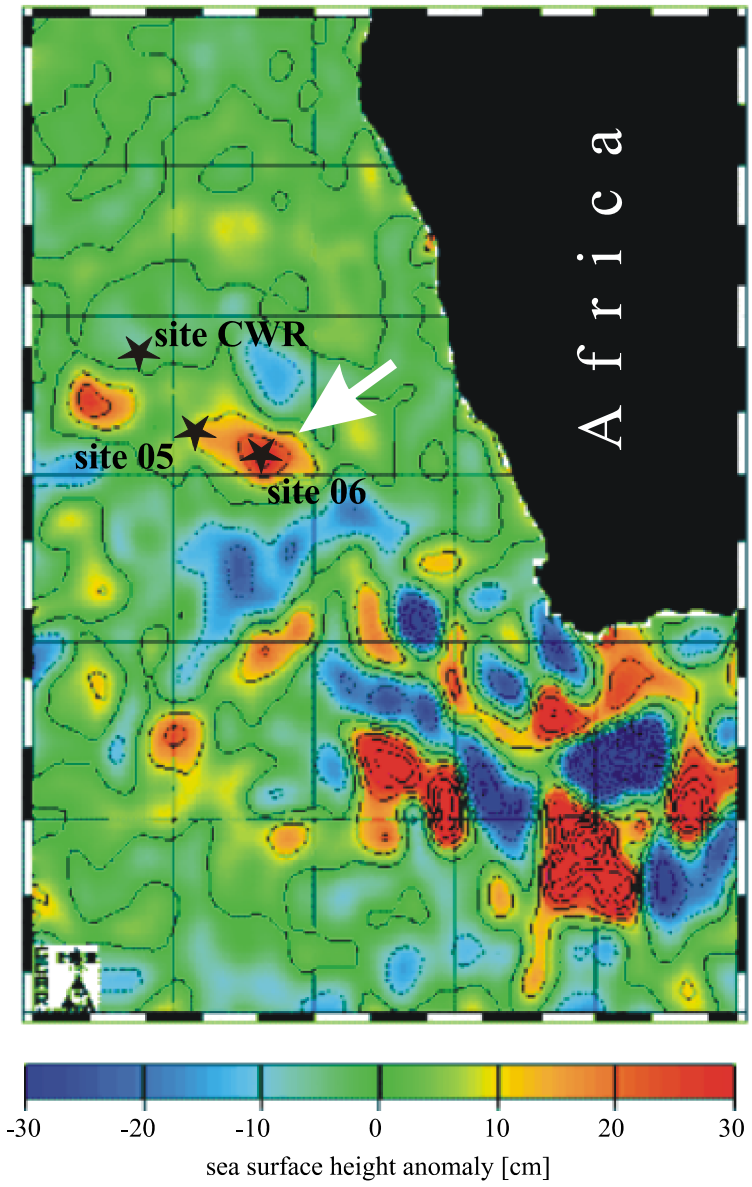

Figure 6.1: Sea surface altimetry image (TOPEX/Poseidon; positive anomaly in red, negative in blue) from February 18, 2000 and location of three sampling stations from this study. The centre of long-lasting eddy "W" (marked by arrow) was at the moment of sampling (22/2/2000) exactly at the station 06.

2. MATERIAL AND METHODS

The area of the Cape Basin off southwestern Africa has been monitored for spawning and decay of Agulhas rings since 1992 using TOPEX/Poseidon satellite altimetry (Gründlingh, 1995; Goñi et al., 1997; Schouten et al., 2000). Aided by SSH images we sampled the centre of the long-lived eddy "W" in the northern Cape Basin during the first MARE expedition in February 2000 (Fig. 6.1). Depth-stratified plankton tows (Tab. 6.1; Fig. 6.1) were collected in the centre of the eddy (station 06), at its edge (station 05), and outside in the surrounding ocean (station CWR). Each station covered nine depth intervals from the upper 800 m depth interval of the water column. The plankton was collected using a Hydrobios Multinet system modified for oblique towing and equipped with 100µm plankton nets (chapters 2 and 5). At the same sites, the entire water column was profiled using a Neill-Brown CTD-rosette sampler (Veth, 2000). In addition, two Technicap PPS5 sediment traps were deployed below the centre of the eddy, one at the site 06 (water depth 5036 m), and another outside the eddy at the CWR site (water depth 2700 m), both moored 250 m above the sea floor. The traps had a sampling area of 1 m^2 and collected an integrated 6-months sample of pelagic particles settling to the sea floor. For processing of foraminiferal samples from traps and plankton tows and the taxonomic determination I followed the procedure as described in chapters 4 and 5. The foraminiferal standing stocks are calculated following the method from chapters 2 and 5. In addition to the plankton tow, CDT and sediment trap sampling, we also recovered the bottom sediments by a box corer at the CWR site during the MARE III cruise (February 2001; 174P03-6). The sampling and processing of the box core and its stratigraphy are described in the chapter 4. In this chapter are presented the results of the foraminiferal analysis from the uppermost 0.5 cm of the sediment.

Table 6.1: Position of the stations and sampling techniques applied in this study.

station	coordinates [°]		sampling technique			
	lat.	long.	pl. tows	CTD	sed. trap	box core
CWR	27.0 S	3.9 E	+	+	+	+
05	28.8 S	6.3 E	+	+		
06	29.2 S	8.2 E	+	+	+	

3. THE EDDY "W"

In October 1999 the Agulhas eddy named "W" was one of the most prominent features on the sea surface height (SSH) images of the Cape Basin (http://ibis.grdl.noaa.gov/SAT/hist/tp_products /topex.html). It was situated in the central Cape Basin, approximately at the latitude of the Cape Town. During the austral spring and early summer it migrated northwards for approximately 5° latitude and lost in intensity. The SSH image of 18th February 2000 (Fig. 6.1) was used for pinpointing the station 06, just in the centre of the ring. The eddy "W" stayed for approximately two

weeks at the site 06 and then migrated westwards over the Walvis Ridge. In May 2000 it disappeared from the SSH images. During April/May 2000 another smaller Agulhas eddy was in the vicinity, southwards from the site 06. However, this eddy disintegrated before fully reaching the site. Although situated centrally within the "Agulhas Eddy Corridor" (Garzoli and Gordon, 1996; Schouten et al., 2000), the CWR site was not crossed by the fleeting eddies during the entire sediment trap sampling period (February-July 2000).

The crucial assumption being made here is that SSH anomalies in the southeastern Atlantic Ocean are undeniably Agulhas rings (Schouten et al., 2000). Indeed it has been shown that gross of the SSH variability in the Cape Basin arises from passing Agulhas rings only (Garzoli and Gordon, 1996; Garzoli et al., 1996). In addition, e.g. van Aken et al. (2003) have demonstrated by extensive seagoing hydrographic investigations the relationship between TOPEX/Poseidon SSH anomalies and in-situ measured properties of the rings. Most of the time the SSH position of the ring centre is within 50 km, or half a degree, of the actual centre (Schouten et al., 2000). SeaWiFS satellite images of the surface chlorophyll-a concentration (chapter 4) show that all stations were oligotrophic, outside the direct influence from the Benguella upwelling at the time of the plankton tow sampling. Yet, tongues of nutrient-rich water spreading from the Benguela upwelling zone did approach the station 06 from July to September 2000.

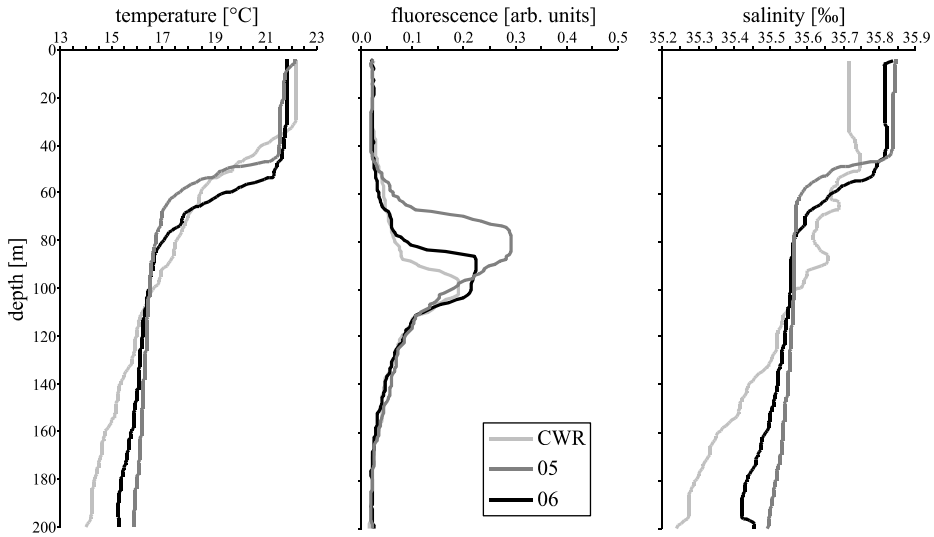

Figure 6.2: Temperature, fluorescence and salinity profiles for the upper 200 m of the water column measured by the CTD-rosette sampler at three study sites from figure 6.1.

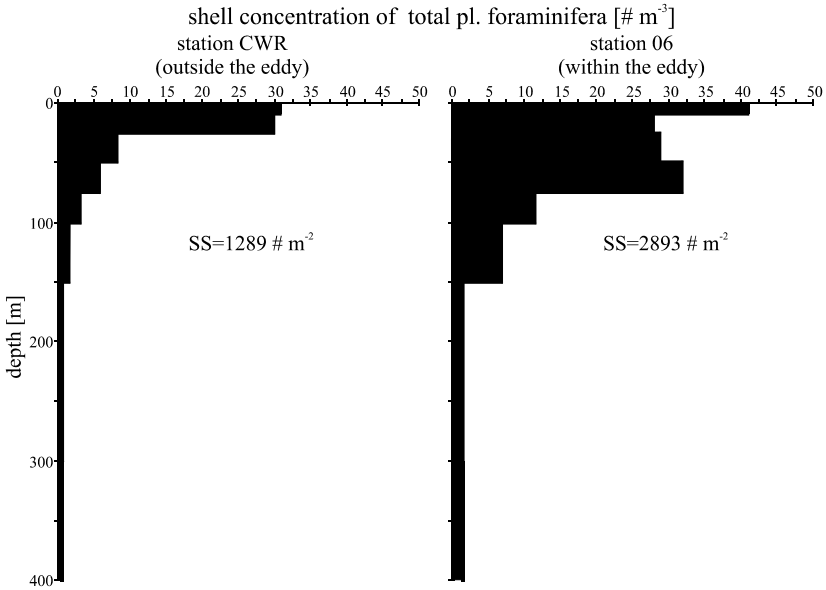

Figure 6.3: Shell concentration of total planktic foraminifera sampled by plankton tows within the eddy "W" (right panel) and in the surrounding oligotrophic gyre (left panel). Numbers refer to the total foraminiferal shell standing stocks in the productive zone calculated following method described in chapters 2 and 5.

4. RESULTS

4.1. Physical properties

During plankton tow sampling and CTD profiling (22 Feb. 2000; station 06) the eddy "W" was situated in the northern Cape Basin. It was eminently distinguishable on the SSH image (Fig. 6.1) by its elevated surface. Although clearly recognisable on the TOPEX/Poseidon satellite image, the CTD profiles taken in the centre of the eddy and outside in the open ocean, were similar (Fig. 6.2). The same temperature of the surface mixed layer (±22°C) and prominent deep fluorescence maximum at ±100 m characterised both profiles. In both cases the fluorescence maximum was below the surface mixed layer. The centre of the eddy differed from the surrounding water by an approximately 0.1‰ higher salinity, deeper surface mixed layer (60 m in the ring vs. 35 m outside) and by a somewhat broader and stronger fluorescence maximum.

4.2. Foraminiferal assemblages

I compared the foraminiferal concentration profiles in the upper water column collected by plankton tows (Figs. 6.3-6.5) with the export fluxes from the sediment traps and the accumulation

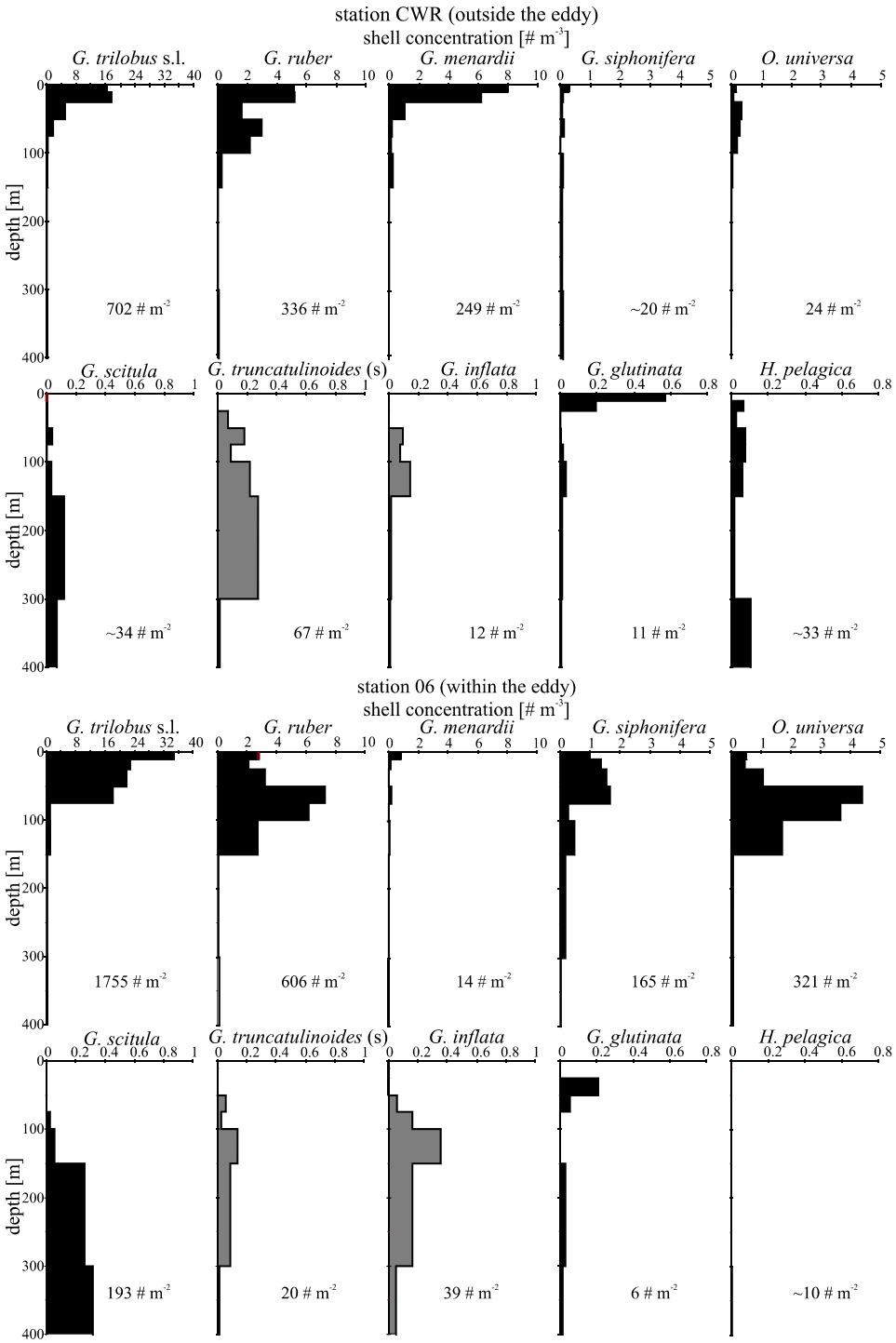
station CWR (outside the eddy)
shell concentration [# m-3]
G. trilobus s.l.
G. ruber
G. menardii
G. siphonifera
O. universa
G. scitula
G. truncatulinoides (s)
G. inflata
G. glutinata
H. pelagica
depth [m]
702 # m-2
336 # m-2
249 # m-2
~20 # m-2
24 # m-2
~34 # m-2
67 # m-2
12 # m-2
11 # m-2
~33 # m-2
station 06 (within the eddy)
shell concentration [# m-3]
1755 # m-2
606 # m-2
14 # m-2
165 # m-2
321 # m-2
193 # m-2
20 # m-2
39 # m-2
6 # m-2
~10 # m-2

Figure 6.4 (previous page): Shell concentration profiles of 10 major foraminiferal species from the plankton tows sampled within and outside the eddy "W" given for the upper 400 m of the water column. Species given in black belong to the typical Agulhas leakage fauna (Peeters et al., 2004). Numbers refer to the standing stocks in the productive zone of the particular species calculated following method from chapters 2 and 5.

flux from the core top sediment (Fig. 6.6). The selected stations represent the foraminiferal assemblages within the eddy (station 06) and the surrounding oligotrophic gyre (CWR station), respectively. In addition, quantitative analysis of the plankton tow samples was performed also at station 05, situated at the eddy's edge.

4.2.1. Water column fauna

In February 2000 the foraminiferal standing stock within the eddy "W" was more than two times higher than in the surrounding oligotrophic ocean (Fig. 6.3). The highest total foraminiferal concentrations were restricted to the surface mixed layer (SML) at both stations. Yet, within the eddy, the foraminiferal concentrations showed two maxima, one within the uppermost tow interval and another at the base of the SML. By contrast, in February 2000 the surrounding ocean was characterised by a shallow SML (Fig. 6.2) and high foraminiferal concentrations were restricted to the uppermost 25 m (Fig. 6.3). The standing stocks at both stations were dominated by tropical, shallow-dwelling species such as *G. trilobus* s.l. and *G. ruber* (Figs. 6.4 and 6.6). *O. universa*, *G. siphonifera* and *G. scitula* were frequent only within the eddy and showed maximum concentrations in the subsurface. Remarkably, the tropical *G. menardii* was absent of within the eddy, while this species was the third most dominant in the surroundings and showed the second highest concentration in the uppermost tow interval. For the other species, deep-dwelling *Globorotalia truncatulinoides* (sin) and *Globorotalia inflata* showed similar concentrations and vertical distributions at both sites, whereas *Globigerinita glutinata* and *Hastigerina pelagica* were rare. Quantitative analysis performed on the tow material collected at station 05, situated at the edge of the eddy "W" (Fig. 6.1), showed significantly increased plankton standing stocks compared to not only the surrounding ocean, but also to the centre of the eddy (Fig. 6.5). The concentration of organic matter was approximately 5 times higher, and the concentration of the particulate inorganic matter exceeded 15 to 45 times the values from the eddy and the surrounding, respectively (Fig. 6.5).

4.2.2. Export fluxes

The relative abundances of major species from the plankton tow and sediment trap assemblages were strikingly similar in spite of the long sampling interval of the traps, covering an integrated 6-month period from February to July 2000 (Fig. 6.5). As in the water column standing stocks, the warm-water species *G. trilobus* s.l. and *G. ruber* dominated also the exported flux intercepted by the traps at both sites. Only minor differences between the plankton tow and sediment trap assemblages were manifested by the increased relative abundance in the export flux of *G. siphonifera* at the CWR site and by the increased relative abundance of *G. inflata* together with *G. siphonifera* at the site 06, respectively. In contrast, *O. universa* and *G. scitula* showed higher relative abundance in the water column within the eddy "W" than in the export flux underneath it.

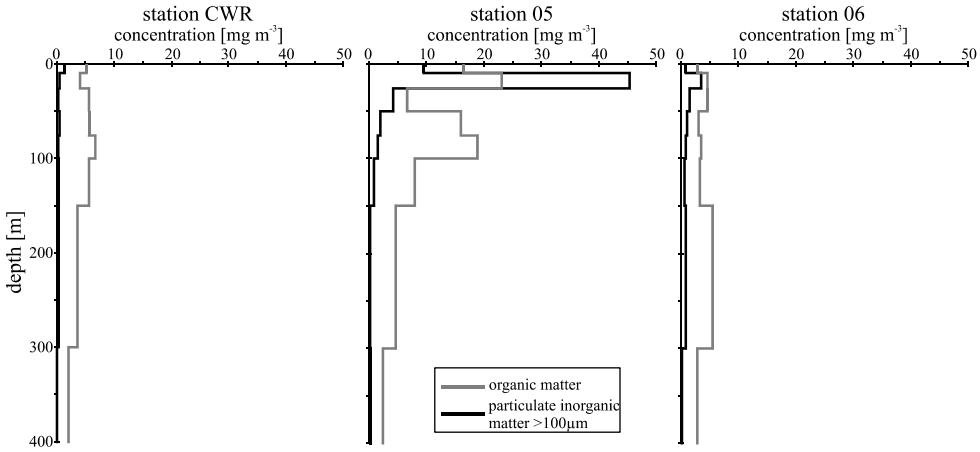

Figure 6.5: Concentration of organic and particulate inorganic matter larger than 100 µm from the plankton tows sampled at three study sites from figure 6.1. The organic matter is calculated as dry bulk weight minus weight of the ashed residue.

4.2.3. Core-top sediment assemblages

Since the water depth at the site 06 (5036 m) is deeper than that of the calcite lysocline (i.e. the depth at which calcite becomes undersaturated or the level of the onset of carbonate dissolution) and the Carbonate Compensation Depth (i.e. the depth below which the rate of calcite dissolution exceeds the rate of deposition) we sampled the sediment surface only at the shallow CWR site (2700 m). The ^{14}C and ^{210}Pb analyses showed that the topmost sediment at the CWR site is modern in age and the mixing rates are very low (chapter 4).

The centennial average accumulation flux preserved in the Walvis Ridge sediment differed in foraminiferal assemblage from those in the export flux and standing stocks sampled at the same site. In contrast to the composition of the fauna in the water column standing stocks and in the sediment trap fluxes, which were dominated by *G. trilobus* s.l. and *G. ruber*, approximately one third of the normalised foraminiferal assemblage in the uppermost 0.5 cm of the sediment was composed of *G. inflata*. Also some other secondary species within the water column and export flux assemblages such as sinistral *G. truncatulinoides*, *G. glutinata* and *G. scitula* showed a significant increase in the relative abundance within the surface sediment. In addition to the conventional enumeration of foraminiferal species, which considers on average 300 shells per sample (chapters 2-5), I analysed more than 5000 foraminiferal shells from the sieve size fraction >150 µm in the CWR sediment in search for *Globoquadrina hexagona*. Yet, this species was neither recognised in the sediment sample, nor in the traps or plankton tows.

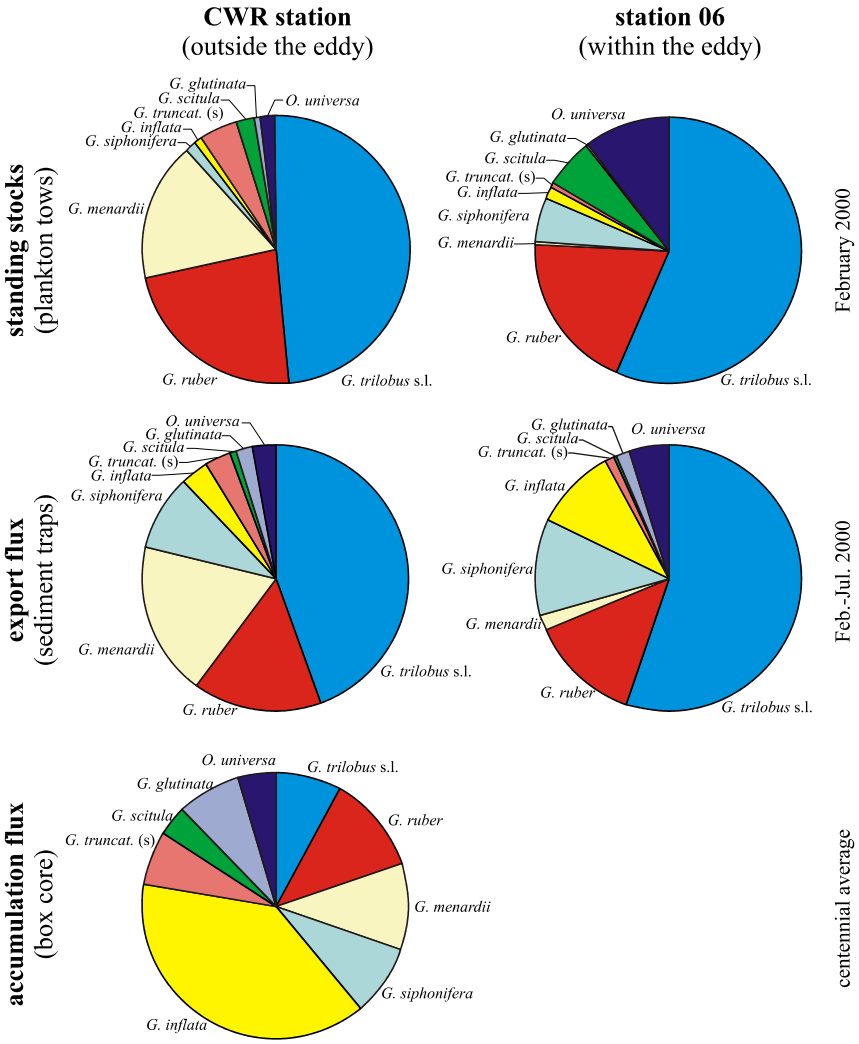

Figure 6.6: Relative abundance of 9 major foraminiferal species normalised to 100%, sampled within and outside the eddy "W", in the water column (February plankton tows), export flux (integrated February to July sediment traps) and accumulation flux (core top sediment).

5. DISCUSSION

The physical properties of a young, freshly formed eddy from the Agulhas retroflection zone in the southern Cape Basin have been recently in-situ studied by van Aken et al. (2003). This eddy was distinguished from the surrounding water by higher temperature and salinity values, and a deeper surface mixed layer. The foraminiferal assemblages of a young Agulhas eddy were characterized by high standing stocks and the dominance of tropical-subtropical species (Peeters et al., 2004). The most dominant among 10 characteristic Agulhas leakage species were *G. trilobus* s.l., *G. ruber* and *G. siphonifera*.

Due to a strong air-sea interaction (Olson et al., 1992), the positive sea surface temperature anomaly disappeared by the time the eddy "W" reached the northern Cape Basin. Yet, the ring was still clearly visible at SSH images (Fig. 6.1). Although the eddy lost some of its original physical and faunal signatures during its migration for more than a year from the Indian to the Atlantic Ocean, several characteristics were still recognizable. It was distinguished from the surroundings by a deeper surface mixed layer, higher salinity and higher foraminiferal standing stocks (Figs. 6.2-6.3). The foraminiferal assemblages were dominated by the same species (i.e. *G. trilobus* s.l., *G. ruber* and *G. siphonifera*), characteristic of a freshly formed ring (Peeters et al., 2004). However, the contrast between the physical and faunal characteristics of the eddy and the surrounding oligotrophic water of the subtropical gyre was weak (Fig. 6.4). It is partly therefore, and not just due to the faunal changes, that it is difficult to clearly identify a mature eddy based only on foraminiferal assemblages, without additional support from the satellite-derived sea surface altimetry.

In a number of paleostudies on Cape Basin sediments, *G. menardii* was attributed to have originated in the Indian Ocean and its presence in the sediment record was interpreted as indicative for the "open Cape valve" (Berger and Wefer, 1996b; Rau et al., 2002), i.e. interconnection between the Indian and Atlantic Ocean. My results suggest that this species does not belong to the typical mature ring fauna. Instead in the ring assemblages, I found an order of magnitude higher standing stocks of *G. menardii* in the adjacent subtropical gyre (Fig. 6.4). In addition, this species does not appear in the modern, freshly formed Agulhas eddies in relative abundances higher than 2% (Peeters et al., 2004, supplementary information S5). Therefore it is more likely that during interglacials, when ocean fronts shifted southward (Wefer and Berger, 1996a), this species re-seeded the Cape Basin from the subtropical Atlantic, rather than from the Indian Ocean (see Fig. 3 from Berger and Wefer, 1996b). This implies that the reappearance of *G. menardii* in the sediment records of the Cape Basin, and in particular in its northern part, can not be directly interpreted as evidence for the opening and closing of the "Cape valve".

Surprisingly high concentrations of organic and particulate inorganic matter were recorded at the station 05, situated at the edge of the eddy "W" (Fig. 6.5). These concentrations were not only higher than in the surrounding oligotropic ocean, but also compared to the centre of the eddy, suggesting a significantly increased productivity and high faunal standing stocks. The flow velocities of the rotating eddy increase with the distance from its centre till the inner edge, where they drop due to the friction with the surrounding water. The velocities are the highest at the top of the thermocline and decrease with depth (van Aken et al., 2003). Therefore, drastically increased standing stocks recorded at station 05 may be the result of an "upwelling like" process in the turbulent zone at the

interface between the eddy and the surrounding water. Such mixing process could introduce nutrients from the subsurface into the surface mixed layer, enhancing productivity in the otherwise predominantly oligotrophic environment.

The integrated February-July export fluxes recorded by the sediment traps at stations CWR and 06 mirror to a large extent the water column standing stocks from February 2000 (Fig. 6.6). This suggests stable conditions in the productive zone during the entire period of trap sampling. The increased dominance of *G. inflata* in the deposition fluxes coupled with decreasing foraminiferal diversity and abundance of the warm water species accompany transition from oligotrophic to mesotrophic conditions along the Benguela trophic gradient (chapter 4). Therefore increased export fluxes of *G. inflata* suggest increased productivity, in particular at the site 06 situated ca. 200 km closer to the Benguela upwelling zone. Such enhanced productivity occurred probably at the end of the sampling period when this site was approached by the filaments of nutrient-rich water spreading from the Benguela upwelling zone or, more likely, subsurface nutrients became available due to the wind-induced winter deepening of the surface mixed layer (Figs. 4.3-4.4). On the other hand, higher relative abundance of *O. universa*, *G. scitula* and *G. ruber* in the February water column of the same site appear related to the passing eddy.

The dominance of *G. inflata* and distinct assemblages of the CWR core-top sediment, in contrast to the February plankton tow and February to July sediment trap assemblages, point to the strong overprint by the seasonal bloom. Approximately 25% of the annual flux in this area is deposited during the short, but prominent spring maximum in October (chapter 4). This seasonal event dilutes the already very weak Indian Ocean signal that remained in the mature eddy and makes it untraceable in the fossil record. In all studied samples I did not find any *G. hexagona*, species endemic in Indian Ocean waters. Therefore, I can not firmly trace the fingerprint of Indian Ocean inflow by the foraminiferal assemblages in the water column and surface sediments of the northern Cape Basin.

6. ACKNOWLEDGMENTS

I thank the captains, crews and shipboard scientific parties of R/V Pelagia and R/V Agulhas for the assistance during the MARE cruises. This work was financially supported by the Dutch Ministry of Education, Arts and Science within the Netherlands - Bremen Oceanography (NEBROC) program. The MARE program (Mixing of Agulhas Rings Experiment) was financed by the Clivarnet project of the Netherlands Organization for Scientific Research (NWO - ALW).

REFERENCES

Berger, W.H. & Wefer, G., 1996a. Central themes of South Atlantic circulation. In: G. Wefer, W.H. Berger, G. Siedler & D.J. Webb (Eds), *The South Atlantic: Past and Present Circulation.* Springer-Verlag, Berlin, Heidelberg: pp. 1-11.

Berger, W.H. & Wefer, G., 1996b. Expeditions into the past: Paleoceanographic studies in the South Atlantic. In: G. Wefer, W.H. Berger, G. Siedler & D.J. Webb (Eds), *The South Atlantic: Past and Present Circulation*. Springer-Verlag, Berlin, Heidelberg: pp. 363-410.

Byrne, D.A., Gordon, A.L. & Haxby, W.F., 1995. Agulhas eddies: a synoptic view using Geosat ERM data. *Journal of Physical Oceanography, 25* (5): 902-917.

Chen, M.-T., Chang, Y.-P., Chang, C.-C., Wang, L.-W., Wang, C.-H. & Yu, E.-F., 2002. Late Quaternary sea-surface temperature variations in the southeast Atlantic: a planktic foraminifer faunal record of the past 600000 yr (IMAGES II MD962085). *Marine Geology, 180* (1-4): 163-181.

de Ruijter, W.P.M., 1982. Asymptotic analysis of the Agulhas and Brazil Current systems. *Journal of Physical Oceanography, 12* (4): 361-373.

de Ruijter, W.P.M., Biastoch, A., Drijfhout, S.S., Lutjeharms, J.R.E., Matano, R.P., Pichevin, T., van Leeuwen, P.J. & Weijer, W., 1999. Indian-Atlantic interocean exchange: dynamics, estimation and impact. *Journal of Geophysical Research, 104* (C9): 20885-20910.

Flores, J.-A., Gersonde, R. & Sierro, F.J., 1999. Pleistocene fluctuations in the Agulhas Current Retroflection based on the calcareous plankton record. *Marine Micropaleontology, 37*: 1-22.

Garzoli, S.L. & Gordon, A.L., 1996. Origins and variability of the Benguela Current. Journal of Geophysical Research, 101(C1): 897-906.

Garzoli, S.L., Gordon, A.L., Kamenkovich, V., Pillsbury, D. & Duncombe Rae, C., 1996. Variability and sources of the southeastern Atlantic circulation. *Journal of Marine Research, 54* (6): 1039-1071.

Goñi, G.J., Garzoli, S.L., Roubicek, A.J., Olson, D.B. & Brown, O.B., 1997. Agulhas ring dynamics from TOPEX/Poseidon satellite altimeter data. *Journal of Marine Research, 55* (5): 861-883.

Gordon, A.L., 1985. Indian-Atlantic transfer of thermocline water at the Agulhas retroflection. *Science, 227* (4690): 1030-1033.

Gordon, A.L., 1996. Communication between oceans. *Nature, 382* (6590): 399-400.

Gründlingh, M.L., 1995. Tracking eddies in the southeast Atlantic and southwest Indian oceans with TOPEX/Poseidon. *Journal of Geophysical Research, 100* (C12): 24977-24986.

Lutjeharms, J.R.E., 1996. The exchange of water between the South Indian and South Atlantic Oceans. In: G. Wefer, W.H. Berger, G. Siedler & D.J. Webb (Eds), *The South Atlantic: Present and past circulation.* Springer-Verlag, Berlin Heidelberg: pp. 125-162.

Lutjeharms, J.R.E. & van Ballegooyen, R.C., 1988. The retroflection of the Agulhas Current. *Journal of Physical Oceanography, 18* (11): 1570-1583.

Olson, D.B., R.A., F. & Gordon, A.L., 1992. Convective modifications of water masses in the Agulhas. *Deep-Sea Research I, 39* (1A): 163-181.

Peeters, F.J.C., Acheson, R., Brummer, G.-J.A., De Ruijter, W.P.M., Schneider, R., Ganssen, G., Ufkes, E. & Kroon, D., 2004. Vigorous exchange between the Indian and Atlantic oceans at the end of the past five glacial periods. *Nature, 430* (7000): 661-665, doi:10.1038/nature02785.

Peterson, R.G. and Stramma, L., 1991. Upper-level circulation in the South Atlantic Ocean. *Progress in Oceanography, 26* (1): 1-73.

Rau, A.J., Rogers, J., Lutjeharms, J.R.E., Giraudeau, J., Lee-Thorp, J.A., Chen, M.-T. & Waelbroeck, C., 2002. A 450 kyr record of hydrological conditions on the western Agulhas Bank Slope, south of Africa. *Marine Geology, 180*: 183-201.

Schouten, M.W., de Ruijter, W.P.M., van Leeuwen, P.J. & Lutjeharms, J.R.E., 2000. Translation, decay and splitting of Agulhas rings in the southeastern Atlantic Ocean. *Journal of Geophysical Research, 105* (C9): 21913-21925.

Shannon, L.V. & Nelson, G., 1996. The Benguela: large scale features and processes and system variability. In: G. Wefer, W.H. Berger, G. Siedler & D.J. Webb (Eds), *The South Atlantic: Present and past circulation*. Springer-Verlag, Berlin Heidelberg: pp. 163-210.

van Aken, H.M., van Veldhoven, A.K., Veth, C., de Ruijter, W.P.M., van Leeuwen, P.J., Drijfhout, S.S., Whittle, C.P. & Rouault, M., 2003. Observations of a young Agulhas ring, Astrid, during MARE in March 2000. *Deep-Sea Research II, 50* (1): 167-195.

Veth, C., 2000. *RV Pelagia Cruise Report: Cruise 64PE155, Project MARE-1, Mixing of Agulhas Rings Experiment.* NIOZ, Texel: 42 pp.

Weijer, W., de Ruijter, W.P.M., Dijkstra, H.A. & van Leeuwen, P.J., 1999. Impact of interbasin exchange on the Atlantic overturning circulation. *Journal of Physical Oceanography, 29* (9): 2266-2284.

Weijer, W., de Ruijter, W.P.M. & Dijkstra, H.A., 2001. Stability of the Atlantic overturning circulation: Competition between Bering Strait freshwater flux and Agulhas heat and salt sources. *Journal of Physical Oceanography, 31* (8): 2385-2402.

Na novu plovidbu

Vedri se nebo. Sunce se rađa.
Plovi iz luke jedna lađa;
Jedna što dugo stajaše u doku,
Sva izbijena, s ranama na boku.
More, ko mati, vuče je na krilo.
Ljulja je, šapće: Ništa nije bilo.

Dobriša Cesarić (1902-1980)

7. Samenvatting

1. PLANKTONISCHE FORAMINIFEREN

Planktonische foraminiferen zijn eencellige organismen behorend tot de Klasse Foraminifera van het Fylum Granuloreticulosa uit het Rijk der Protista (eencellige eukaryoten). Ze werden bijna twee eeuwen geleden ontdekt en voor het eerst beschreven door D'Orbigny (1826). Tijdens hun levenscyclus vormen deze vrij in het water zwevende beestjes een spiraalvormig gewonden kalkschelpje, samengesteld uit meerdere kamers. Ze leven voornamelijk in het bovenste deel van de open oceanische waterkolom waar zij hun verticale positie kunnen bepalen door aanpassing van het drijfvermogen. De taxonomie, traditioneel gebaseerd op de morfologie van de schelp (schelpvormen en typen schelpoppervlak in Fig. 1.1), omvat ongeveer 44 recent levende soorten (Hemleben et al., 1989). Twee hoofdgroepen worden onderscheiden gebaseerd op aan- of afwezigheid van stekels, respectievelijk spinose en niet-spinose soorten (Murray, 1897). Over het algemeen zijn spinose soorten vleeseters en grazen vooral op copepoden, terwijl niet-spinose soorten zich voeden met algen, zoals voor het eerst werd geconstateerd door Rhumbler (1911). Meerdere soorten zijn echter omnivoor en grazen op zowel fytoplankton als op dierlijke prooi. Sommige, in het bijzonder spinose soorten, kunnen symbiotische algen bevatten, voornamelijk dinoflagellaten.

Omgevingskarakteristieken van het bovenste deel van de waterkolom, zoals temperatuur en voedselaanbod, bepalen de soortensamenstelling van de fauna in de verschillende wereldoceanen (o.a. Bé en Tolderlund, 1971). Naast andere factoren is het door die verbondenheid aan het ecosysteem dat met behulp van planktonische foraminiferen omstandigheden van vroegere oceanen achterhaald kunnen worden. Ze worden dan ook tot een van de belangrijkste hulpmiddelen in de paleoceanografie gerekend. De voortplantingscyclus van vele, zo niet alle soorten, eindigt met de gametogenese van het volwassen individu. Gametogenese is de seksuele reproductie waarbij het voortplantende individu een groot aantal gameten loslaat, die later zullen samensmelten tot zygoten waaruit zich de juvenielen ontwikkelen (Hemleben et al., 1989). Na gametogenese zinkt de lege kalkschelp van de adult naar de oceaanbodem. Schelpjes van foraminiferen vormen dan ook een hoofdcomponent van de pelagische oceaansedimenten boven de carbonaat-compensatiediepte (diepte waar beneden de snelheid van carbonaatoplossing groter is dan die van carbonaatafzetting). Door de bovengenoemde wijze van voortplanten zal de carbonaatproductie in de bovenste laag van de oceaan direct gerelateerd zijn aan de depositieflux van schelpjes naar de zeebodem, waardoor de eigenschappen van het water waarin de organismen leefden worden omgezet in een fossiel signaal in het sediment (Fig. 1.2). Ryan en Pitman (1998) verklaarden in hun rapport over de hoogtepunten van het "Ocean Drilling Program" uit eerster dagen, dat de sedimentaire laag van de oceaanbodem een

soort virtuele bibliotheek van informatie is. Onze niet volledige kennis van de ecologie van foraminiferen is wellicht een van de meest beperkende factoren om de informatie opgeslagen in deze "bibliotheek van de zeebodem" te achterhalen. Deze studie richt zich daarom op het ontrafelen van het script van deze bijzondere bibliotheek door het vastleggen van biologische en chemische eigenschappen van recente foraminiferen met de bedoeling om de interpretatie van vroegere oceaanomgevingen te verbeteren.

2. PROXIES IN DE PALEOCEANOGRAFIE

Karakteristieken van vroegere oceanen, zoals paleotemperatuur, paleosaliniteit en paleoproductie, zijn niet direct meetbaar. Zij kunnen echter wel worden afgeleid uit andere nog wel meetbare parameters, die op hun beurt weer zijn gerelateerd aan de niet meer meetbare. Zulke indicatoren worden proxies genoemd. In de paleoceanografie dienen zij om de vroegere omgevingsvariabelen te bepalen, door interpretatie van de meetresultaten in termen van de omstandigheden die zij weerspiegelen. Planktonische foraminiferen behoren tot één van de belangrijkste paleoceanografische proxies. De samenstelling van hun kalkschelp en soortensamenstelling van de associaties uit het verleden worden gebruikt om vroegere temperatuur, saliniteit, ijsvolume, zeespiegelniveau, oceaancirculatie en stratificatiediepte te achterhalen. Deze omgevingsvariabelen kunnen worden vastgesteld aan de hand van de analogie tussen de fossiele schelpjes die in de oceaansedimenten worden aangetroffen en de huidig levende soorten in het bovenste deel van de waterkolom. Gezien de brede toepassing van planktonische foraminiferen en hun grote belang voor oceaan- en klimaatreconstructies, vormt een grondig begrip van het gedrag van recente soorten de basis voor betrouwbare reconstructies van paleohydrografische omstandigheden. Veldobservaties van levende populaties zijn daartoe noodzakelijk, omdat deze in direct verband gebracht kunnen worden met de fysische en chemische eigenschappen van de omringende waterkolom. Een correcte interpretatie van vroegere omstandigheden is echter niet alleen afhankelijk van een volledig begrip van de ecologie van de afzonderlijke soorten. Het bronsignaal van foraminiferen, geëxporteerd vanuit de productieve zone (dat deel van de waterkolom waar foraminiferen leven en hun schelp maken, Fig. 1.2) kan namelijk ook zijn beïnvloed door de mate van preservatie tijdens transport naar de diepzee. Immers, processen zoals ongelijke oplossing van soorten en diagenese (de verandering van sedimenten onder invloed van fysische en (bio)chemische processen) kunnen het oorspronkelijke signaal zodanig wijzigen dat het de reconstructie van de specifieke oceaan- en klimaatvariabelen bemoeilijkt.

Het hoofddoel van deze studie was om de ecologische voorkeuren van recente planktonische foraminiferen vast te stellen en hun reacties op veranderingen in de omgeving. Dit proefschrift richt zich daarom op een aantal vragen met betrekking tot de gevoeligheid van foraminiferensoorten ten aanzien van temperatuur, productiviteit, stratificatiediepte, verticale en laterale verspreiding, populatiedynamiek en seizoenvariabiliteit in schelpproductie en -export. Ook werd aandacht besteed aan de preservatie in sedimenten en het effect van een variabele schelpproductie (over verschillende seizoenen en van jaar tot jaar) naar de fossiele associaties, door accumulatiefluxen van foraminiferen uit het sediment te vergelijken met jaarlijkse depositiefluxen uit sedimentvallen.

3. DE WALVISRUG EN OMSTREKEN

Deze studie werd uitgevoerd in het centrale deel van de Walvisrug, in de Zuidoost Atlantische Oceaan (Fig. 1.3). In dit deel van de Atlantische Oceaan wordt de hydrografie grotendeels bepaald door de Zuid Atlantische subtropische wervel. De centrale Walvisrug bevindt zich onder invloed van de noordwaarts stromende oostelijke flank van deze wervel, beter bekend als de oceanische tak van de Benguelastroom (Peterson en Stramma, 1991; Garzoli en Gordon, 1996), met voornamelijk voedselarm oppervlaktewater. Oostelijk van het studiegebied wordt het oppervlaktewater gedomineerd door de langs de kust stromende tak van de Benguelastroom, die geassocieerd wordt met een windgestuurde opstromingszone langs het Zuid Afrikaanse en Namibische continentale plat (18˚-34˚ Z). In deze zone wordt het oppervlaktewater aflandig getransporteerd door de zuidoostelijke passaatwinden. Kouder en voedselrijk water, afkomstig uit diepere lagen, komt daarvoor in de plaats. Benguela- opstromingscellen zijn het gehele jaar door actief en produceren uitlopers die incidenteel tot 600 km zeewaarts kunnen reiken (Lutjeharms en Stokton, 1987). Hoewel het één van de grootste opstromingsgebieden van de wereld is (Shannon en Nelson, 1996), heeft het Benguela-opstromingssysteem geen directe invloed op de oceanografische condities van het water boven de Walvisrug, dat onafgebroken oligotroof blijft (Fig. 4.3).

Een ander prominent hydrografisch aspect van de Zuidoost Atlantische Oceaan is de instroom van warm en zout water van de Agulhasstroom vanuit de Indische naar de Atlantische Oceaan rondom Kaap de Goede Hoop (Schouten et al., 2000, 2002). Terwijl het grootste deel van dit water weer terugstroomt naar de Indische Oceaan, lekt een kleiner deel in het Kaapbekken. Dit gebeurt in de vorm van grootschalige ringen, die af en toe de Atlantische Oceaan binnenkomen en in het Benguelasysteem kunnen binnendringen. Deze Agulhasringen zijn tegen de klok in draaiende watermassa's met een relatief hoge dichtheid. De ringen hebben een doorsnede van 100 tot 250 km en reiken 500 tot 1000 m diep (Lutjeharms, 1996; van Aken et al., 2003). Nadat ze zich eenmaal in het Benguelasysteem bevinden, migreren ze gestaag noordwaarts, waarbij ze warmte en saliniteit afstaan aan het omringende water. De toevoeging van dit warme en zoute water is een belangrijk element van de wereldwijde thermohaliene circulatie en één van de meest bepalende factoren voor de warmte- en zoutbalans van de Zuid Atlantische Oceaan (Gordon, 1985; Gordon et al., 1992).

4. KORTE SCHETS VAN HET ONDERZOEK

4.1. Materialen en methoden

Het centrale deel van het Walvisruggebied in de Zuidoost Atlantische Oceaan, ongeveer 1300 km westelijk van de Afrikaanse kust, bevindt zich buiten de invloeden van de kustzone en de Benguela-opstroming (Fig. 1.3). Het wordt gekenmerkt door overwegend stabiele condities met gedurende het grootste deel van het jaar lage concentraties aan voedingsstoffen in de ondiepe gemengde oppervlaktelaag en een lage temperatuurgradiënt. Het gebied vormt daardoor een geschikte omgeving om de individuele eigenschappen en de respons van foraminiferensoorten te kunnen bepalen en kwantificeren. Het CWR (Central Walvis Ridge) bemonsteringsstation vormt het

referentiekader voor alle ecologische studies die in dit proefschrift gepresenteerd worden. Een aantal andere locaties rondom de CWR werden bemonsterd om aanvullende regionale gegevens te verzamelen, waardoor het effect van veranderingen in de Zuidoost Atlantische hydrografie op de diepzee carbonaatsedimentatie kon worden vastgesteld (Fig. 1.3; Tab. 1.1). Materiaal werd verzameld met behulp van verschillende bemonsteringstechnieken tijdens de drie MARE vaartochten in februari 2000, juli/augustus 2000 en februari 2001 (Tab. 1.1). Waterkolomeigenschappen zoals temperatuur, saliniteit en fluorescentie werden in-situ gemeten met behulp van een CTD (Conductiviteit Temperatuur Dieptemeter) gecombineerd met een bemonsteringssysteem voor water (flessenrozet, Fig. 1.4a). De flessen werden op gewenste diepten gevuld met zeewater en aan boord of later in het laboratorium geanalyseerd op voedingsstofgehalte en isotopen samenstelling. Plankton van de bovenste 800 tot 1000 m van de waterkolom werd bemonsterd met planktonnetten, die verticaal door het water gesleept werden. Het apparaat dat hiervoor gebruikt werd is een door het NIOZ gemodificeerd Hydrobios Multinet systeem, voorzien van twee doorstroommeters en vijf netten, elk met een maaswijdte van 100 μm, opgehangen in een stalen frame en bestuurd via een PC-deckunit (Fig. 1.4b). Dit maakte kwantitatieve bemonstering van foraminiferen en ander plankton mogelijk op nauwkeurig bepaalde diepte-intervallen. De netten werden geopend en gesloten tijdens het scheef naar boventrekken achter een langzaam varend schip, elk een volume van 20 tot 1000 m^3 zeewater doorlatend (Fig. 1.5). De bemonsterde intervallen waren gewoonlijk groter voor de trekken in diep water waar de planktonconcentraties laag zijn en kleiner in de fotische zone, waar het plankton overvloedig is (Fig. 1.2; Tab. 2.1). Zo werd het dichtslibben van de netten voorkomen, terwijl tegelijk voldoende materiaal kon worden verzameld voor taxonomische en chemische analyses. Bezinkende deeltjes werden verzameld met behulp van tijdreeks-sedimentvallen. Sedimentvallen zijn trechtervormige apparaten, verankerd dicht bij de bodem met een openingsdiameter van 1 m^2 aan de brede bovenkant en uitgerust met een carrousel van 24 monsterpotjes aan de nauwe onderzijde, geprogrammeerd om te roteren in gelijke tijdsstappen van meestal 7 of 8 dagen. Oppervlaktesediment werd bemonsterd met een boxcorer, in dit geval een 55 cm hoge en 50 cm brede metalen cilinder met een gewicht aan de bovenkant. Door de zwaartekracht was deze cilinder in staat snel naar de zeebodem te zinken om de bovenste decimeters van het sediment te doorboren, terwijl het zich bij het intrekken van de kabel sloot met een deksel.

4.2. Populatiedynamiek van planktonische foraminiferen

Hoofdstuk 2 richt zich op de populatiedynamiek van foraminiferen. In dit onderdeel van het proefschrift werd een methode ontwikkeld om drie begrippen te kwantificeren (Fig. 2.3): de diepte van de productieve zone (deel van de waterkolom waar planktonische foraminiferen leven), de populatiedichtheid (aantal schelpjes per m^2 van deze zone) en de verversingstijd ("turnover time", tijd die nodig is voor complete vervanging van de populatie door de volgende generatie). De berekening van de verversingstijd werd op twee onafhankelijke manieren uitgevoerd. De ene manier maakte gebruik van de depositieflux van foraminiferen (bezinkende schelpjes naar de zeebodem, uitgedrukt in aantal per m^2 per dag), een gegeven uit de sedimentvallen nabij de zeebodem. De andere methode nam juist de informatie afkomstig uit de planktonnetten, de zo genoemde exportconcentratie (dode schelpjes bezinkend vanuit de productieve zone, uitgedrukt in aantal per m^3). Een eenvoudig model werd ontwikkeld om de betekenis van deze verversingstijd aan te tonen. Het toonde aan dat de "turnover time" kan worden geïnterpreteerd als de gemiddelde levensduur van een foraminiferensoort

indien de populatie in een min of meer stabiele toestand verkeert waarbij populatieaanwas en sterfte met elkaar in evenwicht zijn (Fig. 2.8 en 2.9). Daarnaast toonde het model ook aan dat in een groeiende populatie verversingstijden toenemen, terwijl ze afnemen in slinkende populaties. Bij toepassing van deze methoden op de CWR resultaten van planktonnetten en sedimentvallen bleek dat de ondiep levende spinose soorten *Globigerinoides trilobus* en *Globigerinoides ruber* (Fig. 1.1d) de meest consistente waarden opleverden, met de minste afwijking van de stabiele toestand. De verversingstijd van deze twee soorten in de zuidelijke zomer impliceerde een gemiddelde levensduur van ongeveer twee weken. Niet-spinose, diep levende soorten toonden verversingstijden van niet meer dan zes weken. Deze bevindingen op de CWR benadrukken dat een complete verversing van een planktonische foraminiferenpopulatie binnen de productieve zone eerder een kwestie van weken is dan van een seizoen of van een jaar, zoals in vorige studies werd verondersteld voor sommige diep levende soorten.

4.3. Maancycli versus seizoeneffecten in depositiefluxen

Hoofdstuk 3 gaat nader in op de populatiedynamiek door het bestuderen van de invloed van de maandstand op de reproductie van foraminiferen. Een dergelijke maangestuurde reproductie werd voor het eerst aangetoond in laboratoriumkweken van *Hastigerina pelagica* (Fig. 1.1a) en is gesuggereerd voor verscheidene andere planktonische foraminiferen. Dit zou mogelijk een belangrijke bron zijn van temporele variatie in laterale en verticale verspreiding van levende soorten en een potentieel sturend mechanisme van korte termijn carbonaatfluxen. Het zou kunnen bijdragen aan de totale carbonaatflux van 5.7 Gt per jaar in de pelagische oceaan. In het veld zijn maanoscillaties in de voortplantingscyclus van foraminiferen nooit zo duidelijk waargenomen als bij de gekweekte *H. pelagica* en deze soort is dan ook tot nu toe de enige waarvoor een endogene maancyclus is aangetoond in het laboratorium. In dit proefschrift wordt voor het eerst gedemonstreerd dat maanperiodiciteit de *H. pelagica* schelpdepositiefluxen bepaalt op 2700 m diepte in de vrije natuur. De depositieflux van deze soort vertoonde op de CWR een uitgesproken 30-dagen cycliciteit, waarbij maxima gemiddeld 12 ½ dag na volle maan vielen. Na correctie op de bezinksnelheid kon het moment van reproductie worden vastgesteld op 5 dagen na volle maan, in overeenstemming met eerdere waarnemingen uit labcultures. Geen van de overige soorten van de Walvisrug beschreef, binnen het 16 tot 90 dagendomein van deze studie, een maangerelateerde of andere periodiciteit in depositieflux. Zij leken eerder door seizoeneffecten beïnvloed dan dat zij maangestuurd waren, implicerend dat reproductie binnen het maandomein continu was. Waarnemingen lieten zien dat *H. pelagica* dit continue productiesignaal naar het sediment niet heeft beïnvloed aangezien zij een zeldzame soort is met lage fluxen en een lage begraafefficiëntie (slechte preservatie). Deze studie toont daarmee aan dat maangestuurde reproductie geen waarneembaar effect heeft op pelagische carbonaatproductie en op accumulatiefluxen in de diepzee. Dit resultaat zal de interpretatie van de verspreidingspatronen van foraminiferen langs ecologische en fysische gradiënten in de bovenste delen van de oceaan vergemakkelijken. Uit het feit dat maanperiodiciteit in de depositiefluxen van *H. pelagica* werd waargenomen, blijkt de hoge nauwkeurigheid van de sedimentval-monstername op deze plek, vooral gezien de broosheid van de soort en de diepte van de verankering.

4.4. Seizoenexport en preservatie langs een trofische gradiënt

Waarnemingen van deeltjesfluxen uit verschillende delen van de wereldoceanen tonen aan dat planktonpopulaties over het algemeen dynamisch gedrag vertonen. Hoofdstuk 4 richt zich op seizoenvariaties in de overwegend voedselarme Zuid Atlantische subtropische wervel. Hiertoe werden tijdreeksen van depositiefluxen op de CWR van fytoplankton (diatomeeën en silicoflagellaten), zoöplankton (foraminiferen en pteropoden) en andere biogene deeltjes uit de sedimentvallen vergeleken met soortgelijke gegevens uit oppervlaktesediment van een boxcorer genomen op dezelfde locatie. De depositiefluxen van alle hoofdcomponenten vertoonden prominente maxima samenvallend met de zuidelijke lente. De start van deze productiviteitscyclus werd geïnitieerd door een verdieping van de oppervlaktemenglaag als gevolg van verhoogde windkracht laat in de herfst. Nutriëntentoevoer vanuit de onderlaag resulteerde in een verhoogde productiviteit (Fig. 4.4b). Aan het eind van de winter werd door het ondieper worden van de menglaag de toevoer van nutriënten afgesneden, wat leidde tot de instorting van de productiviteit. Als gevolg hiervan bereikte in de vroege lente in minder dan een maand, bijna 25% van de totale jaarlijkse massaflux de (nabije) zeebodem. De populatiegrootte van zowel diatomeeën als foraminiferen werd geassocieerd met hetzelfde proces van nutriëntentoevoer in de oppervlaktemenglaag, ondanks dat het fluxmaximum van de diatomeeën in de sedimentval een week vooruit liep op dat van de foraminiferen. Het tijdsverschil werd toegeschreven aan de combinatie van de enerzijds snellere reactie van fytoplankton op voedselbeperking en de anderzijds langzamere bezinking van diatomeeën ten opzichte van de zwaardere foraminiferen. Principale componentanalyse van de depositieflux tijdreeksen vertoonde sterk seizoengebonden foraminiferengroepen, terwijl diatomeeën zich volgens bloei- en niet-bloeiperiode groepeerden. *Globorotalia inflata* (Fig. 1.1f) en de kleine licht verkiezelde *Nitzschia bicapitata* overheersten de jaardeposities van foraminiferen en diatomeeën met respectievelijk 25 en 60%. Een belangrijke uitzondering op het algemene seizoenpatroon vormde de diep levende foraminifeer *Globorotalia truncatulinoides* (Fig. 1.1e), met depositiemaxima buiten het productieseizoen. De linksgewonden vorm toonde maxima vroeg in de winter en laat in het voorjaar, de rechtsgewonden vorm uitsluitend laat in het voorjaar. Een dergelijk verschil in seizoengebonden voorkomen van de twee verschijningsvormen van *G. truncatulinoides* pleit eerder voor een afzonderlijke taxonomische status dan van slechts een windingvariant binnen de soort zelf. Dit is in overeenstemming met resultaten uit recente DNA studies en suggereert dat genetisch verschillende soorten een verschillende seizoenaliteit hebben. Afbraak van organisch materiaal en oplossing van biogeen silicaat op het grensvlak van water en sediment resulteerde in slechte preservatie en daarmee samenhangend aanzienlijke veranderingen in soortensamenstelling van het kiezelfytoplankton. Van alle deeltjescomponenten werden alleen de foraminiferenschelpjes volledig bewaard in de oppervlaktelaag van het sediment teruggevonden. Het zijn dus vooral de foraminiferen (b.v. *G. inflata*) die het signaal van de bovenste delen van de oceaan vastleggen in de bodem, omdat zij nauwelijks hinder ondervinden van oplossing of fragmentatie en primair in staat zijn de seizoengebonden productiviteitsveranderingen weer te geven.

In het laatste deel van hoofdstuk 4 werden de CWR gegevens geplaatst in de context van een productiviteitsgradiënt door het Benguelasysteem, van het hoog productieve opstromingsgebied nabij de kust van Namibië naar het voedselarme deel in de subtropische wervel. Het CWR station completeerde, als eindlid, het voedselarme extreem. Langs deze gradiënt bleken de gemeten fluxmaxima zowel gerelateerd aan de winterminima van de oppervlaktewatertemperatuur als aan de

daarmee samenhangende dieptemaxima van de oppervlaktemenglaag, waarbij een zeewaartse verschuiving werd waargenomen, het eerst optredend langs de kust in augustus en twee maanden later op de CWR locatie. De overgang van oligotrofe naar mesotrofe condities werd gekenmerkt door een toename van *G. inflata* gekoppeld aan een afname van de diversiteit van foraminiferen en warmwater soorten, terwijl in de diatomeeënassociaties de kleine en licht verkiezelde *N. bicapitata* plaatsmaakte voor groter en zwaarder verkiezelde soorten. Dichter bij het opstromingsgebied ging de overgang van mesotrofe naar eutrofe condities gepaard met een afname in dominantie van *G. inflata* gecombineerd met een toename van koudwater soorten zoals *Globigerina bulloides*, de rechtsdraaiende *Neogloboquadrina pachyderma* en uiteindelijk de linksdraaiende *N. pachyderma* samen met *Turborotalita quinqueloba*. Hoewel de totale fluxen van deeltjescomponenten kustwaarts toenamen bleken de verschillen vrij klein, hetgeen slechts een gematigd hogere productiviteit en depositie impliceert langs de Namibische continentale rand in vergelijking met die in de subtropische wervel.

4.5. Zuurstofisotopen-ecologie van recente planktonische foraminiferen

In foraminiferenschelpjes wordt de $\delta^{18}O$, de verhouding tussen het zware en lichte zuurstofisotoop (ratio $^{18}O/^{16}O$) gemeten als afwijking van een standaard, bepaald door de isotopenverhouding en de temperatuur van het omringende zeewater. Als zodanig is in het $\delta^{18}O$ signaal van fossiele schelpjes uit sedimenten de ecologie van levende foraminiferen vastgelegd, te weten de diepte van calcificatie, seizoengebonden variaties in voorkomen, depositieflux en het "vitaal effect" (dat wil zeggen de wijze waarop het $\delta^{18}O$ signaal uit het omringende zeewater wordt opgenomen in het schelpje). Dit primaire signaal uit de productieve zone kan tijdens bezinking naar de zeebodem en tijdens begraving veranderd zijn door bijvoorbeeld aangroei van koudwater calciet in diep water, gedeeltelijke oplossing of diagenese. In hoofdstuk 5 werden verkregen ecologische inzichten van foraminiferensoorten gecombineerd met de zuurstofisotopenverhoudingen van hun schelpjes, om een beter begrip te verkrijgen over de habitat van soorten, de diepte van calcificatie, seizoengebonden variaties in voorkomen in het bovenste deel van de waterkolom en om de schatting van de oppervlaktewatertemperatuur op basis van het $\delta^{18}O$ signaal uit schelpjes te verbeteren. Om het proces naar sedimentpreservatie verder te ontrafelen werden de $\delta^{18}O$ gegevens uit het netplankton van de CWR vergeleken met de $\delta^{18}O$ van de jaardepositieflux uit de sedimentvallen en met het fossiele $\delta^{18}O$ signaal uit het oppervlaktesediment.

De basis van de productieve zone van foraminiferen (Z_{BPZ}) werd berekend gebruikmakend van de methode ontwikkeld in hoofdstuk 2 en werd vergeleken met de uit de $\delta^{18}O$ profielen afgeleide $Z_{BPZ.}$ De uitkomsten van deze twee onafhankelijke benaderingen kwamen grotendeels overeen, suggererend dat zowel uit de concentratie van schelpjes als uit de $\delta^{18}O$ samenstelling ervan een betrouwbare schatting kan worden gemaakt van het dieptebereik van de productieve zone van de betreffende soort. Uit de resultaten van het CWR station en van nog drie andere locaties in het zuidelijke Kaapbekken (Fig. 1.3) kwam *Globigerinita glutinata* (Fig. 1.1c) als beste proxy naar voren voor de watertemperatuur van het zeeoppervlak. Deze soort calcificeert in evenwicht met de verwachte $\delta^{18}O$ samenstelling van het omringende zeewater, vertoonde constante waarden met de diepte en was de enige soort van de CWR die geen verandering in het fossiele $\delta^{18}O$ signaal vertoonde. In overeenstemming met het fluxmaximum in het vroege voorjaar, dat door diepe wintermenging werd teweeggebracht (hoofdstuk 4), reflecteerde het $\delta^{18}O$ signaal van *G. glutinata*

uit het sediment nauwkeurig de wintertemperatuur van het zeewateroppervlak op de CWR locatie. Fossiele schelpjes van *G. ruber* (Fig. 1.1d), een soort die algemeen beschouwd wordt als ondiep levende soort en zodoende gebruikt wordt als proxy voor oppervlaktetemperatuur, bleken ook $\delta^{18}O$ waarden in het sediment te hebben die een goede schatting van de wintertemperatuur op de CWR locatie opleverden. Echter, onze planktonnetvangsten lieten zien dat de calcificatiezone van *G. ruber* altijd reikt tot het diepe chlorofylmaximum dat zich tot ver onder de oppervlaktemenglaag kan bevinden. Op de CWR locatie was dit het geval van het najaar tot het voorjaar (hoofdstuk 4), waardoor het geëxporteerde $\delta^{18}O$ signaal gedeeltelijk gevormd werd in kouder water dan dat van het oppervlak, met als gevolg een aanzienlijke onderschatting van de oppervlaktewatertemperatuur met meer dan 2 °C. Verder is gebleken dat *G. truncatulinoides* (Fig. 1.1e) calcificeert in $\delta^{18}O$ evenwicht met het omringende water binnen de zone met maximale schelpconcentraties, maar dat de diepte van die zone afhangt van de grootte van de schelp. Bij grote exemplaren wordt overigens wel een deel van het calciet gevormd in ondieper en warmer water, maar het gewichtsdeel <250 µm bleek te verwaarlozen ten opzichte van dat van de gehele schelp (Fig. 5.9). De resultaten van de netvangsten op de CWR lieten zien dat de $\delta^{18}O$ van de linksgewonden *G. truncatulinoides* met een maximale schelpdiameter van ~400 µm de watertemperatuur op ongeveer 350 m diepte weerspiegelt en die met een diameter van 250 µm de temperatuur op ongeveer 200 m diepte. Door gebruik te maken van de afwijking in $\delta^{18}O$ van de verschillende groottefracties in het sediment is het mogelijk de temperatuurgradiënt in de waterkolom te schatten.

4.6. Planktonische foraminiferen in een volgroeide Agulhasring

Hoofdstuk 6 beschrijft de faunasamenstelling in een volgroeide, tot in het noordelijke Kaapbekken doorgedrongen Agulhasring. Foraminiferenassociaties en fysische eigenschappen van de ring werden vergeleken met die van het omringende water en met de depositieflux, met als doel het effect van de ringen op de sedimentatiepatronen in het noordelijke Kaapbekken en Walvisrug te evalueren. De bestudeerde ring was op het moment van bemonstering duidelijk herkenbaar op de altimetrische beelden van het zeeoppervlak in de vorm van een verhoging ten opzichte van het omgevende water, veroorzaakt door de tegen de wijzers van de klok in roterende beweging. De ring werd onderscheiden van de omringende oceaan door een enigszins hoger zoutgehalte, een diepere oppervlaktemenglaag en hogere populatiedichtheden van planktonische foraminiferen. De samenstelling van de ringfauna was identiek aan eerder geïdentificeerde associaties in pas gevormde ringen van het zuidelijke Kaapbekken. Het verschil in fauna met de omgevende oceaan was echter gering, ondanks de duidelijke herkenbaarheid van de ring in de altimetrie. Opmerkelijk was echter wel de afwezigheid in de ring van de tropische soort *Globorotalia menardii* (Fig. 1.1b), terwijl deze soort in het omringende oceaanwater overvloedig aanwezig was. In verschillende paleostudies van dit gebied, is de soort vaak verondersteld oorspronkelijk uit de Indische Oceaan te komen en werd daarom geïnterpreteerd als “open klep van de Kaap”, waarmee een volledige interglaciale uitwisseling tussen de Indische en Atlantische Oceaan bedoeld werd. Echter, *G. menardii* behoorde niet tot de typische fauna van de hier bestudeerde volgroeide Agulhasring en evenmin tot die van de pas gevormde ringen uit het zuidelijke Kaapbekken. Het is daarom waarschijnlijker dat de soort in het Kaapbekken terechtkwam vanuit de subtropische Atlantische Oceaan door het zuidwaarts verschuiven van oceaanfronten tijdens interglacialen, in plaats van dat zij via Agulhasringen vanuit de Indische Oceaan in het bekken doordrong.

8. Sažetak

1. PLANKTONSKE FORAMINIFERE

Planktonske foraminifere su jednostanični organizmi unutar stabla Granuloreticulosa (carstvo Protista) otkrivene gotovo prije dva stoljeća, koje je po prvi put opisao D'Orbigny (1826). Za vrijeme njihovog životnog ciklusa ove slobodno plutajuće životinje tvore spiralnu karbonatnu ljušturu koja se sastoji od više klijetki. Planktonske foraminifere žive uglavnom u fotičkoj zoni otvorenog oceana, ali prilagodbom vlastite plovnosti mogu kontrolirati vertikalnu poziciju unutar vodenog stupca i tako obitavati na dubinama i od nekoliko stotina metara. Njihova taksonomija se tradicionalno zasniva na izgledu ljušture (oblik tijela i klijetki i tip njihove površine; sl. 1.1) i obuhvaća otprilike 44 recentne vrste (Hemleben et al., 1989). Na temelju prisutnosti ili odsutnosti bodlji izdvajaju se dvije osnovne skupine, takozvane bodljikave i nebodljikave vrste (Murray, 1897). Bodljikave vrste obično su mesožderi koji se hrane uglavnom kopepodima (veslonošcima), a nebodljikave vrste jedu alge, što je po prvi put zapazio Rhumbler (1911), premda su mnoge vrste svejedi koji se hrane i fitoplanktonom i životinjskom lovinom. Dio uglavnom bodljikavih vrsta može sadržavati simbionte (većinom dinoflagelate). Karakteristike okoliša u gornjem dijelu vodenog stupca, kao što su temperatura ili dostupnost hrane određuju sastav vrsta u svjetskim oceanima (Bé i Tolderlund, 1971). Između ostalih čimbenika upravo ta povezanost s ekosustavom čini planktonske foraminifere jednim od glavnih pomagala u paleooceanografskim istraživanjima, jer omogućuje rekonstrukciju uvjeta u drevnim oceanima. U reproduktivnom ciklusu mnogih, ako ne i svih vrsta, život završava gametogenezom, spolnim razmnožavanjem, gdje roditeljski organizam oslobađa velik broj gameta koje spajanjem stvaraju zigote i dalje se razvijaju u nove organizme (Hemleben et al., 1989). Nakon gametogeneze prazna karbonatna ljuštura roditeljskog organizma tone na dno oceana. Stoga ovaj način razmnožavanja direktno povezuje pelagičku proizvodnju karbonata u gornjem sloju oceana s taloženjem ljuštura na oceanskom dnu, prenoseći osobitosti okoliša u kojem je jedinka živjela u fosilni zapis oceanskih naslaga (sl. 1.2). Taloženje ljuštura foraminifera predstavlja značajan dio biogenog detritičnog toka („particulate flux") i čini većinu sedimentnog pokrivača dna pelagičkog oceana iznad karbonatne kompenzacijske dubine (dubine ispod koje količina otapanja karbonata nadmašuje količinu taloženja ljuštura). Stoga sedimentni pokrivač oceanskog dna predstavlja virtualnu knjižnicu informacija (Ryan i Pitman, 1998). Naše razumijevanje ekologije plaktonskih foraminifera je vjerojatno jedan od bitnih ograničavajućih čimbenika u razotkrivanju informacija pohranjenih u toj knjižnici oceanskog dna. Ovo istraživanje nastoji doprinijeti odgonetavanju "zapisa" te osobite "knjižnice" proučavajući biološke i kemijske karakteristike recentnih planktonskih foraminifera, s ciljem boljeg tumačenja drevnog oceanskog okoliša.

2. PALEOOCEANOGRAFSKI POKAZATELJI

Osobitosti drevnog oceanskog okoliša, kao što su paleotemperatura, paleosalinitet ili paleoprodukcija nisu direktno mjerljive. Pa ipak, one mogu biti razlučene iz drugih, direktno mjerljivih vrijednosti, povezanih s nama zanimljivim svojstvima oceana, koja ne možemo direktno izmjeriti. To su takozvani pokazatelji ("proxies"). U paleooceanografiji oni služe za određivanje osobitosti paleookoliša, kroz interpretaciju mjernih rezultata, u smislu uvjeta koje naznačuju. Planktonske foraminifere su jedan od glavnih paleooceanografskih alata (pokazatelja). Njihove zajednice i kemijski sastav njihovih karbonatnih ljušturica služe procjeni temperature, saliniteta, produkcije, sveopćeg obima leda i razine mora, oceanskih struja i stratifikacije iz prošlosti. Te osobitosti mogu biti procijenjene na temelju analogije fosilnih ljuštura nađenih na dnu oceana i vrsta koje trenutno obitavaju u gornjem dijelu današnjih oceana. Radi takve široke primjene planktonskih foraminifera i njihove velike važnosti za oceanografske i klimatološke rekonstrukcije nužno je potpuno razumijevanje ponašanja današnjih vrsta, jer to predstavlja osnovu za pouzdanu procjenu drevnih hidrografskih uvjeta. Stoga su terenska opažanja na živim zajednicama neophodna jer samo ona omogućuju direktnu usporedbu sastava zajednica i kemije njihovih karbonatnih ljuštura s fizikalnim i kemijskim osobitostima oceanske vode u kojoj žive.

Ova knjiga obrađuje niz pitanja povezanih s odnosom između foraminiferskih zajednica i temperature, proizvodnje ili stratifikacije vodenog stupca koji ih okružuje, njihovu vertikalnu i lateralnu rasprostranjenost, dinamiku zajednica i sezonske promjene u proizvodnji i izvozu ljuštura. Pa ipak, ispravna interpretacija drevnih uvjeta okoliša iz foraminiferskih naslaga nije ovisna samo o potpunom razumijevanju ekologije vrsta. Foraminiferni izvorni signal odaslan iz proizvodne zone (gornjeg dijela vodenog stupca u kojemu foraminifere žive i izlučuju svoju ljušturu; sl. 1.2) je ovisan o stupnju očuvanosti za vrijeme puta prema morskom dnu i nakon taloženja u sklopu dubokooceanskih sedimenata. Procesi djelomičnog otapanja i dijageneze mogu promijeniti izvorni signal i stoga utjecati na rekonstrukciju pojedinih karakteristika oceana ili klime. U svrhu utvrđivanja očuvanosti sedimenata i utjecaja sezonskih i međugodišnjih varijacija u proizvodnji ljuštura na sastav sedimenata morskog dna, ja sam ispitao i karakter akumulacijskog toka taloga („sediment accumulation flux") foraminiferskih ljuštura i usporedio ga s prosječnim godišnjim taloženjem (sl. 1.2).

3. PODRUČJE HRPTA KITOVA

Ovo istraživanje je izvršeno na središnjem dijelu Hrpta kitova (Walvis Ridge) u jugoistočnom Atlantskom oceanu (sl. 1.3) Hidrografija jugoistočnog Atlantika je uglavnom kontrolirana Suptropskim južnoatlantskim vrtlogom. Središnji dio Hrpta kitova je pod utjecajem istočnog ogranka tog vrtloga koji struji prema sjeveru a poznat je kao oceanski krak Bengvelske struje (Peterson i Stramma, 1991; Garzoli i Gordon, 1996) s uglavnom oligotrofnim uvjetima pri površini. Istočno od područja istraživanja površinskom cirkulacijom dominira obalni krak Bengvelske struje. On je povezan s vertikalnim strujanjem prema površini (= „upwelling") izazvanim vjetrom duž južnoafričkog i namibijskog šelfa (18˚ - 34˚ S). Površinska voda je u ovom području tjerana

jugoistočnim pasatnim vjetrovima od obale pa je zamjenjuje podpovršinska hladna voda bogata hranjivim tvarima. Bengvelske ćelije vertikalnog strujanja prema površini su aktivne cijele godine, a ogranci povremeno dosežu i 600 kilometara od obale (Lutjeharms i Stokton, 1987). Premda jedno od najvećih svjetskih područja vertikalnog strujanja prema površini (Shannon i Nelson, 1996), Bengvelski „upweling" sustav nema direktnog utjecaja na oceanografske uvjete iznad središnjeg Hrpta kitova, koji u tom smislu ostaju oligotrofni tijekom cijele godine (sl. 4.3).

Druga upadljiva značajka hidrografije sjeveroistočnog Atlantika je utjecanje tople i slane Aguljaške struje iz Indijskog oceana u Atlantik oko Rta dobre nade (Schouten et al., 2000, 2002). Veći dio Aguljaške struje se lomi i vraća natrag u Indijski ocean, a samo se manji probija u Kapsku zavalu. Proboj se događa u obliku vrtloga velikih dimenzija koji povremeno ulaze u Atlantik i prodiru u Bengvelski sustav. Aguljaški vrtlozi su tijela relativno guste vode, 500 do 1000 m duboki i 100 do 250 km široki, koji se vrte suprotno kazaljci na satu. Nakon što prodru u Bengvelski sustav, oni putuju na sjever i polagano izmjenjuju toplinu i slanost s vodom koja ih okružuje. Ovaj dotok tople i slane vode je važna karika u svjetskom lancu termohalinske cirkulacije i jedan od najvažnijih čimbenika toplinskog i solnog budžeta Južnog Atlantika (Gordon, 1985; Gordon et al., 1992).

4. OKOSNICA ISTRAŽIVANJA

4.1. Materijal i metode

Glavni cilj ovog istraživanja bilo je utvrđivanje ekoloških osobitosti modernih zajednica planktonskih foraminifera i njihovih reakcija na promjene u neposrednom okolišu. Foraminifere reagiraju na različite hidrografske značajke koje se u prirodnom okolišu isprepliću, stvarajući složen sustav kontrolnih čimbenika. Područje središnjeg Hrpta kitova u jugoistočnom Atlantskom oceanu (sl. 1.3) je karakteristično po uglavnom stabilnim uvjetima, kao što su niske količine hranjivih tvari unutar plitkog sloja izmiješane površinske vode duž većeg dijela godine i niski sezonski temperaturni raspon, pa pruža prigodu za određivanje pojedinačnih ekoloških osobitosti i reakcija foraminiferskih vrsta. Područje je smješteno približno 1300 km zapadno od afričke obale, izvan domašaja utjecaja s obale i iz Bengvelskog „upweling" sustava. Uzorkovna stanica na središnjem Hrptu kitova (CWI) stoga predstavlja okosnicu ovdje prikazanih ekoloških istraživanja. Na ovoj su stanici uzorci prikupljeni različitim tehnikama uzorkovanja za vrijeme tri MARE ekspedicije u veljači 2000., srpnju/kolovozu 2000. i veljači 2001. (tab. 1.1). Osobitosti vodenog stupca kao što su temperatura, salinitet i fluorescencija mjerene su na licu mjesta pomoću CTD (Conductivity-Temperature-Depth) rozete (sl. 1.4a), koja je ujedno prikupljala uzorke vode za kemijske analize (na pr. sadržaj hranjivih tvari i izotopni sastav) provedene na brodu ili kasnije u laboratoriju.

Plankton iz gornjih 800 do 1000 m vodenog stupca uzorkovan je planktonskim kočama (tows) pomoću Hydrobios Multinet sustava modificiranog na Kraljevskom nizozemskom institutu za istraživanje mora (NIOZ), opremljenog s dva mjerača toka i pet mreža finoće 100 µm u čeličnom okviru, povezanih s kompjuterski kontroliranom komandnom jedinicom na brodu. Naprava je omogućila količinsko uzorkovanje foraminifera i ostalog planktona na točno određenim dubinskim intervalima. Mreže su otvarane i zatvarane u nizu za vrijeme namotavanja, koso tegljene iza broda koji je plovio polagano. Uzorkovale su između 20 i 1000 m^3 morske vode (sl. 1.5). Uzorkovni

razmaci su obično bili širi u dubini gdje je koncentracija planktona niska, a uži u fotičkoj zoni koja obiluje planktonom. Takav pristup je spriječio začepljenje mreža, a istovremeno omogućio prikupljanje dovoljno materijala potrebnog za taksonomske i kemijske analize.

Detritična tvar (particulate matter) koja se taložila na morsko dno prikupljana je pomoću vremenske serije sedimentnih zamki (sediment traps). To su stožaste naprave usidrene na morskom dnu, s otvorom promjera 1 m^2 na gornjoj strani i revolverom s 24 posudice za uzorke na donjoj, užoj strani, koji je programiran za pomicanje u jednakim vremenskim razmacima (obično 7 ili 8 dana) i uzorkovanje čestica koje se talože kroz gornji otvor (sl. 6 i 7).

Površinski sediment morskog dna je uzorkovan sandučastom napravom za jezgrovanje (box corer). To je 55 cm visok i 50 cm širok bušaći cilindar s utegom s gornje strane, koji se velikom brzinom spušta prema morskom dnu i pod utjecajem gravitacijske sile prodire nekoliko desetaka centimetara duboko u sediment, te se prilikom izvlačenja zatvara zaklopcem.

Uz CWR stanicu uzorkovano je i nekoliko dodatnih stanica iz istog područja kako bi potkrijepile regionalna biološka i kemijska svojstva vodenog stupca i utjecaj hidrografskih promjena u jugoistočnom Atlantiku na ustroj dubokomorske karbonatne sedimentacije (sl. 1.1; tab. 1.1)

4.2. Dinamika zajednica planktonskih foraminifera

Drugo poglavlje obrađuje populacijsku dinamiku planktonskih foraminifera. U tu sam svrhu razvio metodu za određivanje dubine foraminiferske proizvodne zone (tj. dijela vodenog stupca u kojem vrste žive), veličinu zajednice („standing stock“ tj. broja jedinki po kvadratnom metru proizvodne zone), i vremena obnove („turnover time“ tj. vremena potrebnog za potpunu zamjenu populacije jedne vrste slijedećom generacijom) (sl. 2.3.). Vrijeme obnove je pristupljeno na dva nezavisna načina, jednog preko foraminiferskog toka taloženja („deposition flux“ tj. ljušture koje se talože na morsko dno izražene kao broj ljuštura po kvadratnom metru na dan) uzorkovanih sedimentnim zamkama uz morsko dno, i drugog preko izlazne koncentracije („export concentration“) mrtvih jedinki koje tonu iz proizvodne zone u gornjem dijelu vodenog stupca (broj ljuštura po kubičnom metru morske vode) uzorkovanih planktonskim kočama. Jednostavan model je razvijen kako bi ilustrirao značenje takovog vremena obnove. On je pokazao da vrijeme obnove može biti interpretirano kao prosječni životni vijek foraminiferske vrste samo za zajednice koje su u stabilnom stanju („steady state“) ili su mu vrlo blizu (sl. 2.8 i 2.9). Nadalje, model je pokazao da rastuće zajednice rezultiraju dužim vremenom obnove i, suprotno tome, zajednice koje se smanjuju, rezultiraju kraćim vremenom obnove. Ova metoda je primijenjena na rezultate planktonskih koča i sedimentnih zamki sa CWR stanice iz veljače 2000, srpnja 2000 i veljače 2001, koji su ukazali da su bodljikave plitkomorske vrste *Globigerinoides trilobus* i *Globigerinoides ruber* (sl. 1.1d) imale najpostojanije rezultate i da su njihove zajednice bile najbliže stabilnom stanju. Njihovo vrijeme obnove za vrijeme južnog ljeta je interpretirano kao prosječni životni vijek od oko dva tjedna. Nebodljikave dubokomorske vrste su imale vrijeme obnove koje nije bilo duže od šest tjedana. Nalazi sa CWR stanice ukazuju na to da je potpuna obnova zajednica planktonskih foraminifera unutar proizvodne zone pitanje tjedana a ne sezonski ili čak godišnji ciklus kao što je prethodno bilo sugerirano za neke dubokomorske vrste.

4.3. Mjesečevi ciklusi i sezonske promjene toka taloženja

Poglavlje 3. nadalje obrađuje dinamiku zajednica foraminifera u smislu ciklusa razmnožavanja s (polu)mjesečnom frekvencijom. Takva učestalost je prvi puta demonstrirana na laboratorijskim kulturama vrste *Hastigerina pelagica*, a sugerirana je za više vrsta planktonskih foraminifera iz planktonskih koča i sedimentnih zamki. Stoga bi mjesečevi ciklusi mogli biti važan izvor temporalnih varijacija u vertikalnoj i lateralnoj distribuciji živućih vrsta i potencijalni pogonski mehanizam kratkotrajnih promjena karbonatnog toka koji u pelagičkom oceanu iznosi i do 5.7 Gt na godinu. Pa ipak, kolebanje foraminiferskih ciklusa razmnožavanja s mjesečnom frekvencijom nikada nije bilo opaženo na terenu tako jednoznačno kao u kulturama vrste *H. pelagica*, a to je ujedno i jedina vrsta za koju je bilo moguće dokazati endogeni mjesečev ciklus u laboratoriju. Ja sam predočio prvi terenski dokaz da mjesečna učestalost vrste *H. pelagica* uistinu određuje i njezin tok taloženja na morskom dnu na dubini od 2700 m. Razdoblja najvećeg toka taloženja ove vrste su na CWR stanici pokazala snažnu periodičnost s frekvencijom od 30 dana, a maksimumi su dosezali morsko dno u prosjeku 12.5 dana nakon punog mjeseca. Ako se uzme u obzir vrijeme koje je potrebno za taloženje, to se podudara s razmnožavanjem 5 dana nakon punog mjeseca, kao što je izvorno opaženo u izoliranim kulturama. Takva podudarnost je omogućila analiziranje periodičnosti u razmnožavanju drugih vrsta na osnovi tokova taloženja sa CWR stanice, ali ni jedna od njih nije pokazala mjesečnu ni ikakvu drugu periodičnost unutar domene ovog istraživanja u rasponu od 16 to 90 dana. Umjesto da budu rukovođeni mjesečevim ciklusom, tokovi svih drugih vrsta su bili određeni sezonskom reakcijom, što upućuje na to da je njihovo razmnožavanje kontinuirano u domeni mjesečeva ciklusa. S obzirom da je *H. pelagica* rijetka vrsta s niskim tokom i slabom očuvanošću prilikom ukopa u sediment, takvo neprekidno razmnožavanje drugih vrsta uvelike pojednostavljuje interpretacije foraminiferskih raspodjela unutar ekološki i fizikalno stupnjevitih okoliša gornjeg sloja oceana. Nadalje, ovo je istraživanje pokazalo da razmnožavanje u skladu s mjesečevim ciklusom ne utječe na pelagičku karbonatnu proizvodnju niti na dubokomorske sedimentacijske tokove. Prepoznavanje mjesečeve frekvencije u toku taloženja vrste *H. pelagica* također dokazuje visoku točnost uzorkovanja sedimentnim zamkama na ovoj stanici, posebno kada se uzme u obzir vrlo delikatna ljuštura ove vrste i velika dubina na kojoj su zamke bile usidrene.

4.4. Sezonski izvoz i sedimentna očuvanost duž profila sa stupnjevitom raspodjelom hranidbenih tvari

Slijedovi detritičnih tokova iz raznih područja svjetskih oceana upućuju na sveopće dinamičko ponašanje planktonskih zajednica. Poglavlje 4. obrađuje sezonske promjene u pretežito oligotrofnom Južnoatlantskom centralnom vrtlogu kombinirajući vremenski niz tokova taloženja fitoplanktona (dijatomeja i silikoflagelata), zooplanktona (foraminifera i pteropoda) i drugih biogenih čestica sakupljenih sedimentnim zamkama na CWR stanici i suprotstavljajući ih površinskom sedimentu iz jezgre bušotine s te iste stanice. Markantan maksimum tijekom južnog proljeća obilježio je CWR tokove taloženja svih glavnih sastojaka. Proizvodni ulomak započinje zimskim produbljivanjem površinskog izmiješanog sloja mora, kao reakcija na pojačanu snagu vjetra u kasnu jesen, koja omogućava dotok novih hranjivih tvari iz podpovršinskih slojeva podupirući proizvodnju unutar površinskog izmiješanog sloja (sl. 4.4b). Oplićavanje površinskog izmiješanog sloja na prijelomu zime rezultiralo je prekidom dotoka hranjivih tvari koje je izazvalo urušavanje proizvodnje. Kao

posljedica, gotovo 25% godišnjeg težinskog toka stiglo je na morsko dno za vrijeme samo jednog mjeseca u ranom proljeću. I dijatomejski i foraminiferski vertikalni stupci u gornjem dijelu oceana su bili povezani s istim procesom dotoka hranjivih tvari u površinski izmiješani sloj iako su na morskom dnu njihovi maksimumi tokova taloženja bili razdvojeni za jedan tjedan zbog brže reakcije fitoplanktona na ograničenu dostupnost hranjivim tvarima, a što je još dodatno preoblikovano polaganijim tonjenjem fitoplanktona u odnosu na foraminifere. Analiza osnovnih komponenti (PCA) vremenskog slijeda tokova taloženja razotkrila je izraženu sezonalnost foraminiferskih vrsta, dok su diatomeje bile razvrstane prema razdobljima cvata. Mala *Nitzschia bicapitata* kod diatomeja i *Globorotalia inflata* (sl. 1.1f) kod foraminifera dominirale su godišnjim taloženjem sa 60 odnosno 25%. Dubokomorska foraminifera *Globorotalia truncatulinoides* (sl. 1.1f) je činila važnu iznimku jer nije slijedila općenitu sezonsku raspodjelu. Primjerci s lijevo savijenim ljušturama su se najviše taložili za vrijeme rane zime i kasnog proljeća dok su oni sa desno savijenom ljušturom bili obimni samo za vrijeme kasnog proljeća. Takva različita sezonska reakcija savijanja ljušture kod vrste *G. truncatulinoides* sugerira odvojeni taksonomski status, a ne samo jednostavnu raznovrsnost u namotavanju unutar iste vrste. Ovaj je nalaz u suglasnosti s recentnim DNK istraživanjima, što ujedno upućuje da genetske vrste imaju i različitu sezonalnost.

U zoni dodira vode i sedimenta na morskom dnu intenzivno je raspadanje organske tvari i biogenog kremena rezultiralo vrlo slabom očuvanošću i izraženim promjenama sastava zajednica kremenog fitoplanktona. Od svih detritičnih sastojaka jedino su foraminiferske ljušture pokazale potpunu sačuvanost na površini morskog dna. Tako su *G. inflata* i većina ostalih foraminiferskih vrsta taložene kao posljedica sezonskih promjena u proizvodnji i time su kroz sedimentne zajednice morskog dna sačuvale taj signal iz gornjeg oceana.

CWR podaci su upotrijebljeni kao krajnji član za upotpunjavanje profila sa stupnjevitom raspodjelom hranidbenih tvari kroz Bengvelski sustav, od oligotrofnog Centralnog vrtloga do područja visoke proizvodnje u zoni vertikalnog strujanja prema površini uz namibijsku obalu. Pojava maksimalnih tokova duž tog profila istovremena je s minimalnom površinskom temperaturom mora uz koju je povezana i maksimalna dubina površinskog izmiješanog sloja, premda pokazuje vremenski pomak u smjeru pučine, nastupajući prvo duž obale u ranom kolovozu, a dva mjeseca kasnije i na CWR stanici. Prijelaz s oligotrofnih na mezotrofne uvjete obilježen je povećanom zastupljenošću vrste *G. inflata* zajedno sa smanjenjem foraminiferske raznovrsnosti i zastupljenosti sorti toplog mora, a unutar diatomejskih zajednica mala i slabo okremenjena *N. bicapitata* zamijenjena je većim i jače okremenjenim vrstama. Bliže obalnoj zoni vertikalnog strujanja prema površini prijelaz s mezotrofnih na eutrofne uvjete obilježen je smanjenom zastupljenošću vrste *G. inflata* a povećanom zastupljenošću vrsta hladnog mora: *Globigerina bulloides* i desno savijene *Neogloboquadrina pachyderma*, da bi na kraju zajednice dominirale lijevo savijena *N. pachyderma* zajedno s vrstom *Turborotalita quinqueloba*. Iako su ukupni tokovi čestičnih sastojaka porasli u smjeru obale, razlike su bile prilično male, svjedočeći o samo umjerenijoj proizvodnji i taloženju na namibijskom oceanskom rubu u odnosu na Centralni vrtlog.

4.5. Ekologija izotopa kisika iz ljuštura recentnih planktonskih foraminifera

Sastav izotopa kisika ($\delta^{18}O$) iz ljuštura foraminifera povezan je s temperaturom mora koje ih okružuje i njegovim $\delta^{18}O$. Stoga je $\delta^{18}O$ signal iz ljuštura fosilnih foraminifera u sedimentu određen

njihovom ekologijom, to jest dubinom kalcifikacije i njezinim sezonskim promjenama, vremenskim promjenama toka ljuštura i vitalnim efektom (načinom na koji jedinka uklapa $\delta^{18}O$ signal iz mora koje je okružuje u vlastitu ljušturu). Ovaj izvorni signal iz proizvodne zone može biti promijenjen na putu koji ljuštura prođe prema morskom dnu i nakon zatrpavanja između ostalog dubinskom korastom kalcifikacijom kalcita iz hladnog mora, djelomičnim otapanjem ili dijagenezom. U petom poglavlju ekološke su spoznaje o foraminiferskim vrstama kombinirane sa sastavom izotopa kisika iz njihovih ljuštura (to jest $^{18}O/^{16}O$ razmjerom) radi boljeg razumijevanja dubine na kojoj vrste obitavaju, njihove kalcifikacije i sezonske raspodjele unutar gornjeg dijela vodenog stupca, a sve to da bi usavršili procjenu površinske temperature mora preko $\delta^{18}O$ iz foraminiferskih ljuštura. Da bi dalje razotkrili procese koji povezuju proizvodnju ljuštura s njihovom očuvanošću u sedimentu, $\delta^{18}O$ zapis iz CWR planktonskih koča uspoređen je s $\delta^{18}O$ ljuštura iz godišnjeg toka taloženja prikupljenog sedimentnim zamkama i s fosilnim $\delta^{18}O$ iz površinskih naslaga morskog dna.

Donja granica foraminiferske proizvodne zone (Z_{BPZ}) je izračunata uz pomoć metode razvijene u drugom poglavlju, a zatim je uspoređena s Z_{BPZ} dobivenom iz $\delta^{18}O$ profila. Rezultati dobiveni upotrebom dvije nezavisne metode su se u velikoj mjeri podudarali, svjedočeći o ispravnosti osnovne hipoteze iz drugog poglavlja i sugerirajući da koncentracija ljuštura, kao i njihov $\delta^{18}O$ sastav, može sa sigurnošću biti upotrijebljen za određivanje dubinskog raspona proizvodne zone vrsta. Rezultati sa CWR stanice i tri dopunske stanice iz južne Kapske zavale (sl. 1.3) promiču vrstu *Globigerinita glutinata* (Sl. 1.1c) kao najboljeg pokazatelja površinske temperature mora. Ta vrsta kalcificira ljušturu u ravnoteži s očekivanim sastavom $\delta^{18}O$, pokazuje konstantnu $\delta^{18}O$ vrijednost neovisno o dubini i jedina je CWR vrsta koja nije pokazala nikakve promjene u fosilnom $\delta^{18}O$. Sukladno s njenim maksimalnim tokom u ranom proljeću prouzrokovanim dubokim zimskim miješanjem (4. poglavlje) sedimentni $\delta^{18}O$ signal vrste *G. glutinata* s točnošću odražava zimsku površinsku temperaturu mora na CWR stanici. Sedimentni $\delta^{18}O$ zapis vrste *G. ruber* (sl. 1.1d), koja je općenito smatrana plitkomorskom i stoga često upotrebljavana kao pokazatelj površinske temperature mora, na CWR stanici dala je dobru procjenu zimske površinske temperature mora. Usprkos tome, naši rezultati iz planktonskih koča sugeriraju da se zona kalcifikacije vrste *G. ruber* uvijek proteže do dubokog klorofilnog maksimuma, koji se može nalaziti daleko ispod površinskog izmiješanog sloja. Na CWR stanici to se događa od jeseni do proljeća (4. poglavlje) kada je izlazni $\delta^{18}O$ vrste *G. ruber* djelomično formiran u vodi koja je hladnija od površinske pa tako značajno podcjenjuje stvarnu površinsku temperaturu mora za više od 2ºC. *G. truncatulinoides* (sl. 1.1e) se pokazao kao vrsta koja vrši kalcifikaciju u ravnoteži sa očekivanim sastavom $\delta^{18}O$ u zoni najveće koncentracije ljuštura, a ta je obično dublja za veće ljušture. S obzirom da kalcit iz kućica promjera 250 µm ove vrste pridonosi s manje od 10% mase u kućicama promjera 400 µm, udio kalcita formiranog u plitkoj i toplijoj vodi je u velikim ljušturama beznačajan (sl. 5.9). CWR planktonske koče pokazuju da $\delta^{18}O$ iz lijevo savijenih ljuštura vrste *G. truncatulinoides* s maksimalnim promjerom kućice od približno 400 µm odražava temperaturu mora na dubini od oko 350 m, a one promjera oko 250 µm temperaturu s dubine od oko 200 m. Razlika u $\delta^{18}O$ sastavu između ljuštura različitih veličinskih razreda u sedimentu može stoga biti upotrijebljena za procjenu podpovršinske temperaturne stupnjevitosti.

4.6. Planktonske foraminifere u zrelom Aguljaškom vrtlogu

Šesto poglavlje prikazuje faunalni sastav jednog starog Aguljaškog vrtloga koji je prodro do sjeverne Kapske zavale. Foraminiferske zajednice i fizikalne karakteristike vrtloga suprotstavljene su

onima iz okolnog mora, kao i s tokovima taloženja. Cilj mi je bio odrediti utjecaj takvih vrtloga na sedimentaciju u sjevernoj Kapskoj zavali i na Hrptu kitova. U trenutku uzorkovanja proučeni vrtlog je bio jasno raspoznatljiv na radarskim slikama visine morske površine kao povišenje koje nastaje uslijed njegovog rotacionog gibanja u smjeru suprotnom kazaljci na satu. Vrtlog se razlikovao od okolnog oceana malo višim salinitetom, dubljim površinskim izmiješanim slojem i većom gustoćom foraminiferskih zajednica. Sadržaj faune u vrtlogu bio je sličan zajednicama koje su ranije identificirane u svježe formiranom vrtlogu iz južne Kapske zavale. Pa ipak, kontrast između faunalnih zajednica starog vrtloga i okoline bio je slab, usprkos jasnoj identifikaciji na altimetrijskim slikama morske površine.

Izrazita je bila odsutnost tropske vrste *Globorotalia menardii* (sl. 1.1b) iako je ona bila vrlo rasprostranjena u vodama okolnog jugoistočnog Atlantika. U više paleoloških istraživanja u ovom području pretpostavljeno je da ova vrsta potječe iz Indijskog oceana i da označava „otvoren Kapski ventil“, to jest potpunu interglacijalnu razmjenu između Indijskog i Atlantskog oceana. Moje istraživanje pokazuje da *G. menardii* ne pripada tipičnoj fauni starog vrtloga i u skladu je s nalazima iz svježe formiranih vrtloga iz južne Kapske zavale. Zato je vjerojatnije da za vrijeme inerglacijala, kada se oceanske fronte pomiču na jug, ova vrsta ponovno naseljava Kapsku zavalu iz suptropskog Atlantika, a ne preko Aguljaških vrtloga iz Indijskog oceana.

Appendix

Scanning electron microscope micrographs of foraminiferal and diatom species from the South Atlantic Central Gyre

Neven Lončarić, Jolanda van Iperen & Morris Franken

FORAMINIFERA:

Plate I: *Globigerina bulloides* d'Orbigny, 1826
a-c: plankton tows, CWR (2/2/2001), shallow cast, net 2, 75-100 m
Globigerina falconensis Blow, 1959
d-f: plankton tows, CWR (30/7/2000), deep cast, net 2, 300-500 m

Plate II: *Globigerinoides ruber* d'Orbigny 1839
a-e: sediment trap, CWR, cup 11 (20-28/10/2000); specimen **c** from fine sieve fraction

Plate III: *Globigerinoides trilobus* Reuss, 1850
Globigerinoides trilobus trilobus (=*Globigerina triloba* Reuss, 1850)
a: plankton tows, CWR (2/2/2001), shallow cast, net 2, 75-100 m
b: sediment trap, CWR, cup 1 (1-9/8/2000)
Globigerinoides trilobus sacculifer (= *Globigerina sacculifera* Brady, 1877)
c-f: sediment trap, CWR, cup 1 (1-9/8/2000)

Plate IV: *Globigerinoides tenellus* Parker 1958 (=*Globigerinoides tenella* Parker; =*Globoturborotalita tenella*)
a-b: sediment trap, CWR, cup 3 (17-25/8/2000)
Globigerina rubescens Hofker, 1956 (=*Globoturborotalita rubescens*)
c-d: plankton tows, CWR (2/2/2001), deep cast, net 4, 150-200 m, from fine sieve fraction

Plate V: *Globigerinella siphonifera* d'Orbigny, 1839 (=*Globigerinella aequilateralis* Brady)
a: plankton tows, CWR (2/2/2001), shallow cast, net 1, 100-150 m
b-d: sediment trap, CWR, cup 2 (9-17/8/2000)
e: plankton tows, CWR (2/2/2001), deep cast, net 3, 200-300 m

Plate VI: *Globigerinella calida* Parker, 1962
a-c: sediment trap, CWR, cup 11 (20-28/10/2000)
d-e: sediment trap, CWR, cup 2 (9-17/8/2000), from fine sieve fraction

Plate VII: *Orbulina universa* d'Orbigny, 1839
a: plankton tows, CWR (2/2/2001), shallow cast, net 1, 150-100 m
b: plankton tows, CWR (2/2/2001), shallow cast, net 4, 25-50 m
Sphaeroidinella dehiscens Parker and Jones, 1865
c-e: sediment trap, CWR, cup 1 (1-9/8/2000)

Plate VIII: *Hastigerina pelagica* d'Orbigny, 1839
a, b & e: plankton tows, CWR (2/2/2001), deep cast, net 1, 500-800 m
c: plankton tows, CWR (2/2/2001), deep cast, net 2, 300-500 m
d: sediment trap, CWR, cup 22 (16-24/1/2001)

Plate IX: *Beella digitata* Brady, 1879 (=*Globigerina digitata* Brady; =*Globigerinella digitata* Schott)
a: plankton tows, CWR (2/2/2001), deep cast, net 2, 300-500 m
b-d: plankton tows, CWR (2/2/2001), deep cast, net 4, 150-200 m

Plate X: *Globorotalia inflata* d'Orbigny, 1839
a & c: sediment trap, CWR, cup 1 (1-9/8/2000)
b: plankton tows, CWR (2/2/2001), shallow cast, net 2, 75-100 m
Globorotalia menardii d'Orbigny, 1865
d-e: plankton tows, CWR (2/2/2001), deep cast, net 3, 200-300 m, from fine sieve fraction

Plate XI: *Globorotalia hirsuta* d'Orbigny, 1839
a-b: plankton tows, CWR (2/2/2001), deep cast, net 2, 300-500 m
Globorotalia scitula Brady, 1882
c & e: plankton tows, CWR (2/2/2001), deep cast, net 3, 200-300 m, from fine sieve fraction
d: sediment trap, CWR, cup 2 (9-17/8/2000), from fine sieve fraction

Plate XII: *Globorotalia truncatulinoides* d'Orbigny, 1839
a-b: right-coiled, plankton tows, CWR (2/2/2001), deep cast, net 4, 150-200 m
c: right-coiled, sediment trap, CWR, cup 2 (9-17/8/2000)
d-f: left-coiled, plankton tows, CWR (2/2/2001), deep cast, net 4, 150-200 m

Plate XIII: *Globorotalia crassaformis* Galloway and Wissler, 1927
a-d: sediment trap, CWR, cup 11 (20-28/10/2000)

Plate XIV: *Pulleniatina oblicuiloculata* Parker and Jones, 1865
a-b: sediment trap, CWR, cup 3 (17-25/8/2000)
Globigerinita glutinata Egger, 1893
c & e: sediment trap, CWR, cup 3 (17-25/8/2000), from fine sieve fraction
d & f: plankton tows, CWR (2/2/2001), deep cast, net 3, 200-300 m, from fine sieve fraction

Plate XV: *Neogloboquadrina pachyderma* Ehrenberg, 1861
a-c: sediment trap, CWR, cup 14 (13-21/11/2000), from fine sieve fraction
d: plankton tows, CWR (2/2/2001), shallow cast, net 2, 75-100 m

Plate XVI: *Neogloboquadrina dutertei* d'Orbigny, 1839
a-d: sediment trap, CWR, cup 11 (20-28/10/2000)

DIATOMS:

Plate XVII: *Ethmodiscus gazellae* Hustedt, 1928 (=*Coscinodiscus gazellae* Janisch ex Grunow, 1879)
a & c: sediment trap, CWR, cup 18 (15-23/12/2000)
b: magnification of the valve center from **(c)** with labiate processes ringing hyaline central area

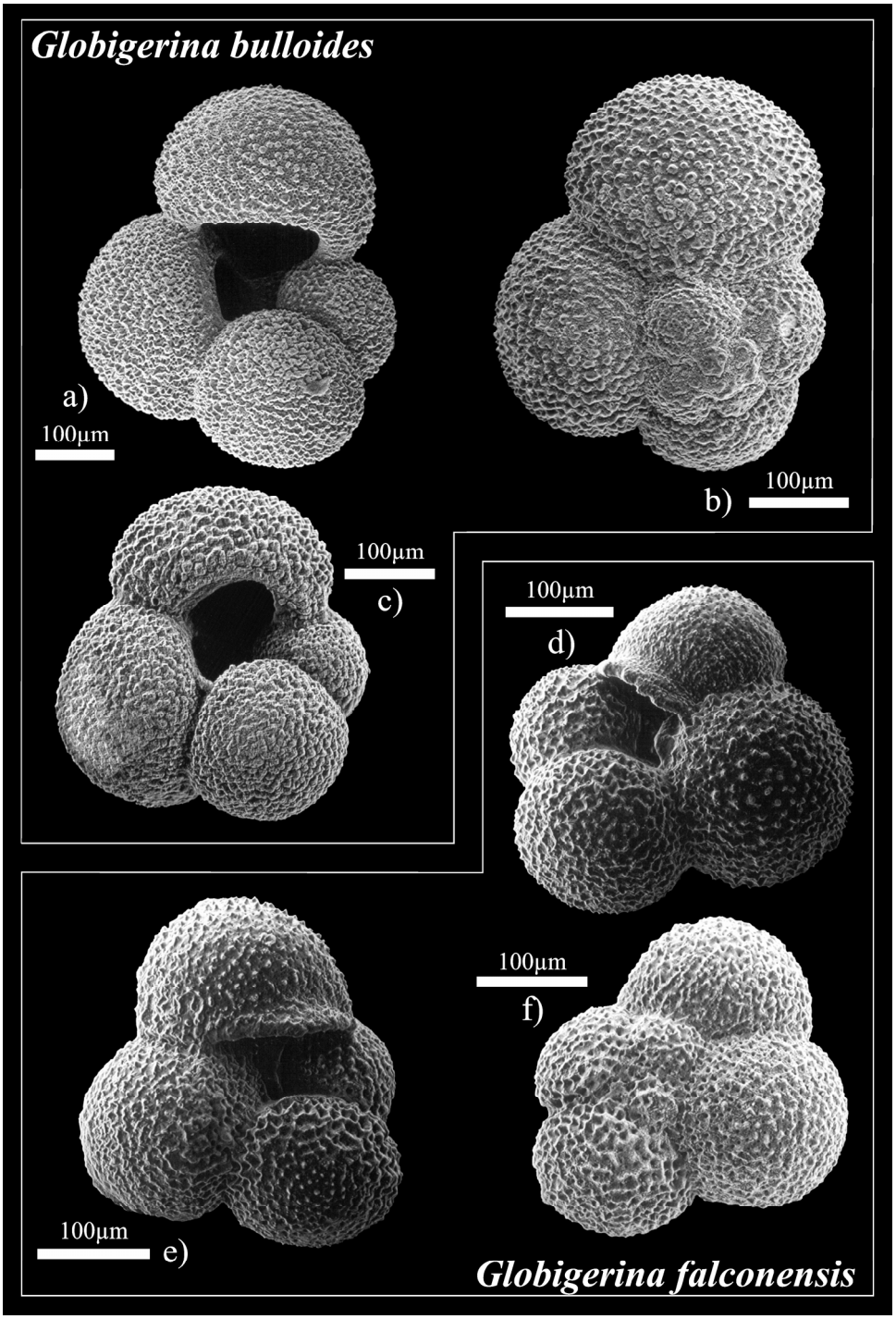
Globigerina bulloides
a)
100µm
b)
100µm
c)
100µm
d)
100µm
e)
100µm
f)
100µm
Globigerina falconensis

PLATE I

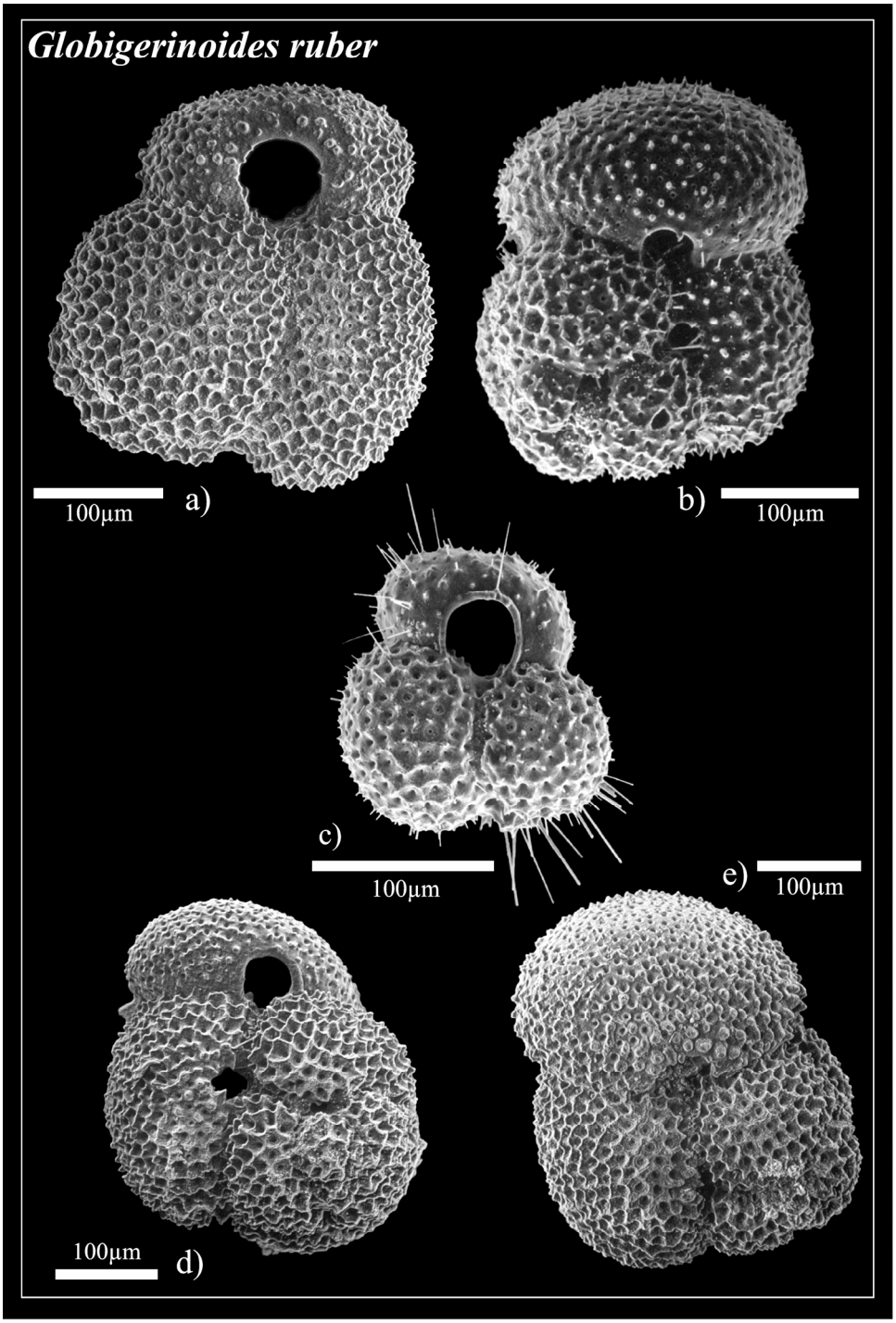
Globigerinoides ruber
a)
100µm
b)
100µm
c)
100µm
e)
100µm
d)
100µm

PLATE II

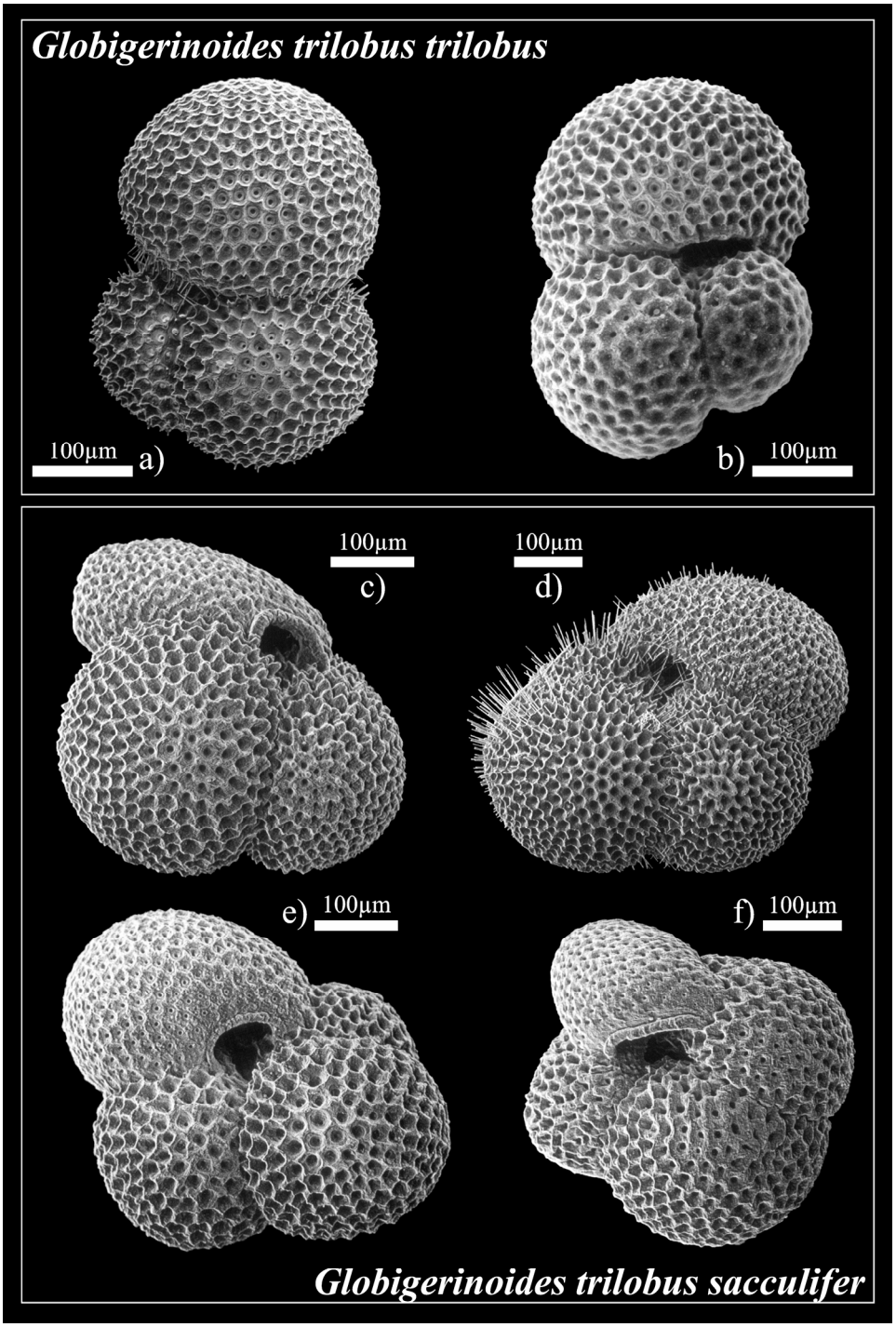
Globigerinoides trilobus trilobus
100µm
a)
b)
100µm
100µm
c)
100µm
d)
e)
100µm
f)
100µm
Globigerinoides trilobus sacculifer

PLATE III

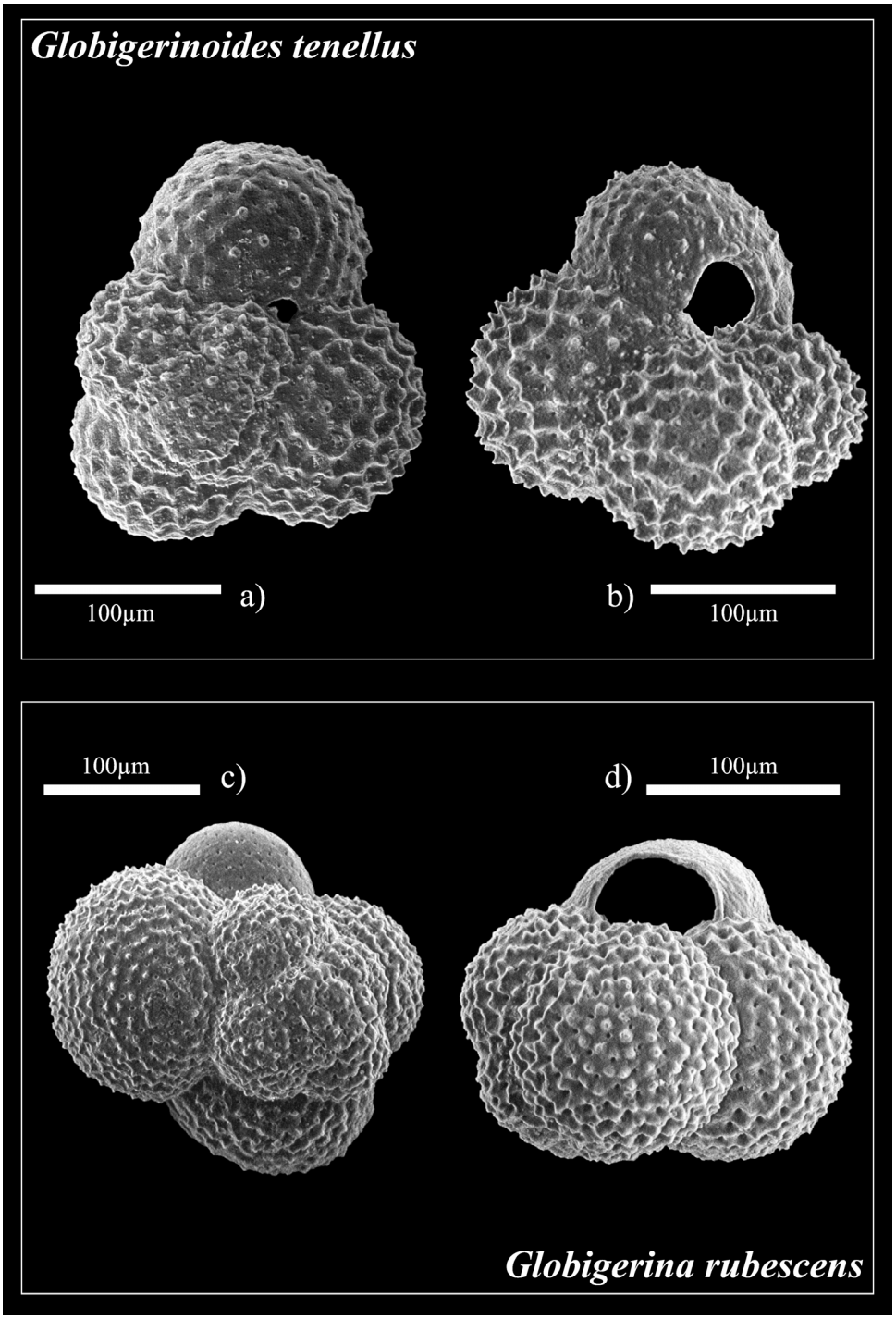
Globigerinoides tenellus
100µm
a)
b)
100µm
100µm
c)
d)
100µm
Globigerina rubescens

PLATE IV

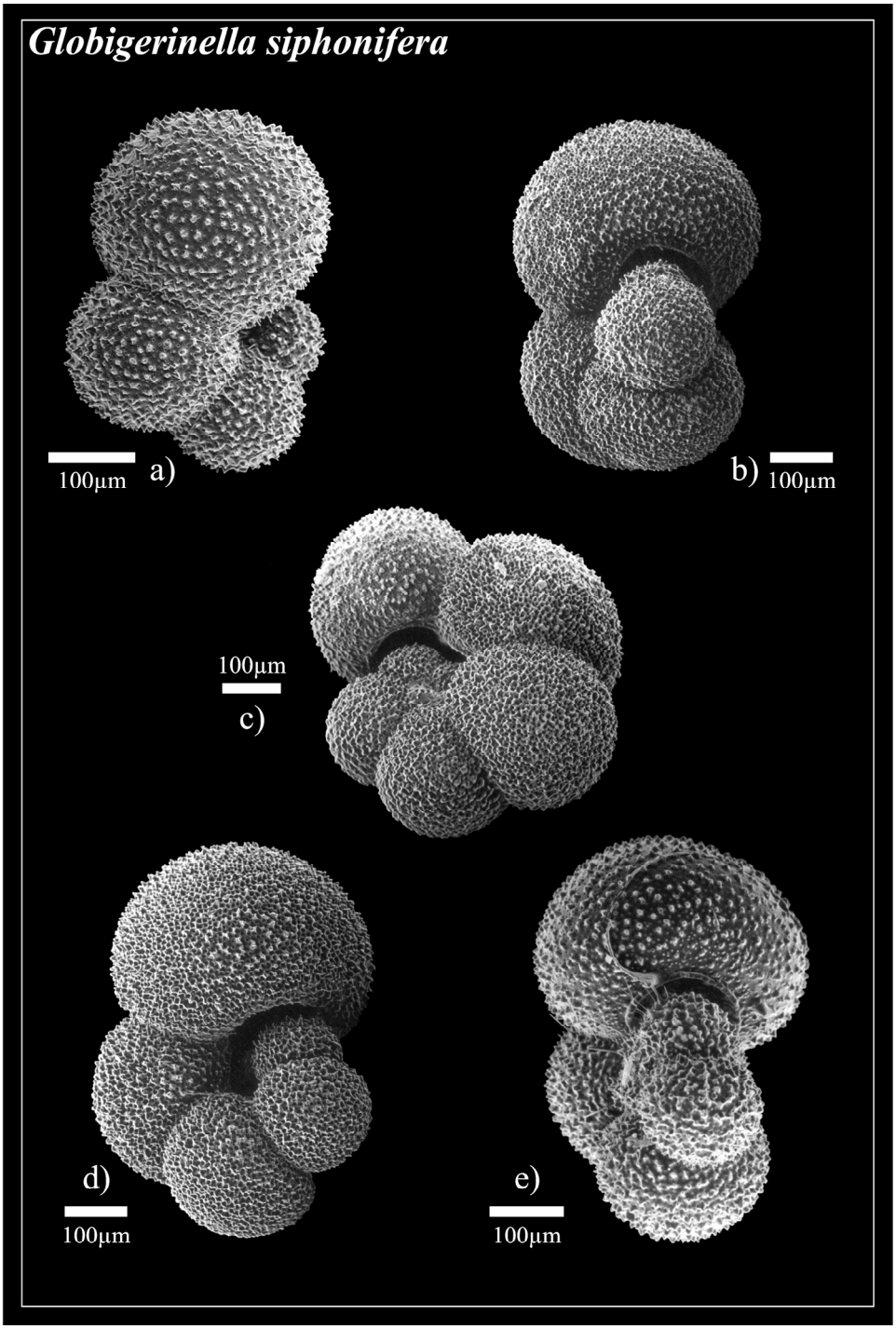
Globigerinella siphonifera
100µm
a)
b)
100µm
100µm
c)
d)
100µm
e)
100µm

PLATE V

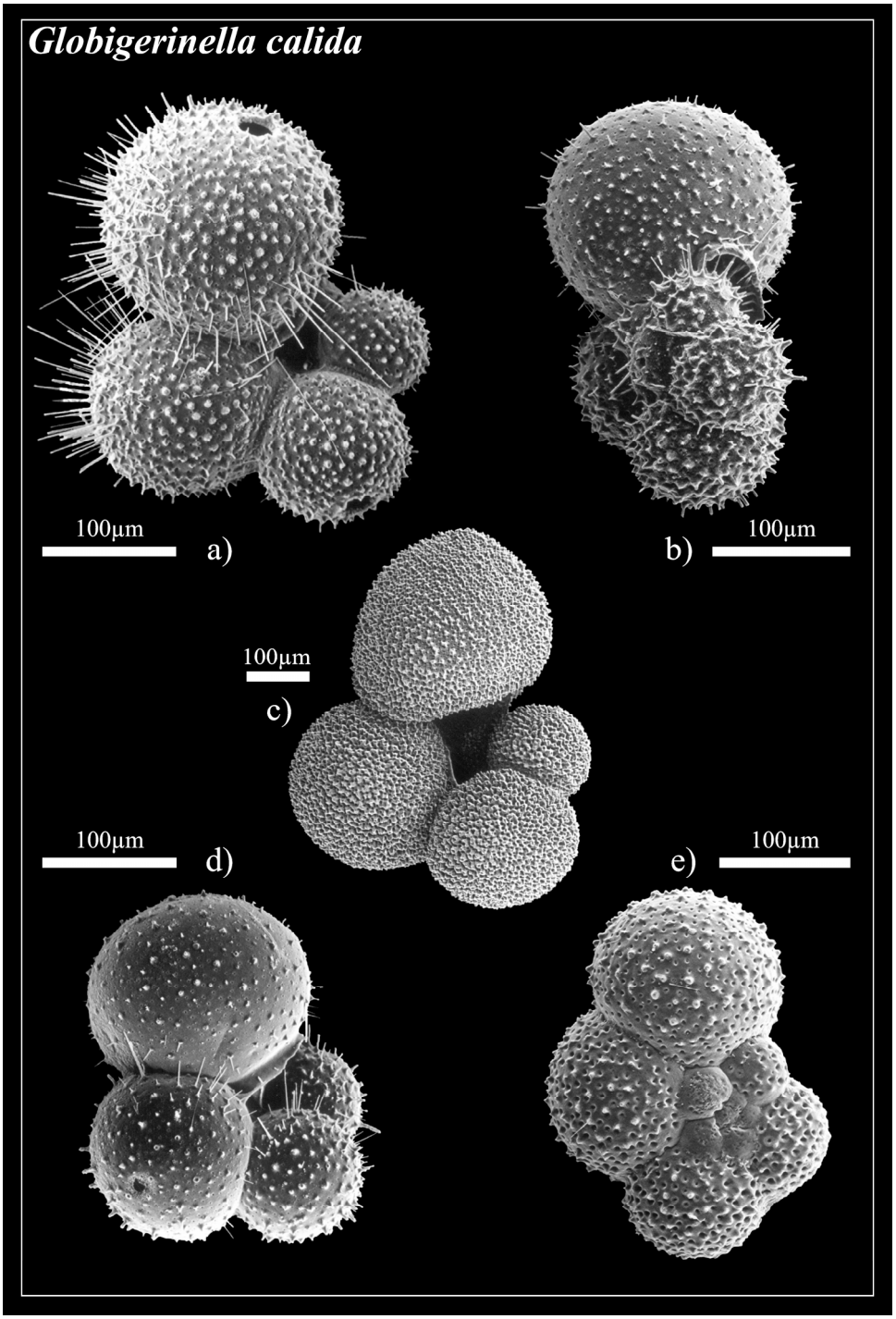
Globigerinella calida
100µm
a)
b)
100µm
100µm
c)
100µm
d)
e)
100µm

PLATE VI

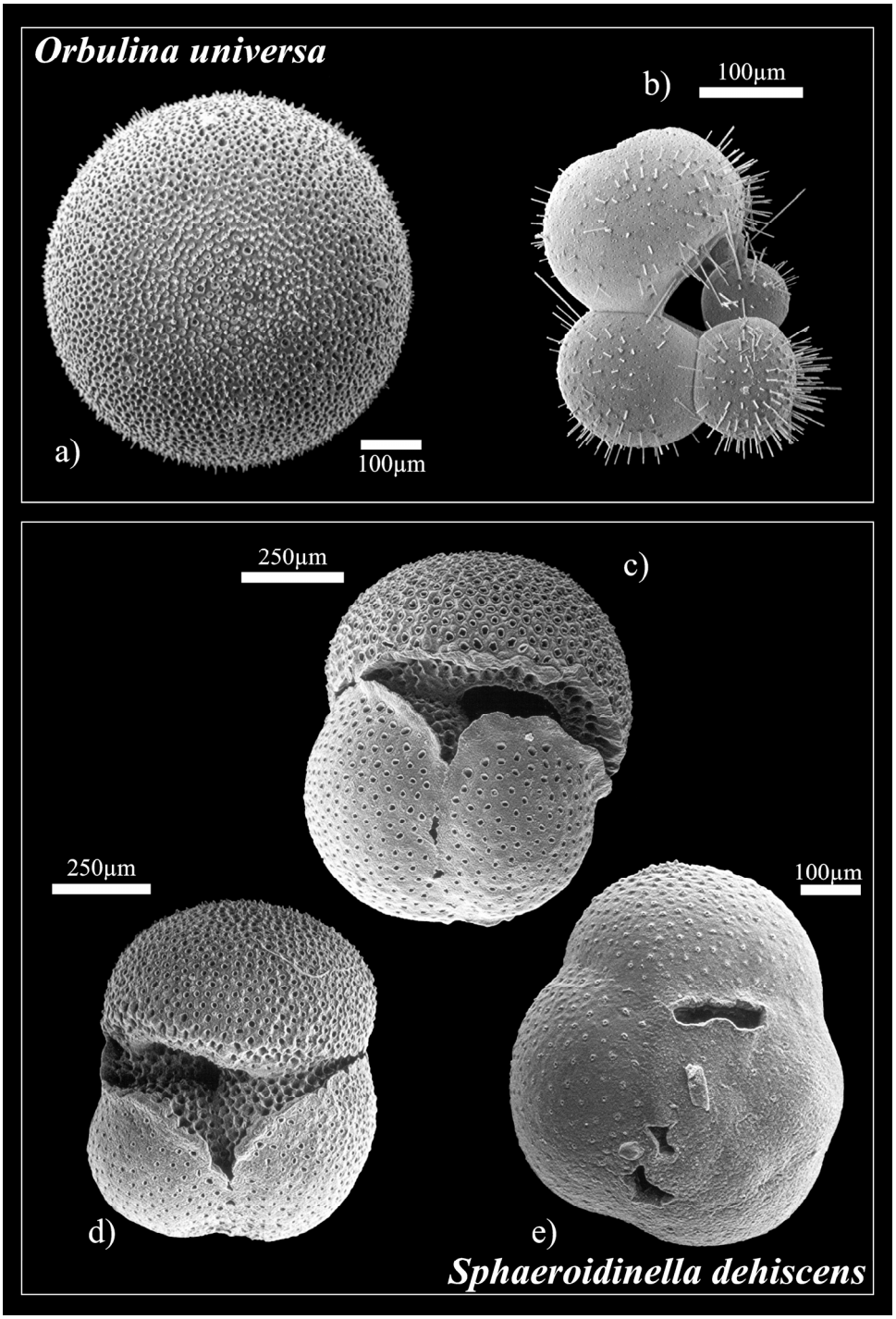
Orbulina universa
a)
100µm
b)
100µm
250µm
c)
250µm
d)
100µm
e)
Sphaeroidinella dehiscens

PLATE VII

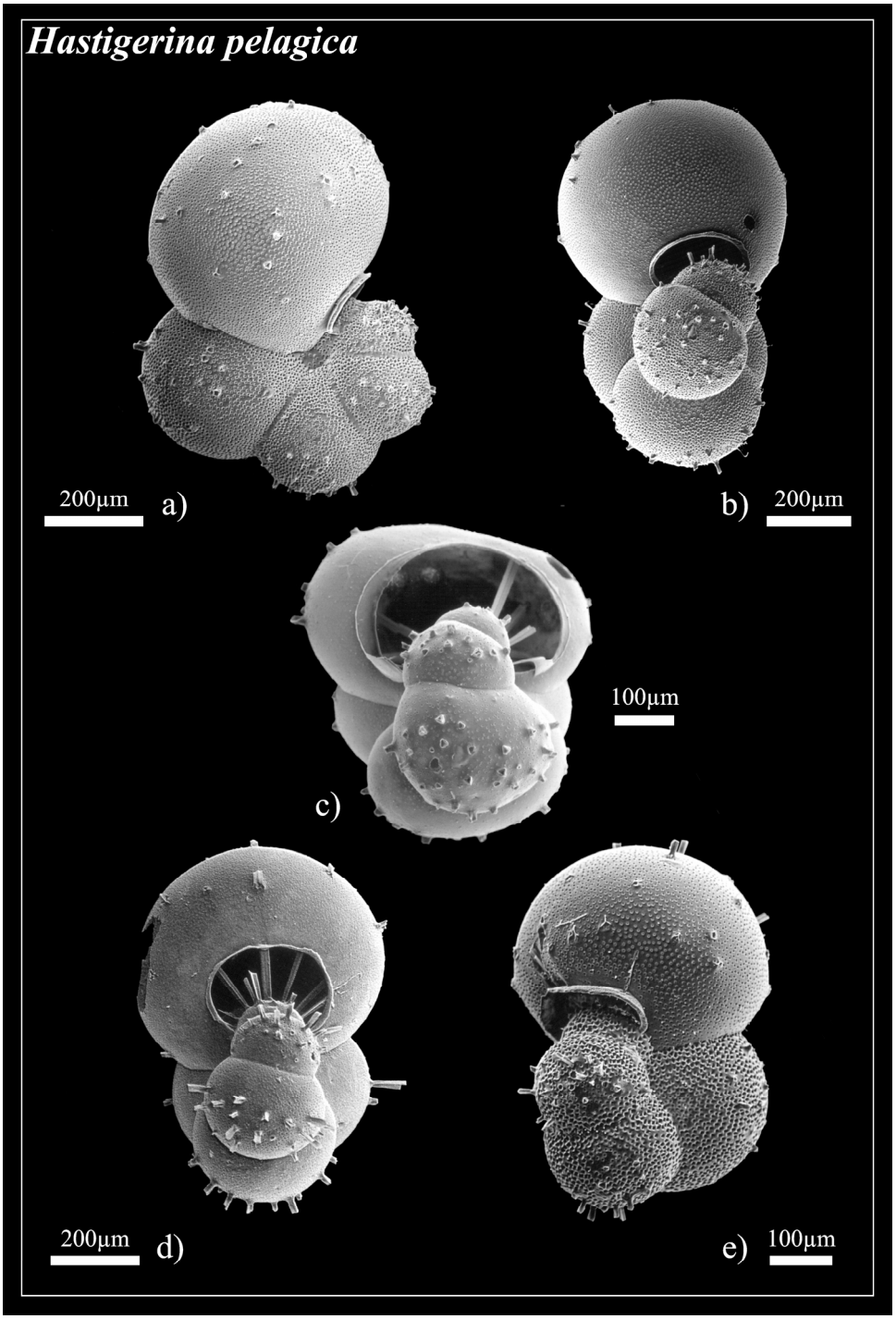

PLATE VIII

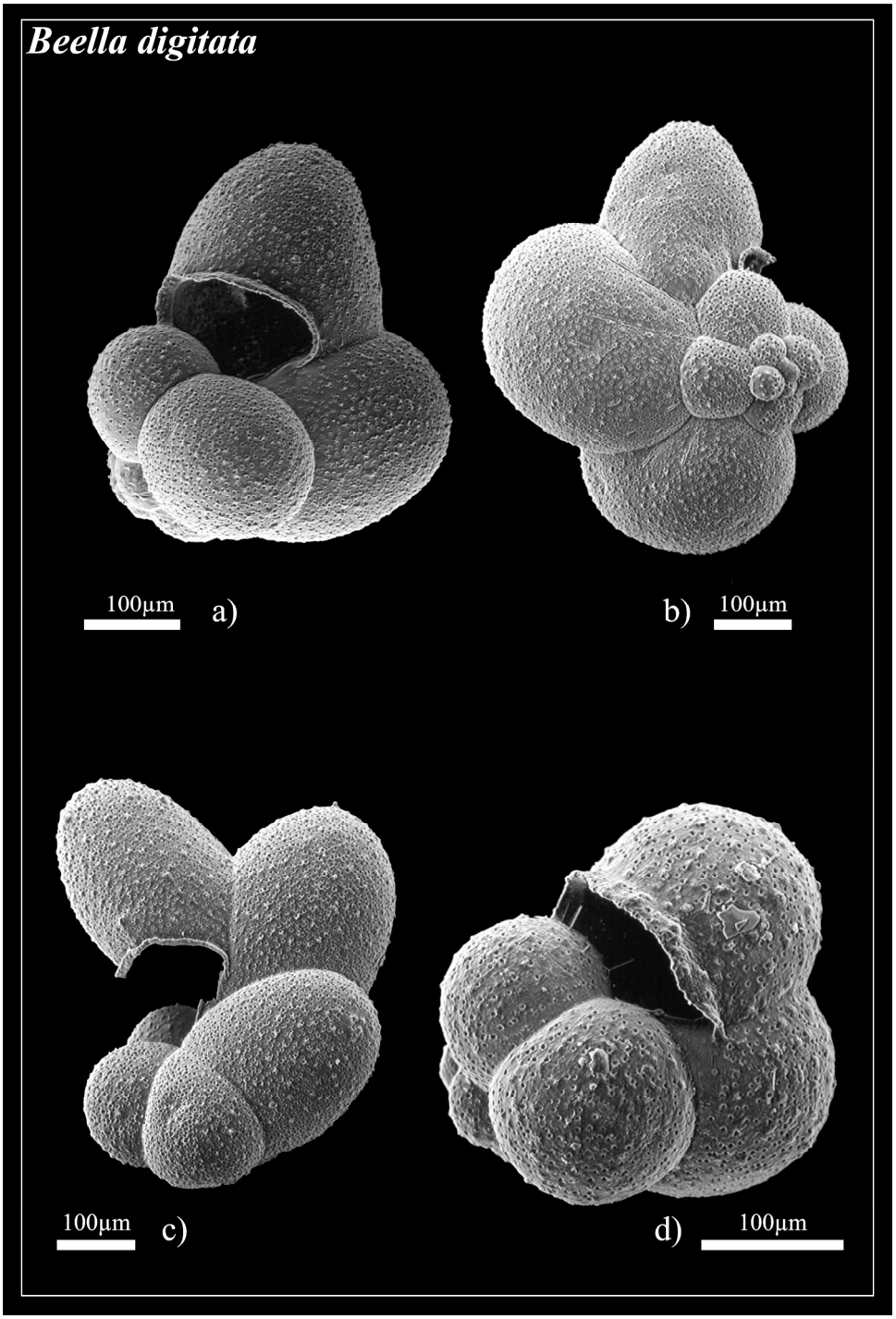

PLATE IX

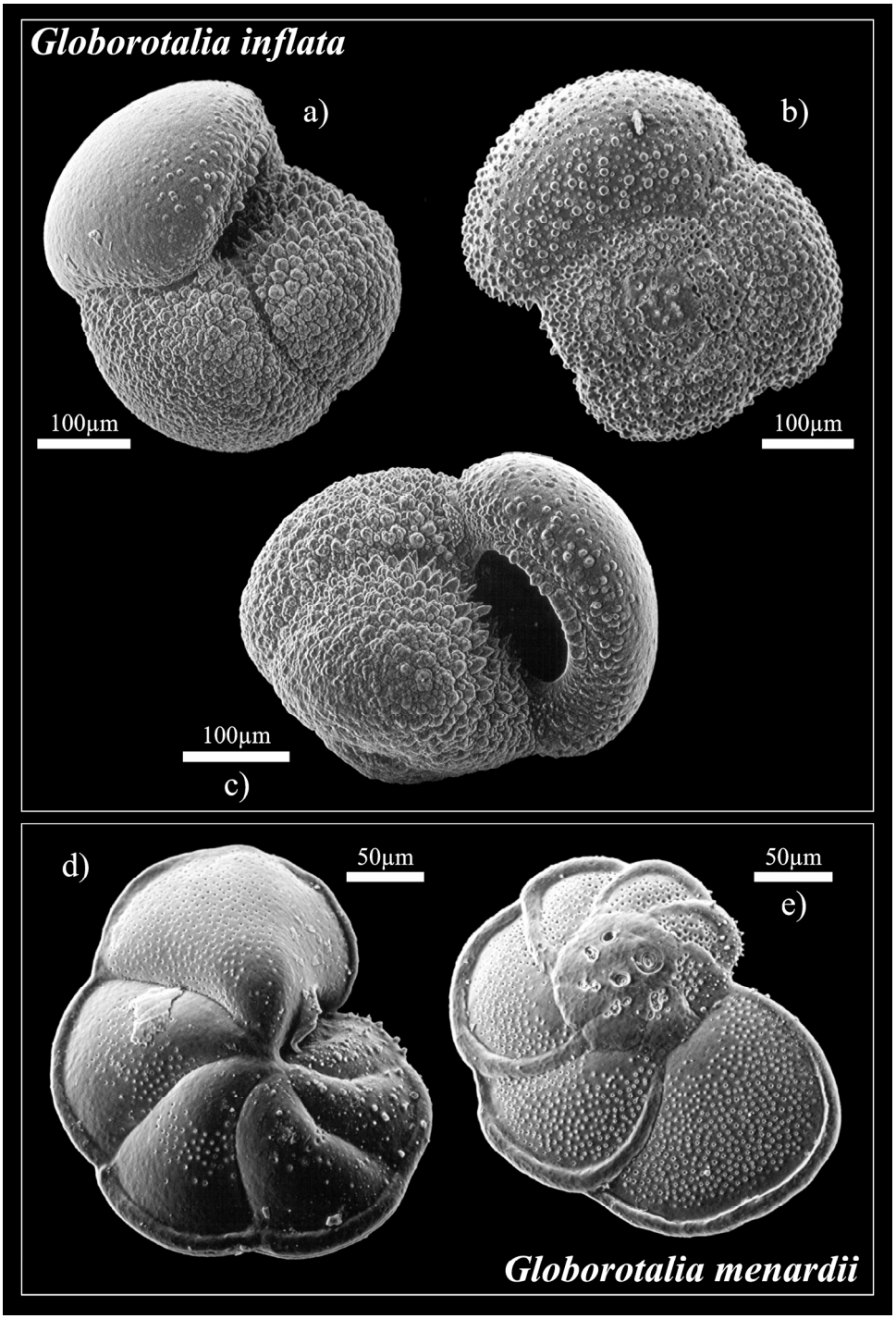
Globorotalia inflata
a)
b)
100µm
100µm
100µm
c)
d)
50µm
50µm
e)
Globorotalia menardii

PLATE X

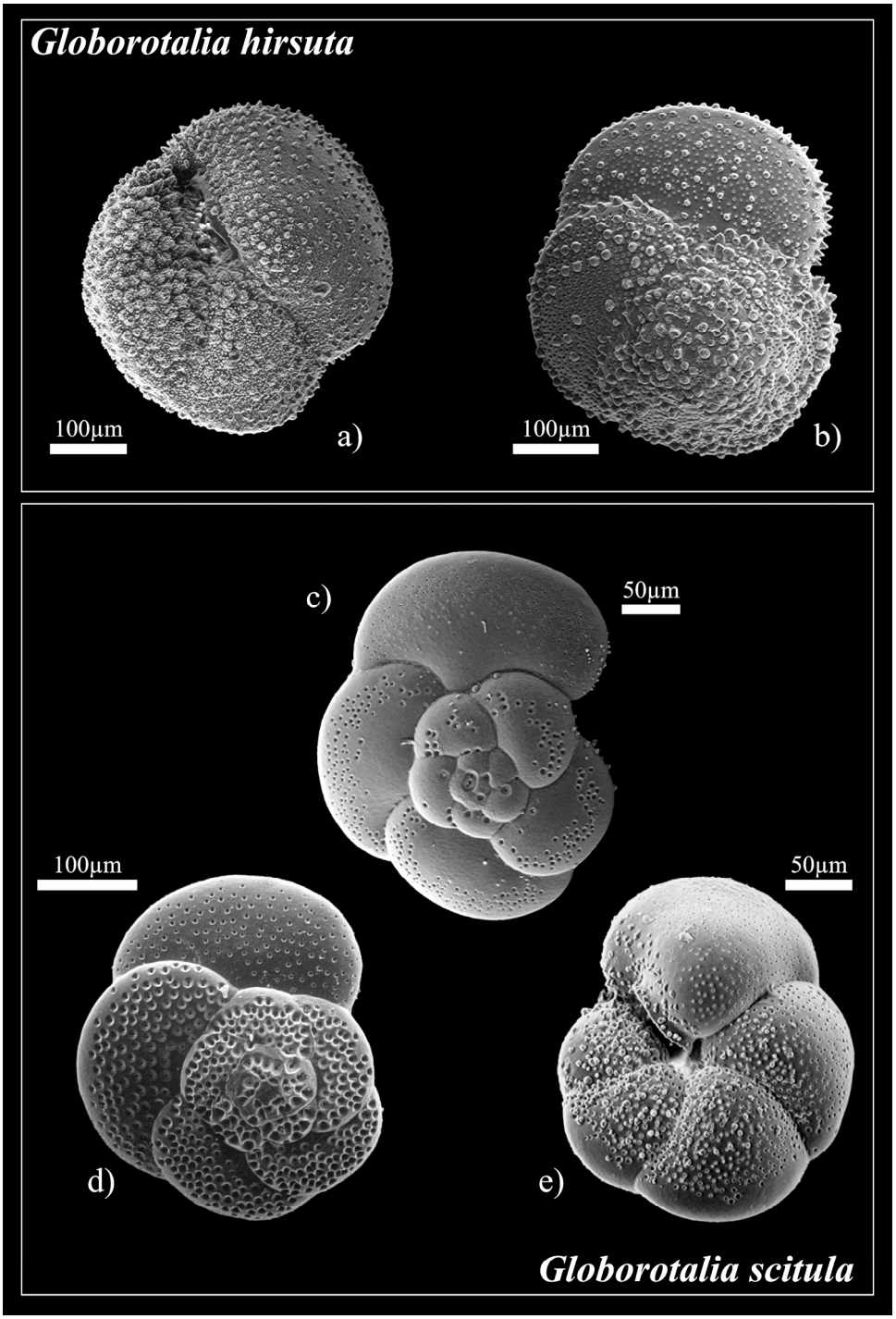
Globorotalia hirsuta
100µm
a)
100µm
b)
c)
50µm
100µm
50µm
d)
e)
Globorotalia scitula

PLATE XI

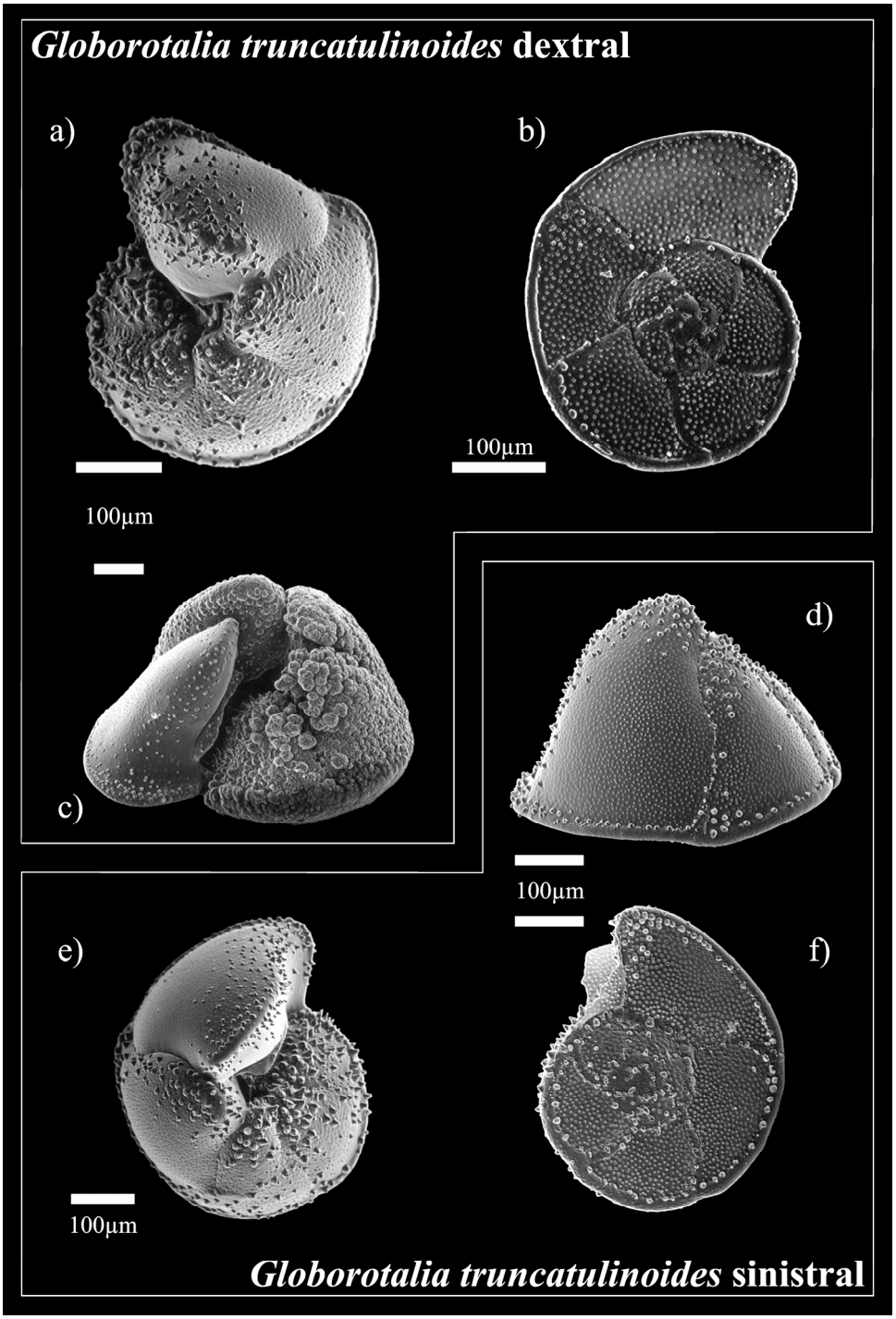
Globorotalia truncatulinoides dextral
a)
b)
100µm
100µm
c)
d)
100µm
e)
f)
100µm
Globorotalia truncatulinoides sinistral

PLATE XII

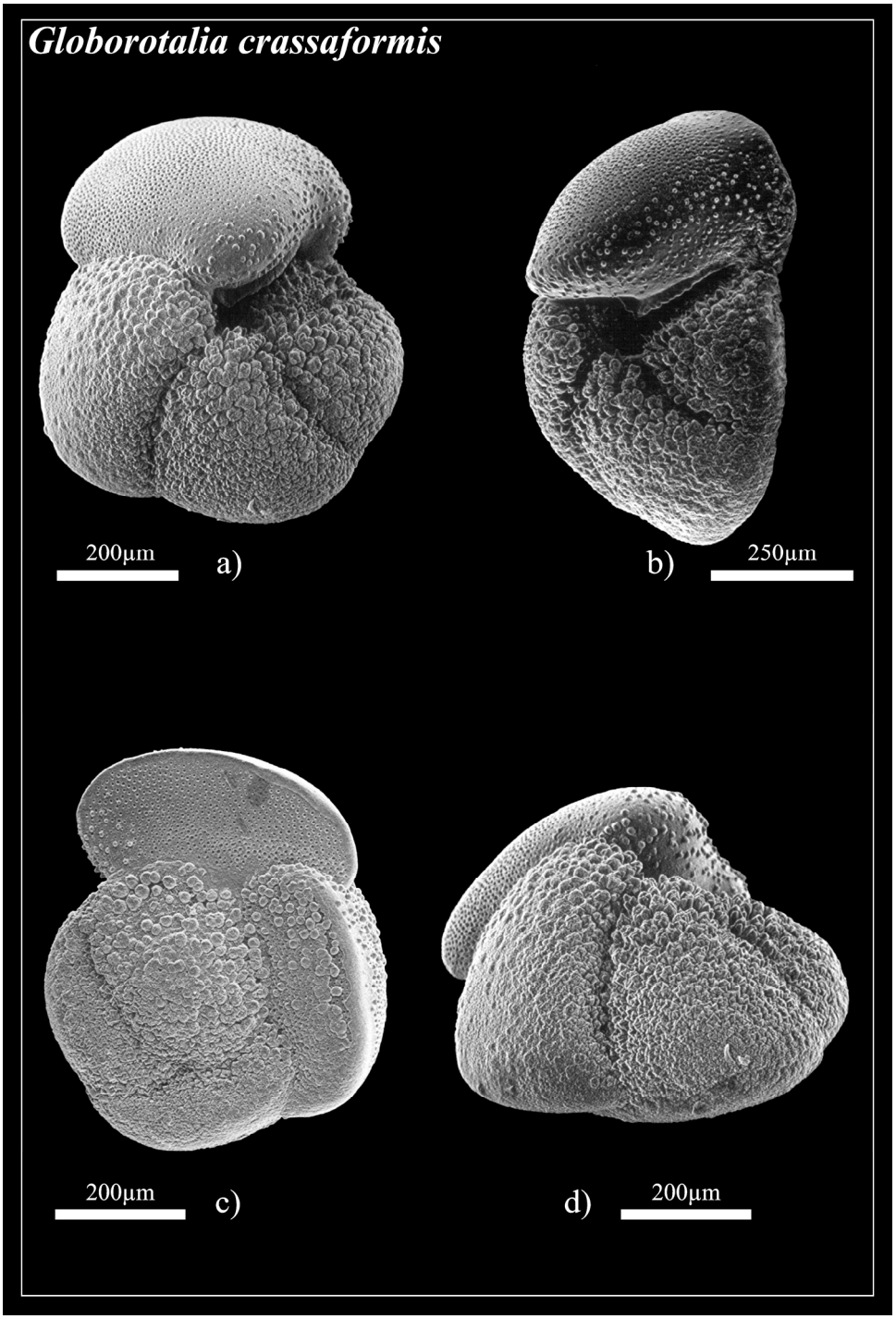

PLATE XIII

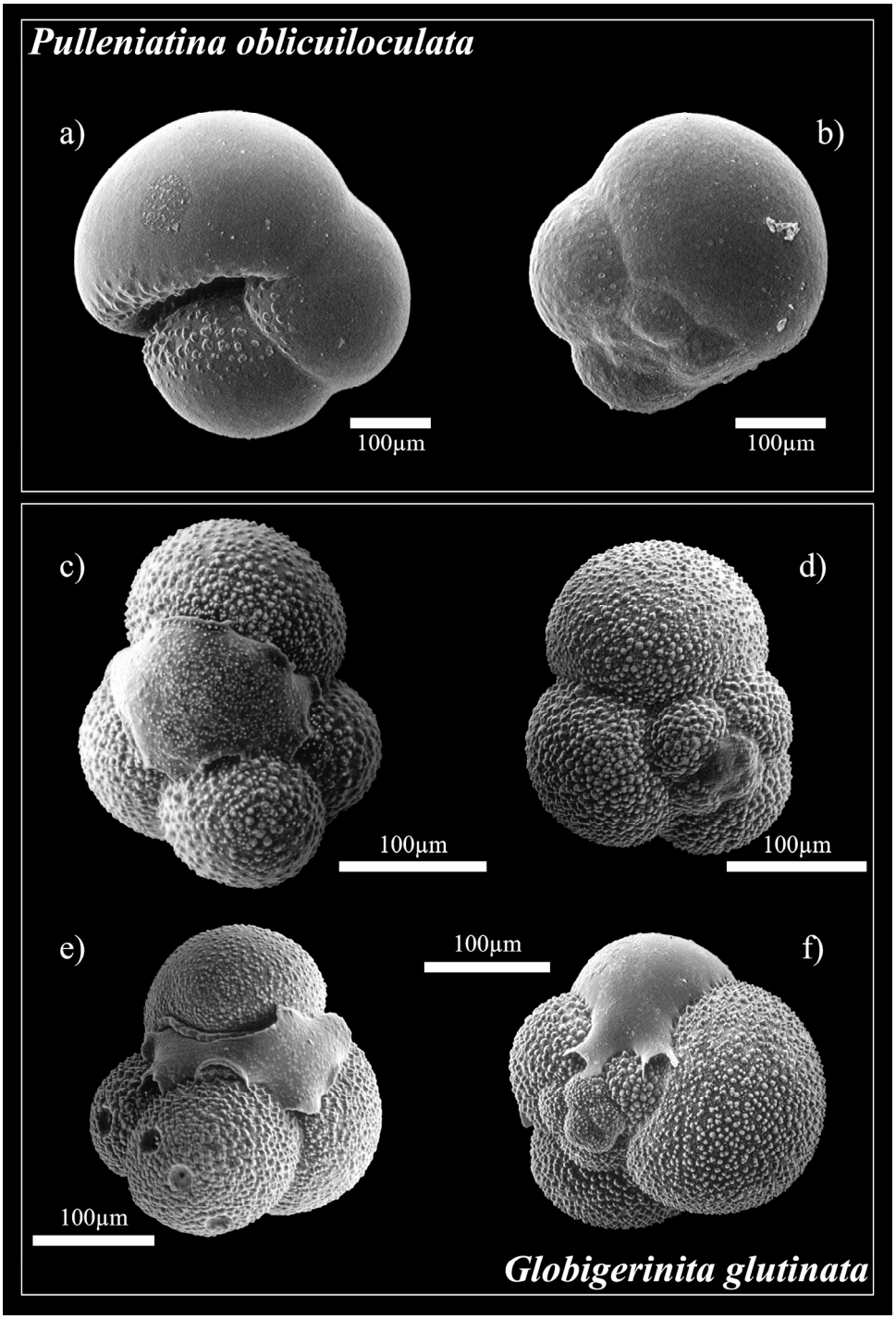
Pulleniatina oblicuiloculata
a)
b)
100µm
100µm
c)
d)
100µm
100µm
e)
100µm
f)
100µm
Globigerinita glutinata

PLATE XIV

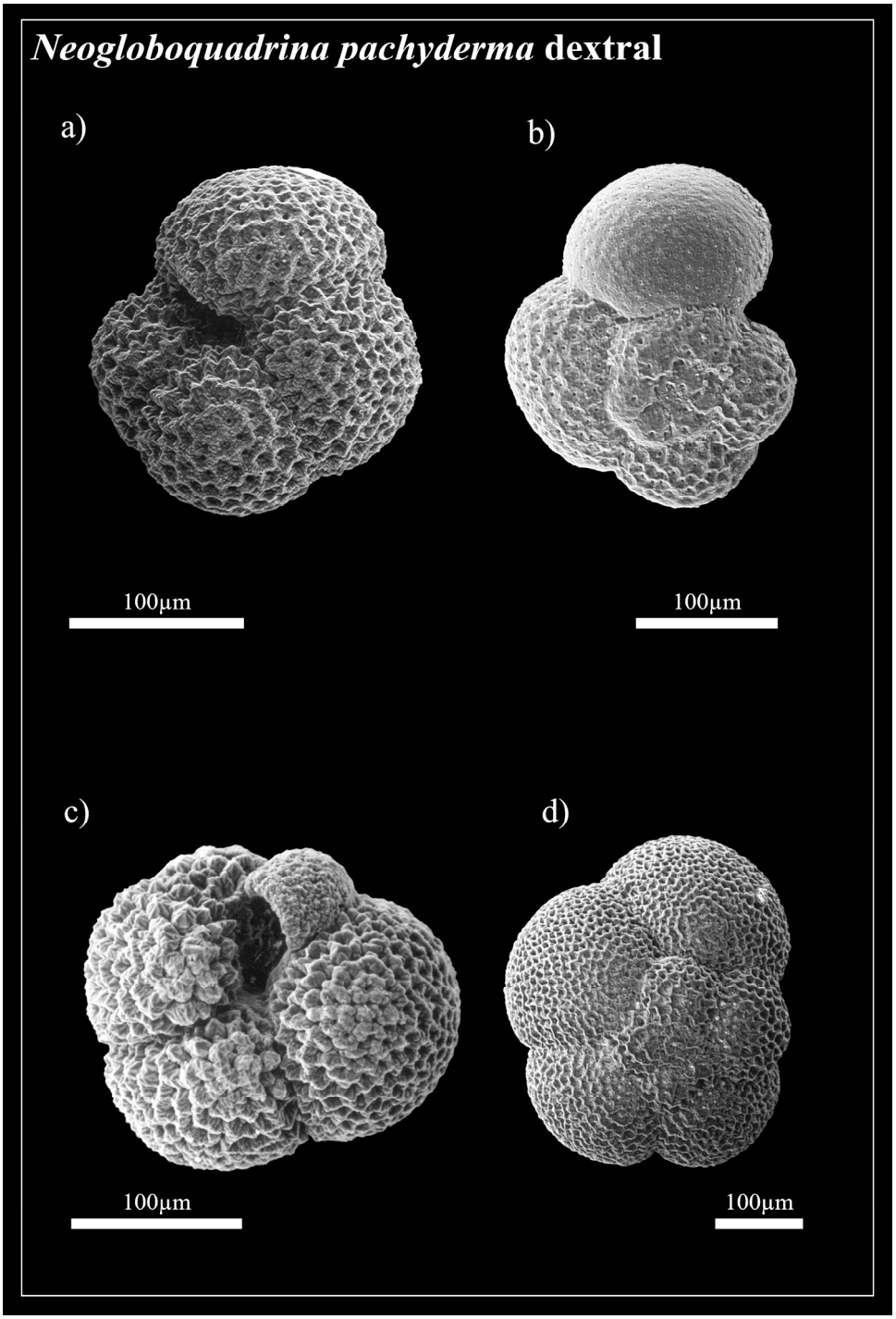
Neogloboquadrina pachyderma dextral
a)
b)
100µm
100µm
c)
d)
100µm
100µm

PLATE XV

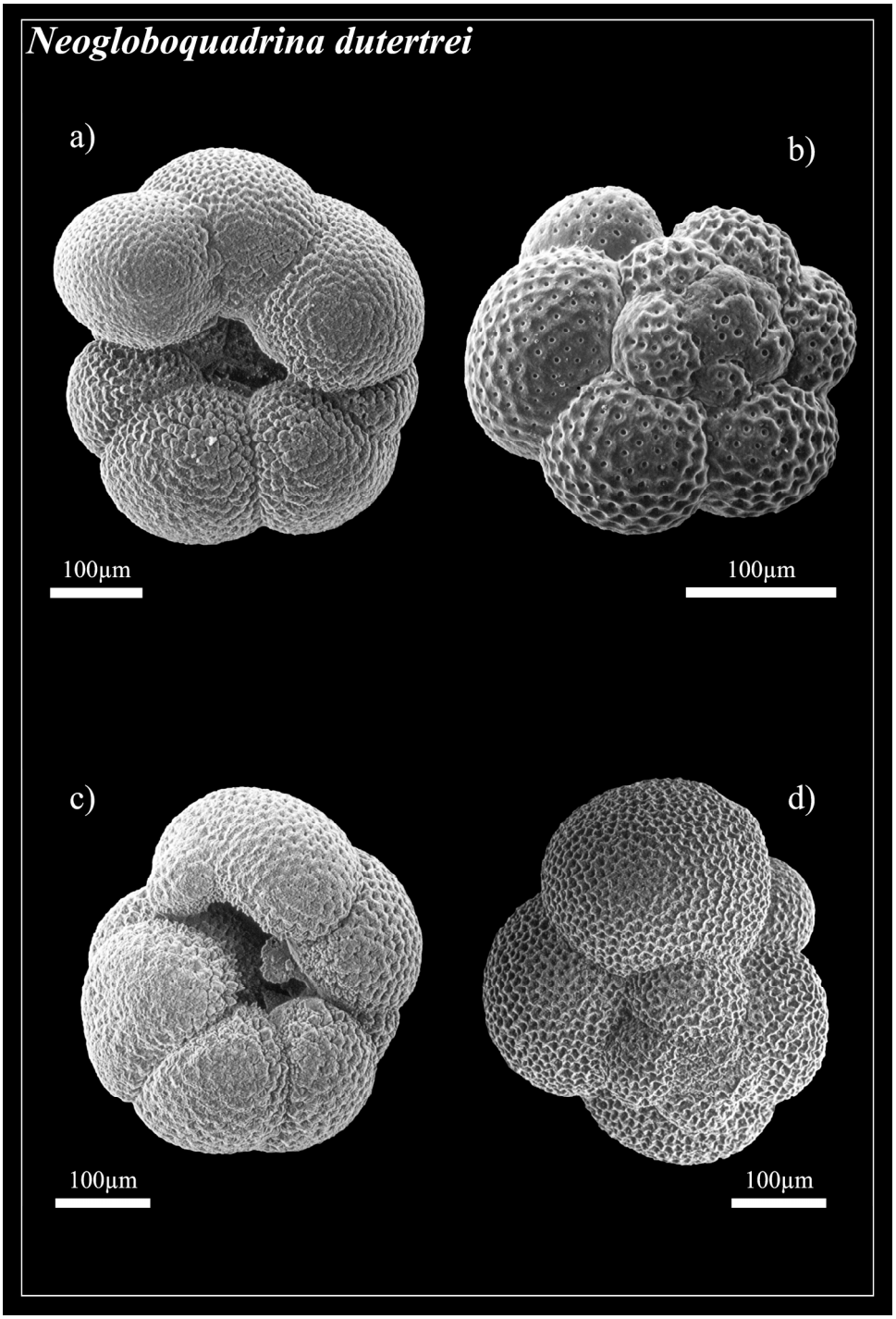

PLATE XVI

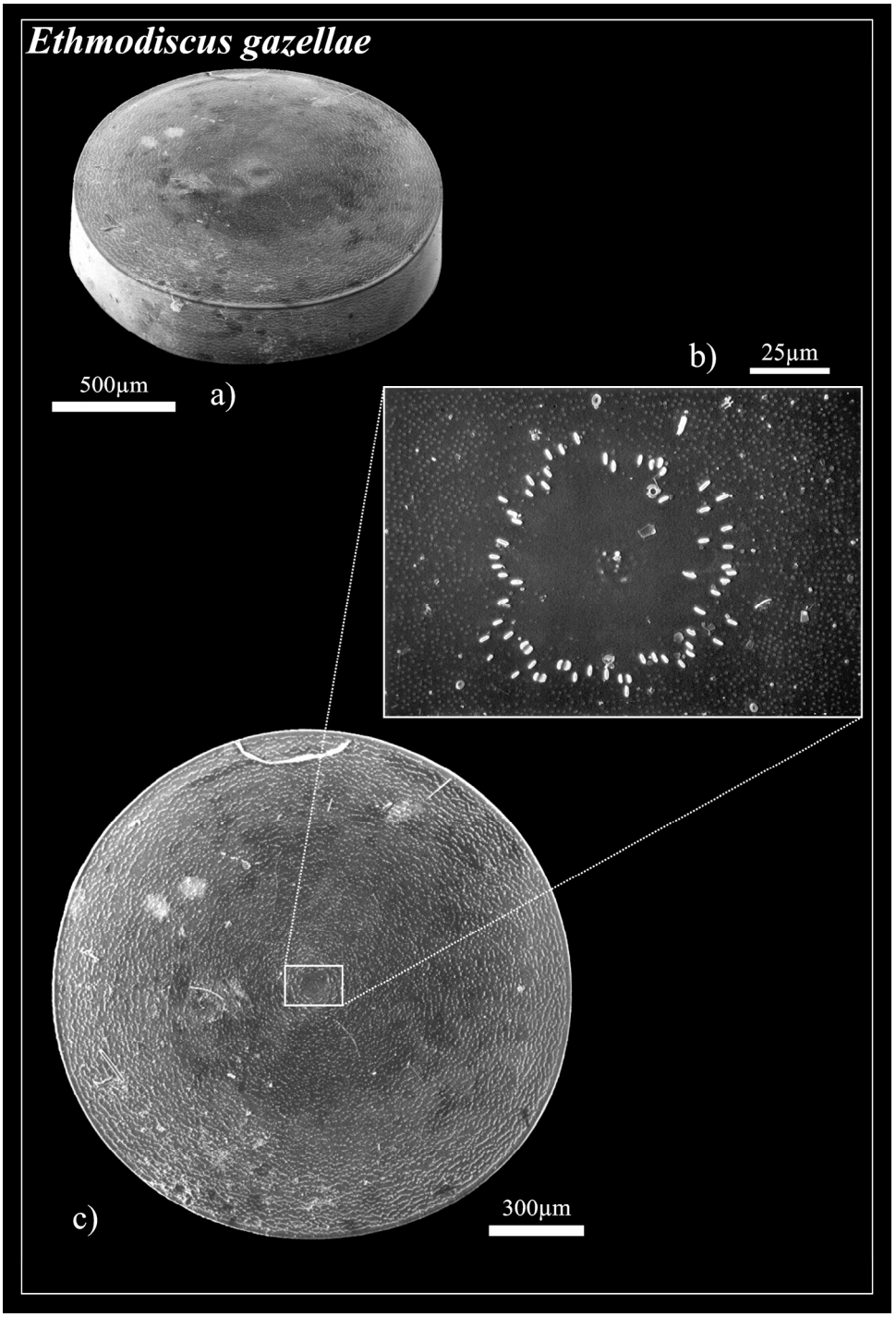

PLATE XVII

SLOTWOORD

Eindelijk, het is zo ver! Ik heb me al heel lang verheugd op het moment om het slotwoord van mijn proefschrift te mogen schrijven, vooral dat ene allerlaatste puntje dat jullie straks zullen zien. Eigenlijk had ik grote plannen met deze paragraaf. Ik wilde me niet alleen beperken tot het opsommen van mensen die op de één of andere manier hierbij betrokken waren. Nee, mijn plan was een essay te schrijven over mijn beleving van Nederland gedurende de tijd dat ik hier verbleef. Geïnspireerd door bijzondere belevenissen en met een muziekje van Nick Cave, Lou Reed of Tom Waits op de achtergrond (trouwe kameraden in Den Helderse nachten) heb ik vaak aantekeningen gemaakt of verhaaltjes opgeschreven met de gedachte: "Dit ga ik straks in het slotwoord gebruiken." Mijn naaste vrienden zullen zich met deze woorden meteen de krantenknipsels aan de muur herinneren of mijn notitieboekje op de TV voor het maken van aantekeningen tijdens het kijken naar het journaal. Maar tja, er moet weer de zoveelste deadline gehaald worden. Het boekje moet morgen naar de drukker, terwijl de meeste aantekeningen ergens onuitgepakt opgeborgen in mijn vaders garage liggen. Dit wordt dan slechts een aankondiging voor de verhalen die misschien ooit nog zullen verschijnen, wellicht in een andere taal waarbij ik me meer op mijn gemak voel. Verhalen over de stroopwafels en maatjes haring, maar ook over de geest van Boudewijn de Groot, absurden van de IND, studentenbeweging uit de polder, verschil tussen waarheid en schijn, C. Darwin vs. Tweede kamer, Mohammed B. & Rita V.,…

Hoewel dit proefschrift op het Koninklijk Nederlands Instituut voor Onderzoek der Zee (NIOZ) is gestart, waren mijn eerste geologische stappen en eerste contact met de wereld van foraminiferen op de Universiteit van Zagreb, waar alles begonnen is. Later, op de Universiteit van Utrecht introduceerde Bert van der Zwaan mij met recente foraminiferen, zowel benthische als planktonische. Bij toeval waren dat de zo'n 100 miljoen jaar jongere "kleinneefjes en kleinnichtjes" van de Adriatische beestjes waarmee ik ooit begonnen ben. In Utrecht mocht ik een kamer delen met Rob Speijer, die moeilijk de talloze keren zal vergeten dat ik zijn naam verkeerd gespeld heb en ook zal hij zich de "gehakt anekdote" waarschijnlijk blijvend herinneren, waardoor hij de hele kamer moest herinrichten. Die anekdote heeft Henko de Stigter geïnspireerd voor het maken van mijn eerste Sinterklaas cadeautje. Henko was in Utrecht een vastberaden begeleider en later een zeer goede vriend die mij altijd bijstond wanneer het echt nodig was. Mijn eerste echte paleoceanografiche stappen zijn gemaakt op Instituto Geológico e Mineiro, Departamento de Geologia Marinha (Rijks Geologische Dienst van Portugal). Naast de nieuwe en boeiende ervaringen met de vaartochten, allerlei soorten bemonsteringen, eerste praatjes op congressen, het maken van de eerste posters en het schrijven van de eerste artikelen, mocht ik drie en half jaar lang genieten van de lekkere hapjes, het mooie weer en kon ik me verdiepen in het rijke Portugese geschiedeniserfgoed. *Muito obrigado pelos bons momentos que partilhámos e por tudo o que me ensinaram. Tenho saudades dos meus amigos Portugueses!* En toen kwam ik op het Koninklijk NIOZ waar ik, dankzij de NEBROC beurs (Netherlands Bremen Oceanography) geregeld door Fred Jansen en na twee jaar ODP werk (Ocean Drilling Program), in 2000 aan het MARE project (Mixing of Agulhas Rings Experiment) begon, dat nu dan met dit boekje als resultaat hopelijk tot de doctorstitel zal leiden. Op het NIOZ werd mijn deel van het MARE werk begeleid door Geert-Jan Brummer, een project en samenwerking dat verre van soepel verliep maar waarop we, denk ik achteraf gezien, beiden trots kunnen zijn, omdat het ons

gelukt is onder moeilijke omstandigheden dit tot een afgerond geheel te brengen. vanuit de VU heeft Dick Kroon alles gecoördineerd. Ik blijf het gemak bewonderen, waarmee hij in een mum van tijd van het ene op het andere onderwerp kon overschakelen en toch overal actief bij betrokken kon blijven. Frank Peeters was betrokken bij de MARE vaartochten, hoofdstuk 5 en heeft additionele gegevens over *G. glutinata* geleverd om mijn theorie over deze soort te ondersteunen.

Ik kan met zekerheid zeggen dat dit proefschrift niet zou bestaan zonder hulp van Jolanda van Iperen. Niet alleen dat ze een grote wetenschappelijke bijdrage aan hoofdstuk 4 heeft geleverd (diatomeeën data en statistische bewerkingen), maar zij heeft de steun gegeven daar waar ik die het meest nodig had. In mijn eeuwige gevecht met de Nederlandse bureaucratie zijn honderden brieven, verzoeken, aanvragen en klachten door haar nagekeken. Vele telefoontjes zijn gepleegd en vele deuren werden geopend die ik zelf niet of moeilijk kon openen. Zij was ook mijn rechter hand bij de opmaak van dit "op afstand gemaakte" boek. Zeker niet onbelangrijk waren de vele prachtige plekjes van Nederland die ze mij heeft laten zien en de uitleg die ze daarbij altijd kon geven. Van berenklauwen tot orchideeën, van cantharellen tot parasolzwammen en van zeevonkjes tot kemphanen. Ik zal onze schitterende fietstochtjes ontzettend missen.

In de bijna 3000 uren dat ik op de TESO boot heb doorgebracht, heb ik in het bijzonder genoten van de gesprekken met Michiel Kienhuis, een goed voorbeeld dat Nederlanders wel degelijk verstand hebben van lekker koken. Veel geklets heeft eindelijk geresulteerd dat ik zelfs Resi mocht ontmoeten! Michiel heeft ook veel geholpen met het oplossen van allerlei computer problemen. Peter Vooijs en Joke Mulder van de NIOZ personeelsadministratie hebben veel "papierwerk" voor mij gedaan. In de Potvis en later in Den Helder, op het NIOZ of op de Pelagia waren er vele aangename momenten of boeiende discussies die ik onder andere gevoerd heb met Peter, Bas, Jérôme, Txetxu, Christian, Micha, Anne-Claire, Sjerry, Aad, Johan, Wim B., Els, Henk dH., Henko, Rineke, Furu, Thomas, Tjeerd, Fred, Erik, Erica, Wim vR., Geert-Jan, Helmut, Hein, Klaas, Yann, Patrick, Henk F., Phil, Astrid, Karel, Santiago, Sharyn, Jort, Yvonne, Sebastiaan, Lydie, Marianne, Katja, Jan, Oscar, Anna, Harry, Marcel, Swier, Judith en vele anderen. Op de VU waren Martin van Breukelen en Hubert Vonhof erg behulpzaam met het gebruik van de massa spectrometer. Martin vond het zelfs niet erg om 's weekends speciaal voor mij naar de VU te komen. Niet te vergeten dat ik, werkend op Texel en wonend in Den Helder, mijn gebrekkig Portugees toch niet helemaal verleerd ben en dat ik de hele tijd toegang tot mijn lieveling hapjes had. Dat allemaal dankzij mijn "Portuguese connection": Teresa Amaro, Sara Cleto en Joana Cardoso. *Meninhas, muito obrigado!*

Ten slotte draag ik dit boekje op aan mijn ouders, die deze lange tijd zo ver waren maar toch zo dichtbij. Te weten dat ik onder alle omstandigheden onvoorwaardelijk op hun steun kan rekenen heeft mij de kracht gegeven om deze levensepisode succesvol af te ronden. *Dragi mama i tata, bili ste dugo tako daleko a opet tako blizu. Već sama spoznaja da na Vas uvijek mogu računati dala mi je snage ovu životnu epizodu uspješno privesti kraju. Puno Vam hvala za sve!*

En daarom allemaal een GROTE BEDANKT!

Zagreb, 30 oktober, 2005 ●

CURRICULUM VITAE

Addresses:

nevenl@nioz.nl (until 1/Jan/2006)
karlobag@excite.com
neven.loncaric@zg.t-com.hr

Education:

2000 – 2005	Ph.D. research at the Royal Netherlands Institute for Sea Research (NIOZ) - Texel and the Faculty of Earth and Life Sciences of the Vrije Universiteit, Amsterdam, The Netherlands (supervised by Prof. Dr. D. Kroon)
1992 – 1994	M.Sc. courses in geology of sedimentary rocks, with emphasis on micropaleontology/ oceanography at the Faculty of Earth Sciences of the Utrecht University, The Netherlands (thesis supervisor Prof. Dr. B. van der Zwaan)
1988 - 1991	B.Sc. courses in geology at the Faculty of Mining, Geology and Petroleum Engineering of the University of Zagreb, Croatia
1984	graduated at the MIOC – Zagreb, Croatia (high school for mathematics and informatics)

Professional activities:

Sep/98 – Sep/05 research position at the NIOZ – Department of Marine Chemistry and Geology working as micropaleontologist/paleoceanographer on the material collected in the SE Atlantic:

- ODP leg 175: planktic foraminifera, Mid-Pleistocene Revolution
- MARE project (Mixing of Agulhas Rings Experiment): ecology of recent planktic foraminifera

Jun/97 - Sep/97 guest scientist at the GEOMAR, Kiel within the group of Prof. Dr. R. Zahn working on sediment cores recovered during the Meteor 39-1 cruise and SIMMAX modern analog technique SST estimations

Apr/95 - Sep/98 junior scientist at the IGM – DGM, Lisbon, Portugal working within the research group of Dr. F. Abrantes as micropaleontologist / paleoceanographer on:

- ENAM project (European North Atlantic Margin): sedimentation patterns at the continental margin, Heinrich events
- Portuguese Continental Margin project: paleo SST estimations and Holocene climate oscillations along the Portuguese continental margin

Major fellowships and grants:

2002/03 Mixing of Agulhas Rings Experiment (MARE) research fellowship (12 months)
1998/02 Netherlands – Bremen Oceanography (NEBROC) research fellowship (50 months)
1996/98 Portuguese science foundation research fellowship (18 months)
1995/96 ENAM research fellowship (18 months)

2004 CNRS, Gif sur Yvette cruise & travel grant (Indian and Southern Ocean)
2001 IMAGES travel grant (Sapporo, Japan)
2000 NWO (Dutch Science foundation) travel grant, (Cavtat, Croatia)
1999 INQUA travel grant (Durban, South Africa)
1999 ODP travel grant (Ventura, CA, USA)

Participations in scientific expeditions:

2004 R/V Marion Dufresne (Réunion - Mauritius - Mayotte - Crozet - Kerguelen - Réunion) (chief scientists: Dr. E. Michel & Dr. C. Waelbroeck, CNRS, Gif sur Yvette, France)
2000 MARESECS & MARE by R/V Pelagia (Dakar – Walvis Bay – Cape Town) (chief scientist: Dr. G.-J. Brummer, NIOZ, Texel, The Netherlands)
1997 R/V Meteor leg 39-1 (Las Palmas - Brest) (chief scientist: Prof. Dr. R. Zahn, GEOMAR, Kiel, Germany)
1996 IMAGES II by R/V Marion Dufresne (Réunion - Cape Town - Walvis Bay - Cape Town - Réunion) (chief scientist: Dr. P. Bertrand, Bordeaux University, France)

Peer- reviewed publications:

Lončarić, N., G.-J.A. Brummer & D. Kroon, 2005. Lunar cycles and seasonal variations in deposition fluxes of planktic foraminiferal shell carbonate to the deep South Atlantic (central Walvis Ridge)**, Deep-Sea Research I, 52** (7), 1175-1186.

Lončarić, N., F. Peeters, D. Kroon & G.-J.A. Brummer, Oxygen isotope ecology of recent planktic foraminifera at the central Walvis Ridge (SE Atlantic), accepted upon revision in **Paleoceanography**.

Lončarić, N., J.M. van Iperen, D. Kroon & G.-J.A. Brummer, Seasonal export and sediment preservation of diatom, foraminiferal and biogenic mass fluxes in a trophic gradient across the SE Atlantic, submitted to **Progress in Oceanography**.

Salgueiro, E., F. Abrantes, H. Meggers, U. Pflaumann, A. Voelker, **N. Lončarić,** P. Oliveira, H.B. Bartels - Jonsdottir, J. Moreno and G. Wefer, Planktonic Foraminifera from Modern Sediments Reflect Upwelling Patterns off Portugal: Insights from a Regional Transfer Function, in revision for **Quaternary Science Reviews**.

Lončarić, N., G.-J.A. Brummer & D. Kroon, Population dynamics of planktic foraminifera at the central Walvis Ridge (SE Atlantic): standing stock, export flux and turnover time, in preparation for **Paleobiology**.

Lončarić, N., G.A. Auffret, F. Abrantes, J.H. Baas, L. Gaspar and C. Pujol, 1998. Late Quaternary sedimentation patterns on the Meriadzek Terrace, Bay of Biscay, **Marine Geology, 152** (1-3), 57-73.

Abrantes, F., J.H. Baas, L. Gaspar, H. Hafladison, D. Klitgard-Kristensen, **N. Lončarić** and T. Rasmussen, 1998. Sediment fluxes along the NE European margin: Inferring hydrological changes between 20 and 8 kyr, **Marine Geology, 152** (1-3), 7-23.

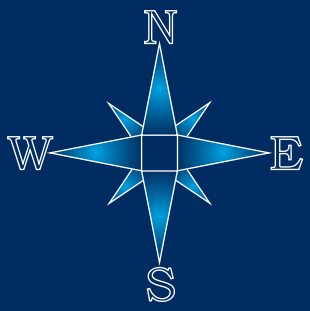

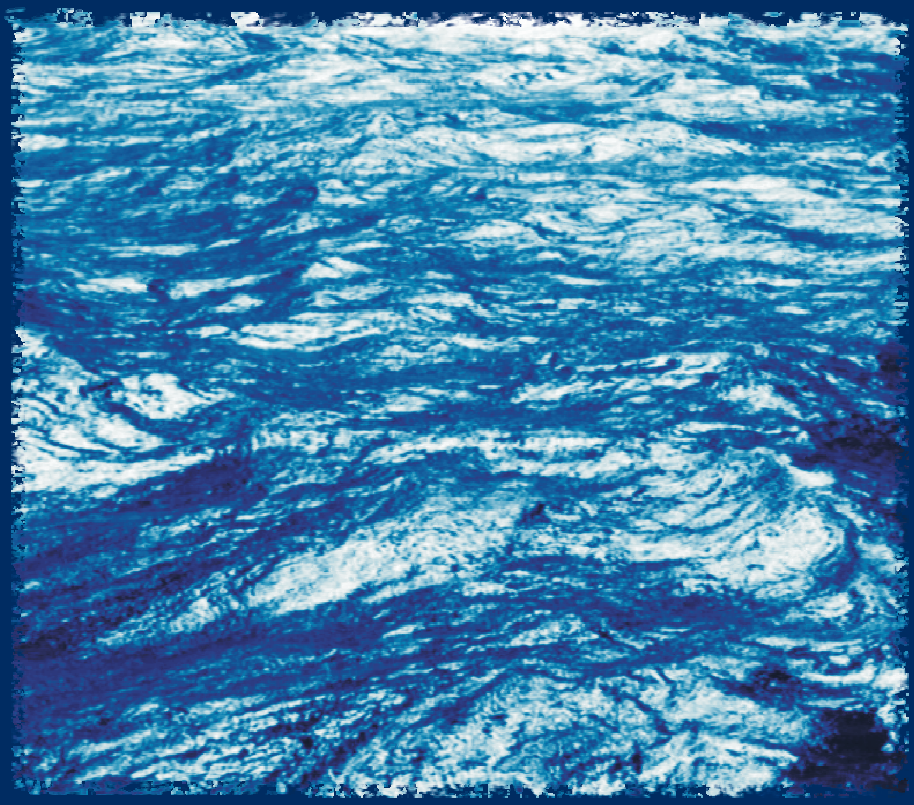

ISBN 90-90201535-X